JYU DISSERTATIONS 172

Ruslan Mokaev

Effective Analytical-Numerical Methods for the Study of Regular and Chaotic Oscillations in Dynamical Systems

UNIVERSITY OF JYVÄSKYLÄ
FACULTY OF INFORMATION TECHNOLOGY

JYU DISSERTATIONS 172

Ruslan Mokaev

Effective Analytical-Numerical Methods for the Study of Regular and Chaotic Oscillations in Dynamical Systems

Esitetään Jyväskylän yliopiston informaatioteknologian tiedekunnan suostumuksella
julkisesti tarkastettavaksi yliopiston Agora-rakennuksen Gamma-salissa
joulukuun 14. päivänä 2019 kello 12.

Academic dissertation to be publicly discussed, by permission of
the Faculty of Information Technology of the University of Jyväskylä,
in building Agora, Gamma hall, on December 14, 2019 at 12 o'clock noon.

JYVÄSKYLÄN YLIOPISTO
UNIVERSITY OF JYVÄSKYLÄ

JYVÄSKYLÄ 2019

Editors
Timo Männikkö
Faculty of Information Technology, University of Jyväskylä
Ville Korkiakangas
Open Science Centre, University of Jyväskylä

Copyright © 2019, by University of Jyväskylä

Permanent link to this publication: http://urn.fi/URN:ISBN:978-951-39-7989-8

ISBN 978-951-39-7989-8 (PDF)
URN:ISBN:978-951-39-7989-8
ISSN 2489-9003

ABSTRACT

Mokaev, Ruslan
Effective analytical-numerical methods for the study of regular and chaotic oscillations in dynamical systems
Jyväskylä: University of Jyväskylä, 2019, 84 p. (+included articles)
(JYU Dissertations
ISSN 2489-9003; 172)
ISBN 978-951-39-7989-8 (PDF)

This dissertation examines the difficulties in analyzing the onset of oscillations in the process of loss of stability in various nonlinear dynamical systems. The study of the onset of oscillations originated with the discovery of periodic regimes in automatic control systems, as well as with the discovery of chaos associated with attempts to explain a laminar fluid flow becoming turbulent. One of the first methods revealing and analyzing stability of periodic oscillations applied to automatic control systems with one scalar nonlinearity was the Andronov point-mapping method, which is applicable only to piecewise linear systems of low order. Van der Pol, Krylov and Bogolyubov suggested the harmonic balance method, which is applicable to systems of arbitrary dimension with scalar nonlinearity of a general form. However, this method is approximate and may incorrectly predict the loss of stability and existence of oscillations.

In this dissertation, for systems with one scalar nonlinearity, the discussion of the classical harmonic balance and the point-mapping methods has been carried out. Advantages and disadvantages of the locus of a perturbed relay system (LPRS) method, which is an extension of the harmonic balance method, were discussed and new examples demonstrating difficulties of studying scenarios of the loss of stability and onset of oscillations in relay systems were presented.

None of the above mentioned methods are applicable when oscillations emerging in the system after the loss of stability demonstrate complex chaotic behavior. Such phenomenon was first noticed by famous scientist Lorenz in the study of turbulent convection of a fluid layer. One of the first explanations to the birth of such oscillations was given via a homoclinic bifurcation, in which a homoclinic oscillation appears in the phase space. In general, proving the existence of a homoclinic oscillation and giving a full description of the loss of stability and the onset of chaos via a homoclinic bifurcation remain open challenges.

In this dissertation, for a class of Lorenz-like systems, the conditions of the existence of a homoclinic oscillation have been analytically obtained and a numerical investigation of several new homoclinic bifurcation scenarios have been carried out. For the Lorenz system, to visualize unstable periodic oscillations, which may appear during homoclinic bifurcations and are embedded in chaotic attractor, the Pyragas control algorithm has been implemented.

Keywords: global stability, periodic and homoclinic oscillations, chaos

TIIVISTELMÄ (ABSTRACT IN FINNISH)

Mokaev, Ruslan
Tehokkaita analyyttis-numeerisia menetelmiä dynaamisten systeemien säännöllisten ja kaoottisten värähtelyjen tutkimiseen
Jyväskylä: University of Jyväskylä, 2019, 84 s. (+artikkelit)
(JYU Dissertations
ISSN 2489-9003; 172)
ISBN 978-951-39-7989-8 (PDF)

Työssä kehitetään uusia menetelmiä dynaamisten systeemien värähtelyjen tutkimiseen. Tutkimusalueen juuret ovat yhtäältä automaattisten ohjausjärjestelmien analyysissä ja toisaalta virtausten turbulenssin syntymekanismeissa. Vanhimpia metodeja ovat Andronovin pistemenetelmä, joka soveltuu paloittain lineaaristen ohjausjärjestelmien toimintapisteiden ja stabiiliuden tutkimiseen, sekä harmonisen tasapainon menetelmä (Van der Pol, Krylov, Bogolyubov), joka soveltuu yleisille systeemeille, joissa on yksi epälineaarinen elementti. Menetelmä ei kuitenkaan ole tarkka, vaan voi antaa vääriä ennusteita systeemin stabiiliudesta.

Tässä työssä vertaillaan yhden epälineaarisuuden sisältäville systeemeille em. menetelmiä sekä pistemenetelmän laajennusta, LPRS-menetelmää (Locus of Perturbed Relay System). Osoittautui, että menetelmät täydentävät toisiaan aidosti ja eri menetelmien avulla voitiin löytää uusia, ennen tuntemattomia esimerkkejä piilevistä kaoottisista värähtelijöistä.

Monimutkaisemmille systeemeille, joissa on useampi epälineaarinen komponentti ja värähtely on kaoottista, edelliset menetelmät eivät ole riittäviä. Kaoottisille värähtelyille on monta syntymekanismia, joista tunnetuin on niin sanottu homokliininen bifurkaatio, jossa tasapainossa olevaan järjestelmään syntyy toimintapisteen muuttuessa spontaanisti periodinen värähtely. Tämän ilmiön löysi meteorologi Lorenz tutkiessaan turbulenssin syntyä ilmakehässä.

Yleisessä tapauksessa kysymys siitä, voiko systeemiin syntyä homokliininen värähtely ja voiko systeemi siirtyä tätä kautta kaoottisen värähtelyn tilaan, on avoin.

Tässä työssä on johdettu joukolle Lorenzin mallin kaltaisia systeemejä ehdot, joiden vallitessa niissä esiintyy homokliininen värähtely. Tämä on mahdollistanut useiden uusien bifurkaatioskenaarioiden numeerisen tarkastelun. Osana numeerista tarkastelua on toteutettu Pyragasin säätöalgoritmi, jonka avulla voidaan visualisoida kaoottisen värähtelyn sisään piiloutuneita, epästabiileja, periodisia värähtelyjä.

Avainsanat: globaali stabiilius, periodisia ja homokliiniset värähtelyt, kaaos

Author

Ruslan Mokaev
Faculty of Information Technology
University of Jyväskylä
Finland
Faculty of Mathematics and Mechanics
St. Petersburg State University
Russia

Supervisors

Professor Pekka Neittaanmäki
Faculty of Information Technology
University of Jyväskylä
Finland

Professor Nikolay V. Kuznetsov
Faculty of Information Technology,
University of Jyväskylä
Finland,
Faculty of Mathematics and Mechanics
St. Petersburg State University
Russia

Professor Timo Tiihonen
Faculty of Information Technology
University of Jyväskylä
Finland

Reviewers

Professor Marius-F. Danca
Department of Mathematics and Computer Science,
Avram Iancu University, Cluj-Napoca
Romania
Romanian Institute of Science and Technology
Cluj-Napoca
Romania

Professor Sergei Abramovich
School of Education and Professional Studies
State University of New York at Potsdam
USA

Opponent

Professor Vladimir Rasvan
Department of Automation
Electronics and Mechatronics
University of Craiova, Craiova, Dolj
Romania

ACKNOWLEDGEMENTS

This thesis was completed in the Doctoral School of the Faculty of Information Technology, University of Jyväskylä.

I would like to express my sincere gratitude to my supervisors Prof. Pekka Neittaanmäki, Prof. Nikolay V. Kuznetsov and Prof. Timo Tiihonen for their guidance, productive discussions, additional comments and continuous support. I am also very grateful to the reviewers of the thesis, Prof. Marius-F. Danca and Prof. Sergei Abramovich, for their fruitful remarks and valuable comments.

I am extending my heartfelt thanks to Prof. Igor Boiko for the countless number of productive conversations and substantive discussions.

I am very much obliged to Ivan Evlashev, Mikhail Kropotov and Prof. Timo Tiihonen for their improvements of English and Finnish languages and grammars.

This work would not have been possible without support from the Faculty of Information Technology and Russian Science Foundation (project 19-41-02002).

I would like to extend my deepest gratitude to my parents Ludmila Mokaeva and Nazir Mokaev and to my brother Timur Mokaev for their love and endless support for everything I do.

This work is dedicated to the memory of Gennady A. Leonov (1947-2018), who was a co-founder of the Finnish-Russian Educational & Research program organized within the agreement between the University of Jyväskylä, Finland and Saint-Petersburg State University, Russia.

LIST OF ACRONYMS

PMM	Point-Mapping Method
HBM	Harmonic Balance Method
LPRS	Locus of a Perturbed Relay System

LIST OF FIGURES

LIST OF TABLES

CONTENTS

LIST OF INCLUDED ARTICLES

PI G.A. Leonov, N.V. Kuznetsov, M.A. Kiseleva, R.N. Mokaev. Global Problems for Differential Inclusions. Kalman and Vyshnegradskii Problems and Chua Circuits. *Differential Equations, Vol. 53, No. 13, PP. 1671–1702, https://doi.org/10.1134/S0012266117130018*, 2017.

PII E.D. Akimova, I.M. Boiko, N.V. Kuznetsov, R.N. Mokaev. Analysis of oscillations in discontinuous Lurie systems via LPRS method. *Vibroengineering PROCEDIA, Vol. 25, PP. 177–181, https://doi.org/10.21595/vp.2019.20817*, 2019.

PIII N.V. Kuznetsov, O.A. Kuznetsova, D.V. Koznov, R.N. Mokaev, B.R. Andrievsky. Counterexamples to the Kalman Conjectures. *IFAC-PapersOnLine, Vol. 51, I. 33, PP. 138–143, https://doi.org/10.1016/j.ifacol.2018.12.107*, 2018.

PIV N.V. Kuznetsov, O.A. Kuznetsova, T.N. Mokaev, R.N. Mokaev, M.V. Yuldashev, R.V. Yuldashev. Coexistence of hidden attractors and multistability in counterexamples to the Kalman conjecture. *Proceedings of the* 11^{th} *IFAC Symposium on Nonlinear Control Systems*, 2019 (accepted to IFAC-PapersOnLine).

PV E.V. Kudryashova E.V., Kuznetsov N.V., Kuznetsova O.A., Leonov G.A., Mokaev R.N. Harmonic Balance Method and Stability of Discontinuous Systems. *In: Matveenko V., Krommer M., Belyaev A., Irschik H. (eds) Dynamics and Control of Advanced Structures and Machines. Springer, Cham, PP. 99–107, https://doi.org/10.1007/978-3-319-90884-7_11*, 2019.

PVI N.V. Kuznetsov, T.N. Mokaev, E.V. Kudryashova, O.A. Kuznetsova, R.N. Mokaev, M.V. Yuldashev, R.V. Yuldashev. Stability and Chaotic Attractors of Memristor-Based Circuit with a Line of Equilibria. *Lecture Notes in Electrical Engineering, PP. 639–644, https://doi.org/10.1007/978-3-030-14907-9_62*, 2020.

PVII G.A. Leonov, R.N. Mokaev, N.V. Kuznetsov, T.N. Mokaev. Homoclinic Bifurcations and Chaos in the Fishing Principle for the Lorenz-like Systems. *International Journal of Bifurcation and Chaos, Vol. 30 (accepted, preprint https://arxiv.org/pdf/1802.07694.pdf)*, 2020.

PVIII N.V. Kuznetsov, T.N. Mokaev, R.N. Mokaev, O.A. Kuznetsova, E.V. Kudryashova. A lower-bound estimate of the Lyapunov dimension for the global attractor of the Lorenz system. *preprint, arXiv:1910.08740, https://arxiv.org/pdf/1910.08740.pdf*, 2019.

1 INTRODUCTION AND STRUCTURE OF THE WORK

1.1 Introduction

The necessity of studying stability and limiting dynamical regimes (attractors) arises in classical theoretical and applied problems. One of the first such problems was related to the design of automatic control (regulators) systems, which ensured the transition of the controlled object to the operating regime and its stability with respect to external disturbances. For the first dynamical models of the control systems the operating regime corresponds to a *globally stable* equilibrium state (or a stationary set).

A classic example of such a dynamical model is the model suggested by I.A. Vyshnegradsky (Vyshnegradsky, 1877) in his stability analysis of the Watt governor – a mechanism used to maintain a constant speed of rotation of a turbine shaft. For the closed dynamic model "machine + governor" Vyshnegradsky studied an approximate linear mathematical model without dry friction and proposed the stability conditions of the desired operating regime corresponding to the equilibrium state (trivial attractor).

Soon it became clear that local stability of the equilibrium state (a necessary condition for the existence of an operating regime) is not a sufficient condition for global stability, and thus, Vyshnegradsky's results were criticized. In a similar regulation system with dry friction it was demonstrated (Léauté, 1885) that the loss of global stability might be related with by existence of non-trivial oscillating periodic working regimes (called lately limit cycles (Poincare, 1892, 1893, 1899)) could appear. Thus, the important question of rigorous proof of global stability and the validation of the Vyshnegradsky procedure of linearizing the system by discarding dry friction remained open.

Afterwards, A.A. Andronov and A.G. Maier (Andronov and Maier, 1944) shown that conditions obtained by Vyshnegradsky are sufficient for global stability using specially developed point-mapping method, which was designed for analysis of oscillations in a special case of low-order nonlinear systems with

piecewise-linear nonlinearities.

For stability analysis of general nonlinear systems with one nonlinearity an approximate method, called the harmonic balance method, was developed (van der Pol, 1926; Krylov and Bogolyubov, 1937). It allowed one to detect the existence of periodic oscillations, whose presence indicates the loss of global stability of a system. For a special case of relay systems with nonlinearity $\mathtt{sign}(\cdot)$ the harmonic balance method was further developed (see (Tsypkin, 1984; Boiko, 2008) and others), which allowed to get more accurate prediction on existence of periodic oscillations. However, all these methods may not find all periodic oscillations, especially the so-called *hidden oscillations* (Leonov and Kuznetsov, 2013; Leonov et al., 2015; Kuznetsov et al., 2018b; Kuznetsov, 2016, 2018a,b, 2019, 2020), which basin of attraction is not connected with equilibrium states, and which are "hidden" somewhere in the phase space.

In more general cases, when there are several scalar nonlinearities in the system, the classical harmonic balance method and its extensions, as well as the point-mapping method, could not be applied for the stability analysis. Another obstacle for application of these methods is related to the fact that the loss of global stability in a system could lead to the birth of not only periodic, but also *chaotic* oscillations.

The discovery of the first chaotic attractor is connected with the work of the famous American meteorologist E. Lorenz (Lorenz, 1963), who proposed a mathematical model of fluid convection in a two-dimensional layer and numerically discovered a chaotic limit regime in this model.

In order to study and predict the appearance of chaotic dynamics in the Lorenz system, researchers considered various scenarios of the loss of global stability and appearance of chaotic attractors. One of the first such scenarios of the transition to chaos, deeply studied in the works of the scientific school of L.P. Shilnikov (Afraimovich et al., 2014), is connected with the appearance in a phase space of a homoclinic orbit (homoclinic bifurcation). In the vicinity of this homoclinic bifurcation, depending on the parameters of the system, both stable and unstable periodic orbits (UPOs) can arise before and after the appearance of a homoclinic orbit. Note that chaotic dynamics may be related with the countable number of unstable periodic orbits (e.g., embedded in a chaotic attractor), which are hard to detect.

1.2 Structure of the work

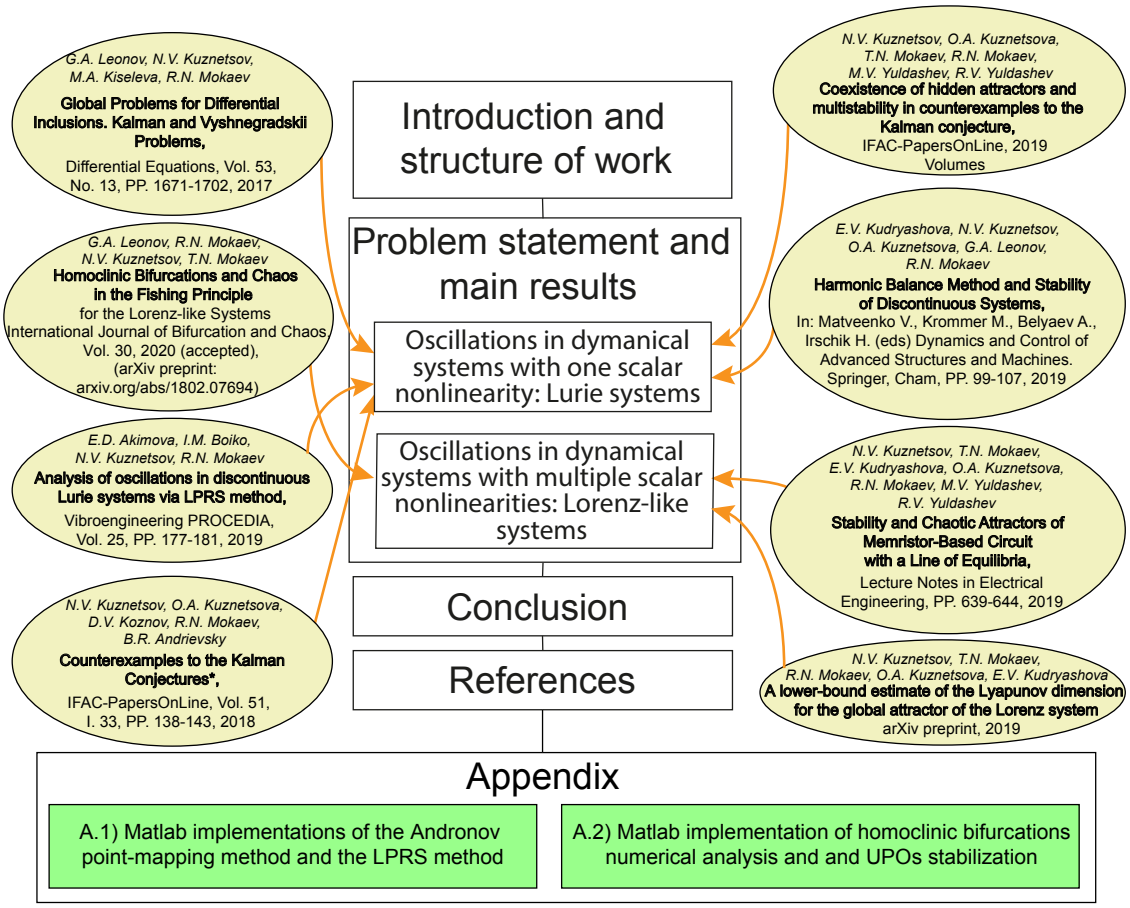

FIGURE 1 Structure of the chapters and their connection with included articles.

1.3 Included articles and author's contribution

The main results were published in the eight included articles. In **(PI; PIII)** author studied the famous Kalman conjecture and introduced a new counterexample representing a system with a hidden chaotic oscillation (coexisting with hidden periodic oscillation with respect to stable equilibrium point), which could not be found by approaches that were used previously. In **PII** author illustrated advantages of the locus of a perturbed relay system method (LPRS) in comparison with the classical harmonic balance method and described limitations of both methods. In **PIV** author studied the Kalman conjecture and introduced a new counterexample representing a system with three coexisting hidden limit cycles in its phase space. In **PV** author described limitations of the classical harmonic balance method on the example of three known nonlinear systems and demonstrated that while this method may give correct results it still may give incorrect prediction on the existence of periodic oscillations and, therefore, on the global stability. In **PVI** author implemented a procedure for visualization of attractors in the vicinity of the line of equilibria in a memristor model. In **PVII** author proved the existence of homoclinic orbit and provided a numerical analysis of different homoclinic bifurcation scenarios in the Lorenz-like systems. In **PVIII** author implemented the Pyragas algorithm for localization of unstable periodic orbits (UPOs) embedded in Lorenz attractor.

In all the above publications author contribution is in writing, proving analytical theorems and numerical modeling.

The results of this study were also reported at the 39^{th} International JVE Conference (St. Petersburg, Russia, 2019) and the 11^{th} IFAC Symposium on Nonlinear Control Systems (Vienna, Austria, 2019); at the seminars of the Department of Applied Cybernetics (St. Petersburg State University), and at the seminars of the Faculty of Information Technology (University of Jyväskylä).

2 PROBLEM STATEMENT AND MAIN RESULTS

2.1 Oscillations in dynamical systems with one scalar nonlinearity: Lurie systems

In this section, following papers **PI-PV**, the problem of analysis of oscillations and describing scenarios of the loss of stability in dynamical systems with one scalar nonlinearity are considered.

2.1.1 Global stability and oscillations

In 1877 Vyshnegradsky published his famous work on the Watt regulator, where he considered the following nonlinear dynamic model (here we consider its Lurie form (Lurie and Postnikov, 1944) - linear part plus nonlinearity, depending only on measurable outputs) of the regulator (see, e.g., **PI**):

$$\dot{x} = Ax + B\varphi(\sigma), \qquad \sigma = Cx, \tag{1}$$

with

$$A = \begin{pmatrix} 0 & 0 & 1 \\ -1 & 0 & 0 \\ -a_v & 1 & -b_v \end{pmatrix}, \quad B = \begin{pmatrix} 0 \\ 0 \\ -1 \end{pmatrix}, \quad C = \begin{pmatrix} 0 \\ 0 \\ 1 \end{pmatrix}^T, \quad \varphi(\sigma) = \frac{1}{2}\operatorname{sign}\sigma.$$

He performed 'linearization' (by discarding nonlinearity φ) in the vicinity of regime, analyzed its local stability and obtained corresponding conditions:

$$a_v > 0, b_v > 0, a_v b_v > 1. \tag{2}$$

Vyshnegradsky supposed that this necessary conditions of local stability would imply also the global stability.

However, soon in similar regulation system with dry friction non-trivial oscillating periodic regimes (Léauté, 1885) were discovered (called lately limit cycles (Poincare, 1892, 1893, 1899)). Thus, Zhukovsky criticized Vyshnegradsky

approach and posed a problem of rigorous justification of Vyshnegradsky conclusion (Zhukovsky, 1909).

For analysis of periodic oscillations in dynamical systems of low order and with piecewise-linear nonlinearities, Andronov developed a point-mapping method (see, e.g., (Andronov et al., 1937)), which was used by Andronov and Maier (Andronov and Maier, 1944) for rigorous analysis of Vyshnegradsky system. It was shown that there are no periodic oscillations in the system if condition (2) is met and, therefore, local stability implies global stability for the system. However, for nonlinear systems with nonlinearities of general form this method could not be applied.

2.1.2 Harmonic balance method

For analysis of periodic oscillations in nonlinear systems with one scalar nonlinearity of general form a classical harmonic balance method was developed in the 192x–193x in the works of van der Pol (van der Pol, 1926), Krylov and Bogolyubov (Krylov and Bogolyubov, 1937). This method is as follows (see (Leonov and Kuznetsov, 2013) and (Khalil, 2002), P. 450–457): suppose there is a periodic solution $a\cos\omega_0 t$ in system (1). Then frequency w_0 can be found from

$$\operatorname{Im} W(j\omega_0) = 0, \tag{3}$$

where $W(s)$ is a transfer function of system (1):

$$W(s) = C(A - Is)^{-1}B, \tag{4}$$

and amplitude a can be found from harmonic balance equation

$$\int_0^{\frac{2\pi}{\omega_0}} \varphi(a\cos(\omega_0 t))\cos(\omega_0 t)dt = ak\int_0^{\frac{2\pi}{\omega_0}} (\cos(\omega_0 t))^2 dt, \tag{5}$$

where k is a linearization coefficient:

$$k = -(\operatorname{Re} W(j\omega_0))^{-1}. \tag{6}$$

For relay systems with $\operatorname{sign}(\sigma)$ nonlinearity this method allows to calculate amplitude analytically:

$$a = \frac{4}{\pi k}. \tag{7}$$

For instance, this method allowed to obtain the same conditions (2) for the global stability of Vyshnegradsky system (see e.g. Gelig et al. (1978)). However, since the classical harmonic balance method is an approximate method of periodic solutions searching, it appeared that the method may be wrong in two directions: it can show that there are no periodic oscillations while they actually exist in the phase space (Leonov and Kuznetsov, 2013) and, on the contrary, shows that there are oscillations, although in fact they do not exist (Leonov and Kuznetsov, 2018a).

For instance, following (Keldysh, 1944), let us consider Keldysh[1] model of the suppression of flutter with one degree of freedom and show that the classical harmonic balance method may predict existence of periodic solutions, while in reality they do not exist. Keldysh system in Lurie form is as follows:

$$A = \begin{pmatrix} 0 & 1 \\ -1 & -\mu \end{pmatrix}, B = \begin{pmatrix} 0 \\ -1 \end{pmatrix}, C = \begin{pmatrix} 0 \\ 1 \end{pmatrix}^T, \quad \varphi(\sigma) = (\Phi + \kappa\sigma^2)\mathrm{sign}(\sigma). \tag{8}$$

Using the classical harmonic balance method, Keldysh formulated the following result: *If*

$$-2.08\sqrt{\Phi\kappa} < \mu, \tag{9}$$

then all trajectories of (8) *converge to the rest segment; If*

$$\mu < -2.08\sqrt{\Phi\kappa}, \tag{10}$$

then there are two periodic trajectories (limit cycles). Other trajectories behave as follows. The trajectories, emerging from infinity, tend to the external limit cycle. The domain between two limit cycles is filled with trajectories unwinding from the internal (unstable) limit cycle and winding onto external (stable) limit cycle. The stability domain bounded by the internal limit cycle is filled with trajectories tending to one of the possible equilibrium on the rest segment.

Using Lyapunov-type theorems for systems with discontinuous right-hand side it can be shown (see (Leonov and Kuznetsov, 2018b)) that if

$$-2\sqrt{\Phi\kappa} < \mu, \tag{11}$$

then any solution (in the Filippov sense (Filippov, 1960)) of (8) converges to the stationary segment $[-\Phi, \Phi]$. Thus, Keldysh's estimate of the global stability region (9) is close to the rigorous analytical estimate, but doesn't coincide as in the case of the Vyshnegradsky system. Fig. 2 shows the bifurcation of collision of the external limit cycle and the stationary segment (see **PV**). In this numerical experiment both limit cycles have disappeared, while Keldysh's estimate (10) holds.

The opposite effect can be observed in the Keldysh system (see (Keldysh, 1944), Eq. 2, P. 34) of flutter suppression with two degrees of freedom, where $\Phi = 1,\ \kappa = 0$ and

$$a_{11} = a_{22} = b_{22} = c_{11} = c_{22} = 0, a_{21} = m_1^2 + \beta^2,\ a_{12} = m_2^2 + \beta^2,$$
$$b_{11} = -1,\ b_{12} = b_{21} = 2\beta,\ c_{12} = c_{21} = 1.$$

[1] Mstislav Keldysh was the president of the Soviet Union Academy of Sciences during 1961-1975.

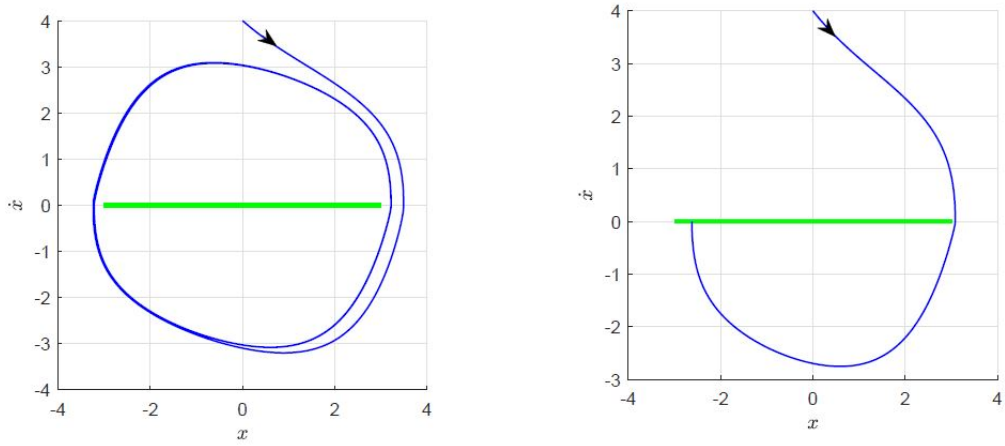

a) b)

FIGURE 2 Numerical analysis of the Keldysh system with one degree of freedom and $\lambda = 0, \Phi = 3, \kappa = 1$. a) $\mu = -3.85792$: outer trajectory attracts to the limit cycle around rest segment. b) $\mu = -3.6287$: limit cycle 'disappeared'.

Lurie form of this system is

$$\begin{aligned} \mathrm{A} &= \begin{pmatrix} 0 & 1 & 0 & 0 \\ -(m_1^2+\beta^2) & -2\beta & 0 & -\lambda \\ 0 & 0 & 0 & 1 \\ 0 & 1 & -(m_2^2+\beta^2) & -2\beta \end{pmatrix}, \mathrm{B} = \begin{pmatrix} 0 \\ -1 \\ 0 \\ 0 \end{pmatrix}, \\ \mathrm{C} &= \begin{pmatrix} 0 \\ 0 \\ 0 \\ 1 \end{pmatrix}^T, \varphi(\sigma) = \mathrm{sign}(\sigma), \end{aligned} \tag{12}$$

where λ is a linear parameter of damper; $m_1 = 0.9, m_2 = 1.1$, β is a parameter. Transfer function of system (12) is

$$W(s) = \frac{s^2}{s^4 + a_3 s^3 + (a_2 + \lambda)s^2 + a_1 s + a_0}, \tag{13}$$

where $a_0 = (m_1^2 + \beta^2)(m_2^2 + \beta^2)$, $a_1 = 2\beta(m_1^2 + m_2^2 + 2\beta^2)$, $a_2 = m_1^2 + m_2^2 + 6\beta^2$, $a_3 = 4\beta$.

The rest segment of system (12) is

$$\Lambda = \{(x_1, x_2, x_3, x_4) \in \mathbb{R}^4 \mid x_2 = x_3 = x_4 = 0, -\tfrac{1}{a_0} \le x_1 \le \tfrac{1}{a_0}\}. \tag{14}$$

Applying the Routh-Hourwitz criterion to find a stability sector of the linearized system $\dot{\mathrm{x}} = A\mathrm{x} + k\, b\, c^*\mathrm{x}$, we obtain

$$\left(-4\beta^2 - \lambda - \frac{(m_1^2 - m_2^2)^2}{2(m_1^2 + m_2^2 + 2\beta^2)}, +\infty \right).$$

Consider system (12) with parameter values

$$\beta = 0.01, \lambda = -0.041. \tag{15}$$

According to the classical harmonic balance method, this system has only one unstable periodic solution with frequency $\omega_{unst} = 1.005037312$ (see (3)). However, using numerical integration (Piiroinen and Kuznetsov, 2008) with initial data in the vicinity of the rest segment (14), we can localize two additional asymmetric periodic solutions (see Fig. 3), which are self-excited with respect to the rest segment. Therefore, this classical method requires further development.

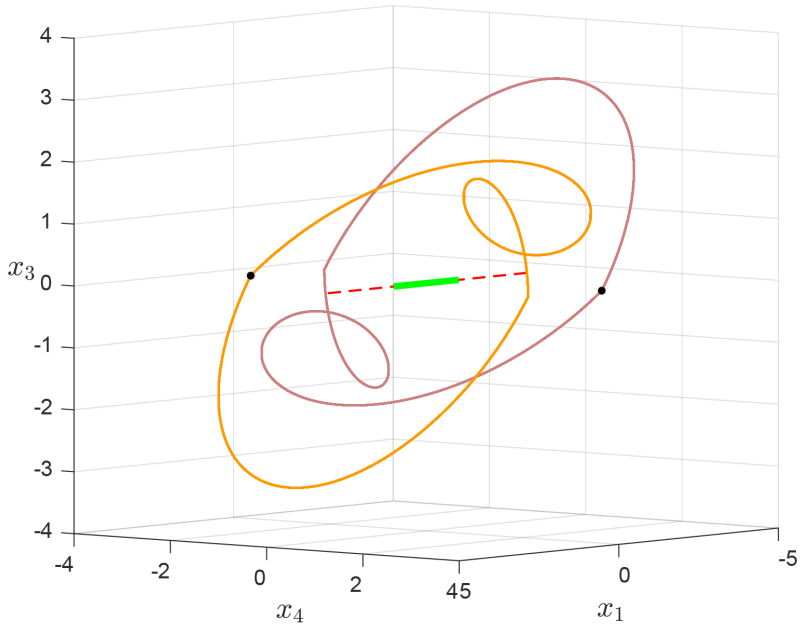

FIGURE 3 Two self-excited (with respect to rest segment) asymmetric periodic solutions of the Keldysh system with $\lambda = 0, \Phi = 1, \kappa = 0$ and $\beta = 0.01$ and $\lambda = -0.041$.

2.1.3 Aizerman and Kalman conjectures

An interesting connection can be observed between the classical harmonic balance method and the absolute stability theory (see, e.g., (Gelig et al., 1978; Khalil, 2002; Rasvan, 2006a,b)), in which the main focus was on the selection of classes of nonlinear systems for which necessary and sufficient conditions for global stability coincide, which imply the absence of non-trivial limiting oscillations (as was in the case of Vyshnegradsky system). The history of attempts to solve this problems is connected with the Aizerman (Aizerman, 1949) and Kalman (Kalman, 1957) conjectures on global stability of Lurie systems with nonlinearity satisfying generalized Routh-Hurwitz criterion and with attempts to construct counterexamples to these conjectures. It can be shown that for systems in Lurie form (1) satisfying conditions of Aizerman or Kalman conjectures, the classical harmonic balance method states that this systems have no periodic solutions.

Aizerman formulated his problem in 1949, while being inspirited by the discussion of the work (Andronov and Maier, 1944) at the Andronov's scientific seminar in the Institute of Automation and Remote Control (USSR Academy of Sciences, Moscow) (Bissell, 1998) and it is as follows: consider system (1) where $\varphi(\sigma)$ is a continuous piecewise-differentiable scalar function and $\varphi(0) = 0$. Suppose that for all $k \in (0, K)$, where K is a positive number or $+\infty$ and any solution of system (1) with $\varphi(\sigma) = k\sigma$ tends to a unique stable equilibrium state. Then for system (1) with any nonlinearity $\varphi(\sigma)$ satisfying the property

$$0 < \varphi(\sigma) < K\sigma, \ \sigma \neq 0,$$

all solutions tend to the unique stable equilibrium state.

In 1957, Kalman formulated a more restrictive conjecture on global stability, where in addition to the conditions from the Aizerman conjecture, it was required that the derivative of nonlinearity belongs to the linear stability sector: if at the points of differentiability $\varphi(\sigma)$ the condition

$$0 < \varphi'(\sigma) < K, \tag{16}$$

is satisfied, then all solutions tend to a unique stable equilibrium state.

Analytical approaches to obtain counterexamples to these conjectures (see, e.g., (Barabanov, 1988)) were based on application of Andronov point-mapping method to nonlinear systems with discontinuous nonlinearity `sign(·)`, which made it possible to analytically integrate their periodic solutions. And after periodic solutions were found, transition to the nonlinear system with piece-wise continuous and continuous nonlinearities ('smoothing' of discontinuous nonlinearity) was performed. Difficulties of numerical search for periodic oscillations in systems that represent counterexamples to Aizerman and Kalman conjectures arise because of multistability, when different attracting oscillations coexist in the phase space and their number and mutual disposition are unknown. At the same time, non-trivial oscillations coexisting with the locally stable equilibrium state are hidden oscillations[2], for which it is not straightforward how to find initial data for their visualization.

2.1.4 Extensions of harmonic balance method

Harmonic analysis of periodic solutions in Lurie systems with relay nonlinearities was extended and new methods were introduced, e.g., Tsypkin method

[2] The classification of attractors as being hidden or self-excited was proposed in (Leonov and Kuznetsov, 2013; Leonov et al., 2015; Kuznetsov et al., 2018b): an oscillation is called self-excited if its basin of attraction intersects with any vicinity of an unstable equilibrium and, thus, it can be visualized numerically by a trajectory srating from a point in a neighborhood of unstable equilibrium; otherwise it is called a hidden oscillation and its basin of attraction is not connected with equilibria and could be small. This classification became a basis for the *theory of hidden oscillations*, which has been developed by N. Kuznetsov in recent publications (Kuznetsov, 2016, 2018a,b, 2019, 2020). This theory represents the modern stage of Andronov's theory of oscillations.

(Tsypkin, 1984) and its further development, which is called the locus of a perturbed relay system approach (the LPRS method) (Boiko, 2005, 2008). This methods made it possible in many cases to refine the results (both existence prediction and parameters estimation), obtained by the classical harmonic balance method. Let us focus on the LPRS method (Boiko, 2008), which is as follows: consider a system in a form

$$\begin{aligned} &\dot{\mathrm{x}} = A\mathrm{x} + Bu, \\ &y = C\mathrm{x}, \\ &u = \begin{cases} +c, & \text{if } \sigma = f_0 - y \geq b \text{ or } \sigma > -b, u(t-0) = c \\ -c, & \text{if } \sigma = f_0 - y \leq b \text{ or } \sigma < b, u(t-0) = -c. \end{cases} \end{aligned} \tag{17}$$

where $A \in \mathbb{R}^{n\times n}$, $B \in \mathbb{R}^{n\times 1}$, $C \in \mathbb{R}^{1\times n}$ are matrices, and $u(t-0)$ is the control value at the time immediately preceding the current time, f is a cumulative input (disturbance) to the system transposed to the relay input, u is the control, y is the output, σ is the error signal, c is the amplitude of the relay, $2b$ is the hysteresis value of the relay function $u = u(\sigma)$. Note that system (1) defines an ideal relay (without hysteresis) and is special case of system (17).

For system (17) a complex function of frequency $J(w)$, called the locus of a perturbed relay system (LPRS), was introduced in (Boiko, 2008):

$$\begin{aligned} J(w) = -0.5C\big[A^{-1} + \tfrac{2\pi}{\omega}(I - e^{\frac{2\pi}{\omega}A})^{-1}e^{\frac{\pi}{\omega}A}\big]B + \\ + \mathrm{i}\tfrac{\pi}{4}C(I + e^{\frac{\pi}{\omega}A})^{-1}(I - e^{\frac{\pi}{\omega}A})A^{-1}B. \end{aligned} \tag{18}$$

Imaginary part of the function defined in that way contains information about the frequency ω of a periodic solution for the system and the real part of $J(\omega)$ contains information about the amplitude a and transfer properties of the relay with respect to a small bias at its input.

With available LPRS of a system, symmetric periodic solutions can be found exactly through solving the following algebraic equation for the frequency ω_0 (see Fig. 4):

$$\operatorname{Im} J(\omega_0) = -\frac{\pi b}{4c}. \tag{19}$$

For the relay without hysteresis $b = 0$ and frequency ω_0 of a periodic oscillation can be found from equation

$$\operatorname{Im} J(\omega_0) = 0, \tag{20}$$

and corresponding amplitudes can be found from

$$a = -\frac{4\operatorname{Re} J(\omega_0)}{\pi}. \tag{21}$$

2.1.5 Problems of frequency analysis

To illustrate advantages and limitations of the LPRS method let's apply this method to system (12) (see, e.g., **(PI; PIII; PV; PIV)**) with

$$\lambda = 0, \Phi = 1, \kappa = 0. \tag{22}$$

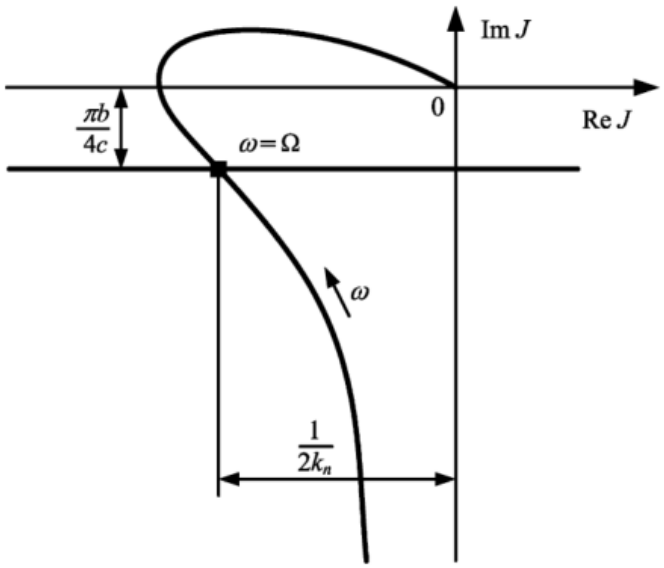

FIGURE 4 The LPRS of relay system and oscillation analysis.

Its sector of linear stability is the following interval

$$\left(-4\beta^2 - \frac{(m_1^2 - m_2^2)^2}{2(m_1^2 + m_2^2 + 2\beta^2)}, +\infty \right), \tag{23}$$

therefore, it satisfies generalized Routh-Hurwitz criterion and according to the classical harmonic balance method, this system has no periodic solutions.

However, using LPRS method, for system (22) with $\beta = 0.03$ we can obtain values of frequency $\omega = 0.5272504$ and initial data (see Table. 2) of a symmetric self-excited periodic oscillation (see Fig. 5,6)[3]. A narrower frequency range of $[0.4, 0.8]$ for the respective part of the LPRS, containing the sought periodic solution, is given in Fig. 6. In addition, this solution can be visualized via numerical modeling from the vicinity of the rest segment (stationary set of system (22)) (see Fig. 7).

However, using Andronov point-mapping method it is possible to get initial data and values of parameters of two hidden limit cycles, that are not found by the LPRS method (see Fig. 8). Their parameters and initial data are presented in Table 1. Note that it is also possible to obtain initial data and parameters of self-excited limit cycle that was already found using numerical modeling and the LPRS method.

Finally, we can apply one of the methods for numerical localization of hidden oscillations in multidimensional dynamical systems, which is based on homotopy and numerical continuation method. The idea is to construct a sequence of similar systems such that for the first (starting) system the initial point for numerical computation of oscillating solution (starting oscillation) can be obtained analytically. Then the transformation of this starting oscillation in the phase space is tracked numerically while passing from one system to another (initial data for

[3] The analysis of the candidate points shows that only one point of intersection of the LPRS and the horizontal axis corresponds to an actual periodic oscillation.

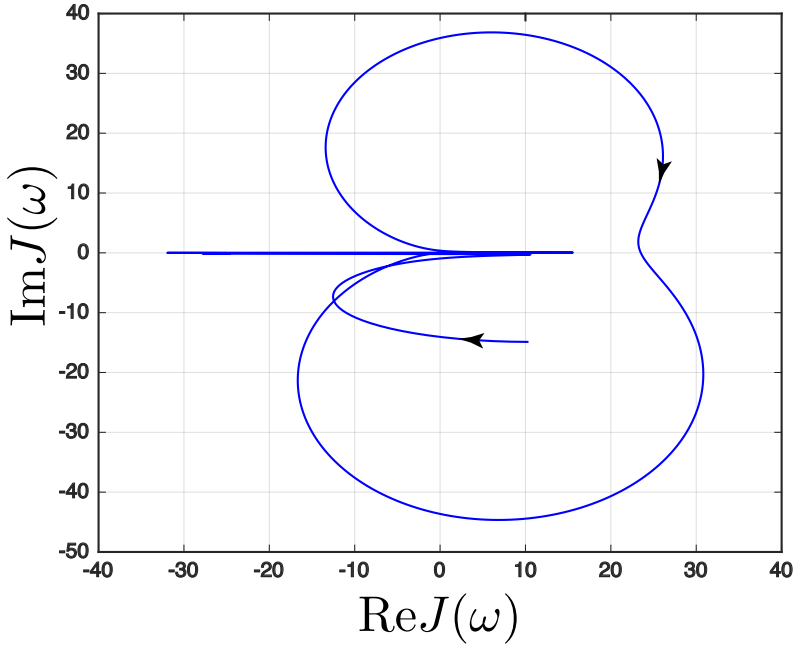

FIGURE 5 The LPRS of the Keldysh system with $\lambda = 0, \Phi = 1, \kappa = 0$ and $\beta = 0.03$.

TABLE 1 Parameters and initial data of two hidden periodic oscillations of the Keldysh system with $\lambda = 0, \Phi = 1, \kappa = 0$ and $\beta = 0.03$.

ω	0.672578885438731
T	9.341930654098658

a) Parameters

x_1	$\pm$0.625205162606947
x_2	$\pm$3.732409707265053
x_3	$\pm$0.0
x_4	$\mp$3.475416972869716

b) Initial data

TABLE 2 Parameters and initial data of a self-excited periodic oscillation of the Keldysh system with $\lambda = 0, \Phi = 1, \kappa = 0$ and $\beta = 0.03$.

ω	0.527252701490018
T	11.916838528135139

a) Parameters

x_1	-0.212347571833203
x_2	1.671123725917290
x_3	0.0
x_4	-1.478087381572674

b) Initial data

numerical modeling of oscillation in the next system is a last point of oscillation in previous system); the last system corresponds to the system in which an attractor is searched (see, e.g., (Kuznetsov et al., 2018a)). Applying this approach to system (22) and passing from $\beta = 0.03$ to $\beta = 0.1$, it is possible to localize a chaotic solution and a periodic solution (see Fig. 9) in the phase space of system (22) with $\beta = 0.1$.

This chaotic oscillation (as well as periodic one) remains under the reverse scenario of discontinuous Aizerman-Pyatnitsky approximation (Aizerman and

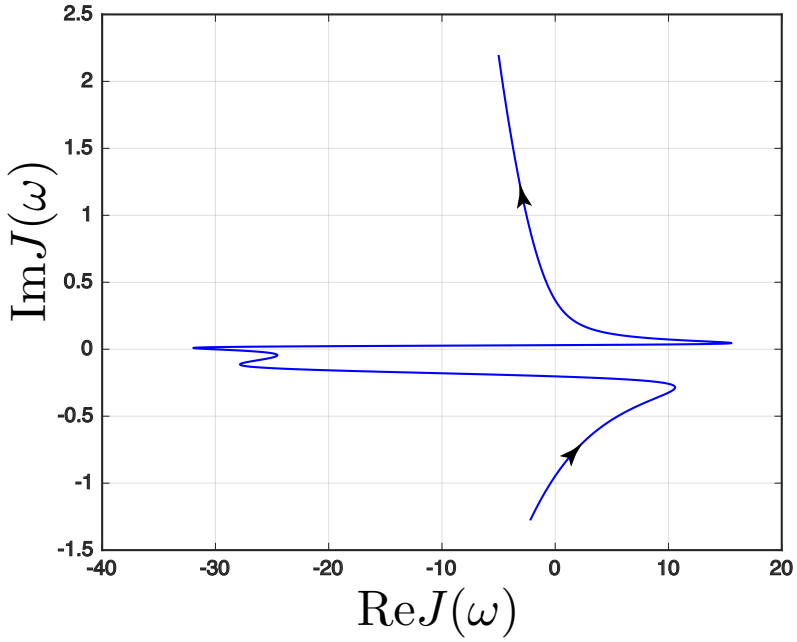

FIGURE 6 The LPRS of the Keldysh system with $\lambda = 0, \Phi = 1, \kappa = 0$ and $\beta = 0.03$ in the range of $[0.4, 0.8]$. The frequency of 0.4 corresponds to the lower end point of the LPRS, and 0.8 corresponds to the higher end point.

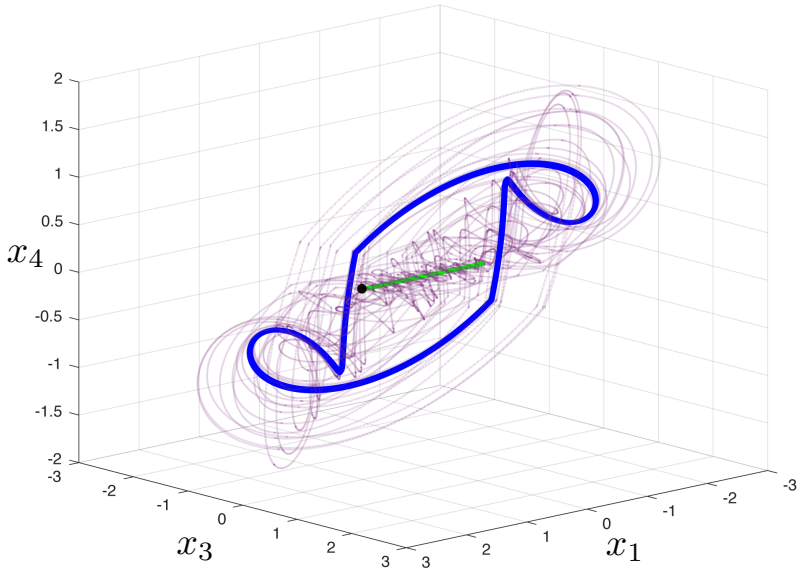

FIGURE 7 From initial point in vicinity of rest segment it is possible to arrive at a limit cycle in the Keldysh system with $\lambda = 0, \Phi = 1, \kappa = 0$ and $\beta = 0.03$.

Pyatnitskiy, 1974), i.e., transition from system (22) with nonlinearity $\varphi(\sigma) = \operatorname{sign}\sigma$ to the system (22) with smooth nonlinearity $\varphi(\sigma) = \tanh(\frac{\sigma}{N})$, where N is a sufficiently small number. This approximation is organized using the numerical continuation method while changing the nonlinearity of system (22) as follows:

$$\varphi(\sigma) = \operatorname{sign}(\sigma) + \varepsilon\left(\tanh(\sigma/N) - \operatorname{sign}(\sigma)\right),$$

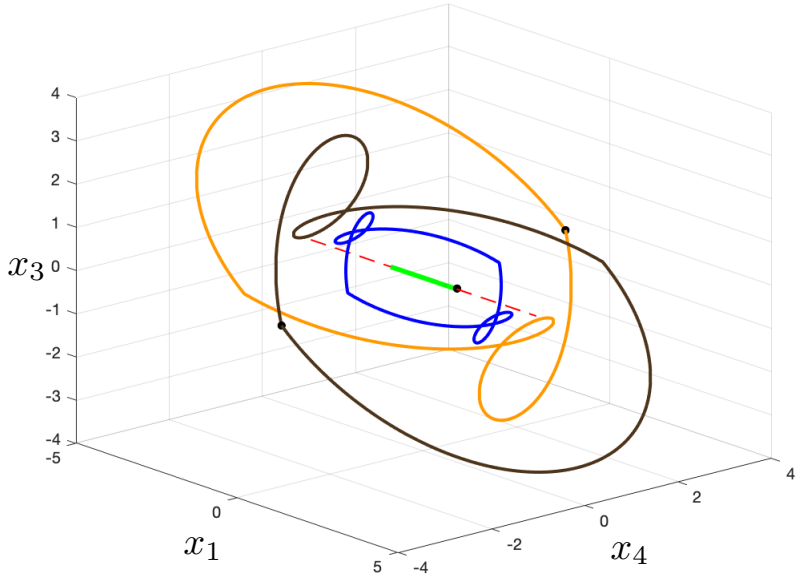

FIGURE 8 Three coexisting limit cycles in the Keldysh system with $\lambda = 0, \Phi = 1, \kappa = 0$ and $\beta = 0.03$: one is a self-symmetric self-excited and two are hidden with the respect to rest segment.

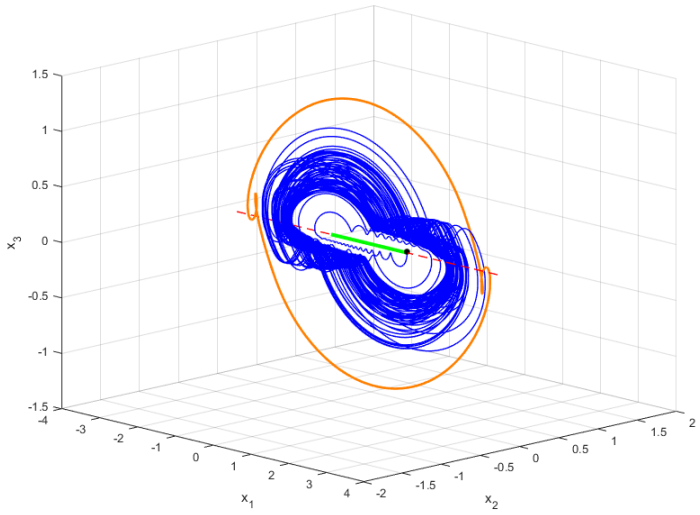

FIGURE 9 Coexisting chaotic and periodic solutions of the Keldysh system with $\lambda = 0, \Phi = 1, \kappa = 0$ and $\beta = 0.1$ (subspace (x_1, x_2, x_3)).

for ε increasing from 0 to 1 with the step 0.1 and $N = 0.05$. During this transition chaotic and periodic oscillations preserved (see **PI**). These oscillations coexist with unique locally stable equilibrium state and, therefore, they are hidden. This configuration represents the first counterexample to the Kalman conjecture with chaotic dynamics (see **PIII**). Note that this chaotic dynamics could not be found neither using the classical harmonic balance method or its extensions on relay systems, nor using point-mapping method.

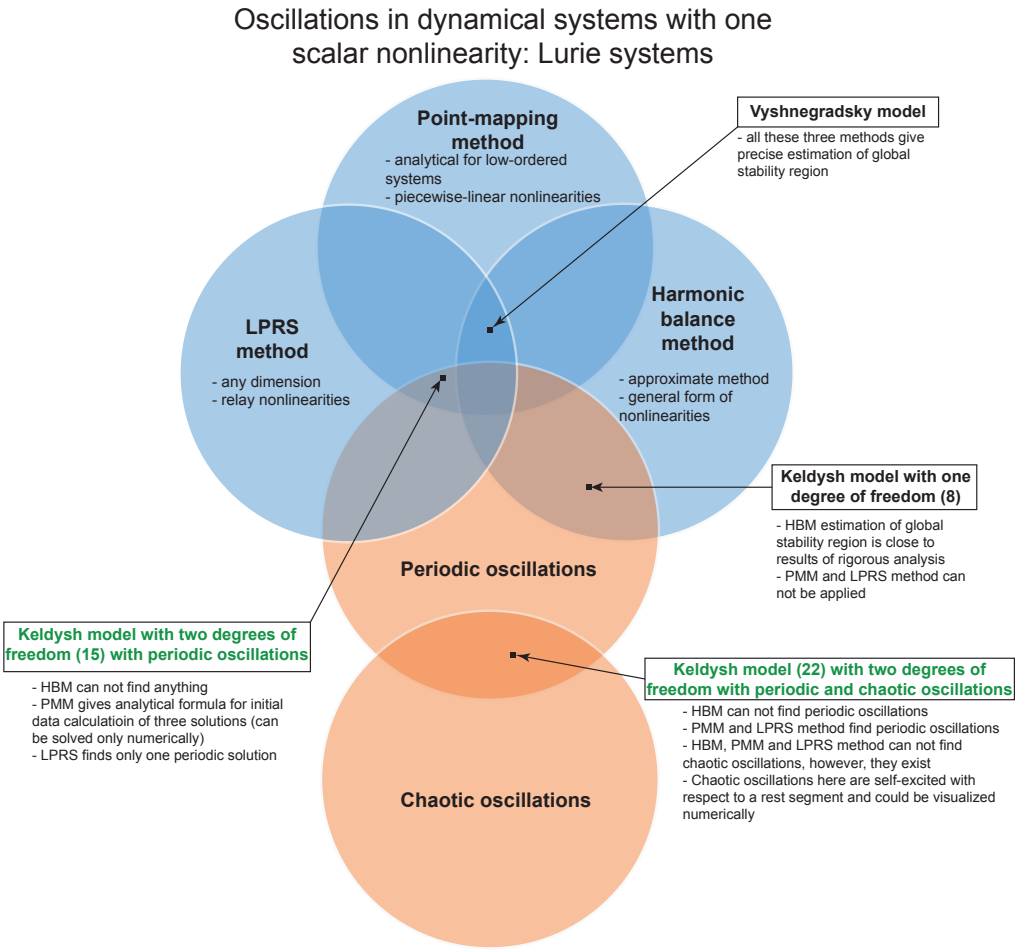

FIGURE 10 Schematic explanation of results on analysis of oscillations and the loss of global stability in Lurie systems.

2.1.6 Conclusion

In this section (see Fig. 10), on the example of Keldysh's models we revealed advantages and limitations of the classical harmonic balance method and the LPRS method of oscillations analysis. Difficulties of analysis of oscillations in Lurie systems with one scalar nonlinearity are connected with the problems of localization of hidden oscillations and possible birth of chaotic regimes. For analytical and numerical analysis of chaotic behavior it is necessary to develop special methods. Some of these methods are presented and discussed in the next section.

2.2 Oscillations in dynamical systems with multiple scalar nonlinearities: Lorenz-like systems

In this section, following papers **PVI-PVIII**, the difficulties in studying the scenarios of the loss of stability and transition to chaos are discussed.

2.2.1 Global stability and chaotic oscillations

In 1963 famous meteorologist E. Lorenz for the first time demonstrated (Lorenz, 1963) that conditions of the loss of stability could be related not only with the emergence of periodic oscillations, but also with the appearance of chaotic oscillations.

A chaotic behavior was discovered in the following Lorenz system[4] with two scalar quadratic nonlinearities:

$$\begin{cases} \dot{x} = -\sigma(x-y), \\ \dot{y} = rx - dy - xz, \\ \dot{z} = -bz + xy, \end{cases} \tag{24}$$

which describes a convection of fluid in a two-dimensional layer. Here $d = 1$, $\sigma > 0$ is a Prandtl number, $r > 0$ is a Rayleigh number, $b > 0$ is a parameter that determines the ratio of the vertical and horizontal dimensions of the convection cell. For $r < 1$ system (24) has only one globally stable equilibrium $S_0 = (0,\, 0,\, 0)$, and for $r > 1$ the equilibrium S_0 turns into a saddle, while two new symmetric equilibria appear:

$$S_{\pm} = \big(\pm\sqrt{b(r-1)}, \pm\sqrt{b(r-1)}, r-1\big), \tag{25}$$

which stability depends on the values of parameters. Remark that system (24) is also encountered in other mechanical and physical problems, for example, in the problem of fluid convection in a closed annular tube (Rubenfeld and Siegmann, 1977), for describing the mechanical model of a chaotic water wheel (Tel and Gruiz, 2006), the model of a dissipative oscillator with an inertial nonlinearity (Neimark and Landa, 1992), and the dynamics of a single-mode laser (Oraevsky, 1981).

Since the form of system (24) and the chaotic nature of possible oscillations do not allow to apply classical methods, which were considered in Chapter 1, the

[4] The Lorenz model is a subject of research for more than 50 years and still is actively studied. See e.g. recent papers in *Nature* (Stewart, 2000), and *Science* (Voosen, 2019). One of the challenging problems is to verify the existence of hidden attractors in the Lorenz-like models (Mokaev, 2016; Chen et al., 2017; Yuan et al., 2017; Sprott and Munmuangsaen, 2018; Kuznetsov et al., 2018b; Kuznetsov and Mokaev, 2019). This problem arise, in particular, since in numerical computation of a trajectory over a finite-time interval it is difficult to distinguish a *sustained chaos* from a *transient chaos* (a transient chaotic set in the phase space, which can persist for a long time).

challenge for researchers is to develop necessary and sufficient stability criteria and study all possible scenarios of the loss of stability and transition to chaos. Another challenging task in the study of the loss of global stability is to search and visualize appearing oscillations in the phase space of dynamical system (which in the general case can have a large dimension). The search for persistent oscillations could be simplified if for a system it is possible to prove the *dissipativeness in the sense of Levinson* (see e.g. (Leonov et al., 2015)) – a property, which ensures the existence of a global bounded absorbing set containing a global attractor. It is known that the Lorenz system (24) has this property and its absorbing set is defined as follows:

$$\mathcal{B} = \left\{(x, y, z) \in \mathbb{R}^3 \mid \tfrac{1}{2}(x^2 + y^2 + (z - r - \sigma)^2) \leq \tfrac{b^2(\sigma+r)^2}{2(b-1)}\right\}. \tag{26}$$

For three-dimensional systems[5] it is possible to use the following special analytical method (Smith, 1986; Leonov, 1991; Kuznetsov et al., 2016; Kuznetsov, 2016) to obtain analytical conditions for the global stability, when all their trajectories tend to equilibria. Rewrite system (24) in the general form

$$\dot{u} = f(u),\ f:\ U \subseteq \mathbb{R}^3 \to \mathbb{R}^3, \tag{27}$$

and consider its linearization

$$\dot{q} = J(u(t, u_0))q \tag{28}$$

along the solution $u(t, u_0)$ existing for $t \in [0, \infty)$ with $u(0, u_0) = u_0 \in U$. Here f is continuously differentiable vector-function, $J(u_0) = Df(u_0)$ is the 3×3 Jacobian matrix, $\det J(u_0) \neq 0$, $\forall u_0 \in U$.

To check the global stability of system (27), it is sufficient to choose a specific nonsingular 3×3 matrix S and differentiable scalar function $V:\ U \subseteq \mathbb{R}^3 \to \mathbb{R}^1$, and to verify the following condition:

$$\lambda_1(u_0, S) + \lambda_2(u_0, S) + \dot{V}(u_0) < 0, \tag{29}$$

where $\lambda_1(u_0, S)$, $\lambda_2(u_0, S)$ are eigenvalues of the matrix $\frac{1}{2}\left(SJS^{-1} + (SJS^{-1})^*\right)$, and derivative of the function V is taken with respect to system (27).

For the Lorenz system (24), this technique gives the following result (see, e.g. (Leonov, 2012)): if the inequality

$$r \leq \frac{(\sigma + b)(b + 1)}{\sigma} \tag{30}$$

holds, then any solution tends to an equilibrium as $t \to +\infty$.

[5] The development of similar methods in the general case for high-dimensional systems is still an open problem.

2.2.2 Scenario of transition to chaos via a homoclinic bifurcation

Condition (30), for the fixed values $\sigma = 10$, $b = 8/3$ and r varying, completes the classical scenario of transition to chaos in the Lorenz system (Sparrow, 1982), which contains the so-called homoclinic bifurcation (Afraimovich et al., 2014) and connected with the appearance of a homoclinic orbit in the phase space. As r increases, the phase space of the Lorenz system is a subject to the following sequence of bifurcations. For $0 < r < 1$, there is a globally asymptotically stable zero equilibrium S_0. For $r > 1$, equilibrium S_0 is a saddle, and a pair of symmetric equilibria $S_\pm$ appears, but if $r \leq r_{gs} \approx 4.64$ all solutions still tend to a stationary set. For $r_{gs} < r < r_h \approx 13.926$, the separatrices $\Gamma_\pm$ of equilibria S_0 are attracted to the equilibria $S_{1,2}$. For $r = r_h$, the separatrices $\Gamma_\pm$ form two homoclinic orbits of equilibria S_0 (homoclinic butterfly, see Fig. (11)). For $r_h < r < r_c \approx 24.06$, the separatrices $\Gamma_\pm$ tend to $S_\mp$, respectively. For $r_c < r$, there is a case of multistability: the separatrices $\Gamma_\pm$ are attracted to the attractor, which is self-excited with respect to one equilibrium S_0, and this attractor co-exists with the stable equilibria $S_\pm$ (see Fig. (12)). For $r > r_a \approx 24.74$, the equilibria $S_\pm$ become unstable. Finally, $r = 28$ corresponds to the classical self-excited Lorenz attractor with respect to all equilibria S_0, $S_\pm$ (see Fig. (13)).

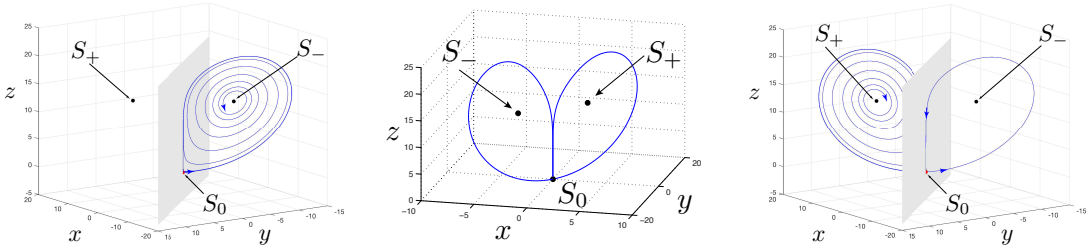

(a) Before homoclinic bifurcation

(b) Homoclinic orbit

(c) After homoclinic bifurcation

FIGURE 11 Numerical visualization of behavior in the phase space of the Lorenz system in the vicinity of homoclinic bifurcation at $r = r_h \approx 13.926$.

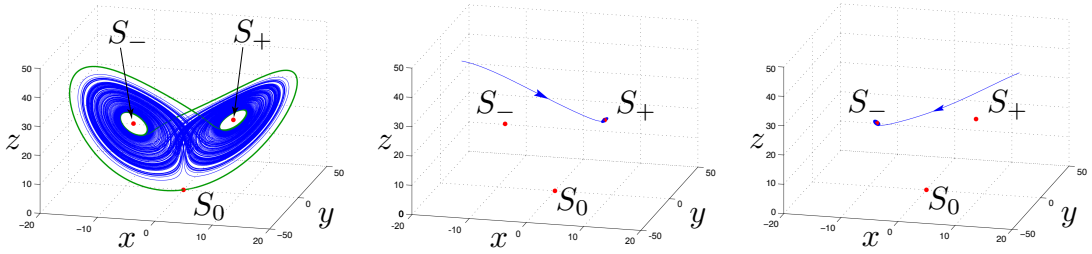

(a) Initial data near the equilibrium S_0

(b) Initial data near the equilibrium S_+

(c) Initial data near the equilibrium S_-

FIGURE 12 Numerical visualization of the self-excited chaotic attractor in the Lorenz system by the trajectories that start in small neighborhoods of the unstable equilibrium S_0. This attractor co-exists with stable equilibria $S_\pm$ (trivial attractors).

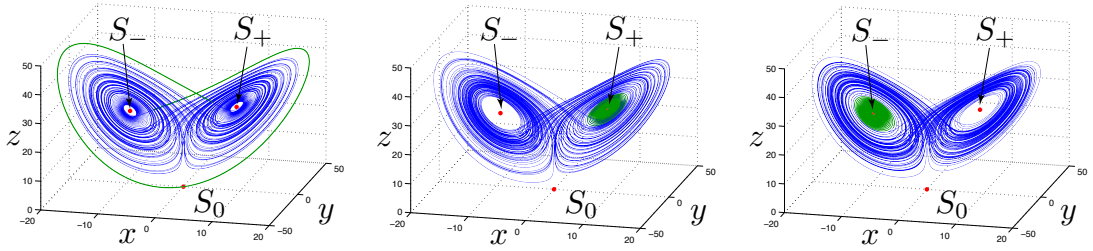

(a) Initial data near the equilibrium S_0

(b) Initial data near the equilibrium S_+

(c) Initial data near the equilibrium S_-

FIGURE 13 Numerical visualization of the classical self-excited chaotic attractor in the Lorenz system by integrating the trajectories with initial data from small neighborhoods of the unstable equilibria $S_{0,\pm}$. Here the separation of the trajectory into transition process and approximation of attractor is rough.

2.2.3 Studying of homoclinic orbits: analytical method

Let us describe a general method for proving the existence of homoclinic trajectories for systems (27) called the *Fishing principle* (Leonov, 2012, 2013, 2014a; Leonov et al., 2015; PVII). Consider an autonomous system of differential equations

$$\dot{\mathrm{x}} = f(\mathrm{x}, q), \quad t \in \mathbb{R}, \quad \mathrm{x} \in \mathbb{R}^n. \tag{31}$$

Here $f(\mathrm{x}, q)$ is a smooth vector-function, $\mathbb{R}^n = \{\mathrm{x}\}$ is a phase space of system (31). Let $\gamma(s), s \in [0,1]$ be a smooth path in the space of the parameter $\{q\} = \mathbb{R}^m$. Consider the following Tricomi problem (Tricomi, 1933; Leonov, 2014b) for system (31) and the path $\gamma(s)$: *is there a point* $q_0 \in \gamma(s)$ *for which system* (31) *with* q_0 *has a homoclinic orbit?*

Consider system (31) with $q = \gamma(s)$ and introduce the following notions. Let $\mathrm{x}(t,s)^+$ be an outgoing separatrix of the saddle point x_0 (i.e. $\lim\limits_{t\to-\infty} \mathrm{x}(t,s)^+ = \mathrm{x}_0$) with a one-dimensional unstable manifold. Define by $\mathrm{x}_\Omega(s)^+$ the point of the first crossing of separatrix $\mathrm{x}(t,s)^+$ with the closed set Ω:

$$\mathrm{x}(t,s)^+ \notin \Omega, \quad t \in (-\infty, T),$$

$$\mathrm{x}(T,s)^+ = \mathrm{x}_\Omega(s)^+ \in \Omega.$$

If there is no such crossing, we assume that $\mathrm{x}_\Omega(s)^+ = \varnothing$ (the empty set).

Theorem 1 ((Leonov, 2012, 2013, 2014a; Leonov et al., 2015; PVII)). *Suppose that for the path* $\gamma(s)$ *there is an* $(n-1)$*-dimensional bounded manifold* Ω *with a piecewise-smooth edge* $\partial\Omega$ *that possesses the following properties:*

(i) *for any* $\mathrm{x} \in \Omega \setminus \partial\Omega$ *and* $s \in [0,1]$*, the vector* $f(\mathrm{x}, \gamma(s))$ *is transversal to the manifold* $\Omega \setminus \partial\Omega$*;*

(ii) *for any* $s \in [0,1]$*,* $f(\mathrm{x}_0, \gamma(s)) = 0$*, the point* $\mathrm{x}_0 \in \partial\Omega$ *is a saddle;*

(iii) *for* $s = 0$ *the inclusion* $\mathrm{x}_\Omega(0)^+ \in \Omega \setminus \partial\Omega$ *is valid;*

(iv) *for* $s = 1$ *the relation* $\mathrm{x}_\Omega(1)^+ = \varnothing$ *is valid (i.e.* $\mathrm{x}_\Omega(1)^+$ *is an empty set);*

(v) *for any* $s \in [0,1]$ *and* $\mathrm{y} \in \partial\Omega \setminus \mathrm{x}_0$ *there exists a neighborhood* $U(\mathrm{y}, \delta) = \{\mathrm{x} \in \mathbb{R}^n \mid |\mathrm{x} - \mathrm{y}| < \delta\}$ *such that* $\mathrm{x}_\Omega(s)^+ \notin U(\mathrm{y}, \delta)$.

If conditions (i)–(v) are satisfied, then there exists $s_0 \in [0,1]$ *such that* $\mathrm{x}(t,s_0)^+$ *is a homoclinic orbit of the saddle point* x_0.

For system (24) with an arbitrary value of parameter d, by using this method it is possible to analytically prove the existence of a homoclinic orbit and make an attempt to study the various scenarios of homoclinic bifurcation numerically (see PII). Using the following smooth change of variables (see, e.g. (Leonov, 2016; Leonov et al., 2017)):

$$\eta := \sigma(y-x), \quad \xi := z - \tfrac{x^2}{b} \tag{32}$$

one can reduce system (24) to the form

$$\begin{cases} \dot{x} = \eta, \\ \dot{\eta} = -(\sigma+d)\eta + \sigma\xi x + \sigma(r-d)x - \frac{\sigma}{b}x^3, \\ \dot{\xi} = -b\xi - \frac{(2\sigma-b)}{b\sigma}x\eta. \end{cases} \tag{33}$$

Then, by changing

$$t := \sqrt{\sigma(r-d)}t, \quad x := \frac{x}{\sqrt{b(r-d)}}, \quad \vartheta := \frac{\eta}{\sqrt{b\sigma}(r-d)}, \quad u := \frac{\xi}{r-d}$$

system (33) can be reduced to the form

$$\begin{cases} \dot{x} = \vartheta, \\ \dot{\vartheta} = -\lambda\vartheta - xu + x - x^3, \\ \dot{u} = -\alpha u - \beta x\vartheta, \end{cases} \tag{34}$$

$$\lambda = \frac{(\sigma+d)}{\sqrt{\sigma(r-d)}}, \quad \alpha = \frac{b}{\sqrt{\sigma(r-d)}}, \quad \beta = \frac{2\sigma-b}{\sigma}.$$

After the transformation, new equilibria have the following form:

$$S_0 = (0,\,0,\,0), \quad S_\pm = (\pm 1,\,0,\,0). \tag{35}$$

For positive α, β, λ the equilibrium state S_0 is always a saddle, and $S_\pm$ are stable equilibria if $\beta < \frac{\lambda(\lambda\alpha+\alpha^2+2)}{(\lambda+\alpha)}$.

The application of the Fishing principle (see Theorem 1) allows us to formulate for system (34) the following result (see **PVII**):

Theorem 2. *Consider a smooth path* $\lambda(s)$, $\alpha(s)$, $\beta(s)$, $s \in [0,\,1)$ *in the parameter space of system* (34). *Let*

$$\begin{aligned} \lambda(0) = 0, \quad \lim_{s\to 1}\lambda(s) = +\infty, \\ \limsup_{s\to 1}\alpha(s) < +\infty, \quad \limsup_{s\to 1}\beta(s) < +\infty \end{aligned} \tag{36}$$

and the following condition holds

$$\alpha(s)\left(\sqrt{\lambda(s)^2+4}+\lambda(s)\right) > 2(\beta(s)-2), \ \ \forall s \in [0,1]. \tag{37}$$

Then there exists $s_0 \in (0,1)$ *such that system* (34) *with* $\alpha(s_0)$, $\beta(s_0)$, $\lambda(s_0)$ *has a homoclinic orbit.*

Corollary 1. *Of particular interest to this study is the following path*

$$\lambda(s) = \frac{s}{\sqrt{1-s}}, \quad \alpha(s) = \delta\sqrt{1-s}, \quad \beta(s) \equiv \beta \in (0,\, 2+\delta), \quad s \in [0,\, 1),\ \delta > 0. \tag{38}$$

This path satisfies all conditions of Theorem 2, and therefore there exists a number $s_0 \in (0,\, 1)$ *such that system* (34) *with parameters* (38) *and* $s = s_0$ *has a homoclinic orbit.*

The equilibrium S_0 is of saddle type and has stable and unstable local invariant manifolds $W^{\mathrm{s}}_{\mathrm{loc}}$ and $W^{\mathrm{u}}_{\mathrm{loc}}$ of dimension $\dim W^{\mathrm{s}}_{\mathrm{loc}} = 2$ and $\dim W^{\mathrm{u}}_{\mathrm{loc}} = 1$, respectively, intersecting at S_0. For S_0 the sign of the saddle value $\sigma_0 = (1-\delta)\sqrt{1-s}$, defined by the sum of real parts of the leading unstable and stable eigenvalues (Shilnikov et al., 2001), depends on the parameter δ.

2.2.4 Studying of homoclinic orbits: numerical method

To study numerically scenarios of homoclinic bifurcations with different signs of the saddle value σ_0 we consider the region of the parameters $\mathcal{B}_{\delta,\beta} = \{\ (\delta,\beta) \mid \delta \in (0,\, 1.1],\ \beta \in (0, 2+\delta)\}$ in the parameter plane (δ,β), which satisfies conditions (38), and for points filling the region $\mathcal{B}_{\delta,\beta}$ calculate the approximate interval $[\underline{s}\,,\bar{s}] \subset (0,1)$, such that within it there exist a homoclinic orbit. We select a grid of points $B_{\mathrm{grid}} \subset \mathcal{B}_{\delta,\beta}$ with the predefined partitioning steps $\delta_{\mathrm{grid}} = \beta_{\mathrm{grid}} = 0.01$ and for each point $(\delta_{\mathrm{curr}}, \beta_{\mathrm{curr}}) \in B_{\mathrm{grid}}$ we choose the partition $0 < s^0_{\mathrm{step}} < 2s^0_{\mathrm{step}} < \ldots, (N-1)s^0_{\mathrm{step}} < 1$ of the interval $(0,1)$ with step $s^0_{\mathrm{step}} = \frac{1}{N} = 0.001$. For the system (34) with parameters $\delta_{\mathrm{curr}}, \beta_{\mathrm{curr}}, \lambda(s_{\mathrm{curr}}), \alpha(s_{\mathrm{curr}})$ we integrate numerically the separatrix $(x_{\mathrm{sepa}}(t), \vartheta_{\mathrm{sepa}}(t), u_{\mathrm{sepa}}(t))$ of the saddle S_0 of system (34) on the chosen time interval $t \in [0, T_{\mathrm{trans}} = 4 \cdot 10^3]$ using the `ode45` solver in MATLAB. Using this numerical routine, we have shown that there are 4 subregions (see **PVII**) with different homoclinic bifurcations (Fig. 14) within the region covered by the given grid of points.

In region $\mathbb{I}$ before bifurcation separatrices $\Gamma^{\pm}(t)$ were attracted to the opposite equilibria $S_{\mp}$ and after bifurcation – to the nearest ones, i.e., to $S_{\pm}$. In this case, during the inverse bifurcation (i.e. while moving from $s = 1$ to $s = 0$), two unstable limit cycles are born from the homoclinic butterfly. This scenario corresponds to the case of the homoclinic bifurcation in classical Lorenz system (see, e.g., (Sparrow, 1982; Wiggins, 1988; Shilnikov et al., 2001)).

In region $\mathbb{III}$ during the bifurcation, one large stable "eight"-type limit collides with the saddle equilibrium S_0 and splits into two stable limit cycles around $S_{\pm}$. Numerical analysis of the separatrices behavior for all $\delta \in [1, 1.1]$, $\beta \in (0, 2+\delta)$ within the chosen partition and the dynamics analysis of the Poincaré map (see **PVII**) give us a reason to state that there is no chaotic dynamics in the vicinity of the homoclinic bifurcation in the case of zero and negative saddle values σ_0.

Also, two new scenarios of homoclinic bifurcation were found. In region $\mathbb{IIII}$, depending on values of parameters δ, β, two symmetric limit cycles $\Theta^{\pm}$ around $S_{\pm}$ coexist with either one stable "eight"-type limit cycle, or a strange attractor

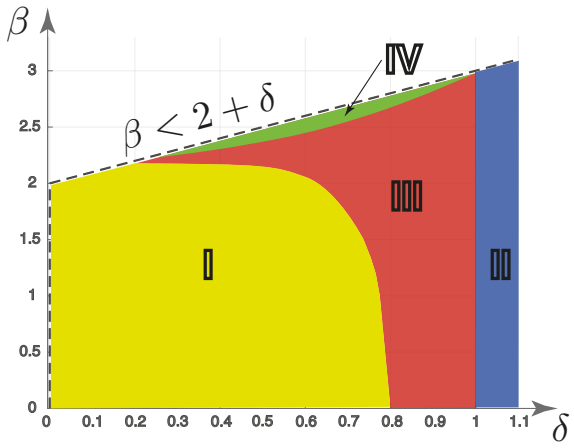

FIGURE 14 Different types of homoclinic bifurcations in the Lorenz-like system with parameters $(\delta, \beta) \in \mathcal{B}_{\delta,\beta}$, and $\lambda(s), \alpha(s), s \in (0,1)$.

which attract the separatrices $\Gamma^{\pm}(t)$. Then this attractor (periodic or strange) loses stability and separatrices $\Gamma^{\pm}(t)$ are attracted to the opposite limit cycles $\Theta^{\mp}$. After the bifurcation the separatrices $\Gamma^{\pm}(t)$ are attracted to the nearest limit cycles $\Theta^{\pm}$. As in the case of the Lorenz system, in this case during the inverse bifurcation, two unstable limit cycles are born from the homoclinic butterfly, but here they separate two stable cycles $\Theta^{\pm}$. For example, for parameter values $\delta = 0.9$, $\beta = 0.2$, the dynamics of separatrices in the phase space is shown in Fig. 15.

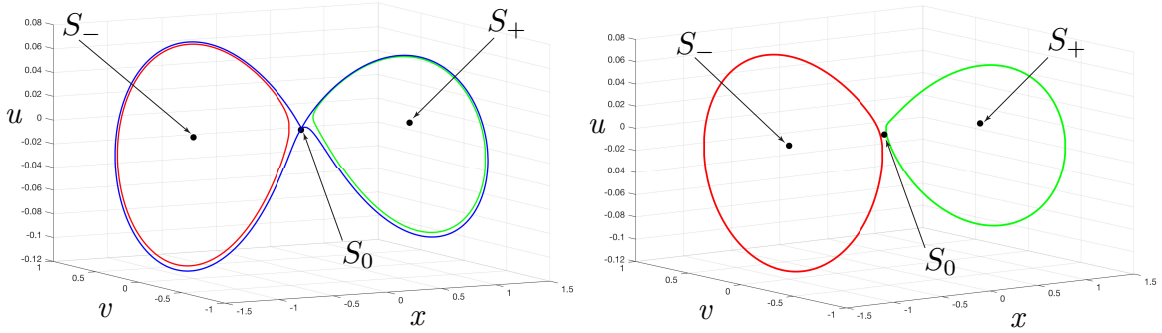

(a) $\underline{s} = 0.06013146057\ldots$ (b) $\bar{s} = 0.06013146058\ldots$

FIGURE 15 Scenario of homoclinic bifurcation the Lorenz-like system with $\delta = 0.9$, $\beta = 0.2$, and $\lambda(s)$, $\alpha(s)$, $s \in [\underline{s}, \bar{s}]$. Two symmetric limit cycles $\Theta^{\pm}$ exist around $S_{\pm}$ at $s = \underline{s}$ before the bifurcation (left subfigure) and at $s = \bar{s}$ after the bifurcation (right subfigure).

For parameter values $\delta = 0.5$, $\beta = 2.2$ the case of coexistence of two symmetric limit cycles $\Theta^{\pm}$ which are self-excited w.r.t $S_{\pm}$, respectively, with a strange attractor self-excited w.r.t S_0 and defined by its separatrix $\Gamma^{+}(t)$ is presented in Fig. 16.

In region $\mathbb{IV}$, when an unstable homoclinic orbit occurs, one strange attractor splits into two (or, if we track the change in the parameter s from 1 to 0, then we can say that two strange attractors merge into one strange attractor). For example, for parameter values $\delta = 0.9$, $\beta = 2.899$, the dynamics of separatrices in

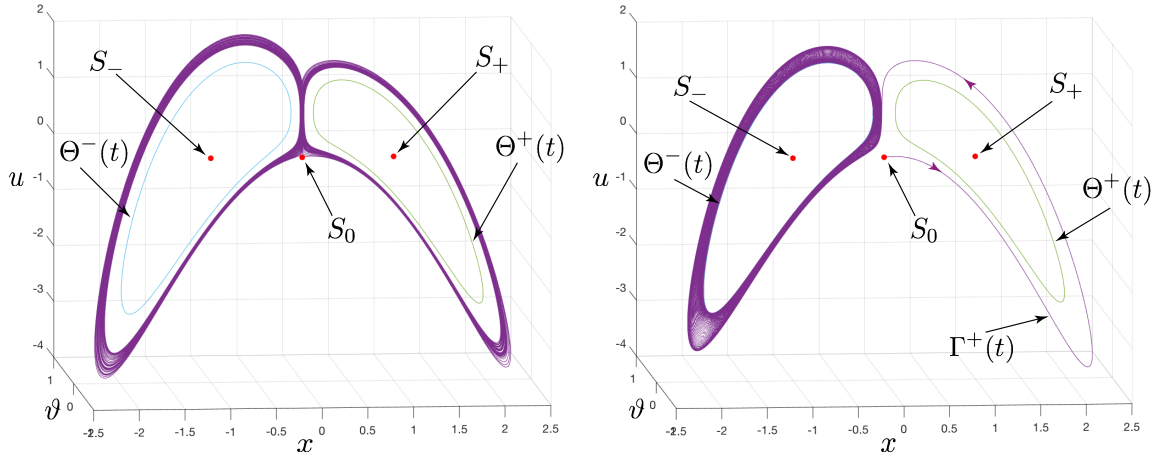

(a) $\underline{s}' = 0.797940743\ldots$ (b) $\underline{s} \in [0.797940744\ldots, 0.80592918053\ldots]$

FIGURE 16 In the Lorenz-like system with $\delta = 0.5$, $\beta = 2.2$, and $\lambda(s)$, $\alpha(s)$, before homoclinic bifurcation the strange attractor co-exists with two stable symmetric limit cycles $\Theta^{\pm}$ at $s = \underline{s}'$ (left subfigure); when it collapses, the separatrix $\Gamma^+(t)$ of the saddle S_0 tends to limit cycle Θ^- at $s = \underline{s}$ (right subfigure), and to limit cycle Θ^+ at $s = \bar{s} = 0.80592918054\ldots$ (after the bifurcation).

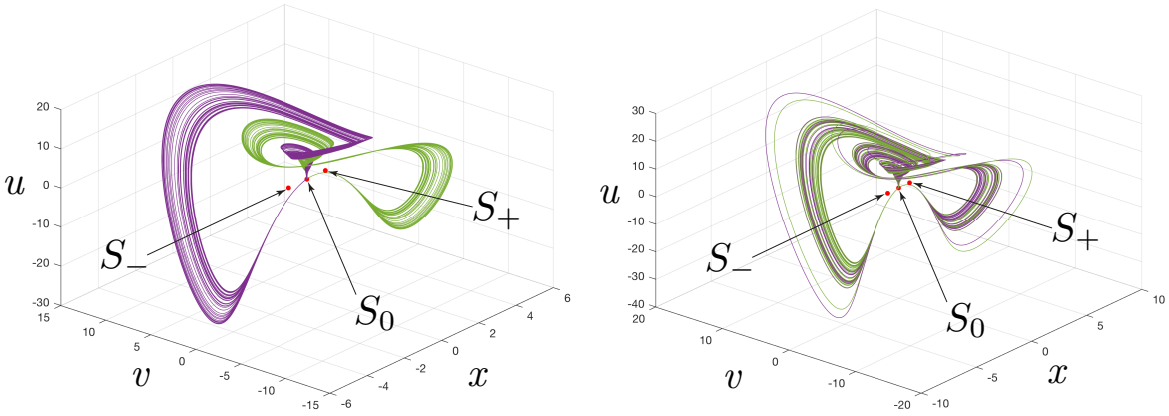

(a) $\bar{s} = 0.7957\ldots$ (b) $\underline{s} = 0.7955\ldots$

FIGURE 17 Scenario of homoclinic bifurcation the Lorenz-like system with $\delta = 0.9$, $\beta = 2.899$, and $\lambda(s)$, $\alpha(s)$, $s \in [\underline{s}, \bar{s}]$. Two separated symmetric strange attractors exist at $s = \bar{s}$ before the bifurcation (left subfigure) and merge at $s = \underline{s}$ after the bifurcation (right subfigure).

the phase space is shown in Fig. 17.

Further study and refinement of these results may require the application of the new numerical methods with a high-performance computing. Also, one could take into consideration recently developed new reliable numerical methods for studying trajectories of dynamical systems (see e.g. Tucker (1999); Liao and Wang (2014); Lozi and Pchelintsev (2015); Kehlet and Logg (2017)) and the existing general numerical tools for the analysis of homoclinic bifurcations (see e.g. Champneys et al. (1996); Doedel and et. al (2007); Homburg and Sandstede (2010)).

Stable periodic orbits that arise in the described scenarios of homoclinic bifurcation can be detected using the standard computational procedure, however, after the disappearance of the homoclinic orbit, unstable periodic orbits (UPOs) can arise in the phase space. Besides, for the case of the sustained chaos, UPOs could be embedded in a chaotic attractor (see e.g. (Afraımovic et al., 1977; Auerbach et al., 1987; Cvitanović, 1991)). One of the effective methods among others for the computation of UPOs is the *delay feedback control* (DFC) approach, suggested by K. Pyragas (Pyragas, 1992) (see also discussions in (Kuznetsov et al., 2015; Chen and Yu, 1999; Lehnert et al., 2011)). This approach allows one to stabilize and study UPOs in various chaotic dynamical systems. Nevertheless, some general analytical results have been obtained (Hooton and Amann, 2012b), showing that DFC has a certain limitation, called the odd number limitation (ONL), which is connected with an odd number of real Floquet multipliers larger than unity. In order to overcome ONL, later Pyragas suggested a modification of the classical DFC technique, which was called the unstable delayed feedback control (UDFC) (Pyragas, 2001).

Let $u^{\mathrm{upo}}(t)$ be an UPO with period $\tau > 0$, $u^{\mathrm{upo}}(t-\tau) = u^{\mathrm{upo}}(t)$, satisfying differential equation (27). To compute the UPO and overcome ONL, we add the UDFC in the following form:

$$\begin{aligned} \dot{u}(t) &= f(u(t)) + KB\left[F_N(t) + w(t)\right], \\ \dot{w}(t) &= \lambda_c^0 w(t) + (\lambda_c^0 - \lambda_c^\infty) F_N(t), \\ F_N(t) &= C^* u(t) - (1-R)\sum_{k=1}^{N} R^{k-1} C^* u(t-kT), \end{aligned} \tag{39}$$

where $0 \le R < 1$ is an extended DFC parameter, $N = 1, 2, \ldots, \infty$ defines the number of previous states involved in delayed feedback function $F_N(t)$, $\lambda_c^0 > 0$, and $\lambda_c^\infty < 0$ are additional unstable degree of freedom parameters, B, C are vectors and $K > 0$ is a feedback gain. For initial condition $u_0^{\mathrm{upo}_1}$ and $T = \tau$ we have

$$F_N(t) \equiv 0,\ w(t) \equiv 0,$$

and, thus, the solution of system (39) coincides with the periodic solution of initial system (27).

For the Lorenz system (24) with parameters $r = 28$, $\sigma = 10$, $b = 8/3$ using (39) with $B^* = (0,1,0)$, $C^* = (0,1,0)$, $R = 0.7$, $N = 100$, $K = 3.5$, $\lambda_c^0 = 0.1$, $\lambda_c^\infty = -2$, one can stabilize (see, e.g., **PVIII**) a period-1 UPO $u^{\mathrm{upo}_1}(t, u_0)$ with period $\tau_1 = 1.5586\ldots$ from the initial point $u_0 = (1,1,1)$, $w_0 = 0$ (see Fig. 18).

Results of this experiment could be verified using various other numerical approaches (see e.g. (Viswanath, 2001; Budanov, 2018; Pchelintsev et al., 2019)), and are in agreement with similar results on the existence of UPOs embedded in the Lorenz attractor (Galias and Tucker, 2008; Barrio et al., 2015). However, the Pyragas procedure, in general, is more convenient for UPOs numerical visualization.

For the initial point $u_0^{\mathrm{upo}_1} \approx (-6.2262, -11.0027, 13.0515)$ on the UPO $u^{\mathrm{upo}_1}(t) = u(t, u_0^{\mathrm{upo}_1})$ the trajectory of system (39) without the stabilization (i.e. with

$K = 0$) on the time interval $[0, T = 100]$ is computed (see Fig. 18b). Denote it by $\tilde{u}(t, u_0^{\text{upo}_1})$ to distinguish this pseudo-trajectory from the periodic orbit $u(t, u_0^{\text{upo}_1})$. One can see that on the initial small time interval $[0, T_1 \approx 11]$, even without the control, the obtained trajectory $\tilde{u}(t, u_0^{\text{upo}_1})$ traces approximately the "true" periodic orbit $u(t, u_0^{\text{upo}_1})$. But for $t > T_1$, without a control, the trajectory $\tilde{u}(t, u_0^{\text{upo}_1})$ diverge from $u^{\text{upo}_1}(t, u_0^{\text{upo}_1})$ and visualize a local chaotic attractor.

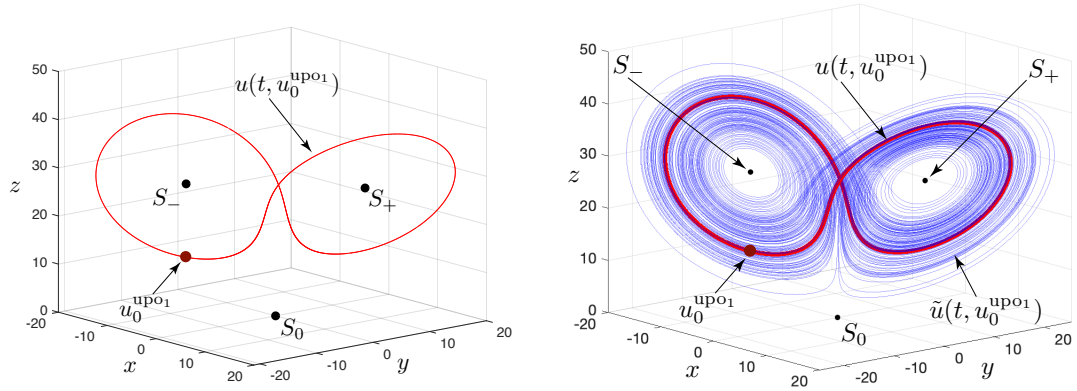

(a) UPO ($K = 3.5$)

(b) Pseudo-trajectory ($K = 0$) and UPO

FIGURE 18 Period-1 UPO $u^{\text{upo}_1}(t)$ (period $\tau_1 = 1.5586\ldots$) stabilized using UDFC method, and pseudo-trajectory $\tilde{u}(t, u_0^{\text{upo}_1})$ ($t \in [0, 100]$) in the system Lorenz with parameters $r = 28$, $\sigma = 10$, $b = 8/3$.

2.2.5 Conclusion

In this section (see Fig. 19), on the example of the classical Lorenz and various Lorenz-like systems, difficulties in analysis of oscillations of dynamical systems with multiple scalar nonlinearities, related to the onset of chaos, are revealed. Analytical and numerical analysis of homoclinic orbits, which are connected with the loss of stability bifurcation and appearance of chaotic oscillations, are performed. Also, an efficient procedure for visualization of unstable periodic orbits embedded in chaotic attractors of the Lorenz system is implemented.

Remark that the obtained results are connected with the problem of calculation of various dimension characteristics (e.g. Lyapunov dimension and topological entropy (Kuznetsov, 2016; Kuznetsov et al., 2018b, 2019b)), and the problem of distinguishing a sustained chaos from a transient chaos in numerical computations of trajectories over finite-time intervals (Chen et al., 2017; Yuan et al., 2017; Sprott and Munmuangsaen, 2018; Kuznetsov et al., 2018b; Kuznetsov and Mokaev, 2019).

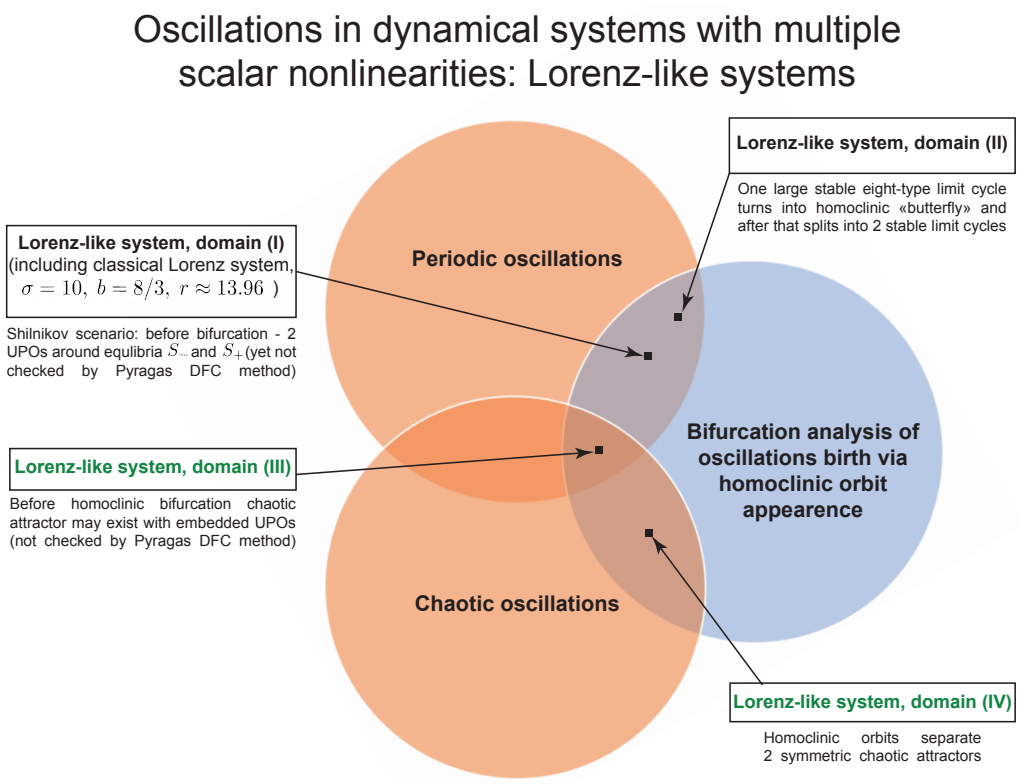

FIGURE 19 Schematic explanation of results on analysis of oscillations and the loss of global stability in the Lorenz-like systems.

3 CONCLUSION

In this thesis effective analytical-numerical methods studying regular and chaotic oscillations in dynamical systems were presented and discussed. For systems with one scalar nonlinearity, the comparative analysis of the classical harmonic balance and the point-mapping methods has been carried out. To study the loss of stability and birth of oscillations in relay systems, the LPRS method, an extension of the classical harmonic balance method specifically tailored for relay systems, was applied. To demonstrate its advantages over the classical harmonic balance method, the Keldysh models of flutter suppression in aircraft control systems were considered. Constraints of existing methods for oscillations analysis, defined by difficulties in localization of hidden oscillations and possible emergence of chaotic regimes, have been described through the study of Keldysh models. Further studies may be undertaken to improve the existing methods with a view to overcoming the outlined difficulties.

Also, the challenges associated with the analysis of the loss of stability and transition to chaos in the systems with multiple scalar nonlinearities have been described. For the class of Lorenz-like systems the existence of a homoclinic orbit tending to a saddle equilibrium was analytically proved and various scenarios of the loss of stability via a homoclinic bifurcation were numerically analyzed. To visualize an unstable periodic orbit which may appear during homoclinic bifurcations and which is embedded in the chaotic attractor, Pyragas time-delayed feedback control algorithm was implemented. Further development of the suggested analytical and numerical methods and their generalization for the case of a homoclinic orbit tending to a saddle-focus equilibrium remain open problems.

YHTEENVETO (SUMMARY IN FINNISH)

Työssä käsitellään menetelmiä dynaamisten järjestelmien stabiiliuden sekä mahdollisten värähtelyjen kaoottisuuden selvittämiseen. Tehokkaimmat menetelmät yhdistävät matemaattista analyysiä ja numeerisia menetelmiä.

Järjestelmille, joissa on yksi epälineaarinen komponentti, tunnetaan useita analyyttisiä menetelmiä. Tässä työssä vertaillaan klassista pistemenetelmää ja harmonisen tasapainon menetelmää sekä pistemenetelmän laajennusta, LPRS-menetelmää (Locus of Perturbed Relay System), joka on kehitetty epäjatkuville niin sanotuille relesysteemeille. Menetelmillä tutkitaan systeemien stabiilisuutta sekä värähtelyjen syntymekanismeja.

Testiesimerkkeinä on käytetty Keldyshin systeemejä, jotka mallintavat lentokoneiden värähtelynhallintamekanismeja. Tutkimus osoitti, että kaikilla menetelmillä oli omia rajoitteitaan värähtelyjen analysoinnissa ja kaoottisten värähtelyjen synnyn ennustamisessa. Tältä osin voidaan tunnistaa useita tarpeita lisätutkimukselle menetelmien edelleen kehittämiseksi.

Myös monimutkaisempien, useita epälineaarisia komponentteja sisältävien, systeemien stabiiliuden ja värähtelyjen syntymekanismien analyysin haasteita kartoitettiin. Yleinen stabiiliusanalyysi on tunnettu avoin ongelma. Tässä työssä tunnistettiin luokka niin sanottuja Lorenz-tyyppisiä systeemejä, joille voitiin analyyttisesti määritellä ehdot, joiden toteutuessa systeemiin syntyy omaehtoinen, homoklininen värähtely. Systeemin numeerinen tarkastelu värähtelyn syntypisteen ympäristössä paljasti lisäksi muita, kaoottisia värähtelymoodeja. Näiden visualisoimiseksi ja analysoimiseksi toteutettiin Pyragasin viiveyhtälökontrolliin pohjautuva menetelmä, jonka avulla voitiin tunnistaa kaoottisen värähtelyn alta epäsäännöllisiä periodisia värähtelymoodeja. Kehitettyjen menetelmien yleistäminen muille systeemityypeille on kiinnostava jatkotutkimuskohde.

REFERENCES

Afraimovich, V., Gonchenko, S.V., L. L., Shilnikov, A. & Turaev, D. 2014. Scientific heritage of LP Shilnikov. Regular and Chaotic Dynamics 19 (4), 435–460.

Afraımovic, V., Bykov, V. & Silnikov, L. 1977. On the origin and structure of the Lorenz attractor. 234 (2), 336–339.

Aizerman, M. & Pyatnitskiy, E. 1974. Foundations of a theory of discontinuous systems: I. Autom.Remote Control 35, 1066-1079.

Aizerman, M. 1949. On a problem regarding stability "in the large" of dynamical systems. Uspekhi Matemat. Nauk 4 (4), 187–188. (in Russian).

Andronov, A. & Maier, A. 1944. The Mizes problem in the theory of direct control and the theory of point transformations of surfaces. Dokl. Akad. Nauk SSSR 43 (2), 58–60. (in Russian).

Andronov, A., Vitt, E. & Khaikin, S. 1937. Theory of Oscillators (in Russian). ONTI NKTP SSSR. [English transl.: Princeton University Press, 1949].

Auerbach, D., Cvitanović, P., Eckmann, J.-P., Gunaratne, G. & Procaccia, I. 1987. Exploring chaotic motion through periodic orbits. Physical Review Letters 58 (23), 2387.

Barabanov, N. 1988. On the Kalman problem. Sib. Math. J. 29 (3), 333-341.

Barrio, R., Dena, A. & Tucker, W. 2015. A database of rigorous and high-precision periodic orbits of the Lorenz model. Computer Physics Communications 194, 76–83.

Bissell, C. 1998. A.A. Andronov and the development of Soviet control engineering. IEEE Control Systems Magazine 18, 56-62.

Boiko, I. 2005. Oscillations and transfer properties of relay servo systems - the locus of a perturbed relay system approach. Automatica 41, 677-683.

Boiko, I. 2008. Discontinuous Control Systems: Frequency-Domain Analysis and Design. Springer London, Limited.

Budanov, V. 2018. Undefined frequencies method. Fundam. Prikl. Mat. 22, 59-71. (in Russian).

Champneys, A., Kuznetsov, Y. & Sandstede, B. 1996. A numerical toolbox for homoclinic bifurcation analysis. International Journal of Bifurcation and Chaos 6, 867–888.

Chen, G., Kuznetsov, N., Leonov, G. & Mokaev, T. 2017. Hidden attractors on one path: Glukhovsky-Dolzhansky, Lorenz, and Rabinovich systems. International Journal of Bifurcation and Chaos in Applied Sciences and Engineering 27 (8). (art. num. 1750115).

Chen, G. & Yu, X. 1999. On time-delayed feedback control of chaotic systems. IEEE Transactions on Circuits and Systems I: Fundamental Theory and Applications 46 (6), 767–772.

Cvitanović, P. 1991. Periodic orbits as the skeleton of classical and quantum chaos. Physica D: Nonlinear Phenomena 51 (1-3), 138–151.

Doedel, E. & et. al 2007. AUTO-07P: Continuation and bifurcation software for ordinary differential equations. ⟨URL:http://www.dam.brown.edu/people/sandsted/auto/auto07p.pdf⟩.

Filippov, A. 1960. Differential equations with discontinuous right-hand side. Mat. Sb. (N.S.) 51 (1), 99-128. (in Russian).

Galias, Z. & Tucker, W. 2008. Short periodic orbits for the Lorenz system. In 2008 International Conference on Signals and Electronic Systems. IEEE, 285–288.

Gelig, A., Leonov, G. & Yakubovich, V. 1978. Stability of Nonlinear Systems with Nonunique Equilibrium (in Russian). Nauka. [English transl: Stability of Stationary Sets in Control Systems with Discontinuous Nonlinearities, World Scientific, 2004].

Homburg, A. J. & Sandstede, B. 2010. Homoclinic and heteroclinic bifurcations in vector fields. Handbook of dynamical systems 3, 379–524.

Hooton, E. & Amann, A. 2012b. Analytical limitation for time-delayed feedback control in autonomous systems. Phys. Rev. Lett. 109, 154101.

Kalman, R. 1957. Physical and mathematical mechanisms of instability in nonlinear automatic control systems. Transactions of ASME 79 (3), 553-566.

Kehlet, B. & Logg, A. 2017. A posteriori error analysis of round-off errors in the numerical solution of ordinary differential equations. Numerical Algorithms 76 (1), 191-210.

Keldysh, M. 1944. On dampers with a nonlinear characteristic. Tr. TsAGI (in Russian) 557, 26-37.

Khalil, H. 2002. Nonlinear Systems. N.J: Prentice Hall.

Krylov, N. & Bogolyubov, N. 1937. Introduction to non-linear mechanics (in Russian). Kiev: AN USSR. [English transl.: Princeton Univ. Press, 1947].

Kuznetsov, N., Alexeeva, T. & Leonov, G. 2016. Invariance of Lyapunov exponents and Lyapunov dimension for regular and irregular linearizations. Nonlinear Dynamics 85 (1), 195-201. doi:10.1007/s11071-016-2678-4.

Kuznetsov, N., Kuznetsova, O., Koznov, D., Mokaev, R. & Andrievsky, B. 2018a. Counterexamples to the Kalman conjectures. IFAC-PapersOnLine 51 (33), 138-143.

Kuznetsov, N., Leonov, G., Mokaev, T., Prasad, A. & Shrimali, M. 2018b. Finite-time Lyapunov dimension and hidden attractor of the Rabinovich system. Nonlinear Dynamics 92 (2), 267-285. doi:10.1007/s11071-018-4054-z.

Kuznetsov, N., Leonov, G. & Shumafov, M. 2015. A short survey on Pyragas time-delay feedback stabilization and odd number limitation. IFAC-PapersOnLine 48 (11), 706-709. doi:10.1016/j.ifacol.2015.09.271.

Kuznetsov, N., Mokaev, T., Kudryashova, E., Kuznetsova, O. & Danca, M.-F. 2019b. On lower-bound estimates of the Lyapunov dimension and topological entropy for the Rossler systems. IFAC-PapersOnLine, 97-102. (15th IFAC Workshop on Time Delay Systems).

Kuznetsov, N. & Mokaev, T. 2019. Numerical analysis of dynamical systems: unstable periodic orbits, hidden transient chaotic sets, hidden attractors, and finite-time Lyapunov dimension. Journal of Physics: Conference Series 1205 (1). doi:10.1088/1742-6596/1205/1/012034. (art. num. 012034).

Kuznetsov, N. 2016. The Lyapunov dimension and its estimation via the Leonov method. Physics Letters A 380 (25-26), 2142-2149. doi:10.1016/j.physleta.2016.04.036.

Kuznetsov, N. 2018a. Plenary lecture “Theory of hidden oscillations”. In 5th IFAC Conference on Analysis and Control of Chaotic Systems.

Kuznetsov, N. 2018b. Plenary lecture “Theory of hidden oscillations”. In 11th Russian Multiconference on Control Problems.

Kuznetsov, N. 2019. Invited lecture “Theory of hidden oscillations and stability of control systems”. In XII All-Russian Congress on Fundamental Problems of Theoretical and Applied Mechanics (Ufa, Russia). (https://www.youtube.com/watch?v=843m-rI5nTM).

Kuznetsov, N. 2020. Theory of hidden oscillations and stability of control systems. Journal of Computer and Systems Sciences International 1. (in press).

Kuznetsov, N. V. 2016. Analytical-numerical methods for the study of hidden oscillations (Habilitation thesis, in Russian). Saint-Petersburg State University.

Léauté, M. 1885. Mémoire sur les oscillations à longue période dans les machines actionnées par des moteurs hydrauliques et sur les moyens de prévenir ces oscillations. Journal de l’école Polytechnique (in French) 55, 1-126.

Lehnert, J., Hövel, P., Flunkert, V., Guzenko, P., Fradkov, A. & Schöll, E. 2011. Adaptive tuning of feedback gain in time-delayed feedback control. Chaos: An Interdisciplinary Journal of Nonlinear Science 21 (4), 043111.

Leonov, G., Andrievskiy, B. & Mokaev, R. 2017. Asymptotic behavior of solutions of Lorenz-like systems: Analytical results and computer error structures. Vestnik St. Petersburg University. Mathematics 50 (1), 15–23.

Leonov, G., Kuznetsov, N. & Mokaev, T. 2015. Homoclinic orbits, and self-excited and hidden attractors in a Lorenz-like system describing convective fluid motion. The European Physical Journal Special Topics 224 (8), 1421-1458. doi:10.1140/epjst/e2015-02470-3.

Leonov, G. & Kuznetsov, N. 2013. Hidden attractors in dynamical systems. From hidden oscillations in Hilbert-Kolmogorov, Aizerman, and Kalman problems to hidden chaotic attractors in Chua circuits. International Journal of Bifurcation and Chaos in Applied Sciences and Engineering 23 (1). doi:10.1142/S0218127413300024. (art. no. 1330002).

Leonov, G. & Kuznetsov, N. 2018a. On flutter suppression in the Keldysh model. Doklady Physics 63 (9), 366-370.

Leonov, G. & Kuznetsov, N. 2018b. On the Keldysh problem of flutter suppression. AIP Conference Proceedings 1959 (1). doi:10.1063/1.5034578. (art. num. 020002).

Leonov, G. 1991. On estimations of Hausdorff dimension of attractors. Vestnik St. Petersburg University: Mathematics 24 (3), 38-41. [Transl. from Russian: Vestnik Leningradskogo Universiteta. Mathematika, 24(3), 1991, pp. 41-44].

Leonov, G. 2012. General existence conditions of homoclinic trajectories in dissipative systems. Lorenz, Shimizu-Morioka, Lu and Chen systems. Physics Letters A 376, 3045-3050.

Leonov, G. 2013. Shilnikov chaos in Lorenz-like systems. International Journal of Bifurcation and Chaos 23 (03). doi:10.1142/S0218127413500582. (art. num. 1350058).

Leonov, G. 2014a. Fishing principle for homoclinic and heteroclinic trajectories. Nonlinear Dynamics 78 (4), 2751-2758.

Leonov, G. 2014b. Rössler systems: estimates for the dimension of attractors and homoclinic orbits. Doklady Mathematics 89 (3), 369–371.

Leonov, G. 2016. Necessary and sufficient conditions of the existence of homoclinic trajectories and cascade of bifurcations in Lorenz-like systems: birth of strange attractor and 9 homoclinic bifurcations. Nonlinear Dynamics 84 (2), 1055–1062.

Leonov, G. A. 2012. Lyapunov functions in the attractors dimension theory. Journal of Applied Mathematics and Mechanics 76 (2), 129-141.

Liao, S. & Wang, P. 2014. On the mathematically reliable long-term simulation of chaotic solutions of Lorenz equation in the interval [0,10000]. Science China Physics, Mechanics and Astronomy 57 (2), 330–335.

Lorenz, E. 1963. Deterministic nonperiodic flow. J. Atmos. Sci. 20 (2), 130-141.

Lozi, R. & Pchelintsev, A. 2015. A new reliable numerical method for computing chaotic solutions of dynamical systems: the Chen attractor case. International Journal of Bifurcation and Chaos 25 (13), 1550187.

Lurie, A. & Postnikov, V. 1944. On the stability theory of control systems. Prikl. Mat. Mekh. 8 (3), 246–248. (in Russian).

Mokaev, T. 2016. PhD thesis "Localization and dimension estimation of attractors in the Glukhovsky-Dolzhansky system". Jyväskylä studies in computing 240.

Neimark, Y. I. & Landa, P. S. 1992. Stochastic and Chaotic Oscillations. Dordrecht, The Netherlands: Kluwer Academic Publishers.

Oraevsky, A. N. 1981. Masers, lasers, and strange attractors. Quantum Electronics 11 (1), 71–78.

Pchelintsev, A., Polunovskiy, A. & Yukhanova, I. 2019. The harmonic balance method for finding approximate periodic solutions of the Lorenz system. Tambov University Reports. Series: Natural and Technical Sciences 24, 187-203. (in Russian).

Piiroinen, P. T. & Kuznetsov, Y. A. 2008. An event-driven method to simulate Filippov systems with accurate computing of sliding motions. ACM Transactions on Mathematical Software (TOMS) 34 (3), 13.

Poincare, H. 1892, 1893, 1899. Les methodes nouvelles de la mecanique celeste. Vol. 1-3. Paris: Gauthiers-Villars. [English transl. edited by D. Goroff: American Institute of Physics, NY, 1993].

van der Pol, B. 1926. On relaxation-oscillations. Philosophical Magazine and Journal of Science 7 (2), 978-992.

Pyragas, K. 1992. Continuous control of chaos by selfcontrolling feedback. Phys. Lett. A. 170, 421-428.

Pyragas, K. 2001. Control of chaos via an unstable delayed feedback controller. Phys. Rev. Lett. 86, 2265-2268.

Rasvan, V. 2006a. Four Lectures On Stability. Control Engineering and Applied Informatics 8 (2), 13–20.

Rasvan, V. 2006b. Three lectures on dissipativeness. In Automation, Quality and Testing, Robotics, 2006 IEEE International Conference on, Vol. 1. IEEE, 167–177.

Rubenfeld, L. A. & Siegmann, W. L. 1977. Nonlinear dynamic theory for a double-diffusive convection model. SIAM Journal on Applied Mathematics 32 (4), 871–894.

Shilnikov, L. P., Shilnikov, A. L., Turaev, D. V. & Chua, L. 2001. Methods of Qualitative Theory in Nonlinear Dynamics: Part 2. World Scientific.

Smith, R. 1986. Some application of Hausdorff dimension inequalities for ordinary differential equation. Proc. Royal Society Edinburg 104A, 235-259.

Sparrow, C. 1982. The Lorenz Equations: Bifurcations, Chaos, and Strange Attractors. Springer New York. Applied Mathematical Sciences.

Sprott, J. & Munmuangsaen, B. 2018. Comment on "A hidden chaotic attractor in the classical Lorenz system". Chaos, Solitons & Fractals 113, 261-262.

Stewart, I. 2000. Mathematics: The Lorenz attractor exists. Nature 406 (6799), 948–949.

Tel, T. & Gruiz, M. 2006. Chaotic dynamics: An introduction based on classical mechanics. Cambridge University Press.

Tricomi, F. 1933. Integrazione di unequazione differenziale presentatasi in elettrotechnica. Annali della R. Shcuola Normale Superiore di Pisa 2 (2), 1-20.

Tsypkin, Y. 1984. Relay Control Systems. Cambridge: Univ Press.

Tucker, W. 1999. The Lorenz attractor exists. Comptes Rendus de l'Academie des Sciences - Series I - Mathematics 328 (12), 1197 - 1202.

Viswanath, D. 2001. The Lindstedt–Poincaré technique as an algorithm for computing periodic orbits. SIAM review 43 (3), 478–495.

Voosen, P. 2019. How far out can we forecast the weather? Scientists have a new answer. Science. doi:10.1126/science.aax0032.

Vyshnegradsky, I. 1877. On regulators of direct action. Izvestiya St. Petersburg Technological Inst. 1. (in Russian).

Wiggins, S. 1988. Global Bifurcations and Chaos. Analytical Methods. New York: Springer.

Yuan, Q., Yang, F.-Y. & Wang, L. 2017. A note on hidden transient chaos in the Lorenz system. International Journal of Nonlinear Sciences and Numerical Simulation 18 (5), 427-434.

Zhukovsky, N. 1909. Theory of regulation of the course of machines. Tipo-litgr. T-va I. N. Kushnerev and Co. (in Russian).

APPENDIX 1 MATLAB IMPLEMENTATIONS OF THE ANDRONOV POINT-MAPPING METHOD AND THE LPRS METHOD

APPENDIX 1.1 Implementation of the Andronov point-mapping method for the Keldysh system

LISTING 1.1 **symSolOde1.m** – function that defines the exact solution of system (12) in the subregion $\Sigma^+ = \{\sigma = c^* x > 0\}$.

```
function sol = symSolOde1(m1, m2, b)

syms X_1 X_2 X_3 X_4 real

C1 = - ( (b^2 + m2^2) * X_1 + 2 * b * X_2 + X_3 ...
                                - 1 / (m1^2 + b^2) ) / ...
                                                (m1^2 - m2^2);
C2 = ( (m1^2 + b^2) * X_1 + 2 * b * X_2 + X_3 ...
                                - 1 / (b^2 + m2^2) ) / ...
                                                (m1^2 - m2^2);
C3 = - ( b * (b^2 + m2^2) * X_1 + ...
                     (3*b^2 + m2^2) * X_2 + ...
                                3 * b * X_3 + X_4 - ...
                                  b / (m1^2 + b^2) ) / ...
                                   ( m1 * (m1^2 - m2^2) );
C4 = ( b * (m1^2 + b^2) * X_1 + ...
                     (m1^2 + 3*b^2) * X_2 + ...
                                3 * b * X_3 + X_4 - ...
                                  b / (b^2 + m2^2) ) / ...
                                   ( m2 * (m1^2 - m2^2) );
syms t positive

x1(t) = 1 / ( (m1^2 + b^2) * (b^2 + m2^2)) + ...
                 C1 * exp(-b*t) * cos(m1*t) + ...
                     C2 * exp(-b*t) * cos(m2*t) + ...
                         C3 * exp(-b*t) * sin(m1*t) + ...
                                 C4 * exp(-b*t) * sin(m2*t);
x2(t) = - exp(-b*t) * ...
                   ( (C1 * b - C3 * m1) * cos(m1*t) + ...
                     (C2 * b - C4 * m2) * cos(m2*t) + ...
                     (C1 * m1 + C3 * b) * sin(m1*t) + ...
                         (C2 * m2 + C4 * b) * sin(m2*t));
x3(t) = exp(-b*t) * ( ...
  (-(m1^2 - b^2) * C1 - 2 * m1 * b * C3) * cos(m1*t) + ...
```

```
35    ( (b^2 - m2^2) * C2 - 2 * b * m2 * C4) * cos(m2*t) + ...
36    ( 2 * m1 * b * C1 - (m1^2 - b^2) * C3) * sin(m1*t) + ...
37      ( 2 * b * m2 * C2 + (b^2 - m2^2) * C4) * sin(m2*t) );
38  x4(t) = exp(-b*t) * ( ...
39    ( (3 * m1^2 - b^2) * b * C1 - (m1^2 - 3 * b^2) * m1 * C3)
       * cos(m1*t) + (-(b^2 - 3 * m2^2) * b * C2 + (3 * b^2 -
      m2^2) * m2 * C4) * cos(m2*t) + ( (m1^2 - 3 * b^2) * m1 *
       C1 + (3 * m1^2 - b^2) * b * C3) * sin(m1*t) + (-(3 * b
      ^2 - m2^2) * m2 * C2 - (b^2 - 3 * m2^2) * b * C4) * sin(
      m2*t) );
40
41  sol = [x1(t); x2(t); x3(t); x4(t)];
42
43  end
```

LISTING 1.2 **symSolOde2.m** – function that defines the exact solution of system (12) in the subregion $\Sigma^- = \{\sigma = c^* x < 0\}$.

```
1   function sol = symSolOde2(m1, m2, b)
2
3   syms X_1 X_2 X_3 X_4 real
4
5   C1 = - ( (b^2 + m2^2) * X_1 + 2 * b * X_2 + X_3 + ...
6                                       1 / (m1^2 + b^2) ) / ...
7                                             (m1^2 - m2^2);
8   C2 = ( (m1^2 + b^2) * X_1 + 2 * b * X_2 + X_3 + ...
9                                       1 / (b^2 + m2^2) ) / ...
10                                            (m1^2 - m2^2);
11  C3 = - ( b * (b^2 + m2^2) * X_1 + ...
12          (3*b^2 + m2^2) * X_2 + ...
13                    3 * b * X_3 + X_4 + ...
14                                  b / (m1^2 + b^2) ) / ...
15                                    ( m1 * (m1^2 - m2^2) );
16  C4 = ( b * (m1^2 + b^2) * X_1 + ...
17          (m1^2 + 3*b^2) * X_2 + ...
18                    3 * b * X_3 + X_4 + ...
19                                  b / (b^2 + m2^2) ) / ...
20                                    ( m2 * (m1^2 - m2^2) );
21  syms t positive
22
23  x1(t) = - 1 / ( (m1^2 + b^2) * (b^2 + m2^2)) + ...
24              C1 * exp(-b*t) * cos(m1*t) + ...
25                  C2 * exp(-b*t) * cos(m2*t) + ...
26                      C3 * exp(-b*t) * sin(m1*t) + ...
27                              C4 * exp(-b*t) * sin(m2*t);
28  x2(t) = - exp(-b*t) * ...
```

```
    ( (C1 * b - C3 * m1) * cos(m1*t) + ...
            (C2 * b - C4 * m2) * cos(m2*t) + ...
                (C1 * m1 + C3 * b) * sin(m1*t) + ...
                    (C2 * m2 + C4 * b) * sin(m2*t));
x3(t) = exp(-b*t) * ( ...
  (-(m1^2 - b^2) * C1 - 2 * m1 * b * C3) * cos(m1*t) + ...
  ( (b^2 - m2^2) * C2 - 2 * b * m2 * C4) * cos(m2*t) + ...
  ( 2 * m1 * b * C1 - (m1^2 - b^2) * C3) * sin(m1*t) + ...
     ( 2 * b * m2 * C2 + (b^2 - m2^2) * C4) * sin(m2*t) );
x4(t) = exp(-b*t) * ( ...
  ( (3 * m1^2 - b^2) * b * C1 - (m1^2 - 3 * b^2) * m1 * C3)
    * cos(m1*t) + (-(b^2 - 3 * m2^2) * b * C2 + (3 * b^2 -
   m2^2) * m2 * C4) * cos(m2*t) + ( (m1^2 - 3 * b^2) * m1 *
    C1 + (3 * m1^2 - b^2) * b * C3) * sin(m1*t) + (-(3 * b
   ^2 - m2^2) * m2 * C2 - (b^2 - 3 * m2^2) * b * C4) * sin(
   m2*t) );

sol = [x1(t); x2(t); x3(t); x4(t)];

end
```

LISTING 1.3 **findRootsChebFun.m** – auxiliary routine to find function zeros using the Chebfun package.

```
function out = findRootsChebFun(symFunc, tInterval)
    fun = matlabFunction(symFunc);
    out = roots(chebfun(fun, tInterval));
end
```

LISTING 1.4 **determineNextSwitch.m** – function of finding the switching moment and the corresponding point on a trajectory.

```
function [tSwitch,xSwitch] = determineNextSwitch(odeNum,m1,
   m2,b,x0,tEnd,vpaPrecision)

    syms t positive
    syms X_1 X_2 X_3 X_4 real

    symSolOde = str2func(['symSolOde', int2str(odeNum)]);
    sol = symSolOde(m1, m2, b);

    sol_x1 = subs(sol(1), {X_1, X_2, X_3, X_4}, {x0(1), x0
   (2), x0(3), x0(4)});
    sol_x2 = subs(sol(2), {X_1, X_2, X_3, X_4}, {x0(1), x0
   (2), x0(3), x0(4)});
    sol_x3 = subs(sol(3), {X_1, X_2, X_3, X_4}, {x0(1), x0
```

```
    (2), x0(3), x0(4)});
12   sol_x4 = subs(sol(4), {X_1, X_2, X_3, X_4}, {x0(1), x0
    (2), x0(3), x0(4)});
13
14   % Define the moment of switching numerically:
15   tRoots = findRootsChebFun(sol_x3, [0, double(tEnd)]);
16   tRoots = tRoots(abs(tRoots) > 1e-12);
17
18   if ~isempty(tRoots)
19       digitsOld = digits;
20       digits(vpaPrecision);
21
22       % Specify the moment of switching using VPA:
23       tSwitch = vpasolve(sol_x3, t, tRoots(1));
24       if tSwitch < 0
25           return;
26       end
27
28       % Define the coordinate of switching using VPA:
29       xSwitch = formula(...
30           [vpa(subs(sol_x1, t, tSwitch), vpaPrecision);
31            vpa(subs(sol_x2, t, tSwitch), vpaPrecision);
32            vpa(subs(sol_x3, t, tSwitch), vpaPrecision);
33            vpa(subs(sol_x4, t, tSwitch), vpaPrecision)]);
34       digits(digitsOld);
35   else
36       tSwitch = tEnd; xSwitch = [];
37   end
38 end
```

LISTING 1.5 **integrateTrajectory.m** – function to simulate trajectories of the Keldysh system (12) with nonlinearity $\varphi(x) = \operatorname{sign}(x)$.

```
1  function traj = integrateTrajectory(m1,m2,beta,x0,tEnd,
     vpaPresision)
2
3  digitsOld = digits;
4  digits(vpaPrecision);
5
6  a1 = (2*(m1^2+beta^2))*beta+2*beta*(m2^2+beta^2);
7  a0 = (m1^2+beta^2)*(m2^2+beta^2);
8
9  syms t positive
10
11 traj = {}; tCurr = 0;
12
```

```
13 if x0(3) < 0
14     [tSwitch, xSwitch] = determineNextSwitch(1, m1, m2,
   beta, x0, tEnd-tCurr, vpaPresision);
15     traj = cat(1, traj, {1, x0, tSwitch});
16     x0 = xSwitch;
17 else
18     [tSwitch, xSwitch] = determineNextSwitch(2, m1, m2,
   beta, x0, tEnd-tCurr, vpaPresision);
19     traj = cat(1, traj, {2, x0, tSwitch});
20     x0 = xSwitch;
21 end
22 tCurr = tCurr + tSwitch;
23
24 while tCurr < tEnd
25     if x0(4) > 0
26         [tSwitch, xSwitch] = determineNextSwitch(2, m1, m2,
    beta, x0, tEnd-tCurr, vpaPresision);
27         traj = cat(1, traj, {2, x0, tSwitch});
28         x0 = xSwitch;
29     elseif x0(4) < 0
30         [tSwitch, xSwitch] = determineNextSwitch(1, m1, m2,
    beta, x0, tEnd-tCurr, vpaPresision);
31         traj = cat(1, traj, {1, x0, tSwitch});
32         x0 = xSwitch;
33     else
34         if a0 * x0(1) + a1 * x0(2) > 1
35             [tSwitch, xSwitch] = determineNextSwitch(1, m1,
    m2, beta, x0, tEnd-tCurr, vpaPresision);
36             traj = cat(1, traj, {1, x0, tSwitch});
37             x0 = xSwitch;
38         elseif  a0 * x0(1) + a1 * x0(2) < -1
39             [tSwitch, xSwitch] = determineNextSwitch(2, m1,
    m2, beta, x0, tEnd-tCurr, vpaPresision);
40             traj = cat(1, traj, {2, x0, tSwitch});
41             x0 = xSwitch;
42         else
43             fprintf('Sliding mode detected!\n');
44             if x0(2) > 0
45                 tSliding = (1 - (a0 * x0(1) + a1 * x0(2)))/
   a0/x0(2);
46                 traj = cat(1, traj, {3, x0, tSliding});
47                 x0 = [(1 - a1*x0(2)) / a0; x0(2); 0; 0];
48
49                 traj = cat(1, traj, {2, x0, tSwitch});
50                 x0 = xSwitch;
```

```
51              elseif x0(2) < 0
52                  tSliding = (-1 - (a0 * x0(1) + a1 * x0(2)))
    /a0/x0(2);
53                  traj = cat(1, traj, {3, x0, tSliding});
54                  x0 = [(-1 - a1*x0(2)) / a0; x0(2); 0; 0];
55
56                  traj = cat(2, traj, {2, x0, tSwitch});
57                  x0 = xSwitch;
58              else
59                  fprintf('Equilibrium interval is reached!\n
    ');
60                  break;
61              end
62          end
63      end
64      tCurr = tCurr + tSwitch;
65  end
66  save('traj.mat', 'traj');
67
68  digits(digitsOld);
69
70  end
```

LISTING 1.6 **plotTraj2D.m** – auxiliary function drawing a trajectory in a 2D plane.

```
1   function plotTraj2D(traj,m1,m2,b,coordInd2d)
2
3   syms t positive
4   syms X_1 X_2 X_3 X_4 real
5
6   [numArcs, ~] = size(traj);
7
8   figure(1); hold on;
9
10  color = {'red','blue'};
11
12  for iTr = 1 : numArcs
13      symSolOde = str2func(['symSolOde', int2str(traj{iTr, 1})
    ]);
14
15      currSol = symSolOde(m1, m2, b);
16      currIC = traj{iTr, 2};
17      sol_x1 = subs(currSol(coordInd2d{1}), {X_1, X_2, X_3,
    X_4}, ...
18                        {currIC(1), currIC(2), currIC(3),
    currIC(4)});
```

```
19      sol_x2 = subs(currSol(coordInd2d{2}), {X_1, X_2, X_3,
        X_4}, ...
20                      {currIC(1), currIC(2), currIC(3),
        currIC(4)});
21
22      plot3(currIC(coordInd2d{1}), currIC(coordInd2d{2}), '.',
         'markersize', 15, 'Color', 'black');
23      fplot(sol_x1, sol_x2, [0, double(traj{iTr, 3})], 'Color'
        , color{traj{iTr, 1}});
24  end
25  grid on; axis on;
26  xlabel(['x' int2str(coordInd2d{1})], 'FontName', 'Times New
        Roman', 'FontAngle', 'italic', 'FontSize', 21);
27  ylabel(['x' int2str(coordInd2d{2})], 'FontName', 'Times New
        Roman', 'FontAngle', 'italic', 'FontSize', 21);
28  hold off;
29
30  end
```

LISTING 1.7 **plotTraj3D.m** – auxiliary function drawing a trajectory in a 3D subspace.

```
1   function plotTraj3D(traj, m1, m2, b, coordInd3d)
2
3   syms t positive
4   syms X_1 X_2 X_3 X_4 real
5
6   [numArcs, ~] = size(traj);
7
8   figure(1); hold on;
9
10  trajColors = {'red','blue'};
11
12  for iTr = 1 : numArcs
13      symSolOde = str2func(['symSolOde', int2str(traj{iTr, 1})
        ]);
14      currSol = symSolOde(m1, m2, b);
15      currIC = traj{iTr, 2};
16      sol_x1 = subs(currSol(coordInd3d{1}), {X_1, X_2, X_3,
        X_4}, ...
17                      {currIC(1), currIC(2), currIC(3),
        currIC(4)});
18      sol_x2 = subs(currSol(coordInd3d{2}), {X_1, X_2, X_3,
        X_4}, ...
19                      {currIC(1), currIC(2), currIC(3),
        currIC(4)});
20      sol_x3 = subs(currSol(coordInd3d{3}), {X_1, X_2, X_3,
```

```
   X_4}, ...
                    {currIC(1), currIC(2), currIC(3),
   currIC(4)});

    % Plot switching point
    plot3(currIC(coordInd3d{1}), currIC(coordInd3d{2}),
   currIC(coordInd3d{3}), '.', 'markersize', 15, 'Color', '
   black');

    % Plot the arc of trajectory of the regime
    fplot3(sol_x1, sol_x2, sol_x3, [0, double(traj{iTr, 3})
   ], 'Color', trajColors{traj{iTr, 1}});
end

grid on; axis on;
xlabel(['x' int2str(coordInd3d{1})], 'FontName', 'Times New
    Roman', 'FontAngle', 'italic', 'FontSize', 21);
ylabel(['x' int2str(coordInd3d{2})], 'FontName', 'Times New
    Roman', 'FontAngle', 'italic', 'FontSize', 21);
zlabel(['x' int2str(coordInd3d{3})], 'FontName', 'Times New
    Roman', 'FontAngle', 'italic', 'FontSize', 21);
hold off;

end
```

LISTING 1.8 **findPeriodicExact.m** – function for localization of periodic solutions via Andronov's point mapping method.

```
function [solX1,solX2,solX4,solT1,solT2] =
   findPeriodicExact(m1,m2,beta,INIT_GUESS)

syms t t1 t2 positive
syms X_1 X_2 X_3 real
syms X_4 positive

solOde1 = symSolOde1(m1, m2, beta);
solOde2 = symSolOde2(m1, m2, beta);

x1_Ode1 = subs(solOde1(1), {t, X_3}, {-t1, 0});
x2_Ode1 = subs(solOde1(2), {t, X_3}, {-t1, 0});
x3_Ode1 = subs(solOde1(3), {t, X_3}, {-t1, 0});
x4_Ode1 = subs(solOde1(4), {t, X_3}, {-t1, 0});

x1_Ode2 = subs(solOde2(1), {t, X_3}, {t2, 0});
x2_Ode2 = subs(solOde2(2), {t, X_3}, {t2, 0});
x3_Ode2 = subs(solOde2(3), {t, X_3}, {t2, 0});
```

```
x4_Ode2 = subs(solOde2(4), {t, X_3}, {t2, 0});

assume(X_4 > 0); assume(t1 > 0); assume(t2 > 0);
[solX1, solX2, solX4, solT1, solT2] = vpasolve(...
  [x1_Ode2 - x1_Ode1 == 0, x2_Ode2 - x2_Ode1 == 0, ...
   x3_Ode2 - x3_Ode1 == 0, x3_Ode2 == 0, x4_Ode2 - x4_Ode1
   == 0], ...
                                [X_1, X_2, X_4, t1, t2],
   INIT_GUESS);
end
```

LISTING 1.9 **keldyshMain.m** – main function to run an analytical-numerical algorithm for searching for periodic trajectories for the Keldysh system (12) with parameters $m_1 = 0.9$, $m_2 = 1.1$, $\beta = 0.03$.

```
function keldyshMain

vpaPresision = 32;

m1 = vpa('0.9', vpaPresision);
m2 = vpa('1.1', vpaPresision);
beta = vpa('0.03', vpaPresision);

x0 = [vpa('10', vpaPresision); vpa('10', vpaPresision);
     vpa('10', vpaPresision); vpa('10', vpaPresision)];

tEnd = vpa('500', vpaPresision);

traj = integrateTrajectory(m1,m2,beta,x0,tEnd,vpaPresision)
   ;

plotTraj3D(traj, m1, m2, b, {1,2,3});
plotProj(traj, m1, m2, b, {1,2});

INIT_GUESS = [traj{end-1,2}(1), traj{end-1,2}(2), ...
              traj{end-1,2}(4), traj{end-2,3}(1), traj{end
   -1,3}(1)];

[solX1,solX2,solX4,solT1,solT2] = findPeriodicExact(m1,m2,
   beta,INIT_GUESS);

disp(solX1); disp(solX2); disp(solX4);
disp(solT1); disp(solT2);

end
```

APPENDIX 1.2 Implementation of the LPRS method for the Keldysh system

LISTING 1.10 **syst_keldysh.m** – function defining the Keldysh system (12) with parameters $m_1 = 0.9$, $m_2 = 1.1$, $\beta = 0.03$ in the Lurie form.

```
function [A, B, C] = syst_keldysh(m1, m2, beta)

a0 = (m2 ^ 2 + beta ^ 2 ) * (m1 ^ 2 + beta ^ 2);
a1 = 2 * beta * (m2 ^ 2 + m1 ^ 2 + 2 * beta ^ 2);
a2 = m2 ^ 2 + m1 ^ 2 + 6 * beta ^ 2;
a3 = 4 * beta;

A = [0 1 0 0; 0 0 1 0; 0 0 0 1; -a0 -a1 -a2 -a3];
B = [0; 0; 0; 1];
C = [0 0 -1 0];

end
```

We use the following function for the LPRS numerical computation (Boiko, 2008).

LISTING 1.11 **lprs_matr.m** – function for numerical calculation of the locus of a perturbed relay system $J(w)$ (LPRS, see Eq. (18)).

```
function J = lprs_matr(A, B, C, w)
n = size(A,1);
I = eye(n);
AINV = inv(A);
if w == 0
    J = (-0.5 + 1i * 0.25 * pi) * C * AINV * B;
else
    t = 2 .* pi / w;
    EXP_A_T = expm(0.5 * A * t);
    EXP_A_T_2 = expm(A * t);
    re_lprs = -0.5 * C * (AINV + t * inv(I-EXP_A_T_2) *
   EXP_A_T) * B;
    im_lprs = 0.25 * pi * C * inv((I + EXP_A_T))*(I -
   EXP_A_T) * AINV * B;
    J = re_lprs + 1i * im_lprs;
end
```

LISTING 1.12 **keldysh_main.m** – main function to run the LPRS mehod for the Keldysh system (12) with parameters $m_1 = 0.9$, $m_2 = 1.1$, $\beta = 0.03$.

```
function keldysh_main

m1 = 0.9;
```

```
m2 = 1.1;
beta = 0.03;

num_points = 100000;
omega_min = 0.1;
omega_max = 10;

yy_lprs = zeros(1, num_points);
xx = linspace(omega_min, omega_max, num_points);

[A, B, C] = syst_keldysh(m1, m2, beta);

for i = 1 : num_points
   yy_lprs(i) = lprs_matr(A, B, C, xx(i));
end

ht = figure('units','normalized','visible','on');
ht.Renderer='Painters';
plot(yy_lprs, 'Color', [0.5, 0, 0.5], 'LineWidth', 1)
xlabel('\textbf{Re$J$}','Interpreter','latex', 'fontsize',15)
   ;
ylabel('\textbf{Im$J$}','Interpreter','latex', 'fontsize',15,
   'rotation',0);
grid on

end
```

APPENDIX 2 MATLAB IMPLEMENTATION OF HOMOCLINIC BIFURCATIONS NUMERICAL ANALYSIS AND STABILIZATION OF UNSTABLE PERIODIC OSCILLATIONS

APPENDIX 2.1 Implementation of homoclinic bifurcations numerical analysis in the Lorenz-like system

LISTING 2.1 **runDeltaBetaGridScan.m** – script to run a numerical procedure for scanning the region parameters $\mathcal{B}_{\delta,\beta}$ (see Eq. (38)) and studying the behavior of the separatrices of saddle equilibria S_0, $S_\pm$.

```
clear global;

DIR = './GRID_TEST';

delta = 0.5;

betaStep = 0.01;
betaSpan = betaStep : betaStep : 2 + delta - betaStep;

sStep = 0.01;
sSpan = sStep : sStep : 1 - sStep;

% Choosing the vicinity for points near the equilibria S0,
   S1, S2
eqEpsVic.S0 = 1e-16;
eqEpsVic.S12 = 1e-2;

acc = 1e-16; rel_tol = acc; abs_tol = acc; InitialStep =
   acc/10;

radiusInf = 1000;  S1 = [1,0,0]; epsVicS1 = 1e-1;
ODE.solverName = 'ode45';
ODE.options = odeset('RelTol', rel_tol, 'AbsTol', abs_tol,
   'InitialStep', InitialStep, 'NormControl', 'on', 'Events
   ', @(t, x) trajBehaviorEvents(t, x, radiusInf, S1,
   epsVicS1));
ODE.lim = true;

% Integration time:
tEnd.trans = 4000; tEnd.lim = 1000;

% Log options:
```

```
logOption = [];

% Plot options:
plotOptions.symmetric = false;
plotOptions.color = true;
plotOptions.figVisible = 'off';
plotOptions.figSave = true;
plotOptions.axis = [];
plotOptions.view = [];

% Main routing:
deltaBetaGridScan(DIR, delta, betaSpan, sSpan, eqEpsVic,
   ODE, tEnd, logOption, plotOptions);
```

LISTING 2.2 **trajBehaviorEvents.m** – function to detect the events "a trajectory goes outside the sphere" and "a trajectory is in the ε-vicinity of a point".

```
function [value, isterminal, direction] =
   trajBehaviorEvents(~, x, radiusInf, xEq, epsEq)
   value = [sqrt(x(1)^2 + x(2)^2 + x(3)^2) - radiusInf;
                    sqrt((x(1) - xEq(1))^2 + ...
                         (x(2) - xEq(2))^2 + ...
                         (x(3) - xEq(3))^2) - epsEq];
   isterminal = [1; 1];
   direction = [0; 0];
```

LISTING 2.3 **deltaBetaGridScan.m** – numerical procedure for scanning the region of parameters (δ, β) and studying the behavior of separatrices of saddle equilibria S_0, $S_\pm$.

```
function deltaBetaGridScan(DIR, delta, betaList, sList,
   eqEpsVic, ODE, tEnd, logOption, plotOptions)

for iBeta = 1 : length(betaList)
    betaDIR = [DIR '/Delta=' num2str(delta,'%.2g') ...
               '/Beta=', num2str(betaList(iBeta),'%.2g')];
    if ~isequal(exist(betaDIR, 'dir'), 7) % 7 = directory.
        mkdir(betaDIR);
    end
end

numWorkers = feature('numCores');
poolObj = parpool(2*numWorkers);
cleaner = onCleanup(@() delete(poolObj));
parfor iBeta = 1 : length(betaList)

```

```
    beta = betaList(iBeta);

    for iS = 1 : length(sList)

        warning('off','MATLAB:odearguments:RelTolIncrease')
    ;

        s = sList(iS);

        betaDIR = [DIR '/Delta=' num2str(delta,'%.2g') '/
    Beta=', num2str(beta,'%.2g')];

        integrateTraj(betaDIR, delta, beta, s, eqEpsVic,
    ODE, tEnd, logOption, plotOptions);

        warning('on','MATLAB:odearguments:RelTolIncrease');
    end
end

figs2png(delta, betaList, sList);

end
```

LISTING 2.4 **integrateTraj.m** – function for numerical integrating separatrices of saddle equilibria for given parameter values δ, β, s.

```
function sol = integrateTraj(DIR, delta, beta, s, eqEpsVic,
    ODE, tEnd, logOption, plotOptions)

fileName = [DIR, '/s=', num2str(s, '%.16g')];

warning('off','MATLAB:odearguments:RelTolIncrease');

S0 = [0, 0, 0]; S1 = [1, 0, 0]; %S2 = [-1, 0, 0];

% Values of parameters :
alpha = delta * sqrt(1-s); lambda = s / sqrt(1-s);

[V, D] = eig(J(S0, alpha, beta, lambda));
[~, IX] = sort(real(diag(D)), 'descend');

%% Eigenvectors of J in S0
vU_S0 = V(:, IX(1))' / norm(V(:, IX(1))');

[V1, D1] = eig(J(S1, alpha, beta, lambda));
[~, IX1] = sort(real(diag(D1)), 'descend');
```

```
20
21 if ~isempty(logOption)
22     fprintf('%.12g\n', s);
23
24     fprintf('parameters: alpha = %.16g, beta = %.16g,
   lambda = %.16g\n', alpha, beta, lambda);
25
26     fprintf('lambda_1(S0) = %s, lambda_2(S0) = %s, lambda_3
   (S0) = %s\n', ...
27         D(IX(1), IX(1)), D(IX(2), IX(2)), D(IX(3), IX(3)));
    %
28     if real(D(IX(1), IX(1))) > 0
29         fprintf('Eq. S0 is unstable\n');
30     else
31         fprintf('Eq. S0 is stable\n');
32     end
33
34     fprintf('lambda_1(S1) = %s, lambda_2(S1) = %s, lambda_3
   (S1) = %s\n', ...
35         D1(IX1(1), IX1(1)), D1(IX1(2), IX1(2)), D1(IX1(3),
   IX1(3))); %
36     if real(D1(IX1(1), IX1(1))) > 0
37         fprintf('Eq. S1 and S2 are unstable\n');
38     else
39         fprintf('Eq. S1 and S2 are stable\n');
40     end
41 end
42
43 initPointS0 = S0 + eqEpsVic.S0 * sign(vU_S0(1)) * vU_S0;
44 sol.sepaS0 = feval(ODE.solverName, @(t, x) lorenzLikeSyst(t
   , x, alpha, beta, lambda), [0, tEnd.trans], initPointS0,
    ODE.options);
45 if ~isempty(plotOptions)
46     plotLorenzLikeSepa(fileName, sol.sepaS0.x, sol.sepaS0.y
   ', plotOptions);
47     if ODE.lim
48         tLimSpan = linspace(tEnd.trans-tEnd.lim, tEnd.trans
   ,100*tEnd.lim);
49         attrS0 = deval(sol.sepaS0, tLimSpan);
50         plotLimOptions = plotOptions; plotLimOptions.color
   = false;
51         plotLorenzLikeSepa(fileName, tLimSpan, attrS0',
   plotLimOptions);
52     end
53 end
```

```
54
55 if beta > s * (delta + 2 / (delta * (1-s) + s))
56     vU1_S1 = real(V1(:, IX1(1)))' / norm(real(V1(:, IX1(1))
   ));
57     vU2_S1 = imag(V1(:, IX1(1)))' / norm(imag(V1(:, IX1(1))
   ));
58
59     initPointS1 = S1 + eqEpsVic.S12 * (vU1_S1 + vU2_S1) /
   norm(vU1_S1 + vU2_S1);
60     sol.sepaS1 = feval(ODE.solverName, @(t, x)
   lorenzLikeSyst(t, x, alpha, beta, lambda), [0, tEnd.
   trans], initPointS1, ODE.options);
61     if ~isempty(plotOptions)
62         plotLorenzLikeSepa(fileName, sol.sepaS1.x, sol.
   sepaS1.y', plotOptions);
63         if ODE.lim
64             attrS1 = deval(sol.sepaS1, tLimSpan);
65             plotLorenzLikeSepa(fileName, tLimSpan, attrS1',
    plotLimOptions);
66         end
67     end
68 else
69     sol.sepaS1 = [];
70 end
71
72 warning('on','MATLAB:odearguments:RelTolIncrease');
73
74 end
```

LISTING 2.5 **plotLorenzLikeSepa.m** – auxiliary function for plotting and saving phase space pictures of system (34).

```
1  function plotLorenzLikeSepa(fileName, t, traj, plotOptions)
2
3      S0 = [0, 0, 0]; S1 = [1, 0, 0]; S2 = [-1, 0, 0];
4
5      hFigMain = figure; hold on;
6
7      set(hFigMain, 'visible', plotOptions.figVisible);
8
9      plot3(S0(1),S0(2),S0(3), '.','markersize', 15, 'Color',
       'red');
10     plot3(S1(1),S1(2),S1(3), '.','markersize', 15, 'Color',
       'red');
11     plot3(S2(1),S2(2),S2(3), '.','markersize', 15, 'Color',
       'red');
```

```
12
13      plot3(traj(:,1), traj(:,2), traj(:,3));
14      if plotOptions.symmetric
15         plot3(-traj(:,1), -traj(:,2), traj(:,3));
16      end
17      grid on; xlabel('x'); ylabel('v'); zlabel('u');
18
19      if isempty(plotOptions.axis)
20          axis auto;
21      else
22          axis(plotOptions.axis);
23      end
24
25      if isempty(plotOptions.view)
26          view(3);
27      else
28          view(plotOptions.view);
29      end
30
31      if plotOptions.figSave
32          savefig(hFigMain, [fileName, '.fig'], 'compact');
33      end
34
35      if strcmp(plotOptions.figVisible, 'off')
36          close(hFigMain);
37      end
38
39      if plotOptions.color
40          hFigColor = figure; hold on;
41
42          set(hFigColor, 'visible', plotOptions.figVisible);
43
44          plot3(S0(1),S0(2),S0(3), '.', 'markersize',15,'
    Color','red');
45          plot3(S1(1),S1(2),S1(3), '.', 'markersize',15,'
    Color','red');
46          plot3(S2(1),S2(2),S2(3), '.', 'markersize',15,'
    Color','red');
47
48          c = 1:numel(t);       %# colors
49          surf([traj(:,1),traj(:,1)], ...
50               [traj(:,2), traj(:,2)], ...
51               [traj(:,3), traj(:,3)], ...
52               [c(:), c(:)], ...
53                     'EdgeColor','flat', 'FaceColor','none')
```

```
    ;
54          colormap( jet(numel(t)) );
55
56          grid on; xlabel('x'); ylabel('v'); zlabel('u');
57
58          if isempty(plotOptions.axis)
59              axis auto;
60          else
61              axis(plotOptions.axis);
62          end
63
64          if isempty(plotOptions.view)
65              view(3);
66          else
67              view(plotOptions.view);
68          end
69
70          if plotOptions.figSave
71              savefig(hFigColor, [fileName, '_col.fig'], '
    compact');
72          end
73
74          if strcmp(plotOptions.figVisible, 'off')
75              close(hFigColor);
76          end
77      end
78  end
```

LISTING 2.6 **figs2png.m** – auxiliary function to plot and save PNG-images.

```
1   function figs2png(delta, betaList, sList)
2
3   for iBeta = 1 : length(betaList)
4
5       beta = betaList(iBeta);
6
7       for iS = 1 : length(sList)
8           s = sList(iS);
9
10          DIR = ['./GRID_TEST/Delta=' num2str(delta,'%.2g') '
    /Beta=', num2str(beta,'%.2g')];
11          fileName = [DIR, '/' int2str(iS) '-s=', num2str(s,
    '%.16g')];
12
13          if exist(fileName, 'file')
14              hFig = openfig([fileName '.fig'], 'invisible');
```

```
15              set(hFig, 'Position', [1, 1, 200, 200]);
16              print(hFig, '-r300', [fileName, '.png'], '-dpng
    ');
17              close(hFig);
18
19              fileNameNoTrans = [fileName '_noTrans'];
20              hFig2 = openfig([ fileNameNoTrans '.fig'],'
    invisible');
21              set(hFig2, 'Position', [1, 1, 200, 200]);
22              print(hFig2, '-r300', [fileNameNoTrans, '.png'
    ],'-dpng');
23              close(hFig2);
24          end
25      end
26  end
27  end
```

LISTING 2.7 **bifChaoticMain.m** – script to start the procedure for modeling the behavior of a grid of points on a Poincaré section with the sequential application of the Poincaré map.

```
1  function bifChaoticMain
2
3  DIR = './FIG/';
4  delta = 0.9; beta = 2.899;
5
6  sL = 0.7955; sR = 0.7958;
7  numPoincareMaps = 100;
8  isContinue = 0;
9  lorenzLikeSystPoincareSec(DIR,delta,sL,numPoincareMaps,
       isContinue);
10
11 end
```

LISTING 2.8 **lorenzLikeSystPoincareSec.m** – procedure for modeling the behavior of a grid of points on a Poincaré section with the sequential application of the Poincaré map.

```
1  function lorenzLikeSystPoincareSec(DIR, delta, beta, s,
       numPoincareMaps, isCont)
2
3  warning('off', 'MATLAB:odearguments:RelTolIncrease');
4
5  T = 1000;
6
7  alpha = delta * sqrt(1-s); lambda = s / sqrt(1-s);
```

```
8
9  %% Event 1 : Is trajectory in the vicinity of the eq. S0:
10     function [value, isterminal, direction] = isInVic(~, y,
       epsHomoclin, dir)
11         value = norm(y) - epsHomoclin;
12         isterminal = 1;
13         direction = dir;
14     end
15
16 %% Event 2 :
17     function [value, isterminal, direction] = isOnPS0(~, y,
       p, vNorm)
18         value = vNorm(1) * (y(1) - p(1)) + vNorm(2) * (y(2)
      - p(2)) + vNorm(3) * (y(3) - p(3));
19         isterminal = 1;
20         direction = 1;
21     end
22
23 %% Event 3 :
24     function [value, isterminal, direction] = isOnPS1(~, y,
       p, vNorm)
25         value = [vNorm(1) * (y(1) - p(1)) + vNorm(2) * (y(2)
       - p(2)) + vNorm(3) * (y(3) - p(3)), ...
26                 -vNorm(1) * (y(1) + p(1)) - vNorm(2) * (y(2) + p
      (2)) + vNorm(3) * (y(3) - p(3))];
27         isterminal = [1, 1];
28         direction = [1, 1];
29     end
30
31 %% Event 4 :
32     function [value, isterminal, direction] = isTurning(~,
      y, vS, vSS)
33         value = [y(1), y(2), det([y(1), y(2), y(3); vS(1),
      vS(2), vS(3); vSS(1), vSS(2), vSS(3)])];
34         isterminal = [1, 1, 0];
35         direction = [1, -1, 0];
36     end
37
38 %%
39 odeLorenzLike = @(t, x) lorenzLikeSyst(t, x, alpha, beta,
      lambda);
40
41 S0 = [0, 0, 0]; S1 = [1, 0, 0]; S2 = [-1, 0, 0];
42 equilPoints = [S0; S1; S2];
43
```

```
44 %% Stability of the equilibria:
45 [V, D] = eig(J(S0, alpha, beta, lambda));
46 [~, IX] = sort(real(diag(D)), 'descend');
47 fprintf('lambda_1(S0) = %s, lambda_2(S0) = %s, lambda_3(S0)
       = %s\n', D(IX(1), IX(1)), D(IX(2), IX(2)), D(IX(3), IX
   (3)));
48 if real(D(IX(1), IX(1))) > 0
49     fprintf('Eq. S0 is unstable\n');
50 else
51     fprintf('Eq. S0 is stable\n');
52 end
53
54 [~, D1] = eig(J(S1, alpha, beta, lambda));
55 [~, IX1] = sort(real(diag(D1)), 'descend');
56 fprintf('lambda_1(S1) = %s, lambda_2(S1) = %s, lambda_3(S1)
       = %s\n', ...
57         D1(IX1(1), IX1(1)), D1(IX1(2), IX1(2)), D1(IX1(3),
   IX1(3))); %
58 if real(D1(IX1(1), IX1(1))) > 0
59     fprintf('Eq. S1 and S2 are unstable\n');
60 else
61     fprintf('Eq. S1 and S2 are stable\n');
62 end
63
64 %% Eigenvectors of J in S0
65 vU = V(:, IX(1))' / norm(V(:, IX(1))');
66 vS = V(:, IX(2))' / norm(V(:, IX(2))');
67 vSS = V(:, IX(3))' / norm(V(:, IX(3))');
68
69 %% Parameters of ODE solver:
70 acc = 1e-16;
71 rel_tol = acc;
72 abs_tol = acc;
73 InitialStep = acc/10;
74
75 %% Choosing 'epsHomoclin' for init. point in the vicinity
   of the eq.s S0
76 epsHomoclinInit = 1e-16;
77 x_unst_01 = S0 + epsHomoclinInit * vU;
78
79 %% Choosing 'epsVicinity' for placing the Poincare sections
    Pi0
80 epsVicPS0 = 5e-1; %3e-5;
81
82 %% Define P0 - point on the Poincare section Pi_0
```

```
83  P0 = S0 + epsVicPS0 * vS;
84  optionsOnPS0 = odeset('RelTol', rel_tol, 'AbsTol', abs_tol,
        'InitialStep', InitialStep, 'NormControl', 'on', '
    Events', @(t, x) isOnPS0(t, x, P0, -vS));
85
86  [~, sepa] = ode45(odeLorenzLike, [0 T], x_unst_01,
    optionsOnPS0);
87  sepaEnd = sepa(end, :);
88
89  %% Construct a rectangular grid of points on Pi_0
90  wNorm = [det([vS(2), vSS(2); vS(3), vSS(3)]), ...
91          -det([vS(1), vSS(1); vS(3), vSS(3)]), ...
92          det([vS(1), vSS(1); vS(2), vSS(2)])];
93  vPS = cross(vS, wNorm) / norm(cross(vS, wNorm));
94  vPSN = -cross(vS, vPS) / norm(cross(vS, vPS));
95
96  epsPoincareWidth = 2.5e-2; %norm(sepaEnd - P0) + epsVicPS0
    /10;
97  disp(epsPoincareWidth);
98
99  A = det([vS(2), vS(3); vSS(2), vSS(3)]);
100 B = -det([vS(1), vS(3); vSS(1), vSS(3)]);
101 C = det([vS(1), vS(2); vSS(1), vSS(2)]);
102
103 distSepaStMan = abs(A * sepaEnd(1) + B * sepaEnd(2) + C *
    sepaEnd(3)) / (sqrt(A^2 + B^2 + C^2));
104 disp(distSepaStMan);
105
106 horNumSteps = 5;
107 frameThikness = epsPoincareWidth / 2; %epsVicPS0/20;
108
109 epsPoincareHeight = epsPoincareWidth + frameThikness;
110 disp(epsPoincareHeight);
111
112 %% Vertex of the frame
113 frVertex = frameVertex(P0, vPS, vPSN, frameThikness,
    epsPoincareWidth, epsPoincareHeight);
114
115 %% Rectangular on Poincare section Pi0
116 rectHorSize = 6e-2;
117 rectVertSize = 6e-2;
118 rect3D = rectangle3d(P0, vPS, vPSN, rectHorSize,
    rectVertSize);
119
120 %% Distance from saddle to Poincare section Pi1
```

```
121 epsVicPS1 = 1.5 * rectVertSize;
122 P1 = S0 + epsVicPS1 * vU;
123 optionsOnPS1 = odeset('RelTol', rel_tol, 'AbsTol', abs_tol,
        'InitialStep', InitialStep, 'NormControl', 'on', '
    Events', @(t, x) isOnPS1(t, x, P1, vU));
124
125
126 axisSize3D = [];
127
128 %% Check continuation of num. procedure
129 if isCont == 0
130
131     pointsPS0 = frameGrid(P0, vPS, vPSN, frameThikness, ...
132                           epsPoincareWidth, epsPoincareHeight
    , horNumSteps);
133
134     [pointsBackPS0, pointsPS1_1, pointsPS1_2] =
    execPoincareMap(pointsPS0, odeLorenzLike, [0 T],
    optionsOnPS0, optionsOnPS1);
135
136     fileName = [DIR '00'];
137
138     plotPoincareSec(equilPoints, vS, vSS, rect3D, sepa,
    frVertex, pointsPS0, pointsPS1_1, pointsPS1_2,
    pointsBackPS0, axisSize3D, fileName);
139
140     lastIndex = 0;
141     currPointsPS0 = pointsBackPS0;
142     save([DIR 'currPointsPS0.mat'], 'currPointsPS0');
143     preIterPoincareMap = 1;
144 elseif isCont == 1
145     lastIndex = getLastFigIndex(DIR);
146     load([DIR 'currPointsPS0.mat'], 'currPointsPS0');
147     preIterPoincareMap = 0;
148 else
149     return;
150 end
151
152 %% Main loop
153 for iPoincareMap = 1 : numPoincareMaps-preIterPoincareMap
154
155     [currPointsBackPS0, currPointsPS1_1, currPointsPS1_2] =
     execPoincareMap(currPointsPS0, odeLorenzLike, [0 T],
    optionsOnPS0, optionsOnPS1);
156
```

```
157     currIndex = lastIndex+iPoincareMap;
158     fileName = [DIR num2str(currIndex, '%02d')];
159 
160     plotPoincareSec(equilPoints, vS, vSS, rect3D, sepa,
    frVertex, currPointsPS0, currPointsPS1_1,
    currPointsPS1_2, currPointsBackPS0, axisSize3D, fileName
    );
161 
162     currPointsPS0 = currPointsBackPS0;
163     save([DIR 'currPointsPS0.mat'], 'currPointsPS0');
164 end
165 
166 warning('on','MATLAB:odearguments:RelTolIncrease');
167 
168 end
```

LISTING 2.9 **execPoincareMap.m** – function performing the Poincaré map.

```
1  function [pointsBackOnPS0, pointsOnPS1_1, pointsOnPS1_2] =
       execPoincareMap(pointsOnPS0, ode, tInt, optionsOnPS0,
       optionsOnPS1)
2       if ~isempty(pointsOnPS0)
3           numWorkers = feature('numCores');
4           poolObj = parpool(numWorkers);
5           cleaner = onCleanup(@() delete(poolObj));
6 
7           [rPS0, cPS0]  = size(pointsOnPS0);
8           startPointPS0 = pointsOnPS0(:, 1:3);
9           colorPS0 = pointsOnPS0(:, 4:6);
10          pointsOnPS1 = zeros(rPS0, cPS0+1);
11          parfor iPS0 = 1 : rPS0
12              warning('off', 'MATLAB:odearguments:
        RelTolIncrease');
13              [~, currTraj, ~, ~, currIe] = ode45(ode, tInt,
        startPointPS0(iPS0, :), optionsOnPS1);
14              pointsOnPS1(iPS0, :) = [currTraj(end, :),
        colorPS0(iPS0, :), currIe];
15              warning('on', 'MATLAB:odearguments:
        RelTolIncrease');
16          end
17          pointsOnPS1_1 = pointsOnPS1(pointsOnPS1(:, end) ==
        1, 1 : end-1);
18          pointsOnPS1_2 = pointsOnPS1(pointsOnPS1(:, end) ==
        2, 1 : end-1);
19 
20          if ~isempty(pointsOnPS1_1)
```

```
21            [rPS1_1, cPS1_1]  = size(pointsOnPS1_1);
22            pointsBackOnPS0_1 = zeros(rPS1_1, cPS1_1);
23            startPointPS1_1 = pointsOnPS1_1(:, 1:3);
24            colorPS1_1 = pointsOnPS1_1(:, 4:6);
25            parfor iPS1_1 = 1 : rPS1_1
26                warning('off', 'MATLAB:odearguments:
    RelTolIncrease');
27                [~, currTraj] = ode45(ode, tInt,
    startPointPS1_1(iPS1_1, :), optionsOnPS0);
28                pointsBackOnPS0_1(iPS1_1, :) = [currTraj(
    end, :), colorPS1_1(iPS1_1, :)];
29                warning('on', 'MATLAB:odearguments:
    RelTolIncrease');
30            end
31        else
32            pointsBackOnPS0_1 = [];
33        end
34        pointsBackOnPS0 = pointsBackOnPS0_1;
35
36        if ~isempty(pointsOnPS1_2)
37            [rPS1_2, cPS1_2]  = size(pointsOnPS1_2);
38            pointsBackOnPS0_2 = zeros(rPS1_2, cPS1_2);
39            startPointPS1_2 = pointsOnPS1_2(:, 1:3);
40            colorPS1_2 = pointsOnPS1_2(:, 4:6);
41            parfor iPS1_2 = 1 : rPS1_2
42                warning('off', 'MATLAB:odearguments:
    RelTolIncrease');
43                [~, currTraj] = ode45(ode, tInt,
    startPointPS1_2(iPS1_2, :), optionsOnPS0);
44                pointsBackOnPS0_2(iPS1_2, :) = [currTraj(
    end, :), colorPS1_2(iPS1_2, :)];
45                warning('on', 'MATLAB:odearguments:
    RelTolIncrease');
46            end
47        else
48            pointsBackOnPS0_2 = [];
49        end
50        pointsBackOnPS0 = [pointsBackOnPS0;
    pointsBackOnPS0_2];
51     else
52        errorMessage = sprintf('Error: No points on
    Poincare section\n');
53        uiwait(warndlg(errorMessage));
54        return;
55     end
```

```
end
```

LISTING 2.10 **rectangle3d.m** – function specifying the vertices of a rectangular frame on a Poincaré section Σ^{in}.

```
function rect3d = rectangle3d(P0, vHor, vVert, rectHorSize,
    rectVertSize)

    p1 = P0 + rectHorSize * vHor - rectVertSize * vVert;
    p2 = P0 - rectHorSize * vHor - rectVertSize * vVert;
    p3 = P0 - rectHorSize * vHor + rectVertSize * vVert;
    p4 = P0 + rectHorSize * vHor + rectVertSize * vVert;

    rect3d = [p1(:), p2(:), p3(:), p4(:)];
end
```

LISTING 2.11 **frameVertex.m** – function that defines the vertices of the half-frame on the Poincaré section Σ^{in}.

```
function frVertex = frameVertex(midPoint, vHor, vVert, ...
                    frThickness, frInHalfWidth,
   frHalfHeight)

P2 = midPoint + frInHalfWidth * vHor;
P1 = P2 + frThickness * vHor;
P8 = P1 + frHalfHeight * vVert;
P3 = P2 + (frHalfHeight - frThickness) * vVert;
P4 = P3 - 2 * frInHalfWidth * vHor;
P5 = midPoint - frInHalfWidth * vHor;
P6 = P5 - frThickness * vHor;
P7 = P6 + frHalfHeight * vVert;

frVertex = [P1; P2; P3; P4; P5; P6; P7; P8];

end
```

LISTING 2.12 **frameGrid.m** – function that generates the initial half-framed grid of points on the Poincaré section Σ^{in}.

```
function grid = frameGrid(midPoint, vHor, vVert, ...
    frThickness, frInHalfWidth, frHalfHeight, numPoints)

grid = []; currIndex = 1;
%% 1st rectangle
pointRect1 = midPoint + frInHalfWidth * vHor;

stepSize = frThickness / (numPoints-1);
```

```
numPointsVert = floor(frHalfHeight / stepSize) + 1;
col = jet(numPointsVert);

for iPointX = 1 : numPoints
    xp = pointRect1 + (iPointX-1) * stepSize * vHor;
    for iPointY = 1 : numPointsVert
        grid = [grid; xp + (iPointY-1) * stepSize * vVert, col(iPointY, :)];
        currIndex = currIndex+1;
    end
end

%% 2nd rectangle
pointRect2 = midPoint - frInHalfWidth * vHor;

for iPointX = 1 : numPoints
    xp = pointRect2 - (iPointX-1) * stepSize * vHor;
    for iPointY = 1 : numPointsVert
        grid = [grid; xp + (iPointY-1) * stepSize * vVert, col(iPointY, :)];
        currIndex = currIndex+1;
    end
end

numPointsHor = 2 * frInHalfWidth / stepSize + 1;

%% 3nd rectangle
pointRect3 = midPoint + frInHalfWidth * vHor + (numPointsVert-1) * stepSize * vVert;

for iPointX = 1 : numPointsHor-1
    xp = pointRect3 - iPointX * stepSize * vHor;
    for iPointY = 1 : numPoints
        grid = [grid; xp - (iPointY-1) * stepSize * vVert, col(end - (iPointY-1),:)];
        currIndex = currIndex+1;
    end
end

grid(:, 1:3) = grid(:, 1:3) + stepSize * vVert;
end
```

LISTING 2.13 **plotPoincareSec.m** – function for drawing a grid of points on the Poincaré section in the sequential application of the Poincaré map and saving the corresponding pictures.

```
function plotPoincareSec(equilibria, vS, vSS, rect,
   separatrix, frVertex, pointsPS0, pointsPS1_1,
   pointsPS1_2, pointsBackPS0, axisSize3D, fileName)

S0 = equilibria(1, :); S1 = equilibria(2, :); S2 =
   equilibria(3, :);
xPS0 = rect(1, :); yPS0 = rect(2, :); zPS0 = rect(3, :);

fx = @(s,t) vS(1) * s + vSS(1) * t;
fv = @(s,t) vS(2) * s + vSS(2) * t;
fu = @(s,t) vS(3) * s + vSS(3) * t;

epsManifold = 1e1;

hFig1 = figure('Visible','off'); hold on;
axFig1 = gca;

%% Equilibria:
plot3(axFig1, S0(1), S0(2), S0(3), '.', 'markersize', 20, '
   Color', 'black');
plot3(axFig1, S1(1), S1(2), S1(3), '.', 'markersize', 20, '
   Color', 'black');
plot3(axFig1, S2(1), S2(2), S2(3), '.', 'markersize', 20, '
   Color', 'black');

%% 2D stable manifold
fsurf(axFig1, fx, fv, fu, [-epsManifold, epsManifold], '
   EdgeColor', 'none', 'FaceColor', [0.9, 0.9, 0.9]);

%% Separatrix
if ~isempty(separatrix)
    plot3(axFig1, separatrix(:,1), separatrix(:,2),
   separatrix(:,3));
    plot3(axFig1, -separatrix(:,1), -separatrix(:,2),
   separatrix(:,3));
end

%% Poincare section:
hPS1 = fill3(axFig1, xPS0, yPS0, zPS0, 'r'); set(hPS1, '
   FaceAlpha', 0.1);
plotDashedLine(axFig1, [(xPS0(1) + xPS0(4)) / 2, ...
                        (yPS0(1) + yPS0(4)) / 2, ...
                        (zPS0(1) + zPS0(4)) / 2], ...
                        [(xPS0(2) + xPS0(3)) / 2, ...
```

```
                        (yPS0(2) + yPS0(3)) / 2, ...
                        (zPS0(2) + zPS0(3)) / 2]);

%% Half-frame
plotDashedLine(axFig1, frVertex(1, :), frVertex(2, :));
plotDashedLine(axFig1, frVertex(2, :), frVertex(3, :));
plotDashedLine(axFig1, frVertex(3, :), frVertex(4, :));
plotDashedLine(axFig1, frVertex(4, :), frVertex(5, :));
plotDashedLine(axFig1, frVertex(5, :), frVertex(6, :));
plotDashedLine(axFig1, frVertex(6, :), frVertex(7, :));
plotDashedLine(axFig1, frVertex(7, :), frVertex(8, :));
plotDashedLine(axFig1, frVertex(8, :), frVertex(1, :));

%% Grid of points
scatter3(axFig1, pointsPS0(:,1),pointsPS0(:,2),pointsPS0
   (:,3), 36, pointsPS0(:,4:6), 'filled');

if ~isempty(pointsPS1_1)
    scatter3(axFig1, pointsPS1_1(:,1),pointsPS1_1(:,2),
   pointsPS1_1(:,3), 36, pointsPS1_1(:,4:6), 'filled');
end
if ~isempty(pointsPS1_2)
    scatter3(axFig1, pointsPS1_2(:,1),pointsPS1_2(:,2),
   pointsPS1_2(:,3), 36, pointsPS1_2(:,4:6), 'filled');
end

grid(axFig1, 'on');
if  ~isempty(axisSize3D)
    axis(axFig1, axisSize3D);
else
    axis(axFig1, 'auto');
end

xlabel(axFig1, 'x'); ylabel(axFig1, 'y'); zlabel(axFig1, 'z
   ');
view(axFig1, 3);
hold off;

set(hFig1, 'Position', [1, 1, 500, 500]);
savefig(hFig1, [fileName, '_(PS0->PS1).fig'], 'compact');
close(hFig1);

%%
hFig2 = figure('Visible','off'); hold on;
axFig2 = gca;
```

```
76
77 plot3(axFig2, S0(1), S0(2), S0(3), '.', 'markersize', 20, '
   Color', 'black');
78 plot3(axFig2, S1(1), S1(2), S1(3), '.', 'markersize', 20, '
   Color', 'black');
79 plot3(axFig2, S2(1), S2(2), S2(3), '.', 'markersize', 20, '
   Color', 'black');
80
81 %% 2D stable manifold
82 fsurf(axFig2, fx, fv, fu, [-epsManifold, epsManifold], '
   EdgeColor', 'none', 'FaceColor', [0.9, 0.9, 0.9]);
83
84 if ~isempty(separatrix)
85     plot3(axFig2, separatrix(:,1), separatrix(:,2),
   separatrix(:,3));
86     plot3(axFig2, -separatrix(:,1), -separatrix(:,2),
   separatrix(:,3));
87 end
88
89 hPS1 = fill3(axFig2, xPS0, yPS0, zPS0, 'r'); set(hPS1, '
   FaceAlpha', 0.1);
90 plotDashedLine(axFig2, [(xPS0(1) + xPS0(4)) / 2, ...
91                         (yPS0(1) + yPS0(4)) / 2, ...
92                         (zPS0(1) + zPS0(4)) / 2], ...
93                         [(xPS0(2) + xPS0(3)) / 2, ...
94                          (yPS0(2) + yPS0(3)) / 2, ...
95                          (zPS0(2) + zPS0(3)) / 2]);
96
97 %% Half-frame
98 plotDashedLine(axFig2, frVertex(1, :), frVertex(2, :));
99 plotDashedLine(axFig2, frVertex(2, :), frVertex(3, :));
100 plotDashedLine(axFig2, frVertex(3, :), frVertex(4, :));
101 plotDashedLine(axFig2, frVertex(4, :), frVertex(5, :));
102 plotDashedLine(axFig2, frVertex(5, :), frVertex(6, :));
103 plotDashedLine(axFig2, frVertex(6, :), frVertex(7, :));
104 plotDashedLine(axFig2, frVertex(7, :), frVertex(8, :));
105 plotDashedLine(axFig2, frVertex(8, :), frVertex(1, :));
106
107 if ~isempty(pointsPS1_1)
108     scatter3(axFig2, pointsPS1_1(:,1),pointsPS1_1(:,2),
   pointsPS1_1(:,3), 36, pointsPS1_1(:,4:6),'filled');
109 end
110 if ~isempty(pointsPS1_2)
111     scatter3(axFig2, pointsPS1_2(:,1),pointsPS1_2(:,2),
   pointsPS1_2(:,3), 36, pointsPS1_2(:,4:6),'filled');
```

```
112 end
113 scatter3(axFig2, pointsBackPS0(:,1),pointsBackPS0(:,2),
       pointsBackPS0(:,3), 36, pointsBackPS0(:,4:6),'filled');
114 grid(axFig2, 'on');
115 if ~isempty(axisSize3D)
116     axis(axFig2, axisSize3D);
117 else
118     axis(axFig2, 'auto');
119 end
120 xlabel(axFig2, 'x'); ylabel(axFig2, 'v'); zlabel(axFig2, 'u
       ');
121 view(axFig2, 3);
122 hold off;
123
124 set(hFig2, 'Position', [1, 1, 500, 500]);
125 savefig(hFig2, [fileName, '_(PS1->PS0).fig'], 'compact');
126 close(hFig2);
127 end
```

LISTING 2.14 **plotDashedLine.m** – auxiliary function for drawing a dashed line.

```
1 function h = plotDashedLine(ax, pBegin, pEnd)
2
3 h = plot3(ax, [pBegin(1), pEnd(1)], [pBegin(2), pEnd(2)], [
       pBegin(3), pEnd(3)], '--', 'LineWidth', 1.5, 'Color', '
       black');
4
5 end
```

LISTING 2.15 **getLastFigIndex.m** – auxiliary function for determining the number of the last iteration of the Poincaré map and the corresponding picture of the Poincaré section stored in the current folder.

```
1  function lastIndex = getLastFigIndex(DIR)
2
3      figFiles = dir([DIR '/*_(PS0->PS1).fig']);
4
5      if isempty(figFiles)
6          lastIndex = -1;
7      else
8          lastFigName = figFiles(end).name;
9
10         lastFigNameSplited = strsplit(lastFigName, '_');
11
12         lastIndex = ...
13         str2double(cell2mat(lastFigNameSplited(1)));
```

```
    end
end
```

APPENDIX 2.2 Implementation of UPOs stabilization in the Lorenz system

LISTING 2.16 **lorenzSystD.m** – function determines the Lorenz system (24) with additional time-delayed feedback component (see Eq. (39)).

```
function dydt = lorenzSystD(t, y, Z, r, sigma, b, R, nLag,
   eps, K, lambda0_c, lambdaInf_c, lambda_r)

    F = (y(2) - Z(2,1));

    for iLag = 1 : nLag
        F = F + R^iLag * (Z(2, iLag) - Z(2, iLag+1));
    end

    dydt = zeros(4,1);

    restrPerturbCond = abs(F) < eps;

    if restrPerturbCond
        F_u = F + y(4);
    else
        F_u = 0;
    end

    dydt(1) = -sigma * (y(1) - y(2));
    dydt(2) = r * y(1) - y(2) - y(1) * y(3) - K * F_u;
    dydt(3) = - b * y(3) + y(1) * y(2);

    if restrPerturbCond
        dydt(4) = lambda0_c * y(4) + (lambda0_c -
   lambdaInf_c) * F;
    else
        dydt(4) = -lambda_r * y(4);
    end
end
```

LISTING 2.17 **lorenzStabUPO.m** – main function for period-1 UPO stabilization by the Pyragas UDFC method for the Lorenz system (24).

```
function lorenzStabUPO

```

```
r = 28; sigma = 10; b = 8/3;

R = 0.7; nLag = 100; eps = 3; K = 3.5;

lambda0_c = 0.1; lambdaInf_c = -2; lambda_r = 10;

dde = @(t, y, Z) lorenzSystD(t, y, Z, r, sigma, b, R, nLag,
    eps, K, lambda0_c, lambdaInf_c, lambda_r);

tau = 1.558615;

lags = tau * (1 : (nLag+1));

initPoint = [2; 2; 2; 0];

tEnd = 200;

acc = 1e-6; RelTol = acc; AbsTol = acc;
ddeOpt = ddeset('RelTol', RelTol, 'AbsTol', AbsTol);

solDDE = dde23(dde, lags, initPoint, [0, tEnd], ddeOpt);

figure(1); hold on;
plot3(solDDE.y(1,:), solDDE.y(2,:), solDDE.y(3,:), 'Color',
    [0, 0, 1]);
hold off;
grid on; axis on;
xlabel('x'); ylabel('y'); zlabel('z');
view(3);

figure(2);
plot(solDDE.x, solDDE.y(4,:), 'Color', [0, 0, 1]);
grid on; axis on;
xlabel('t');
ylabel('w(t)');
```

ORIGINAL PAPERS

PI

GLOBAL PROBLEMS FOR DIFFERENTIAL INCLUSIONS. KALMAN AND VYSHNEGRADSKII PROBLEMS AND CHUA CIRCUITS

by

G.A. Leonov, N.V. Kuznetsov, M.A. Kiseleva, R.N. Mokaev 2017

Differential Equations, Vol. 53, No. 13, PP. 1671–1702,
https://doi.org/10.1134/S0012266117130018

ISSN 0012-2661, Differential Equations, 2017, Vol. 53, No. 13, pp. 1–32. © Pleiades Publishing, Ltd., 2017.

CONTROL THEORY

Global Problems for Differential Inclusions. Kalman and Vyshnegradskii Problems and Chua Circuits

G. A. Leonov, N. V. Kuznetsov*, M. A. Kiseleva, and R. N. Mokaev

Saint Petersburg State University, St. Petersburg, 199034 Russia
University of Jyväskylä, Jyväskylä, 40014 Finland
**e-mail: nkuznetsov239@gmail.com*

DOI: 10.1134/S0012266117130018

1. INTRODUCTION

The emergence of the theory of differential inclusions is usually associated with works by French mathematician A. Marchaud [1,2] and Polish mathematician S.K. Zaremba [3,4]. However, the development of the theory of differential inclusions was furthered not only by the research in the field of abstract mathematics but also by the studies of particular problems in mechanics (plasticity, dry friction, control with relay elements, tribology, etc.; see, for example, [5–33]). That is to say, along with general considerations and attempts to understand how the notion of derivative is introduced for differential inclusions, there were other trends, related to particular needs of applied problems. First, let us describe this concrete research and then switch to the general definitions of solutions to differential inclusions. In what follows, we consider the classical Vyshnegradskii and Kalman problems and prove theorems on the stability and instability in the large.

1.1. Hartog Model

So, in 1930, J.D. Hartog [34] considered the following equation:

$$m\ddot{x} + kx + F_0 \mathrm{sgn}\,(\dot{x}) = 0, \tag{1}$$

where m, k, F_0 are positive parameters.

Equation (1) can be reduced to the following two-dimensional system:

$$\begin{aligned} \dot{x} &= y, \\ \dot{y} &= -\frac{k}{m}x - \frac{F_0}{m}\mathrm{sgn}\,(y). \end{aligned} \tag{2}$$

Let us consider the question of how a solution to the system in Eq. (2) should be understood and how the value of $\mathrm{sgn}\,(y)$ can be defined at $y = 0$. Let us show that choosing a fixed value for sign at $y = 0$ is incorrect, as in this case, the solution, as a rule, will not exist.

For $y \neq 0$ the right-hand sides of the system in Eq. (2) are continuous and we can take advantage of the classical notion of solution. For example, for $y > 0$ the system takes the form

$$\begin{aligned} \dot{x} &= y, \\ \dot{y} &= -\frac{k}{m}x - \frac{F_0}{m}, \end{aligned} \tag{3}$$

and for $y < 0$:

$$\begin{aligned} \dot{x} &= y, \\ \dot{y} &= -\frac{k}{m}x + \frac{F_0}{m}. \end{aligned} \tag{4}$$

(Reg. No. 1301, 11.2.2017)

Suppose that at some time moment t_0, the trajectory of a continuous system in Eq. (3) or (4) falls on the straight line $y = 0$, i.e., $y(t_0) = 0$. If $kx < -F_0$, the trajectory can be extended naturally into half-space $y > 0$ by virtue of system (3), as the value of dy/dt, found from the second equations in systems (3) and (4), is positive. Similarly, if $y(t_0) = 0$ and $kx > F_0$, then the trajectory can be continued into half-space $y < 0$. In other words, the thus-constructed trajectories weave through ray $y = 0$, $kx < -F_0$ toward increasing y and ray $y = 0$, $kx > F_0$ toward decreasing y.

However, should the trajectory fall into interval $y = 0$, $k|x| < F_0$ at time moment $t = t_0$, the above reasoning is no longer applicable. Indeed, it is impossible to "release" a trajectory into either half-space $y > 0$ (as the derivative dy/dt determined from the second equation in the system in Eq. (3) is less than zero) or half-space $y < 0$ (as the derivative dy/dt determined from the second equation in the system in Eq. (4) is greater than zero). Thus, the trajectories of systems (3), (4) do not "weave" through interval $y = 0$, $k|x| < F_0$ but "dock" on it instead. Therefore, such a trajectory remains within interval $y = 0$, $k|x| < F_0$ while $k|x| < F_0$. Hence it follows that $dy/dt = 0$, and, therefore, if we want our solution to satisfy the system in Eq. (2), we should equate the right-hand side of the second equation in this system to zero. In other words, $\operatorname{sgn}(0) = -kx/F_0$ for $k|x| < F_0$, with the value at $y = 0$ being inconstant.

For definiteness, let us adjoin the boundary $k|x| = F_0$, $y = 0$ to our interval.

According to the above reasoning, instead of the system in Eq. (2), we now consider the system

$$\begin{aligned} \dot{x} &= y, \\ \dot{y} &= -\frac{k}{m}x - \frac{F_0}{m}\xi(x, y), \end{aligned} \tag{5}$$

where

$$\xi(x, y) = \begin{cases} 1 & \text{for } y > 0 \text{ or for } y = 0,\ kx < -F_0, \\ -1 & \text{for } y < 0 \text{ or for } y = 0,\ kx > F_0, \\ -kx/F_0 & \text{for } y = 0,\ k|x| \le F_0. \end{cases} \tag{6}$$

Now let us find the equilibrium state of the system in Eq. (5). By equating the right-hand sides of Eqs. (5) to zero, we arrive at the relations $|x| \le F_0/k$, $y = 0$. That is to say, for $y = 0$ this system has a rest segment $[-F_0/k, F_0/k]$ that consists entirely of the equilibrium state of the system.

The phase portrait of the system in Eq. (5) is shown in Fig. 1.

It is worth mentioning that in 1944, V.M. Keldysh [35] studied a two-dimensional model of damping flutter in aircraft control systems with dry friction, and this model also led to a similar behavior near the discontinuity.

1.2. Autopilot Model

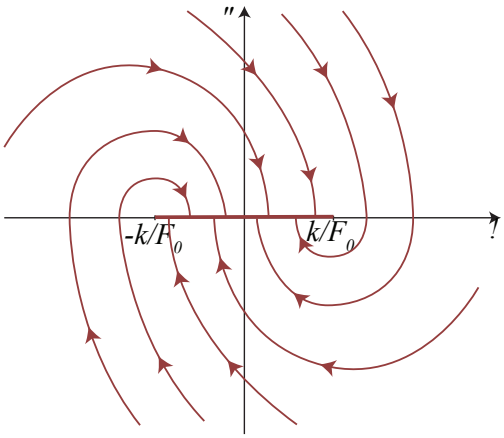

Fig. 1. Phase portrait of system (1). Trajectories tend toward the rest segment $\{|x| \le F_0/k,\ y = 0\}$.

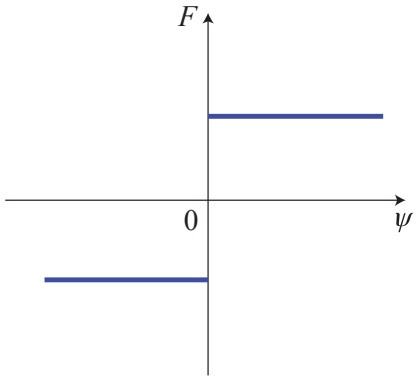

Fig. 2. Nonlinear characteristic of servomotor. The case with no zone of insensitivity.

Later, in 1940s, independent works were published by A.I. Lurie and V.N. Postnikov [36], B.V. Bulgakov [37], and A.A. Andronov[1] and N.N. Bautin [38, 39] in which all of them considered one and the same problem about heading hold of a neutral airplane using autopilot with a constant servomotor speed.

The equations of motion of the system have the following form [38–41]:

$$\begin{aligned} &\ddot{\phi} + M\dot{\phi} = -N\eta, \\ &\dot{\eta} = F(\psi), \\ &\psi = \phi + \beta\dot{\psi} - \frac{1}{a}\eta, \end{aligned} \tag{7}$$

where $F(\psi) = K\operatorname{sgn}\psi$ for $\psi \neq 0$.

Here ϕ is airplane's yaw angle; η is the rudder angle; ψ is the argument of a servomotor that controls the rudder; β is the so-called artificial damping coefficient; $1/a$ is the feedback factor; M, N, and K are positive constants that characterize, respectively, the natural damping of airplane and the rudder and steering gear; and $F(\psi)$ is a nonlinear characteristic of the servomotor.

In [38, 40], the authors considered the characteristic depicted in Fig. 2, which corresponds to the lack of insensitivity.

Using the transformation (dots here denote differentiation with respect to t_{new}; t_{old} and ψ_{old} are t and ψ from Eq. (7))

$$\begin{aligned} &t \equiv t_{new} = Mt_{old}, \\ &z = \frac{M^3}{NK}\ddot{\phi}, \\ &u = \frac{M^3}{NK}(\dot{\phi} + \ddot{\phi}), \\ &\psi \equiv \psi_{old} = \frac{M^3}{NK}\psi_{old} \end{aligned} \tag{8}$$

and renaming

$$M\beta = A, \qquad \frac{M^2}{Na} = B,$$

[1] A.A. Andronov was a student of L.I. Mandelstam. In 1946, A.A. Andronov was elected a member of the Academy of Sciences of the USSR in Department of Technical Sciences to become the first academician in control theory.

we reduce the system in Eq. (7) to the form

$$\begin{aligned} \dot{z} &= -z - \xi(z,u,\psi), \\ \dot{u} &= -\xi(z,u,\psi), \\ \dot{\psi} &= u + (A-1)z - B\xi(z,u,\psi), \end{aligned} \tag{9}$$

where $\xi(z,u,\psi) = \operatorname{sgn}\psi$ for $\psi \neq 0$.

Using a reasoning similar to the above for the system considered by Hartog, we can extend the definition of $\xi(z,u,\psi)$ to $\psi = 0$. Let us write down this extension [38, 40]

$$\xi(z,u,\psi) = \begin{cases} 1 & \text{for } \psi > 0 \text{ or for } \psi = 0,\ u + (A-1)z - B > 0 \\ & \text{or for } \psi = 0,\ u + (A-1)z - B = 0,\ u > A + B, \\ -1 & \text{for } \psi < 0 \text{ or for } \psi = 0,\ u + (A-1)z + B < 0 \\ & \text{or for } \psi = 0,\ u + (A-1)z + B = 0,\ u < -(A+B), \\ \dfrac{1}{B}[(A_1)z + u] & \text{for } \psi = 0,\ |u + (A-1)z| < B \\ & \text{or for } \psi = 0,\ u + (A-1)z - B = 0,\ u > -(A+B) \\ & \text{or for } \psi = 0,\ u + (A-1)z + B = 0,\ u < A + B. \end{cases} \tag{10}$$

The system in Eq. (9) has only one equilibrium state $z = 0$, $u = 0$, $\psi = 0$, which is a stable node for $(A+B)^2 \geq 4B$ (see Fig. 3) or a stable focus for $(A+B)^2 < 4B$ (see Fig. 4).

It should be noted that system trajectories that pass through points $\psi = 0$, $u + (A-1)z - B > 0$ and $\psi = 0$, $u + (A-1)z - B < 0$ cross the plane $\psi = 0$ in directions $\psi > 0$ and $\psi < 0$, respectively. Trajectories tending to the manifold $\psi = 0$, $|u + (A-1)z| < B$ on both sides have opposite directions and join on the manifold. Such a manifold is called the *sliding mode manifold*. A trajectory that is

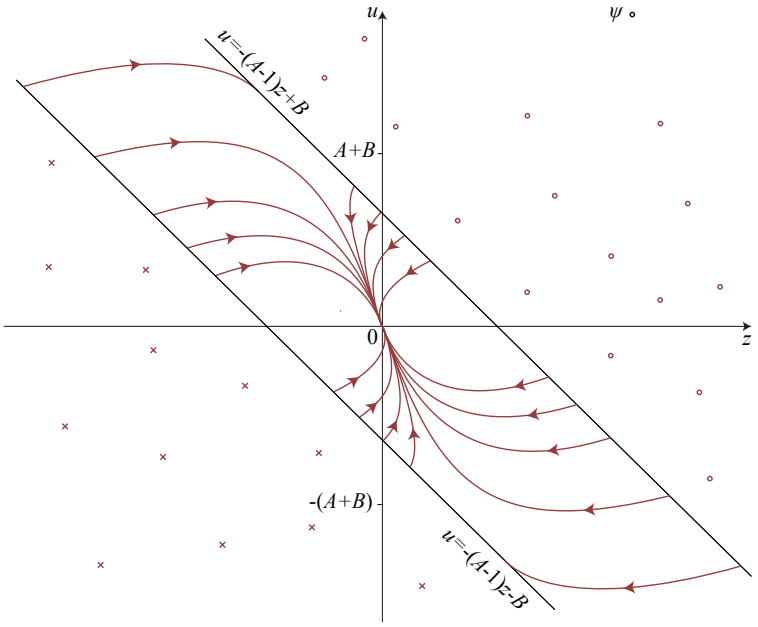

Fig. 3. Phase portrait of system (9) in the case where the equilibrium state $z = 0$, $u = 0$, $\psi = 0$ is a stable node. Here plane $\psi = 0$ is in the drawing plane, and trajectories moving from and toward an observer are marked with the crosses and circles, respectively.

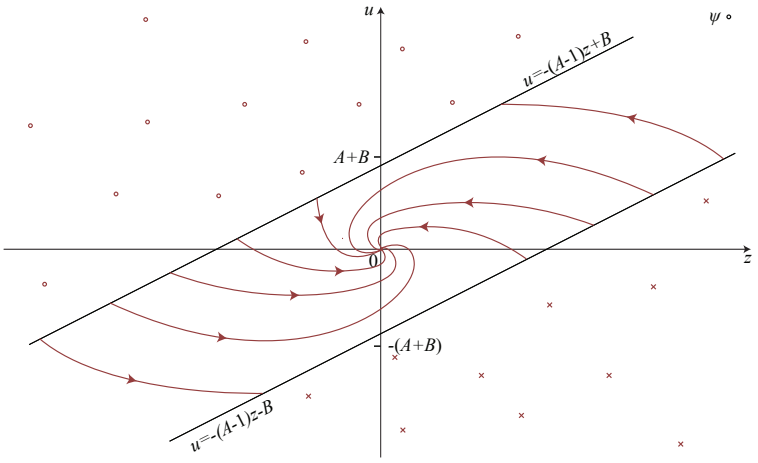

Fig. 4. Phase portrait of system (9) in the case where the equilibrium state $z = 0$, $u = 0$, $\psi = 0$ is a stable focus. Here plane $\psi = 0$ is in the drawing plane, and trajectories moving from and toward an observer are marked with the crosses and circles, respectively.

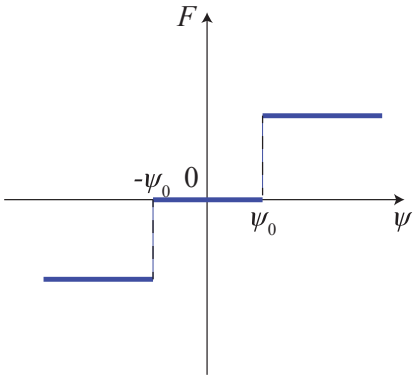

Fig. 5. Nonlinear characteristic of a servomotor with insensitivity zone.

trapped on it either tends to the unique equilibrium state of the system without leaving the limits of the manifold or escapes into half-space $\psi > 0$ or $\psi < 0$ upon reaching the edge of this manifold.

The point transformation method was used in [38,40] to derive conditions under which a control process converges. In particular, it was shown that for

$$A + B > 1 \tag{11}$$

the control process converges for any initial conditions (i.e., the equilibrium state $\phi = \dot{\phi} = \eta = 0$ of the system in Eq. (7) is stable in the large).

In [39,41], it is considered the characteristic shown in Fig. 5, which corresponds to the presence of an insensitivity zone, i.e.,

$$F = \begin{cases} K & \text{for } \psi > 0, \\ -K & \text{for } \psi < 0, \\ 0 & \text{for } -\psi_0 < \psi < \psi_0, \\ a(\dot{\phi} + \beta\ddot{\phi}) & \text{for } \psi = -\psi_0,\ \psi = \psi_0. \end{cases} \tag{12}$$

Assuming $A = M\beta > 0$, $B = \dfrac{M}{Na} > 0$ and introducing

$$t' = Mt, \qquad z = \frac{M^3}{NK}\frac{d^2\phi}{dt'^2},$$
$$u = \frac{M^3}{NK}\left\{\frac{d\phi}{dt'} + \frac{d^2\phi}{dt'^2}\right\},$$

we reduce system (7) to the form

$$\begin{aligned} \frac{dz}{dt'} &= -z + f(u, z, \psi), \\ \frac{du}{dt'} &= f(u, z, \psi), \\ \frac{d\psi}{dt'} &= g(u, z, \psi), \end{aligned} \tag{13}$$

where

$$\begin{array}{llll} f \equiv -1, & g \equiv u + (A-1)z - B & \text{if} & \psi > \psi_0, \\ f \equiv 1, & g \equiv u + (A-1)z + B & \text{if} & \psi < \psi_0, \\ f \equiv 0, & g \equiv u + (A-1)z & \text{if} & |\psi| < \psi_0, \end{array}$$

$$f \equiv -\frac{1}{B}\,u + \frac{1-A}{B}z, \qquad g \equiv 0 \begin{cases} \text{if } \psi = \psi_0, & 0 < u + (A-1)z < B, \\ \text{if } \psi = -\psi_0, & -B < u + (A-1)z < 0. \end{cases}$$

In what follows, we provide a study of solutions to the system in Eq. (13) that is defined by the requirement for $u(t')$, $z(t')$, $\psi(t')$ to be continuous at the points of discontinuity of $f(u, z, \psi)$ and $g(u, z, \psi)$. In particular, we consider the sliding mode manifolds

$$\begin{array}{lll} \sigma: & \psi = \psi_0, & 0 < u + (A-1)z < B, \\ \sigma': & \psi = -\psi_0, & -B < u + (A-1)z < 0. \end{array} \tag{14}$$

The system in Eq. (13) with insensitivity zone has the rest segment $\dot\psi = \eta = 0$, $-\sigma_0 \le \psi \le \sigma_0$. In [39, 41], the stability of this segment was not studied due to complexity of calculations involved in the method of point maps. However, it was shown in [42] that under the condition in Eq. (11), the above rest segment is stable in the large. In other words, the presence of insensitivity zone in the nonlinear characteristic of a servomotor does not alter the stability domain (11), obtained for the case with no insensitivity zone.

Along with the works [38, 39], an independent study [36] was published in which it is continued the study of the control system, considered in [37],

$$\begin{aligned} m\frac{dv}{dt} + kv &= Q, \\ \frac{dr}{dt} &= v, \\ \frac{dQ}{dt} &= -qf_*(\mu), \end{aligned} \tag{15}$$

where r stands for the deviation of a controlled parameter from its value in the equilibrium state; v denotes the rate of change of this parameter; and Q is the coordinate of the control system. In the last equation (servomotor equation), the quantity μ,

$$\mu = av + br + cQ,$$

is the opening of a valve that controls the servomotor movement. Quantities m, k, q, a, b, and c are constant coefficients, while $f_*(\mu)$ is the nonlinear characteristic with a symmetric insensitivity zone and is similar to the characteristic shown in Fig. 5.

Performing the change of variables

$$x_1 = \frac{m}{qT^2}v - \frac{1}{qT}Q,$$
$$x_2 = \frac{1}{qT}Q,$$
$$x_3 = \frac{m\mu}{aqT^2},$$

we reduce the system in Eq. (15) to the form

$$\begin{aligned} \frac{x_1}{d\tau} &= -x_1 + f(x_3), \\ \frac{x_2}{d\tau} &= -f(x_3), \\ \frac{x_3}{d\tau} &= (\alpha - 1)x_1 + \alpha x_3 - rf(x_3), \end{aligned} \tag{16}$$

where $\tau = \dfrac{kt}{m}$, $\alpha = \dfrac{bT}{a}$, $r = \dfrac{cm}{aT}$, $f(x_3) = f_*(\mu)$.

In [36], the second Lyapunov method was used, and Lyapunov functions of the "quadratic form plus integral of nonlinearity" type were employed for the first time. Let us write them out here. For the case $\alpha > 1$, $r + 1 - \alpha > 0$, it is considered the Lyapunov function of the form

$$V = \int_0^{x_3} f(x_3)dx_3 + \frac{\alpha}{2}{x_2}^2 + \frac{\alpha - 1}{2}{x_1}^2.$$

The derivative of V, by virtue of system (16), is as follows:

$$\dot{V} = -(\alpha - 1)[f(x_3) - x_1]^2 - (r + 1 - \alpha)[f(x_3)]^2.$$

In the case where $0 < \alpha < 1$, $r > 0$, they considered the Lyapunov function of the form

$$V = \int_0^{x_3} f(x_3)dx_3 + \frac{1 - \alpha}{2}{x_1}^2 + \frac{\alpha}{2}{x_2}^2.$$

In this case, the derivative of V, by virtue of system (16), has the form:

$$\dot{V} = -(1 - \alpha)x_1^2 - r[f(x_3)]^2.$$

This made it possible to derive the following condition for the control process to be stable:

$$r > 0, \qquad \alpha > 0, \qquad \alpha - 1 - r > 0. \tag{17}$$

It should be noted that by performing the change of variables $z = -x_1$, $u = x_2$, $\psi = x_3$, the system in Eq. (16) can be reduced to system (9), where $A = 2 - \alpha$ and $B = r$.

Thus, the same problem on heading hold for a neutral airplane using autopilot with a constant servomotor speed was considered in [36–39]. In this case, the problem in [36] was the first problem on absolute stability [43]. Results obtained by A.I. Lurie, V.N. Postnikov, and N.N. Bautin gave impetus to the development of not only the theory of absolute stability but also the general theory of discontinuous systems [42,44–49]. A.A. Andronov and N.N. Bautin were the first to rigorously treat

the main peculiarities of discontinuous systems using the example of a three-dimensional system. They described the sliding mode manifold and the way the system behaves when crossing the discontinuity manifold.[2] In turn, generalizing the Lyapunov-type theorems and the absolute stability for discontinuous systems (see, for example, the works by A.Kh. Gelig and G.A. Leonov [42, 50, 51]) and using the Lyapunov function of the "integral of nonlinearity plus quadratic form" type, which was proposed for the first time in the work by A.I. Lurie and V.N. Postnikov, one can consider the problem in a more general form without partitioning trajectories into pieces [42].

1.3. Vyshnegradskii Model

The central problem in the direct control theory was posed by I.A. Vyshnegradskii in 1877. He considered a machine–control system (governor) that can be written as follows [52]:

$$\ddot{x} + B\dot{x} + Ax = y - \frac{1}{2}\operatorname{sgn}\dot{x}, \qquad \dot{y} = -x. \tag{18}$$

The first equation describes the motion of the governor with Coulomb and dry frictions, while the second describes the dynamics of the machine. Parameters A and B are referred to as "the Vyshnegradskii parameters" (or "the chief parameters of the direct control theory").

The system in Eq. (18) can be written in the form of the third-order system

$$\begin{gathered}\dot{u} = Pu + q\varphi(\sigma), \qquad \sigma = r^*u, \qquad \varphi(\sigma) = \frac{1}{2}\operatorname{sgn}(\sigma),\\ u = \begin{pmatrix} x \\ y \\ z \end{pmatrix}, \qquad P = \begin{pmatrix} 0 & 0 & 1 \\ -1 & 0 & 0 \\ -A & 1 & -B \end{pmatrix}, \qquad q = \begin{pmatrix} 0 \\ 0 \\ -1 \end{pmatrix}, \qquad r = \begin{pmatrix} 0 \\ 0 \\ 1 \end{pmatrix}.\end{gathered} \tag{19}$$

In his work [52], I.A. Vyshnegradskii pointed out that given no Coulomb friction (i.e., with $\varphi(\sigma) \equiv 0$), the linear system in Eq. (19) is asymptotically stable if the following relations hold true:

$$A > 0, \qquad B > 0, \qquad AB > 1. \tag{20}$$

To study the dynamics of the nonlinear system in Eq. (19), A.A. Andronov and A.G. Majer [53], on the discontinuity plane

$$S = \{u:\ r^*u = 0 = 0\}, \tag{21}$$

based on the physical properties of Coulomb friction, extended the definition of the nonlinearity

$$\begin{gathered}\hat{\varphi}(u) = \begin{cases} \varphi(r^*u) = \dfrac{1}{2}\operatorname{sgn}(r^*u) & \text{for } u \notin S, \\ \hat{\varphi}_S(u) & \text{for } u \in S, \end{cases}\\ \hat{\varphi}_S(u) = \hat{\varphi}_S(x,y,z) = \begin{cases} 1 & \text{for } Ax + y > \dfrac{1}{2}, \\ -1 & \text{for } -Ax + y < \dfrac{1}{2}, \\ -2Ax + 2y & \text{for } |-Ax + y| \le \dfrac{1}{2}, \end{cases}\end{gathered} \tag{22}$$

and considered the system

$$\dot{u} = Pu + q\hat{\varphi}(u). \tag{23}$$

Here, trajectories that pass through the points of the half-planes $\{z = 0, -Ax + y > 1/2\}$ and $\{z = 0, -Ax + y < -1/2\}$ "pierce" plane $z = 0$ toward $z > 0$ and toward $z < 0$, respectively.

[2] It is worth mentioning that in 1944, M.V. Keldysh [35] provided a nonrigorous description for the behavior of a fourth-order system with a more complex discontinuous nonlinearity.

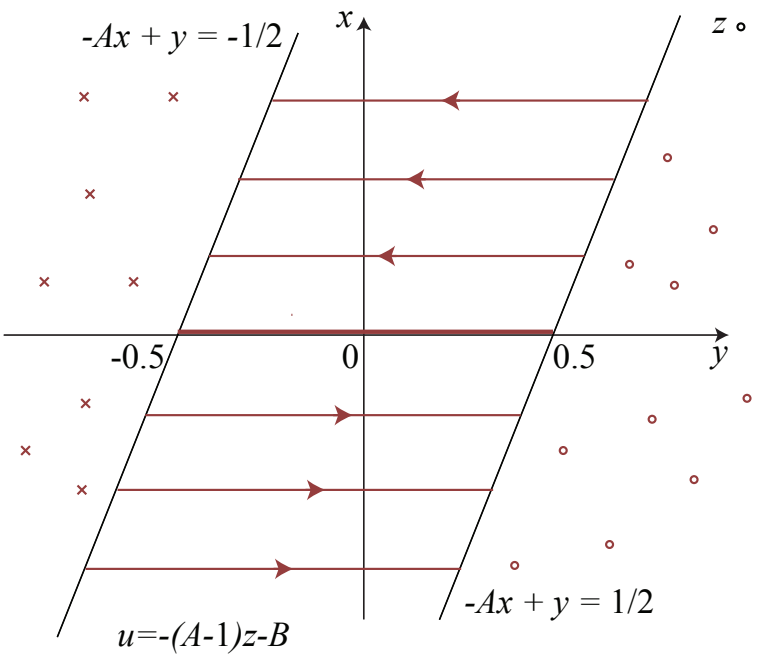

Fig. 6. Phase portrait of system (23). Here, plane $z = 0$ is in the drawing plane, and trajectories moving from and toward an observer are marked with the crosses and circles, respectively.

Domain $\{z = 0, |Ax + y| \le 1/2\}$ is a sliding mode manifold. Trajectories that approach this manifold on both sides have opposite directions. Let us consider in details the trajectories of sliding mode manifold. It can be easily seen that such trajectories are described by the differential equations

$$\dot{x} = 0, \qquad \dot{y} = -x, \qquad \dot{z} = 0, \tag{24}$$

i.e., the sliding mode solutions are straight lines $x(t) = x_0$, $y(t) = -x_0 t + y_0$, $z(t) = 0$, x_0, $y_0 \in \mathbb{R}$. The trajectories of the system in Eq. (23) leave the manifold $\{z = 0, |Ax + y| \le 1/2\}$ via half-line

$$\{-Ax + y = 1/2,\ y < 0,\ z = 0\},$$

heading for half-space $z > 0$, or via half-line

$$\{-Ax + y = -1/2,\ y > 0,\ z = 0\},$$

heading for half-space $z < 0$ (see Fig. 6).

It follows from the extension of definition of $\hat{\varphi}(u)$ that the equilibrium states of the system in Eq. (23) are points $x = 0$, $y = y_0$, $z = 0$, where $y_0 \in [-1/2, 1/2]$, i.e., the equilibrium states of the system in Eq. (23) belong to the sliding mode manifold

$$D = \{u :\ r^* u = 0,\ -r^* P u / r^* q \in [\varphi(0-), \varphi(0+)]\} \tag{25}$$

and fill the rest segment

$$\Lambda = \{u = P^{-1} q s,\ s \in [\varphi(0-), \varphi(0+)]\} = \{x = z = 0,\ y \in [\varphi(0-), \varphi(0+)]\},$$

which is marked in Fig. 6 by the thick line.

One of the results obtained in [53] was the following condition on the absolute stability of the system:

$$AB > 1. \tag{26}$$

The control process converges in this case for any initial conditions, and the curve with equation $AB = 1$ is known as the Vyshnegradskii hyperbola (see Fig. 7).

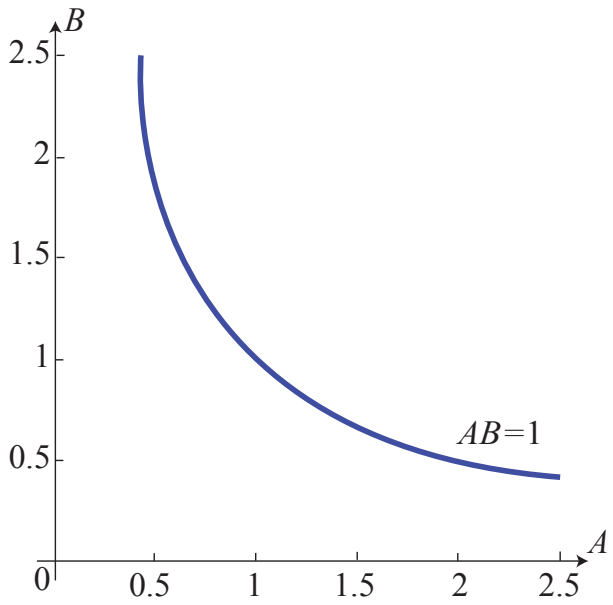

Fig. 7. Domain of parameters of stable systems described by Eqs. (19).

2. DIFFERENTIAL INCLUSIONS. DEFINITIONS OF SOLUTIONS

Let us consider the system

$$\dot{u} = f(t, u), \qquad t \in \mathbb{R}, \qquad u \in \mathbb{R}^n, \tag{27}$$

where $f : \mathbb{R} \times \mathbb{R}^n \to \mathbb{R}^n$ is a piecewise-continuous function with the set of discontinuity points of zero measure.

Most definitions of solutions can be introduced in the following manner: for every point (t, u) in a domain G, we define a set $F(t, u)$ (extending the definition of the discontinuous right-hand side) in the space of dimension n. If f is continuous in (t, u) then set $F(t, u)$ consists of one point and coincides with f at this point. If (t, u) is the point of discontinuity of function f, then $F(t, u)$ is defined one way or another, depending on the definition, i.e., instead of Eq. (27), we consider the differential inclusion

$$\dot{u} \in F(t, u), \tag{28}$$

where $F(t, u)$ is a multi-valued function.

Mathematicians usually pose the problem of defining a multi-valued function F using a given function f, whereas in mechanics, the multi-valued function F is often given.

Definition 1. A solution to the system in Eq. (27) or the counterpart differential inclusion in Eq. (28) is an *absolutely continuous*[3] vector-function $u(t)$, defined on interval I, for which the derivative exists almost everywhere on I and

$$\dot{u}(t) \in F(t, u(t)). \tag{29}$$

[3] Let $I \subset \mathcal{D}_t \subset \mathbb{R}$ be a time interval. A function $u(t) : I \to \mathbb{R}^n$ is called *absolutely continuous* on I if for any positive ε there exists a positive δ such that for any finite sequence of nonoverlapping subintervals (t_{1k}, t_{2k}) from I, where $t_{1k}, t_{2k} \in I$, satisfying

$$\sum_k (t_{2k} - t_{1k}) < \delta,$$

we have

$$\sum_k ||u(t_{2k}) - u(t_{1k})|| < \varepsilon.$$

It is well known that an absolutely continuous vector-function $u(t)$ defined on interval I is differentiable almost everywhere on I. Hereinafter, we imply that the expression "almost everywhere on I" means "for all $t \in I$ for which $\dot{u}(t)$ exists" (see [54, p. 60]).

As mentioned in the introduction, the development of the theory of differential inclusions is usually associated with the works by French mathematician A. Marchaud and Polish mathematician S.K. Zaremba, published in 1934–1936 [1–4]. They studied equations of the form

$$Du \subset F(t,u), \tag{30}$$

where $t \in \mathcal{D}_t \subset \mathbb{R}$, $u \in \mathcal{D}_u \subset \mathbb{R}^n$ and $F(t,u)$ is a multi-valued vector-function that puts every point (t,u) in a certain domain $\mathcal{D} = \mathcal{D}_t \times \mathcal{D}_u$ in correspondence with a set $F(t,u)$ of points from $\mathbb{R}^n$. Marchaud and Zaremba introduced the notions of contingency and paratingency for operator D.

Definition 2. The contingency of a vector-function $u(t)$ at a point t_0 is the set $\operatorname{Cont} u(t_0)$ of all limit points of sequences $\dfrac{u(t_i)-u(t_0)}{t_i-t_0}$, $t_i \to t_0$, $i = 1,2,\ldots$

Definition 3. The paratingency of a vector-function $u(t)$ at a point t_0 is the set $\operatorname{Parat} u(t_0)$ of all limit points of sequences $\dfrac{u(t_i)-u(t_j)}{t_i-t_j}$, $t_i \to t_0$, $t_j \to t_0$, $i = 1,2,\ldots$

T. Wazewski continued Marchaud and Zaremba's research and proved [55] that if $u(t)$ is a solution to the differential inclusion in Eq. (30) in the Marchaud sense (i.e., it is a solution to the equation in contingencies) then vector-function $u(t)$ is *absolutely continuous*.

Introducing the property of absolute continuity for solution $u(t)$ played a key role in the development of the theory of differential inclusions and equations with a discontinuous right-hand side, as it made it possible to avoid using artificial constructions in Definition 2 and Definition 3 and consider ordinary derivative almost everywhere. In what follows, we will consider three possible approaches to extending the definition of discontinuous systems and defining their solutions (various other approaches are discussed, for example, in [47, 54, 56–59]).

2.1. Filippov's Approach

In 1960, A.F. Filippov published his works [44, 60], where he had considered absolutely continuous functions as solutions to a differential equation with a discontinuous right-hand side. Filippov's approach is one of the most popular among other definitions of solutions to systems with discontinuous right-hand side. Following [44], let us consider the system in Eq. (27).

Definition 4. A vector-function $u(t)$, defined on interval I, is called a *solution* to the system in Eq. (27) if it is continuous and almost for all $t \in I$, vector $\dot{u}(t)$ belongs to the minimum closed convex set that contains all $f(t,u')$ when u' runs over almost entire δ-neighborhood of point $u(t)$ in $\mathbb{R}^n$ (for a fixed t), i.e.,

$$\dot{u}(t) \in \prod_{\delta>0} \prod_{\mu N=0} \operatorname{conv} f(t, B(u(t),\delta) - N). \tag{31}$$

Here, the right-hand side in Eq. (31) is called Filippov's extension of the right-hand side of the discontinuous system (27).

Let us consider the case where the system in Eq. (27) is autonomous and vector-function $f(u)$ is discontinuous on a certain smooth surface S in $\mathbb{R}^n$ and continuous in the vicinity of this surface. Let there exist right- and left-hand limits $f_+(u)$ and $f_-(u)$ of vector-function $f(u)$ as point u approaches surface S from one or the other side. Suppose that both vectors $f_+(u)$ and $f_-(u)$ point toward the discontinuous surface S. Then a *sliding mode* emerges. According to Definition 4 (see the formula in Eq. (31)), the definition of the sliding-mode vector field on a discontinuous surface can be extended as follows. Let us construct a plane tangent to surface S at a point u and a segment l that joins the endpoints of vectors $f_+(u)$ and $f_-(u)$. Then, it is possible to construct a vector originating from point u and ending at the point of intersection of the segment and the tangent plane, $f_0 = f_0(u)$. According to Definition 4, vector $f_0(u)$ defines the vector field at point u.

The derived solution to the system in Eq. (27) satisfies Definition 4, but there is a number of important applied problems where Definition 4 cannot be applied. As an example of such a problem,

let us consider the problem of synthesizing controls s_1 and s_2 that are bounded, $|s_1| \le 1$, $|s_2| \le 1$, and optimally quickly map each point $(u_1(0), u_2(0))$ of the system

$$\dot{u}_1 = u_2 s_1, \qquad \dot{u}_2 = s_2 \tag{32}$$

to the zero. It is well known [61] that synthesizing such a control is possible on the entire plane (u_1, u_2). For example, in the first quadrant of the plane, the optimum control will be the control

$$s_1 = \begin{cases} 1 & \text{for } u_1 < 0.5{u_2}^2, \\ -1 & \text{for } u_1 \ge 0.5{u_2}^2, \end{cases} \qquad s_2 = \begin{cases} -1 & \text{for } u_1 \le 0.5{u_2}^2, \\ 1 & \text{for } u_1 > 0.5{u_2}^2. \end{cases} \tag{33}$$

In particular, the trajectory $u_1 = 0.5{u_2}^2$ is optimum. For this trajectory, the system in Eq. (32) takes on the form $\dot{u}_1 = -u_2$, $\dot{u}_2 = -1$. Let us take a point $u = (u_1, u_2)$ on this trajectory and start approaching this trajectory from the side $u_1 < 0.5{u_2}^2$. The limit value of the right-hand side of the system in Eq. (32) has the form $f_+(u) = (u_2, -1)$. If we approach the trajectory from the side $u_1 > 0.5{u_2}^2$, then the limit $f_-(u) = (-u_2, 1)$. As $f_+(u) = -f_-(u)$, then, in this special case, segment l intersects point u, i.e., $f_0(u) = 0$, and, according to Definition 4, the solution in the sliding mode is an equilibrium state. At the same time, $(-u_2, -1)$ is the velocity vector of the optimum trajectory. Thus, the optimum trajectory is not a solution in the sense of Definition 4, proposed by Filippov.

2.2. Aizerman–Pyatnitskii's Approach

Let us consider the approach to defining the solutions of discontinuous systems in terms of approximations by the solutions of continuous systems. This approach was developed in [27, 45, 46] and others.

M.A. Aizerman and E.S. Pyatnitskii [45] suggested a different definition of the solution to equations with discontinuous right-hand side. This definition makes it possible to use ordinary derivative. Let us consider the approach that these authors proposed in a special case when $f(t, u)$ is discontinuous on surface Σ. We consider the sequence of continuous vector-functions $f_\varepsilon(t, u)$ that coincides with $f(t, u)$ outside of the ε-neighborhood of surface Σ and tends to $f(t, u)$ as $\varepsilon \to 0$ at every point that does not belong to Σ. Let $u_\varepsilon(t)$ be a solution to the system

$$\dot{u} = f_\varepsilon(t, u). \tag{34}$$

Definition 5. A solution to the system in Eq. (27) in the Aizerman–Pyatnitskii sense is said to be the limit of any uniformly converging subsequence of solutions $u_{\varepsilon_k}(t)$, viz.

$$u_{\varepsilon_k}(t) \rightrightarrows u(t).$$

Generally speaking, there may exist more than one such limit. Note that this definition extension, introduced in [45], does not always pertain to applied problems.

For example, let us consider the system

$$\dot{u} \in Au + b\phi(\sigma), \qquad \sigma = c^* u, \tag{35}$$

where $\phi(\sigma)$ is the characteristic of dry friction shown in Fig. 8 or Fig. 9, i.e.,

$$\phi(\sigma) = \begin{cases} \operatorname{sgn} \sigma & \text{for } \sigma \ne 0, \\ [-1, 1] & \text{for } \sigma = 0, \end{cases} \qquad \text{or} \qquad \phi(\sigma) = \begin{cases} \operatorname{sgn} \sigma & \text{for } \sigma \ne 0, \\ [-\alpha, \alpha] & \text{for } \sigma = 0. \end{cases} \tag{36}$$

Since the definitions proposed by Filippov and Aizerman–Pyatnitskii only account for nonlinearities for which $\sigma \ne 0$, solutions to the system in Eq. (35) with the dry-friction characteristics presented in Figs. 8 and 9 coincide. This result does not represent the physics of this phenomenon.

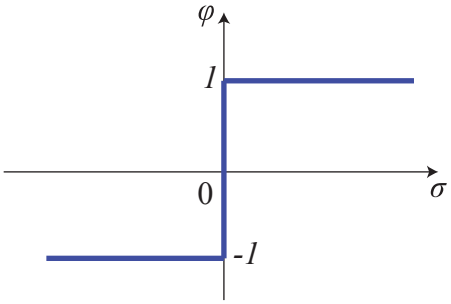

Fig. 8. Dry friction model: the friction of rest does not assume values that are greater in magnitude that sliding friction.

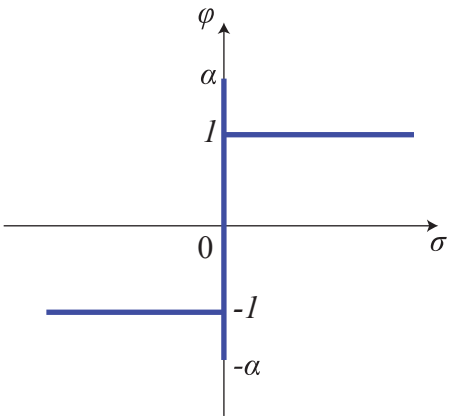

Fig. 9. Dry friction model: the friction of rest may assume values that are greater in magnitude that sliding friction.

In order to take dynamics on the discontinuity surface into account, one needs to consider a more adequate approach, where instead of the system with the discontinuous right-hand side (27), a system with multi-valued right-hand side is studied, i.e., the differential inclusion in Eq. (28) is considered.

2.3. Gelig–Leonov–Yakubovich Approach

As has been demonstrated above, Filippov's definition may yield incorrect results for certain problems in physics, i.e., we should consider a more general class of multi-valued functions $F(t,u)$. One of such generalizations was considered by A.Kh. Gelig, G.A. Leonov, and V.A. Yakubovich in [42]. Further, in order to construct the theory, we should also assume that the multi-valued function $F(t,u)$ is semicontinuous.

Definition 6. A function $F(t,u)$ is said to be *semicontinuous* (upper semicontinuous, β-continuous) at a point (t_0,u_0) if for any $\varepsilon>0$ there exists $\delta(\varepsilon,t,u)$, such that set $F(t,u)$ is contained in the ε-neighborhood of set $F(u_0,u_0)$ when point (t,u) runs over the δ-neighborhood of point (t_0,u_0).

Definition 7. A vector-function $u(t)$, defined on a segment (t_1,t_2), is called a *solution* to Eq. (28) if the multi-valued function $F(t,u)$ is semicontinuous and $\forall(t,u)\in\mathcal{D}$ the set $F(t,u)$ is convex, closed, and bounded.

Unlike in Filippov's extension of definition, here the set $F(t,u)$ is not required to be minimum. The following local theorem on the existence of solutions to a differential inclusion holds true [42].

Theorem 1. *Suppose that a multi-valued function $F(t,u)$ is semicontinuous for all points (t_1,u_1) from the domain*

$$\mathcal{D}_1 \subset \mathcal{D}: \qquad |t_1-t_0| \le \alpha, \qquad |u_1-a| \le \rho,$$

and set $F(t_1,u_1)$ is bounded, convex, and closed. In addition, let us assume

$$\sup|y| = c \qquad for \qquad y \in F(t_1,u_1), \qquad (t_1,u_1) \in \mathcal{D}_1.$$

Then for $|t-t_0| \le \tau = \min(\alpha, \rho/c)$, there exists at least one solution $u(t)$ with the initial data $u(t_0)=a$ that satisfies Eq. (28) in the sense of Definition 1.

Let us also provide here a theorem on the continuability of a solution that stays within a bounded domain [42].

Theorem 2. *If $\forall t \in [0,T)$ a solution to the system in Eq. (28) belongs to a certain compact domain $\mathcal{G}$ from $\mathbb{R}^n$, then $x(t)$ is defined on $[0,T]$ and $x(t) \in \mathcal{G}$.*

Thus, the solution to the system in Eq. (28) is continuable as long as it is finite.

Let us consider the case of the autonomous Eq. (28), which is rather important for applications, specifically, for

$$\frac{du}{dt} \in F(u). \tag{37}$$

The following theorem holds true.

Theorem 3. *Let the ω-limit set Ω of trajectory $u(t,b)$ for the system in Eq. (37) be bounded. Then at least one $u(t,a)$, defined for $t \in (-\infty,+\infty)$ and consisting entirely of ω-limit points, passes through any ω-limit point $a \in \Omega$, i.e., $u(t,a) \subset \Omega$ for $t \in \mathbb{R}^1$.*

The proofs of Theorems 1, 2, and 3 are available in [42].

Various other theorems of the qualitative theory also hold true for the differential inclusion in Eq. (28) (see, for example, [42, 54, 62]).

Now let us consider Eq. (29) with $F(t,u(t)) = Pu(t) + q\phi(r^*u(t))$, i.e.,

$$\dot{u}(t) \in Pu(t) + q\phi(r^*u(t),t) \tag{38}$$

for almost all t (here we assume that $F(t,u(t))$ satisfies the conditions in Definition 7, i.e., $F(t,u(t))$ satisfies the conditions 1; therefore, hereinafter we assume that solution exists for almost all $t \in I$). Here P, q, and r are constant matrices and $\phi(r^*u(t),t)$ is a multi-valued function.

If a matrix q^*q is nonsingular then

$$(q^*q)^{-1}q^*\left[\dot{u}(t) - Pu(t)\right] \in \phi(r^*u(t),t) \tag{39}$$

for almost all t.

The left-hand side in Eq. (39) is called a selector

$$\xi(t) = (q^*q)^{-1}q^*\left[\dot{u}(t) - Pu(t)\right] \tag{40}$$

and is a single-valued function that "concretizes" the multi-valued function $\phi(r^*u(t),t)$ for solution $u(t)$. In other words, the problem in Eq. (38) becomes as follows:

$$\dot{u}(t) = Pu(t) + q\xi(t) \qquad \text{for almost all } t, \tag{41}$$

$$\xi(t) \in \phi(r^*u(t),t). \tag{42}$$

For any solution $u(t)$ there exists a corresponding extension $\xi(t)$. As shown above, if the matrix q^*q is nonsingular then $\xi(t)$ is defined by the relation in Eq. (40) for almost all t and $\xi(t)$ is measurable.

Is there a measurable selector $\xi(t)$ in the case where $\det q^*q = 0$? The following theorem on the existence of a measurable selector, proved by B.M. Makarov specially for [42], plays an important role in studying differential inclusions as it makes it possible to replace a differential inclusion with a differential equation in a fairly general case while retaining the structure of the right-hand side.

Let $F(t,u,\xi)$ be a vector-function defined for $t \in I$, $u \in \mathbb{R}^n$, $\xi \in \mathbb{R}^m$ with values in $\mathbb{R}^n$. Suppose that $\sigma(t,u)$ is a continuous vector-function defined on $I \times \mathbb{R}^n$ with values from $\mathbb{R}^l$, and let $\phi(t,\sigma)$ be a multi-valued function defined on $I \times \mathbb{R}^l$ with values that are subsets of $\mathbb{R}^n$. The following theorem holds [42].

Theorem (Makarov's theorem, [42]). *Let a function F be continuous and ϕ be semicontinuous, with its values being subsets from $\mathbb{R}^n$. Let $u_0(t)$ be an absolutely continuous vector-function on $I \subset \mathcal{D}_t$ that satisfies the following conditions*:

$$\dot{u}_0(t) \in \{F[t,u_0(t),\xi] | \xi \in \mathcal{A}(t)\} \quad \textit{for almost all} \quad t \in I,$$

where

$$\mathcal{A}(t) = \phi[t, \sigma(t,u_0(t))].$$

Then there exists a Lebesgue measurable vector-function ξ_0 in I such that the following relations are valid:

$$\dot{u}_0(t) = F[t,u_0(t),\xi_0(t)], \qquad \xi_0(t) \in \mathcal{A}(t) \quad \textit{for almost all} \quad t \in I.$$

3. VYSHNEGRADSKII PROBLEM

Applying the method of point maps to the qualitative study of piecewise-linear discontinuous systems often proves labourious. Below we will show how the Vyshnegradskii problem can be qualitatively studied by developing the classical Lyapunov's ideas for the case of discontinuous systems.

By using the above theory of differential inclusions, passing from the system in Eq. (19) to the system in Eq. (23) in the work [53] can be substantiated as follows. Proceeding from the physical meaning of a discontinuous nonlinearity, let us perform a *procedure of regularization* of the discontinuous right-hand side of the system in Eq. (19), following Filippov's approach (see Definition 4) and replacing vector-function $f(u) = Pu + q\varphi(r^*u)$ with a semicontinuous multi-valued vector-function $F(u)$ with values that coincide with $f(u)$ outside of discontinuity points and are a minimum convex closed bounded set containing all possible limit points of $f(u)$ as u tends to S at the discontinuity points. Here $F(u)$ can be represented in the form

$$F(u) = Pu + q\Phi(u), \qquad \Phi(u) = \begin{cases} \varphi(r^*u), & r^*u \neq 0, \\ [\varphi(0-), \varphi(0+)], & r^*u = 0 \end{cases} \tag{43}$$

and we can switch from the system in Eq. (19) to the differential inclusion

$$\dot{u} \in F(u) = Pu + q\Phi(u). \tag{44}$$

For any initial data u_0 the differential inclusion in Eq. (44) has a solution (see Theorem 1) $u(t) = u(t,u_0), u(t_0,u_0) = u_0$ (generally speaking, not unique) on a certain time interval $I = [t_0,t_1)$ (while the solution stays bounded) such that $u(t)$ is an absolutely continuous function and has a derivative $\dot{u}(t)$ for almost all $t \in I = [t_0,t_1)$ for which we have

$$\dot{u}(t) \in Pu(t) + q\Phi(u(t)). \tag{45}$$

Outside of the discontinuity plane S, the behavior of the solution $u(t)$ is uniquely determined by the continuous vector field of the system in Eq. (19). For initial data in the discontinuity plane $u_0 \in S$ (or when the solution falls into the discontinuity plane at the time moment t_0), the behavior of the system may not be unique and the dynamics of the vector field can be refined, based on the vector-field dynamics near the discontinuity point and on the requirement for the solution to

be absolutely continuous. The solution with initial data in the discontinuity plane stays in that plane on a certain (maximum) time segment or the infinite interval $u(t) \in S,\ t \in [t_0, t_1]$. Here, the case of $t_0 = t_1$ corresponds to the crossing of the discontinuity surface, while the case of $t_0 < t_1$ corresponds to a sliding mode.

According to Theorem 4, for a solution $u(t)$ there exists such a extended nonlinearity $\hat{\varphi}(t) = \hat{\varphi}(t)$ that for almost all $t \in [t_0, t_1]$ (where derivate $\dot{u}(t)$ exists), we have the relation

$$\dot{u}(t) = Pu(t) + q\hat{\varphi}(t), \qquad \hat{\varphi}(t) \in \Phi(u(t)). \tag{46}$$

If $u_0 \in S$ then while relation $0 \equiv r^*\dot{u}(t) = r^*Pu(t) + r^*q\hat{\varphi}(t)$ holds true, the solution slides along the discontinuity plane $r^*u = x = 0$. Here, for the sliding to take place, it is necessary that $\hat{\varphi}(t) = \hat{\varphi}_S(u(t)) = -r^*Pu(t)/r^*q = y(t) \in \Phi(u(t))|_{r^*u(t)=0} = [\varphi(0-), \varphi(0+)]$ and, thus, sliding is possible in a band D. As matrix P is nonsingular, the sliding band contains the *rest segment*

$$\Lambda = \{u = P^{-1}qs,\ s \in [\varphi(0-), \varphi(0+)]\}.$$

In the case of the crossing (that is, where a trajectory crosses the discontinuity plane) of the discontinuity plane at $t = t_0$, the extension of the definition of the vector field is inessential and, for definiteness, we can define $\Phi(u(t_0))$ based on the continuity of

$$\hat{\varphi}_S(u) = \begin{cases} \varphi(0-), & r^*u = 0, \quad -r^*Pu/r^*q/\rho < \varphi(0-), \\ \varphi(0+), & r^*u = 0, \quad -r^*Pu/r^*q > \varphi(0+). \end{cases} \tag{47}$$

Note that the vector field in the vicinity of the sliding band D prevents the sliding trajectory from hopping off the band before reaching the band edge ∂D. It follows from the construction in Eq. (31) that for initial data from ∂D, the velocity vector is determined uniquely and the solution may not slide along ∂D.

Thus, for all initial data in the system, we have forward uniqueness (as time increases) and the construction in Eq. (31) makes it possible to pass from the differential inclusion in Eq. (44) to the system in Eq. (23) with a discontinuous right-hand side that describes the system dynamics both outside of and on the discontinuity surface.

3.1. Construction of Lyapunov Functions for the Global Stability and Instability Analysis

To simplify the nonlinear analysis, following [63], we perform linear changes of coordinates and time and pass to the system

$$\dot{x} = y - ax - \varphi(x), \quad \dot{y} = z - x, \quad \dot{z} = -ax, \quad a = \frac{1}{A\sqrt{A}}, \quad \varphi(x) = a(BA-1)x + \frac{1}{2\sqrt{A}}\operatorname{sgn}(x),$$

which can be rewritten in the form

$$\dot{u} = Pu + q\varphi(\sigma), \quad \sigma = r^*u, \qquad \varphi(\sigma) = \varphi(x) = a(BA-1)x + \frac{1}{2\sqrt{A}}\operatorname{sgn}(x),$$

$$u = \begin{pmatrix} x \\ y \\ z \end{pmatrix}, \qquad P = \begin{pmatrix} -a & 1 & 0 \\ -1 & 0 & 1 \\ -a & 0 & 0 \end{pmatrix}, \qquad q = \begin{pmatrix} -1 \\ 0 \\ 0 \end{pmatrix}, \qquad r = \begin{pmatrix} 1 \\ 0 \\ 0 \end{pmatrix}.$$

Here, the transfer function of the system has the form

$$W(s) = r^*(P - sI)^{-1}q = \frac{s^2}{s^3 + as^2 + s + a} = \frac{s^2}{(s^2+1)(s+a)}.$$

The corresponding discontinuity surface, sliding mode band, and rest segment take the form

$$\begin{aligned} &S = \{u:\ r^*u = x = 0\}, \\ &D = \{u:\ r^*u = x = 0,\ -r^*Pu/r^*q = y \in [\varphi(0-), \varphi(0+)]\}, \\ &\Lambda = \{u:\ u = -P^{-1}qs,\ s \in [\varphi(0-), \varphi(0+)]\} = \{x = z = 0,\ -P^{-1}q = y \in [\varphi(0-), \varphi(0+)]\}. \end{aligned} \tag{48}$$

The extended nonlinearity has the form

$$\hat{\varphi}(u)=\begin{cases}\varphi(r^*u) & \text{for } u\notin S,\\ \hat{\varphi}_S(u) & \text{for } u\in S,\end{cases}$$

$$\hat{\varphi}_S(u)=\hat{\varphi}_S(x,y,z)=\begin{cases}\varphi(0+) & \text{for } y=-r^*Pu/r^*q>\varphi(0+),\\ \varphi(0-) & \text{for } y=-r^*Pu/r^*q<\varphi(0-),\\ -r^*Pu/r^*q=y-ax & \text{for } y=-r^*Pu/r^*q\in[\varphi(0-),\varphi(0+)].\end{cases}\tag{49}$$

Let

$$h=P^*r=\begin{pmatrix}-A\\ 1\\ -B\end{pmatrix},\qquad \rho=r^*q=-1.$$

Let us consider the Lyapunov function

$$V(u)=V(x,y,z)=\frac{1}{2}(z-x)^2+\frac{1}{2}(y-\hat{\varphi}(x,y,z))^2+ax\hat{\varphi}(x,y,z)-a\int\limits_0^x\varphi(s)ds\geq 0,$$

which is discontinuous.[4] Outside of the discontinuity plane S, function $V(x,y,z)$ is smooth and has the form

$$V(x,y,z)=\frac{1}{2}(z-x)^2+\frac{1}{2}(y-\varphi(x))^2+ax\varphi(x)-a\int\limits_0^x\varphi(s)ds\geq 0,$$

and its derivative along the trajectories of the system in Eq. (43) obeys

$$\dot{V}(x(t),y(t),z(t))=-\varphi'(x(t))(y(t)-ax(t)-\varphi(x(t)))^2\leq 0,\qquad x(t)\neq 0.\tag{50}$$

Note that the form of the system implies that there is no time interval $t\in(t_1,t_2)$ such that $x(t)\equiv\text{const}$. Hence, here we have $V(x(t_1),y(t_1),z(t_1))<V(x(t_2),y(t_2),z(t_2))$.

On the trajectories with the initial data $u_0=(x_0,y_0,z_0)$ on the sliding band D, function $V(x,y,z)$ has the form

$$V(0,y(t),z(t))=\frac{1}{2}z(t)^2+\frac{1}{2}(y(t)-\hat{\varphi}_S(u(t)))^2\equiv z_0^2.\tag{51}$$

In this case, if the trajectory leaves the band after time t then we have the continuity

$$V(0,y(t),z(t))\equiv z_0^2=\lim_{t^+\to t}V(x(t^+),y(t^+),z(t^+)).$$

The crossing of the discontinuity surface $x=0$ occurs for

$$x=0,\qquad y\notin[\varphi(0-),\varphi(0+)],\tag{52}$$

and at the moment of intersection t, for the vector field we have

$$\begin{cases}\dot{x}(t)>0, & y(t)>\varphi(0+)\geq 0,\\ \dot{x}(t)<0, & y(t)<\varphi(0-)\leq 0,\\ \dot{y}(t)=z(t),\\ \dot{z}(t)=0.\end{cases}\tag{53}$$

[4] Other examples of using discontinuous Lyapunov functions are discussed in [20, 64].

In this case, for $t^- > t > t^+$, we have

$$\begin{aligned} &y(t) > \varphi(0+) \geq 0, \qquad \frac{1}{2}(y(t)-\varphi(0-))^2 \geq \frac{1}{2}z(t)^2 + \frac{1}{2}(y(t)-\varphi(0+))^2 = \lim_{t^+\to t} V(t^+), \\ &y(t) < \varphi(0-) \leq 0, \qquad \lim_{t^-\to t} V(t^-) = \frac{1}{2}z(t)^2 + \frac{1}{2}(y(t)-\varphi(0+))^2 \\ &\qquad\qquad \geq \frac{1}{2}z(t)^2 + \frac{1}{2}(y(t)-\varphi(0-))^2 = \lim_{t^+\to t} V(t^+). \end{aligned} \tag{54}$$

It follows from the above that function $V(u)$ possesses the following properties.

I. *For any trajectory $u(t,a)$ function $V(u(t,a))$ is a nonincreasing function of t.*

II. *It follows from $V(u(t,u_0)) = \text{const}$ at $t \geq 0$ that $u(t,u_0) \in D$ for $t \geq 0$.*

III. *For $u \in \Lambda$ we have $V(u) = 0$, and for $u \notin \Lambda$ we have $V(u) > 0$.*

Following [51], let us take a trajectory $u(t,u_0)$ and let u_0^ω be an arbitrary ω-limit point $u(t,a)$. Suppose that $u_0^\omega \notin D$. Then, taking advantage of the continuity of function $V(u)$ outside of D and property I, we arrive at

$$\lim_{t\to+\infty} V(u(t,u_0)) = V(u_0^\omega). \tag{55}$$

Point u_0^ω is visited by a trajectory $u(t,u_0^\omega)$ that consists of the ω-limit points of the trajectory $u(t,u_0)$. For each ω-limit point u_0^ω there exists a subsequence $t_k \to +\infty$ such that $u(t_k,u_0) \to u_0^\omega$. Hence, Eq. (55) implies the equality $V(u(t,u_0^\omega)) \equiv V(u_0^\omega)$. The above and II imply that $u_0^\omega \in D$. Thus, all ω-limit points of the system are situated in D and, therefore, are ω-limit points of the system. However, the set of ω-limit points belonging to D coincides with the segment of rest Λ. Therefore, for all u_0, we have

$$\lim_{t\to+\infty} \min_{v\in\Lambda} \|u(t,u_0) - v\| = 0. \tag{56}$$

Now let us prove the local stability of Λ. In the proof, we cannot benefit from the known reasoning by A.M. Lyapunov in view of function $V(u)$ being discontinuous. However, we will show that there exists such a subsequence of δ-neighborhoods of Λ_δ of the stationary set Λ that collapse to Λ as $\delta \to 0$ and such a sequence of times τ_δ ($\lim_{\delta\to0}\tau_\delta = 0$) that

$$\lim_{\delta\to0} V[u(\tau_\delta,u_0)] = 0 \quad \forall u_0 \in \Lambda_\delta. \tag{57}$$

This assertion implies stability in the small. Indeed, let us fix an arbitrary neighborhood Λ_ε. Based on ε, let us select a number $\delta > 0$ so that the following relations hold true:

$$\begin{aligned} &u(t,u_0) \in \Lambda_{\varepsilon/2} \quad \forall t \in [0,\tau_\delta], \quad u \in \Lambda_\delta, \\ &\sup_{u_0\in\Lambda_\delta} V[u(\tau_\delta,u_0)] < \inf_{u\in\Gamma_\varepsilon} V(u), \end{aligned} \tag{58}$$

where Γ_ε is the boundary of Λ_ε. Property III of function $V(u)$ and the relation in Eq. (57) imply that such δ always exists. Property I of function $V(u)$ and the relations in Eq. (58) imply that $u(t,u_0) \in \Lambda_\varepsilon$ for all $t \geq 0$, and, therefore, the rest segment Λ is locally stable.

Now let us prove the relation in Eq. (57). For $u_0^\omega \in \Lambda$ and satisfying $h^* u_0^\omega = -\rho\varphi(+0)$, function $V(u_0^\omega)$ is continuous with respect to set $L^+ = \{u|\ r^* u_0^\omega \geq 0\}$ and the following estimate holds:

$$V[u(0,u_0)] \leq r_\alpha,$$

where

$$u_0 \in U_\alpha(u_0^\omega) \cap L^+, \qquad \lim_{\alpha\to0} r_\alpha = 0.$$

By $U_\alpha(u_0^\omega)$ we denoted the α-neighborhood of point u_0^ω. It can be easily seen from considering the qualitative picture of the phase space that for a sufficiently small α all trajectories with initial data from set $U_\alpha(u_0^\omega) \cap \{x:\ r^*r < 0\}$ will fall into subspace L^+ within period τ_α. Thus, we have

$$V[u(\tau_\alpha, u_0)] \le r_\alpha, \tag{59}$$

where $u_0 \in U_\alpha(u_0^\omega)$, $\lim_{\alpha\to 0} r_\alpha = 0$.

The estimate in Eq. (59) is proved similarly for the case of $u_0^\omega \in \Lambda$ and $h^* u_0^\omega = -\rho\varphi(-0)$.

Let us consider the case where $u_0^\omega \in \Lambda \cap \overset{\circ}{D}$, where $\overset{\circ}{D}$ is the interior of set D. It can be easily seen that for a sufficiently small α_a that all trajectories with initial data from $U_{\alpha_a}(u_0^\omega)$ will fall onto the sliding mode surface D within time period τ_{α_a}. However, by virtue of the continuity of function $V(u)$ with respect to D, we have

$$V[u(\tau_{\alpha_a}, u_0)] \le r_{\alpha_a},$$

where

$$u_0 \in U_{\alpha_a}(u_0^\omega), \qquad \lim_{\alpha_a\to 0} \tau_{\alpha_a} = 0, \qquad \lim_{\alpha_a\to 0} r_{\alpha_a} = 0.$$

Sets $U_{\alpha_a}(u_0^\omega)$ and $U_\alpha(u_0^\omega)$ form a cover of a certain closed neighborhood $\overline{\Lambda_\delta}$ of the segment of rest Λ. Having selected a finite subcover, based on the Heine–Borel theorem, we define τ_δ as the maximum of all $\tau_{\alpha_a}, \tau_\alpha$ from the subcover. Then we similarly construct r_δ. Thus, the relation in Eq. (57) is proved.

Let $A > 0, B > 0, AB < 1$. Then the discriminant of the cubic equation

$$\Delta = -4B^3 + 1 - 4A^3 + 18 - 27 = -4(B^3 + C^3 + 2) < 0,$$

and, therefore, the equation has one real and two complex conjugate roots $-\gamma, \alpha \pm i\omega$. In this case, the product of the roots is -1 and, hence, the real root is negative (i.e., $\gamma > 0$), while the complex conjugate ones have negative real part (i.e., $\alpha > 0$) due to violation of the stability condition $AB > 1$. Then the system in Eq. (19) can be reduced with a nonsingular transformation to the form

$$P = \begin{pmatrix} \alpha & \omega & 0 \\ \alpha & -\omega & 0 \\ 0 & 0 & -\gamma \end{pmatrix}, \qquad q = \begin{pmatrix} q_1 \\ q_2 \\ q_3 \end{pmatrix}, \qquad r = \begin{pmatrix} r_1 \\ r_2 \\ r_3 \end{pmatrix}. \tag{60}$$

Let us consider the Lyapunov function $V(x, y, z) = x^2 + y^2$. For the derivative along the solutions of the system, we obtain

$$\dot V(x(t), y(t), z(t)) = 2\alpha(x^2(t) + y^2(t)) + q_1 x\varphi(\sigma(t)) + q_2 y\varphi(\sigma(t)) \ge \varepsilon V - c,$$

where c, ε are some positive constants. For sufficiently large $x^2 + y^2 > R$, this implies that $V(x(t), y(t), z(t)) \to +\infty$ as $t \to +\infty$ and, therefore, there is no global stability.

We have thus proved the following assertion.

Theorem. *Let $A > 0$, $B > 0$. If $AB > 1$, then the system in Eq.* (19) *is globally stable* (*all the solutions of the system tend to the rest segment, which is Lyapunov-stable*). *If $AB < 1$ then the system in Eq.* (19) *is not globally stable.*

3.2. Numerical Modeling

The forward uniqueness (as time increases) of the system makes it possible to perform the efficient numerical analysis. Let us provide some examples of modeling the discontinuous system in Eq. (19) with the *MATLAB* package.

4. HIDDEN ATTRACTORS IN THE CHUA SYSTEM

Let us provide an example of modeling discontinuous systems numerically that is based on the Aizerman–Pyatnitskii approach and compare it with the modeling based on the Filippov approach.

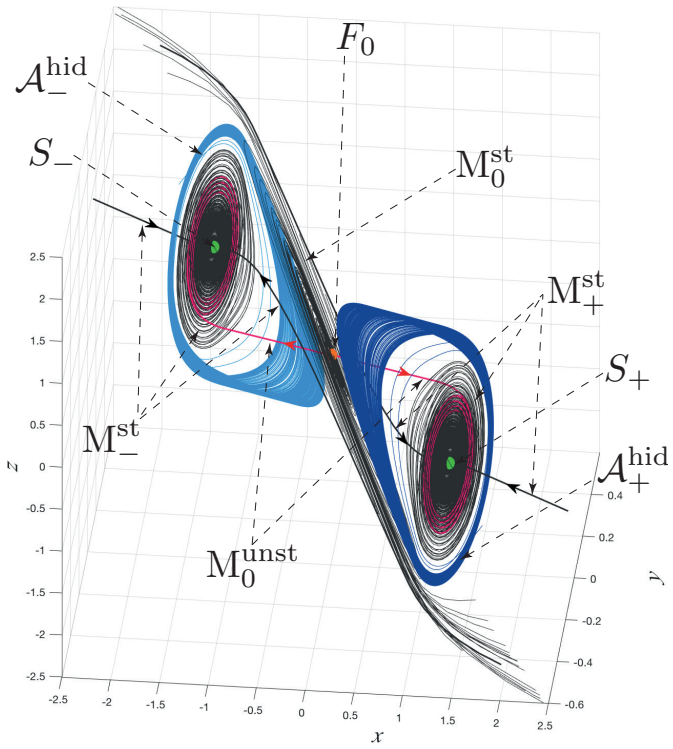

Fig. 10. Two symmetric hidden chaotic attractors $\mathcal{A}_+^{\rm hid}$ and $\mathcal{A}_-^{\rm hid}$ in the classical Chua system. Trajectories from the unstable manifold $M_0^{\rm unst}$ of saddle points F_0 are pulled toward locally stable equilibrium states $S_\pm$; trajectories from the stable manifolds $M_0^{\rm st}$, $M_+^{\rm st}$, and $M_-^{\rm st}$ are attracted toward F_0 or $S_\pm$.

Let us consider the following discontinuous system—a modified Chua system with a discontinuous characteristic [65–67]:

$$\begin{aligned}\dot{x} &= -\alpha(m_1+1)x + \alpha y - \alpha(m_0-m_1)\mathrm{sgn}\,(x),\\ \dot{y} &= x - y + z,\\ \dot{z} &= -\beta y - \gamma z,\end{aligned} \tag{61}$$

where α, β, γ, m_0, m_1 are system parameters.

It was shown in the paper [68] that with the parameters $\alpha = 8.4$, $\beta = 12$, $\gamma = -0.005$, $m_0 = -1.2$, and $m_1 = -0.05$, the classical Chua system (system (61) in which $\mathrm{sgn}\,(x)$ is replaced with $\mathrm{sat}(x) = \frac{1}{2}(|x+1| - |x-1|)$) has the so-called hidden attractor[5] (see Fig. 11 and Fig. 10). In the system considered, there are also the zero equilibrium state of the saddle-focus

[5] To visualize an attractor, it is necessary to choose an initial point in attractor's basin of attraction and observe how the trajectory starting from this initial point after a transient process visualizes the attractor. Thus, from a computational point of view, it is natural to suggest the following classification of attractors, based on the simplicity of finding the basin of attraction in the phase space: an attractor is called a self-excited attractor if its basin of attraction intersects with any open neighborhood of a stationary state (an equilibrium); otherwise, it is called a hidden attractor. Hidden attractors are attractors in the systems without equilibria (see, e.g., electromechanical systems with the Sommerfeld effect [75, 76]), and in the systems with only one stable equilibrium (see, e.g. counterexamples [72, 77] to the Aizerman's and Kalman's conjectures [75, 76]). One of the first related problems is the second part of Hilbert's 16th problem [80] on the number and mutual disposition of limit cycles in two-dimensional polynomial systems where nested limit cycles exhibit hidden periodic oscillations [72, 81, 82]. For the multidimensional systems, the corresponding problem [83] is to determine the number and mutual disposition of attractors and repellers (e.g., in dependence on the degree of polynomials in the right-hand side of the system).

The classification of attractors as being hidden or self-excited was introduced in connection with the discovery of the first hidden Chua attractor [65, 69–71, 84, 85] and then has captured attention of scientists from around the world (see, e.g. [86–116]). By now, hidden attractors have been discovered in various physical, mechanical, and electronic models [117–123].

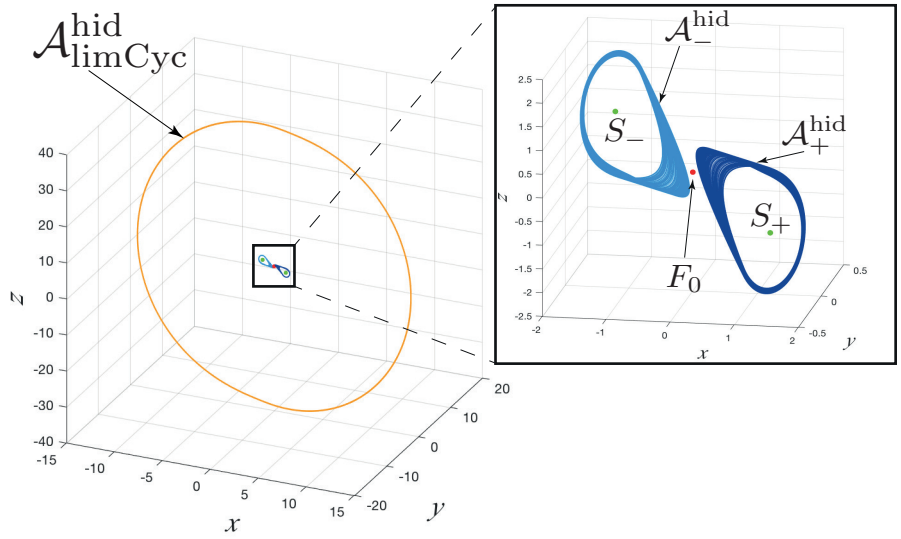

Fig. 11. Co-existence of a hidden periodic attractor (a stable limit cycle $\mathcal{A}^{\text{hid}}_{\text{limCyc}}$) and two symmetric hidden chaotic attractors ($\mathcal{A}^{\text{hid}}_{+}$ and $\mathcal{A}^{\text{hid}}_{-}$).

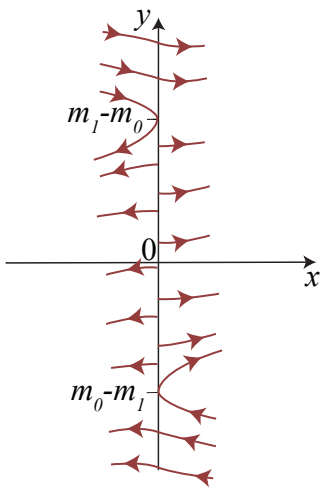

Fig. 12. Behavior of trajectories of system (61) near $x = 0$ for a fixed $z = z_0$, $z_0 \in \mathbb{R}$; unstable manifold of sliding modes: $x = 0$, $|y| \le m_1 - m_0$.

type with a one-dimensional unstable manifold and two symmetric stable equilibrium states $S_\pm$ of the focus-node type:

$$S_\pm = \pm\left(\frac{m_1 - m_0}{m_1 + \frac{\beta}{\beta+\gamma}}, \frac{\gamma(m_1 - m_0)}{(\gamma+\beta)m_1 + \beta}, -\frac{\beta(m_1 - m_0)}{(\gamma+\beta)m_1 + \beta}\right). \tag{62}$$

Now let us revert to considering the modified Chua system in Eq. (61). Let us write down the extension of ξ for $\operatorname{sgn} x$, by repeating the reasoning similar to that for the above-considered systems,

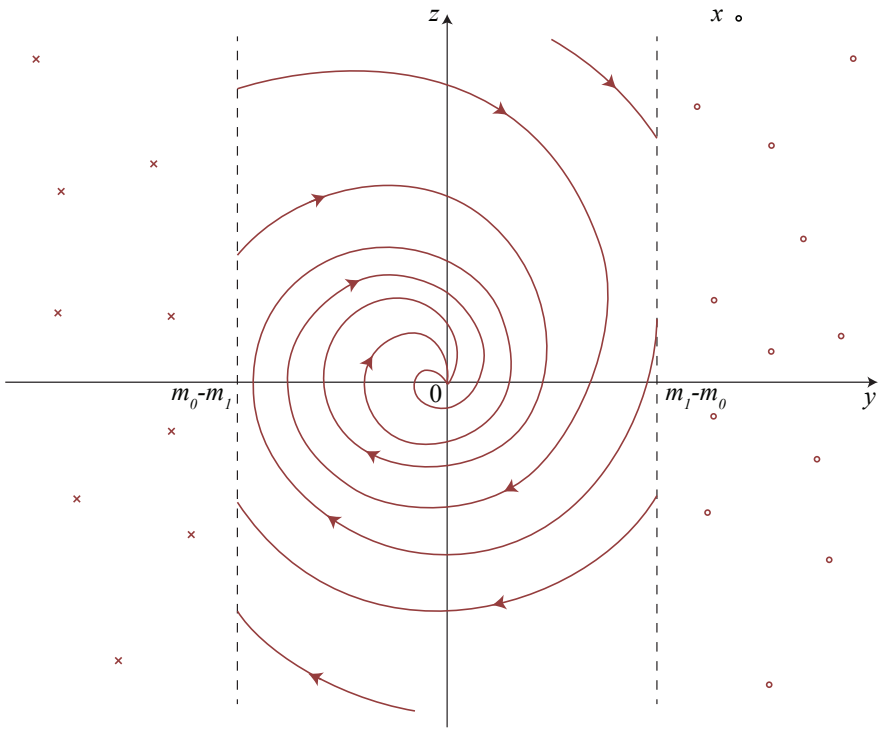

Fig. 13. Phase portrait of system (61): plane $x = 0$ is in the drawing plane, and trajectories moving from and toward an observer are marked, respectively, with the crosses and circles.

viz.

$$\xi(x,y) = \begin{cases} 1 & \text{for } x > 0 \text{ or for } x = 0,\ y > m_1 - m_0, \\ -1 & \text{for } x < 0 \text{ or for } x = 0,\ y < m_0 - m_1, \\ \dfrac{y}{m_0 - m_1} & \text{for } \psi = 0,\ |y| < m_1 - m_0. \end{cases} \tag{63}$$

Similar to the classical Chua system, there are two symmetric stable equilibrium states $S_\pm$ of the saddle-focus type in the system in Eq. (61). The system in Eq. (61) also has the zero equilibrium state, which is situated on an unstable manifold of sliding modes $x = 0$, $|y| \le m_1 - m_0$ (see Fig. 12) and is also a locally stable focus (see Fig. 13).

It proved possible to find a hidden periodic attractor for the system in Eq. (61). In modeling by the Filippov approach, we used a special numerical method described in [124]. To model by the Aizerman–Pyatnitskii approach, one can replace $\operatorname{sgn}(x)$ with

$$\operatorname{sat}_\varepsilon(x) = \frac{1}{2}\left(\left|\frac{x}{\varepsilon} + 1\right| - \left|\frac{x}{\varepsilon} - 1\right| \right),$$

where $\varepsilon > 0$. Decreasing parameter ε makes it possible to obtain the Aizerman–Pyatnitskii solution $(\operatorname{sat}_\varepsilon(x_1) \rightrightarrows \operatorname{sgn}(x_1)$ as $\varepsilon \to 0$, see Fig. 14).

Figure 15 displays hidden attractors modeled by using the Filippov (the "dark" color) and Aizerman–Pyatnitskii (the "light" color) approaches. It can be easily seen that as ε decreases, the two attractors virtually coincide. Also, in this case the Filippov approach coincides with the Gelig–Leonov–Yakubovich approach. These results agree with the assertion of a theorem proved in [67, 125]. Note that unlike in the Vyshnegradskii problem, forward uniqueness is violated due to the presence of an unstable manifold of sliding modes for the system in Eq. (61). Therefore, when modeling on a discontinuity, a necessity arises to use the numerical method based on the Aizerman–Pyatnitskii approach.

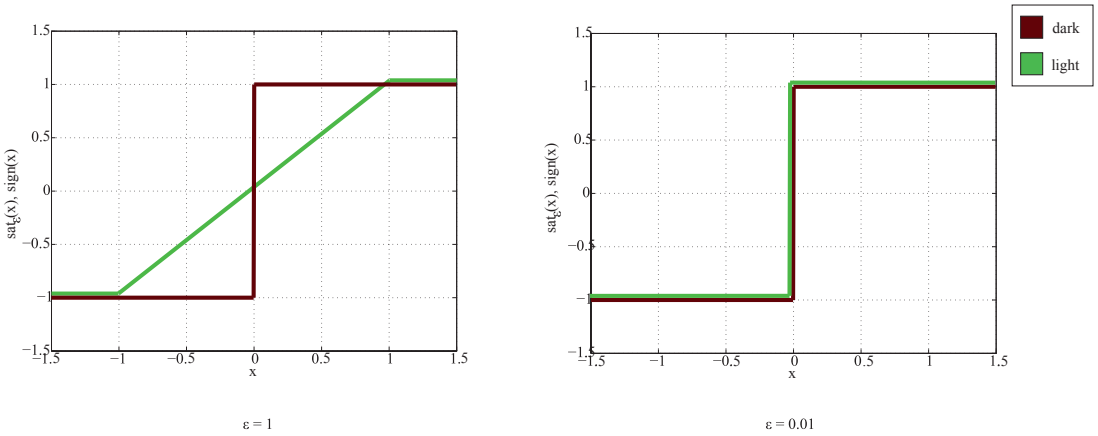

Fig. 14. Graphs of $\mathrm{sat}_\varepsilon(x_1)$ and $\mathrm{sgn}\,(x_1)$.

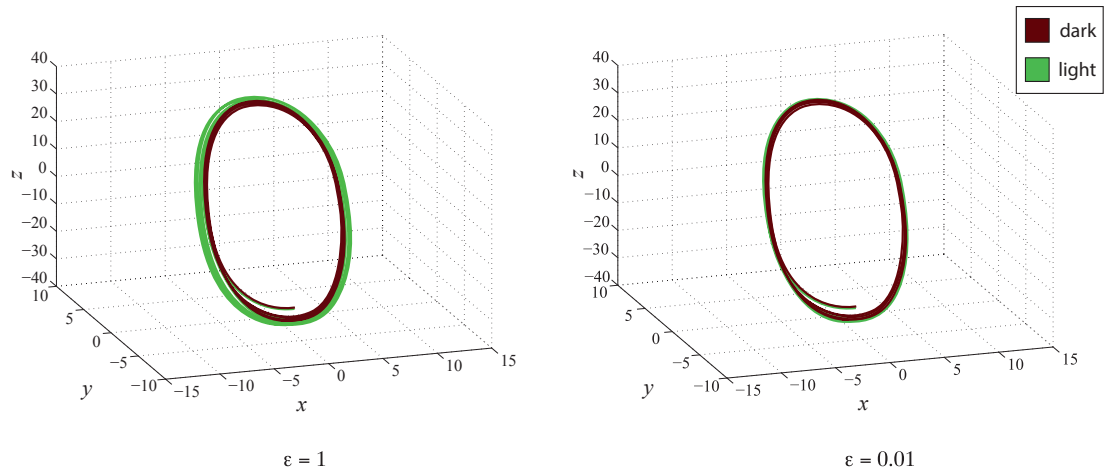

Fig. 15. Hidden attractor in the Chua system. Comparing Filippov and Aizerman–Pyatnitskii approaches.

5. COUNTEREXAMPLE TO THE KALMAN CONJECTURE

The Kalman problem [79] is one of the actual and complicated problems in control theory. It appeals to many due to its simplicity and the clarity of its statement, which we provide below.

Suppose we have the system

$$\dot{x} = A\,x + b\,\varphi(\sigma), \qquad \sigma = c^*x, \tag{64}$$

where A is a constant $n \times n$-matrix, b and c are constant n-dimensional columns, with all values being real; $*$ is the sign of transposition; and φ is a smooth scalar function, $\varphi(0) = 0$, satisfying the condition

$$k_1 \le \varphi'(\sigma) \le k_2, \qquad \sigma \in (-\infty, +\infty), \tag{65}$$

where k_1 is a number or $-\infty$ and k_2 is a number or $+\infty$.

In 1957, R.E. Kalman formulated the following conjecture [79]: *if a linear system* $\dot{x} = A\,x + k\,b\,c^*x$, $k \in [k_1, k_2]$, *is globally asymptotically stable, then the system in Eq.* (64) *is also globally asymptotically stable.* Let us recall that a system is globally asymptotically stable if its zero solution is Lyapunov-stable and $\lim_{t\to+\infty} |x(t, x_0)| = 0$ for any $x_0 \in \mathbb{R}^n$.

This conjecture is known to be true for the case of $n = 1, 2, 3$ [72, 126]. The first attempts to construct a counterexample to this conjecture were made in Fitts' paper [127], where he performed the computer simulation of system (64) for $n = 4$ with the transfer function

$$W(p) = \frac{p^2}{((p+\beta)^2 + 0.9^2)\,((p+\beta)^2 + 1.1^2)} \tag{66}$$

and the cubic nonlinearity $\varphi(\sigma) = K\sigma^3$. As a result of the modeling, Fitts discovered periodic solutions of the system in Eq. (64) for the values of parameters $K = 10$ and $\beta \in (0.01, 0.75)$. However, later N.E. Barabanov showed [126] that the results of the experiments were incorrect for a part of the parameters that Fitts considered, specifically, for $\beta \in (0.572, 0.75)$. The Kalman conjecture was further discussed and doubts in the counterexamples [127] and [126] were raised in [128–130].

Numerical modeling of Fitts' counterexample, i.e., the system in Eq. (64) with the transfer function in Eq. (66) and the cubic nonlinearity $\varphi(\sigma) = 10\,\sigma^3$, could be a challenging task. For example, for $\beta = 0.01$ it was shown [72] that the discovered periodic solution has a very small basin of attraction.

Let us use Eq. (66) to consider an approach to constructing counterexamples to the Kalman conjecture based on the ideas of discontinuous systems. Consider the system in Eq. (64) with $n = 4$, defined by the transfer function in Eq. (66) with a nonlinearity of the type $\varphi(\sigma) = \psi_0(\sigma) = \operatorname{sgn}\sigma$, as the limiting case of the system in Eq. (64) with a "saturation"-type nonlinearity

$$\varphi(\sigma) = \psi_m(\sigma) \equiv \begin{cases} -1, & \sigma \le -m, \\ \dfrac{1}{m}\,\sigma, & -m \le \sigma \le m, \\ 1, & \sigma \ge m, \end{cases} \tag{67}$$

where $0 < m \le N$, N is a sufficiently small positive number. If a local attractor of the system with $\varphi(\sigma) = \psi_0(\sigma)$ does not belong to the sliding mode manifold, then the system in Eq. (64) with $\varphi(\sigma) = \psi_m(\sigma)$ of type (67) possesses an attractor close to that local attractor. In this case, the trajectories of systems with nonlinearities $\psi_0(\sigma)$ and $\psi_m(\sigma)$ can be computed analytically as solutions of linear systems by using Andronov's point mapping method [131].

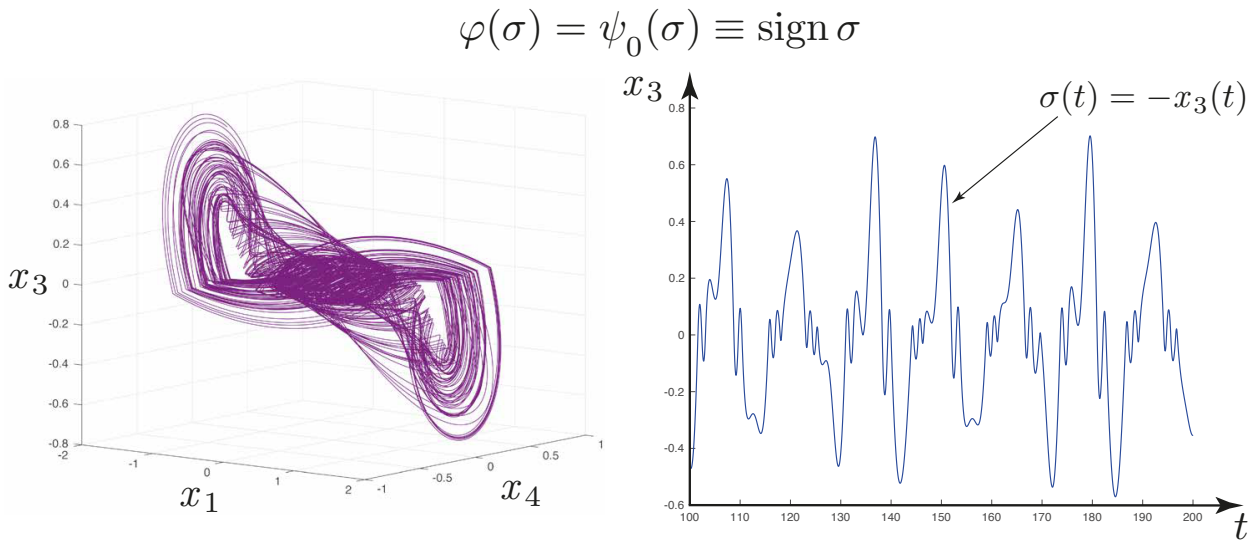

Fig. 16. Strange attractor of system (68) at $\beta = 0.1$ and $\varphi(\sigma) = \psi_0(\sigma) = \operatorname{sgn}\sigma$.

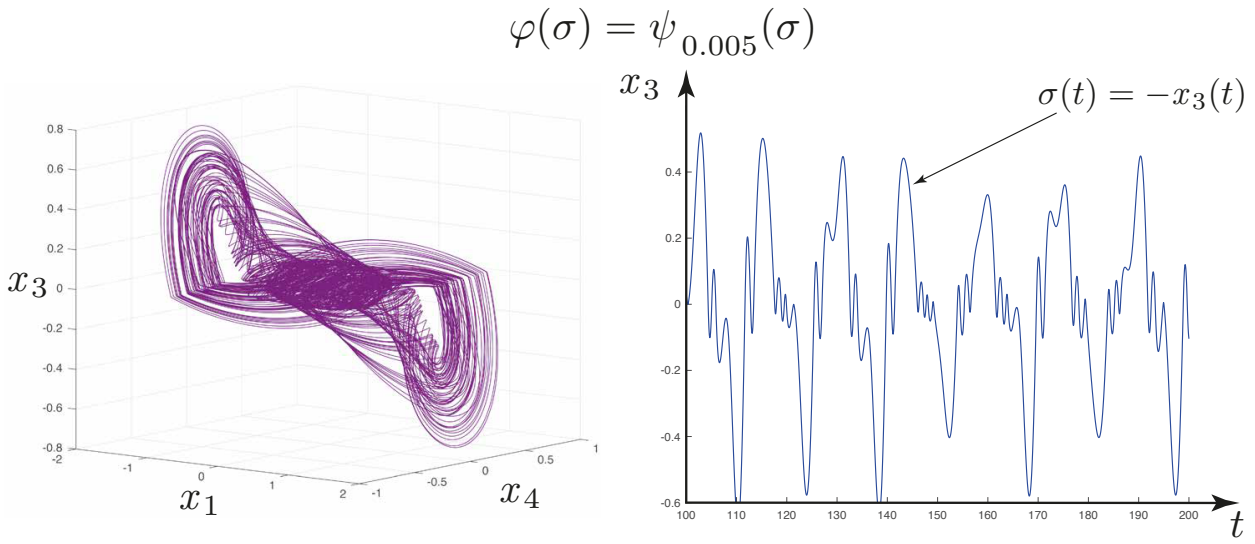

Fig. 17. Strange attractor of system (68) at $\beta = 0.1$ and $\varphi(\sigma) = \psi_m(\sigma)$, $m = 0.005$.

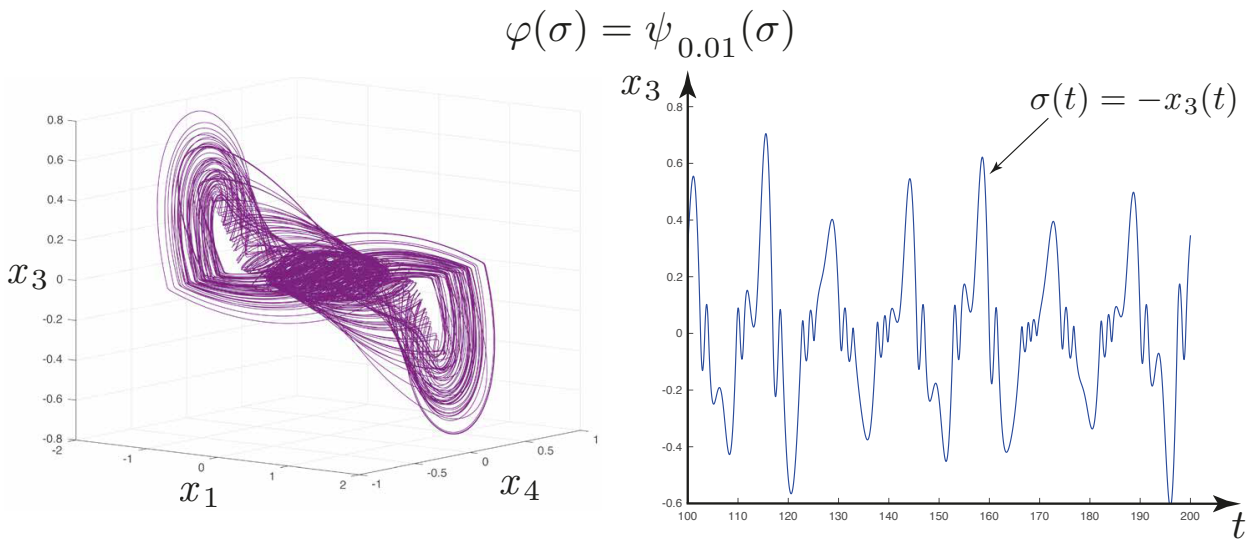

Fig. 18. Strange attractor of system (68) at $\beta = 0.1$ and $\varphi(\sigma) = \psi_m(\sigma)$, $m = N = 0.01$.

Further, let us take advantage of the numerical continuation method [72, 77, 132, 133]. Considering the system from Fitts' example with the nonlinearity

$$\varphi(\sigma) = \chi_\varepsilon(\sigma) \equiv \psi_N(\sigma) + \varepsilon\,(\tanh(\sigma/N) - \psi_N(\sigma))$$

and varying parameter ε from 0 to 1, we can switch from the system with a piecewise-differentiable nonlinearity $\varphi(\sigma) = \psi_N(\sigma)$ to the system with a smooth nonlinearity $\varphi(\sigma) = \tanh(\sigma/N)$.

Deriving the system based on the transfer function in Eq. (66), we arrive at [134]

$$\begin{aligned} &\dot x_1 = x_2, \qquad \dot x_2 = x_3, \qquad \dot x_3 = x_4, \\ &\dot x_4 = -a_0 x_1 - a_1 x_2 - a_2 x_3 - a_3 x_4 + \varphi(\sigma), \end{aligned} \tag{68}$$

where $a_0 = (1.1^2 + \beta^2)(0.9^2 + \beta^2)$, $a_1 = 2\beta(1.1^2 + 0.9^2 + 2\beta^2)$, $a_2 = 1.1^2 + 0.9^2 + 6\beta^2$, $a_3 = 4\beta$,

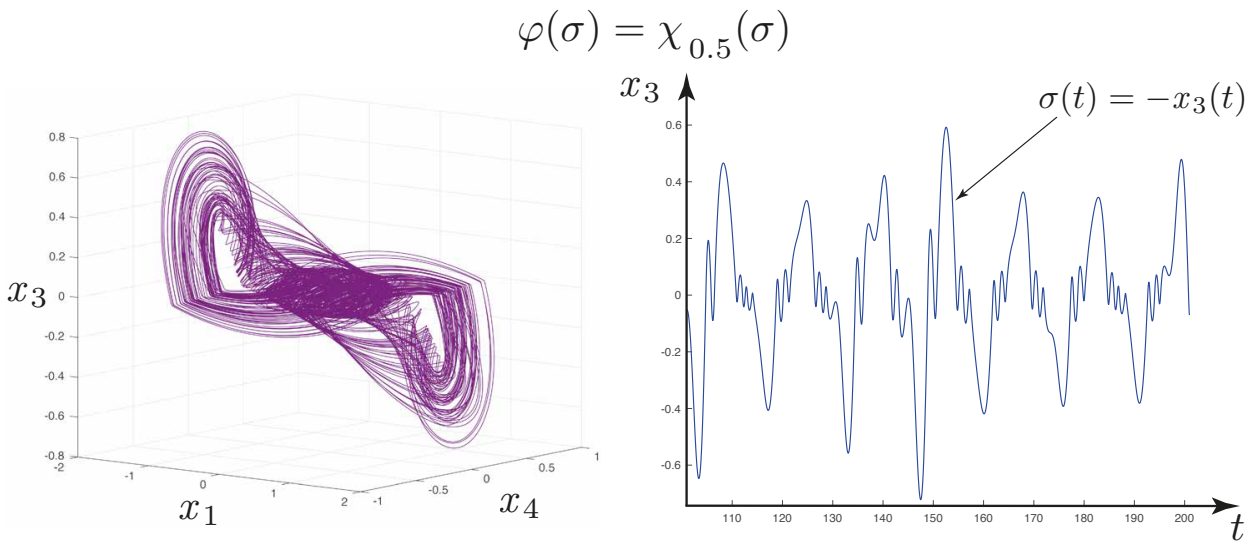

Fig. 19. Strange attractor of system (68) at $\beta = 0.1$ and $\varphi(\sigma) = \chi_\varepsilon(\sigma) \equiv \psi_N(\sigma) + \varepsilon\,(\tanh(\sigma/N) - \psi_N(\sigma))$, $N = 0.01$, $\varepsilon = 0.5$.

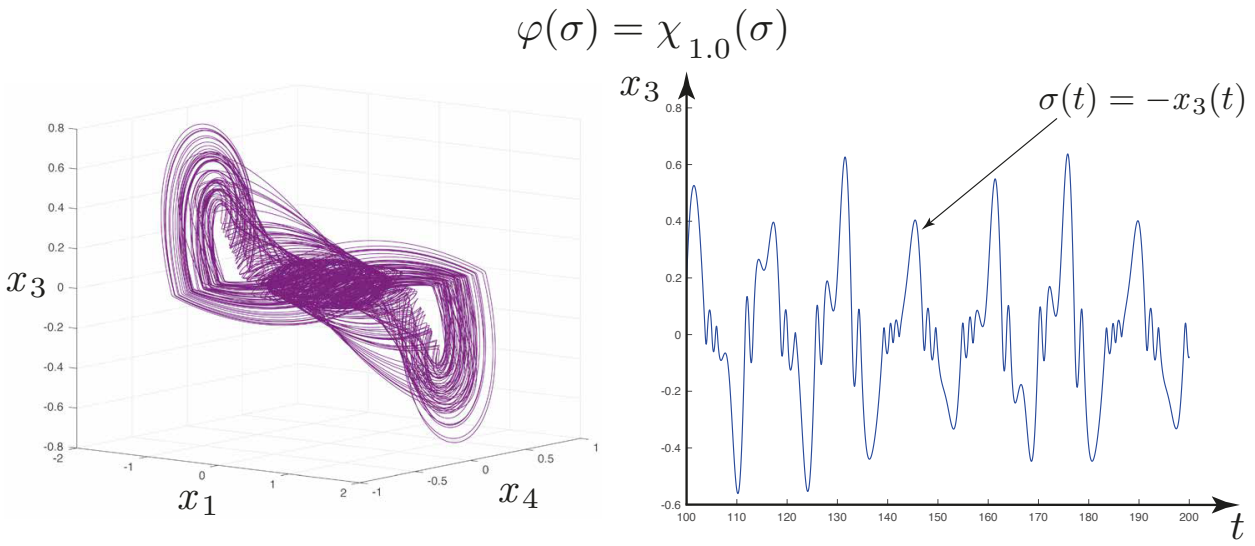

Fig. 20. Strange attractor of system (68) at $\beta = 0.1$ and $\varphi(\sigma) = \chi_\varepsilon(\sigma) \equiv \psi_N(\sigma) + \varepsilon\,(\tanh(\sigma/N) - \psi_N(\sigma))$, $N = 0.01$, $\varepsilon = 1$.

$\sigma = -x_3$. The system in Eq. (68) can be represented in matrix form (64) with the matrices

$$A = \begin{pmatrix} 0 & 1 & 0 & 0 \\ 0 & 0 & 1 & 0 \\ 0 & 0 & 0 & 1 \\ -a_0 & -a_1 & -a_2 & -a_3 \end{pmatrix}, \qquad b = \begin{pmatrix} 0 \\ 0 \\ 0 \\ 1 \end{pmatrix}, \qquad c = \begin{pmatrix} 0 \\ 0 \\ -1 \\ 0 \end{pmatrix}.$$

For $\beta = 0.1$ and $\varphi(\sigma) = \psi_0(\sigma) = \operatorname{sgn}(\sigma)$, the system possesses a local attractor (Fig. 16). This attractor retains after replacing in Eq. (68) the nonlinearity $\varphi(\sigma) = \psi_0(\sigma)$ with the nonlinearity $\varphi(\sigma) = \psi_m(\sigma)$ of form (67) at $0 < m \le N$, $N = 0.01$ (for $m = 0.005$ see Fig. 17; for $m = N = 0.01$ see Fig. 18).

Using the nonlinearity $\varphi(\sigma) = \chi_\varepsilon(\sigma) \equiv \psi_N(\sigma) + \varepsilon\,(\tanh(\sigma/N) - \psi_N(\sigma))$ for ε increasing from 0 to 1 with the step 0.1, we can arrange the transition from the piecewise-differentiable nonlinearity in

Eq. (67), which corresponds to $\varphi(\sigma) = \chi_0(\sigma) = \psi_N(\sigma)$, to the smooth nonlinearity $\varphi(\sigma) = \chi_1(\sigma) = \tanh(\sigma/N)$. Here, the local attractor obtained at the previous steps is retained (Figs. 19, 20).

Thus, a hidden attractor takes place in the system in Eq. (64) with $\varphi(\sigma) = \tanh(\sigma/N)$ for sufficiently small N, and the Kalman conjecture fails for $k_1 < 0$ and $k_2 = +\infty$.

6. CONCLUSION

In this paper various approaches to define the solutions of differential equations with discontinuous right-hand sides and differential inclusions have been described. The theory of such systems started to develop actively once in the middle of the 20th century it became clear that their solutions are absolutely continuous vector-functions and the sliding modes are typical effects for discontinuous systems.

The method of Lyapunov functions proves to be an efficient mathematical tool for the global analysis of discontinuous systems. We have demonstrated how discontinuous Lyapunov functions can be applied to discontinuous systems in the classical Vyshnegradskii problem. It has been revealed that the method of discontinuous approximations and Aizerman–Pyatnitskii ideas are useful when constructing counterexamples to the Kalman problem.

ACKNOWLEDGMENTS

This work was supported by the Russian Science Foundation, project no. 14-21-00041. This paper is a translation of http://www.math.spbu.ru/diffjournal/pdf/leonov_5.pdf from Russian into English done by MAIK.

REFERENCES

1. Marchaud, A., Sur les champs de demi-droites et les équations différentielles du premier ordre, *Bull. Soc. Math. France*, 1934, vol. 62, pp. 1–38.
2. Marchaud, A., Sur les champs continus de demi-cones convexes et leurs integrales, *Compos. Math.*, 1936, vol. 3, pp. 89–127.
3. Zaremba, S.C., Sur une extension de la notion d'équation différentielle, *C. R. Acad. Sci. Paris*, 1934, vol. 199, no. 10, pp. 545–548.
4. Zaremba, S.C., Sur les équations au paratingent, *Bull. Sci. Math.*, 1936, vol. 60, no. 2, pp. 139–160.
5. Agrachev, A.A. and Sachkov, Y.L., *Control Theory from the Geometric Viewpoint*, Encyclopaedia of Mathematical Sciences, vol. 87: *Control Theory and Optimization, II,* Berlin: Springer-Verlag, 2004.
6. Bennett, S., *A History of Control Engineering 1930–1955*, Stevenage, UK: Peter Peregrinus, Ltd., 1993.
7. Brogliato, B., *Nonsmooth Mechanics: Models, Dynamics and Control*, Berlin: Springer-Verlag, 1999.
8. Pfeiffer, F. and Glocker, C., *Multibody Dynamics with Unilateral Contacts*, New York: Wiley, 1996.
9. Utkin, V., *Sliding Modes in Control and Optimization*, Berlin: Springer-Verlag, 1992.
10. Emel'yanov, S.V., *Sistemy avtomaticheskogo upravleniya s peremennoi strukturoi* (Automatic Control Systems of Variable Structure), Moscow: Nauka, 1967.
11. Plestan, F., Shtessel, Y., Bregeault, V., and Poznyak, A., New methodologies for adaptive sliding mode control, *Int. J. Control*, 2010, vol. 83, no. 9, pp. 1907–1919.
12. Poznyak, A.S., Yu, W., Sanchez, E.N., and Perez, J.P., Nonlinear adaptive trajectory tracking using dynamic neural networks, *IEEE Trans. Neural Networks*, 1999, vol. 10, no. 6, pp. 1402–1411.
13. Edwards, C. and Spurgeon, S., *Sliding Mode Control: Theory and Applications*, London: Taylor & Francis, 1998.
14. Arkin ,R.C., *Behavior-Based Robotics*, Cambridge: MIT Press, 1998.
15. Kloeden, P.E. and Marín-Rubio, P., Negatively invariant sets and entire trajectories of set-valued dynamical systems, *Set-Valued Var. Anal.*, 2011, vol. 19, no. 1, pp. 43–57.
16. Goryacheva, I.G., *Contact Mechanics in Tribology*, vol. 61 of *Solid Mechanics and Its Applications*, Boston: Kluwer, 1998.
17. Goryacheva, I.G., Rajeev, P.T., and Farris, T.N., Wear in partial slip contact, *J. Tribol.*, 2001, vol. 123, no. 4, pp. 848–856.
18. Kolesnikov, V.I., *Teplofizicheskie protsessy v metallopolimernykh tribosistemakh* (Thermophysical Processes in Metal–Polymer Tribological Systems), Moscow: Nauka, 2003.

19. Kachanov, L.M., *Osnovy teorii plastichnosti* (Fundamentals of Plasticity Theory), Moscow: Nauka, 1969.
20. Polyakov, A. and Fridman, L., Stability notions and Lyapunov functions for sliding mode control systems, *J. Franklin Inst.*, 2014, vol. 351, no. 4, pp. 1831–1865.
21. Orlov, Y.V., *Discontinuous systems: Lyapunov Analysis and Robust Synthesis under Uncertainty Conditions*, New York: Springer Science & Business Media, 2008.
22. Kershtein, I.M., Klyushnikov, V.D., Lomakin, E.V., and Shesterikov, S.A., *Osnovy eksperimental'noi mekhaniki razrusheniya* (Foundations of Experimental Fracture Mechanics), Moscow: Mosk. Gos. Univ., 1989.
23. Boiko, I., *Discontinuous Control Systems: Frequency-Domain Analysis and Design*, New York: Springer Science & Business Media, 2008.
24. Dolgopolik, M. and Fradkov, A., Nonsmooth and discontinuous speed-gradient algorithms, *Nonlinear Anal.: Hybrid Syst.*, 2017, vol. 25, pp. 99–113.
25. Flugge-Lotz, I., *Discontinuous Automatic Control of Missiles*, Stanford: Stanford Univ., Division of Eng. Mech., 1950.
26. Flugge-Lotz, I., *Discontinuous Automatic Control*, Princeton: Princeton University Press, 1953.
27. Anosov, D.V., Stability of the equilibrium positions in relay systems, *Autom. Remote Control*, 1959, vol. 20, no. 2, pp. 130–143.
28. Neimark, Yu.I., On the sliding mode in relay automatic control systems, *Avtom. Telemekh.*, 1957, vol. 18, pp. 27–33.
29. Venets, V.I., Differential inclusions in convex problems, *Autom. Remote Control*, 1980, no. 40, pp. 1261–1269.
30. Solodovnikov, V.V., *Osnovy avtomaticheskogo regulirovaniya. Teoriya* (Foundations of Automatic Control: Theory), Moscow: Gos. Izd. Mashinostr., 1954.
31. Besekerskii, V.A. and Popov, E.P., *Teoriya sistem avtomaticheskogo regulirovaniya* (Theory of Automatic Control Systems), Moscow: Nauka, 1972.
32. Khalil, H.K., *Nonlinear Systems*, Upper Saddle River: Prentice Hall, 2002.
33. Tsypkin, Y.Z., *Relay Control Systems*, Cambridge: Cambridge Univ. Press, 1984.
34. Hartog, J.D., Forced vibrations with combined viscous and coulomb damping, *The London, Edinburgh, Dublin Philos. Mag. J. Sci.*, 1930, vol. 9, no. 59, pp. 801–817.
35. Keldysh, M.V., On dumpers with nonlinear characteristic, *Tr. TsAGI*, 1944, vol. 557, pp. 26–37.
36. Lur'e, A.I. and Postnikov, V.N., Concerning the theory of stability of regulating systems, *Prikl. Mat. Mekh.*, 1944, vol. 8, no. 3, pp. 246–248.
37. Bulgakov, B.V., Maintained oscillations of automatically controlled systems, *Prikl. Mat. Mekh.*, 1943, vol. 7, no. 2, pp. 97–108.
38. Andronov, A.A. and Bautin, N.N., Motion of a neutral plane equipped with an autopilot and the theory of point transformations of surfaces, *Dokl. Akad. Nauk SSSR*, 1944, vol. 43, no. 5, pp. 197–201.
39. Andronov, A.A. and Bautin, N.N., Stabilisation de route d'un avion neutre par autopilote ayant un vitesse constante et à zone d'insensibilite, *C. R. (Dokl.) Acad. Sci. URSS*, 1945, vol. 46, no. 4, pp. 143–146.
40. Andronov, A.A. and Bautin, N.N., Theory of stabilization of a neutral plane by an autopilot with a constant velocity of the actuator: I, *Izv. Akad. Nauk SSSR, Ser. Tekh. Nauk*, 1955, no. 3, pp. 3–32.
41. Andronov, A.A. and Bautin, N.N., Theory of stabilization of a neutral plane by an autopilot with a constant velocity of the actuator: II, *Izv. Akad. Nauk SSSR, Ser. Tekh. Nauk*,, 1955, no. 6, pp. 54–71.
42. Yakubovich, V. A., Leonov, G.A., and Gelig, A.Kh., *Stability of Stationary Sets in Control Systems with Discontinuous Nonlinearities*, Singapore: World Sci., 2004.
43. Aizerman, M.A. and Gantmakher, F.R., *Absolyutnaya ustoichivost' reguliruemykh sistem* (Absolute stability of Control Systems), Moscow: Akad. Nauk SSSR, 1963.
44. Filippov, A.F., Differential equations with discontinuous right-hand side, *Mat. Sb.*, 1960, vol. 51, no. 1, pp. 99–128.
45. Aizerman, M.A. and Pyatnitskii, E.S., Foundations of a theory of discontinuous systems: I, *Autom. Remote Control*, 1974, vol. 35, pp. 1066–1079.
46. Aubin, J.P. and Cellina, A., *Differential Inclusions: Set-Valued Maps and Viability Theory*, Berlin: Springer-Verlag, 1984.
47. Clarke, F.H., Ledyaev, Y.S., Stern, R.J., and Wolenski, P.R., *Nonsmooth Analysis and Control Theory*, Berlin: Springer-Verlag, 1998.

48. Leine, R.I. and Nijmeijer, H., *Differential Inclusion, Dynamics and Bifurcations of Non-Smooth Mechanical Systems*, Berlin: Springer-Verlag, 2004.
49. Smirnov, G.V., *Introduction to the Theory of Differential Inclusions*, Graduate Studies in Mathematics, vol. 41, Providence: Amer. Math. Soc., 2002.
50. Gelig, A.Kh., Investigation of stability of nonlinear discontinuous automatic control systems with a nonunique equilibrium state, *Autom. Remote Control*, 1964, vol. 25, pp. 1413–148.
51. Leonov, G.A., Stability of nonlinear controllable systems having a nonunique equilibrium position, *Autom. Remote Control*, 1971, vol. 32, no. 10, pp. 1547–1552.
52. Vyshnegradskii, I.A., On direct action controllers, *Izv. S.-Peterb. Tekhnol. Inst.*, 1877, pp. 21–62.
53. Andronov, A.A. and Maier, A.G., Vyshnegradskii problem in direct control theory: I, *Avtom. Telemekh.*, 1947, vol. 8, no. 5, pp. 314–334.
54. Filippov, A. F., *Differential Equations with Discontinuous Righthand Sides*, Dordrecht: Kluwer, 1988.
55. Ważewski, T., Sur une condition équivalente à l'équation au contingent, *Bull. Acad. Polon. Sci. Sér. Sci. Math. Astronom. Phys*, 1961, no. 9, pp. 865–867.
56. Cortes, J., Discontinuous dynamical systems, *IEEE Control Syst.*, 2008, vol. 28, no. 3, pp. 36–73.
57. Krasovskij, N.N., *Stability of Motion: Applications of Lyapunov's Second Method to Differential Systems and Equations with Delay*, Stanford University Press, 1963.
58. Krasovskij, N.N. and Subbotin, A.I., *Game-Theoretical Control Problems*, New York: Springer, 1987.
59. Hermes, H., *Discontinuous Vector Fields and Feedback Control*, New York: Academic, 1967.
60. Filippov, A.F., On certain questions in the theory of optimal control, *J. Soc. Ind. Appl. Math. Ser. A*, 1962, vol. 1, no. 1, pp. 76–84.
61. Boltyanskii, V.G., *Matematicheskie metody optimal'nogo upravleniya* (Mathematical Methods of Optimal Control), Moscow: Nauka, 1969.
62. Tolstonogov, A., *Differential Inclusions in a Banach Space*, Berlin: Springer-Verlag, 2000.
63. Pliss, V.A., *Nekotorye problemy teorii ustoichivosti dvizheniya* (Some Problems of Motion Stability Theory), Leningrad: Leningr. Gos. Univ., 1958.
64. Polyakov, A., Discontinuous Lyapunov functions for nonasymptotic stability analysis, *IFAC Proc. Volumes*, 2014, vol. 47, no. 3, pp. 5455–5460.
65. Kuznetsov, N., Kuznetsova, O., Leonov, G., and Vagaitsev, V., Analytical-numerical localization of hidden attractor in electrical Chua's circuit, *Lect. Notes Electr. Eng.*, 2013, vol. 174, no. 4, pp. 149–158.
66. Kuznetsov, N.V., Kuznetsova, O.A., Leonov, G.A., and Vagaitsev, V.I., Hidden attractor in Chua's circuits, *ICINCO 2011—Proceedings of the 8th International Conference on Informatics in Control, Automation and Robotics*, 2011, vol. 1, pp. 279–283.
67. Leonov, G.A., Kiseleva, M.A., Kuznetsov, N.V., and Kuznetsova, O.A., Discontinuous differential equations: comparison of solution definitions and localization of hidden Chua attractors, *IFAC-PapersOnLine*, 2015, vol. 48, no. 11, pp. 408–413.
68. Kuznetsov, N.V., Kuznetsova, O.A., Leonov, G.A., Mokaev, T.N., and Stankevich, N.V., Hidden attractors localization in Chua circuit via the describing function method, *IFAC-PapersOnLine*, 2017, vol. 50, no. 1, pp. 2651–2656.
69. Kuznetsov, N.V., Leonov, G.A., and Vagaitsev, V.I., Analytical-numerical method for attractor localization of generalized Chua's system, *IFAC-PapersOnLine*, 2010, vol. 4, no. 1, pp. 29–33.
70. Leonov, G.A., Kuznetsov, N.V., and Vagaitsev, V.I., Localization of hidden Chua's attractors, *Phys. Lett. A*, 2011, vol. 375, no. 23, pp. 2230–2233.
71. Leonov, G.A., Kuznetsov, N.V., and Vagaitsev, V.I., Hidden attractor in smooth Chua systems, *Phys. D (Amsterdam, Neth.)*, 2012, vol. 241, no. 18, pp. 1482–1486.
72. Leonov, G.A. and Kuznetsov, N.V., Hidden attractors in dynamical systems. From hidden oscillations in Hilbert–Kolmogorov, Aizerman, and Kalman problems to hidden chaotic attractors in Chua circuits, *Int. J. Bifurcation Chaos Appl. Sci. Eng.*, 2013, 23, no. 1, art. no. 1330002.
73. Leonov, G.A., Kuznetsov, N.V., and Mokaev, T.N., Homoclinic orbits, and self-excited and hidden attractors in a Lorenz-like system describing convective fluid motion, *Eur. Phys. J. Spec. Top.*, 2015, vol. 224, no. 8, pp. 1421–1458.
74. Kuznetsov, N.V., Hidden attractors in fundamental problems and engineering models: A short survey, *Lect. Notes Electr. Eng.*, 2016, vol. 371, pp. 13–25 (Plenary lecture at the International Conference on Advanced Engineering Theory and Applications 2015).

75. Sommerfeld, A., Beitrage zum dynamischen Ausbau der Festigkeitslehre, *Z. d. Vereins deutscher Ingenieure*, 1902, vol. 46, pp. 391–394.
76. Kiseleva, M.A., Kuznetsov, N.V., and Leonov, G.A., Hidden attractors in electromechanical systems with and without equilibria, *IFAC-PapersOnLine*, 2016, vol. 49, no. 14, pp. 51–55.
77. Leonov, G.A. and Kuznetsov, N.V., Algorithms for searching for hidden oscillations in the Aizerman and Kalman problems, *Dokl. Math.*, 2011, vol. 84, no. 1, pp. 475–481.
78. Aizerman, M.A., On a problem concerning the stability in the large of dynamical systems, *Uspekhi Mat. Nauk*, 1949, vol. 4, no. 4, pp. 187–188.
79. Kalman, R.E., Physical and mathematical mechanisms of instability in nonlinear automatic control systems, *Trans. ASME J.*, 1957, vol. 79, no. 3, pp. 553–566.
80. Hilbert, D., Mathematical problems, *Bull. Amer. Math. Soc.*, 1901–1902, no. 8, vol. 437–479.
81. Bautin, N.N., On the number of limit cycles generated on varying the coefficients from a focus or centre type equilibrium state, *Dokl. Akad. Nauk SSSR*, 1939, vol. 24, no. 7, pp. 668–671.
82. Kuznetsov, N.V., Kuznetsova, O.A., and Leonov, G.A., Visualization of four normal size limit cycles in two-dimensional polynomial quadratic system, *Differ. Equations Dyn. Syst.*, 2013, vol. 21, nos. 1–2, pp. 29–34.
83. Leonov, G. and Kuznetsov, N., On differences and similarities in the analysis of Lorenz, Chen, and Lu systems, *Appl. Math. Comput.*, 2015, vol. 256, pp. 334–343.
84. Leonov, G. and Kuznetsov, N., Localization of hidden oscillations in dynamical systems (plenary lecture), *4th International Scientific Conference on Physics and Control*, 2009, http://www.math.spbu.ru/user/leonov/publications/2009-PhysCon-Leonov-plenary-hidden-oscillations.pdf#page=21
85. Kiseleva, M., Kudryashova, E., Kuznetsov, N., Kuznetsova, O., Leonov, G., Yuldashev, M., and Yuldashev, R., Hidden and self-excited attractors in Chua circuit: synchronization and SPICE simulation, *Int. J. Parallel, Emergent, Distrib. Syst.*, 2018, doi:10.1080/17445760.2017.1334776.
86. Sharma, P., Shrimali, M., Prasad, A., Kuznetsov, N., and Leonov, G., Controlling dynamics of hidden attractors, *Int. J. Bifurcation Chaos Appl. Sci. Eng.*, vol. 25, no. 4, art. no. 1550061.
87. Sharma, P., Shrimali, M., Prasad, A., Kuznetsov, N., and Leonov, G., Control of multistability in hidden attractors, *Eur. Phys. J.: Spec. Top.*, 2015, vol. 224, no. 8, pp. 1485–1491.
88. Zhang, X. and Chen, G., Constructing an autonomous system with infinitely many chaotic attractors, *Chaos: Interdiscip. J. Nonlin. Sci.*, 2017, vol. 27, no. 7, art. no. 071101.
89. Li, Q., Zeng, H., and Yang, X.-S., On hidden twin attractors and bifurcation in the Chua's circuit, *Nonlinear Dyn.*, 2014, vol. 77, nos. 1–2, pp. 255–266.
90. Burkin, I.M. and Khien, N.N., Analytical-numerical methods of finding hidden oscillations in multidimensional dynamical systems, *Differ. Equations*, 2014, vol. 50, no. 13, vol. 1695–1717.
91. Li, C. and Sprott, J.C., Coexisting hidden attractors in a 4-D simplified Lorenz system, *Int. J. Bifurcation Chaos Appl. Sci. Eng.*, vol. 24, no. 3, art. no. 1450034.
92. Chen, G., Chaotic systems with any number of equilibria and their hidden attractors, *4th IFAC Conference on Analysis and Control of Chaotic Systems* (plenary lecture), 2015, http://www.ee.cityu.edu.hk/ gchen/pdf/CHEN_IFAC2015.pdf
93. Saha, P., Saha, D., Ray, A., and Chowdhury, A., Memristive non-linear system and hidden attractor, *Eur. Phys. J.: Spec. Top.*, 2015, vol. 224, no. 8, pp. 1563–1574.
94. Feng, Y. and Pan, W., Hidden attractors without equilibrium and adaptive reduced-order function projective synchronization from hyperchaotic Rikitake system, *Pramana*, 2017, vol. 88, no. 4, p. 62.
95. Zhusubaliyev, Z., Mosekilde, E., Churilov, A., and Medvedev, A., Multistability and hidden attractors in an impulsive Goodwin oscillator with time delay, *Eur. Phys. J.: Spec. Top.*, 2015, vol. 224, no. 8, vol. 1519–1539.
96. Danca, M.-F., Hidden transient chaotic attractors of Rabinovich–Fabrikant system, *Nonlinear Dyn.*, 2016, vol. 86, no. 2, pp. 1263–1270.
97. Kuznetsov, A.P., Kuznetsov, S.P., Mosekilde, E., and Stankevich, N.V., Co-existing hidden attractors in a radio-physical oscillator system, *J. Phys. A: Math. Theor.*, 2015, vol. 48, art. no. 125101.
98. Chen, M., Li, M., Yu, Q., Bao, B., Xu, Q., and Wang, J., Dynamics of self-excited attractors and hidden attractors in generalized memristor-based Chua's circuit, *Nonlinear Dyn.*, 2015, vol. 81, pp. 215–226.
99. Pham, V.-T., Rahma, F., Frasca, M., and Fortuna, L., Dynamics and synchronization of a novel hyperchaotic system without equilibrium, *Int. J. Bifurcation Chaos Appl. Sci. Eng.*, vol. 24, no. 6, art. no. 1450087.
100. Ojoniyi, O.S. and Njah, A.N., A 5D hyperchaotic Sprott B system with coexisting hidden attractors, *Chaos Solitons Fractals*, 2016, vol. 87, pp. 172–181.

101. Rocha, R. and Medrano-T, R.O., Finding hidden oscillations in the operation of nonlinear electronic circuits, *Electr. Lett.*, 2016, vol. 52, no. 12, pp. 1010–1011.
102. Borah, M. and Roy, B.K., Hidden attractor dynamics of a novel non-equilibrium fractional-order chaotic system and its synchronisation control, *2017 Indian Control Conference (ICC),* 2017, pp. 450–455.
103. Wei, Z., Pham, V.-T., Kapitaniak, T., and Wang, Z., Bifurcation analysis and circuit realization for multiple-delayed Wang–Chen system with hidden chaotic attractors, *Nonlinear Dyn.*, 2016, vol. 85, no. 3, pp. 1635–1650.
104. Pham, V.-T., Volos, C., Jafari, S., Vaidyanathan, S., Kapitaniak, T., and Wang, X., A chaotic system with different families of hidden attractors, *Int. J. Bifurcation Chaos Appl. Sci. Eng.*, 2016, vol. 26, no. 8, art. no. 1650139.
105. Jafari, S., Pham, V.-T., Golpayegani, S., Moghtadaei, M., and Kingni, S., The relationship between chaotic maps and some chaotic systems with hidden attractors, *Int. J. Bifurcation Chaos Appl. Sci. Eng.*, 2016, vol. 26, no. 13, art. no. 1650211.
106. Dudkowski, D., Jafari, S., Kapitaniak, T., Kuznetsov, N., Leonov, G., and Prasad, A., Hidden attractors in dynamical systems, *Phys. Rep.*, 2016, vol. 637, pp. 1–50.
107. Singh, J. and Roy, B., Multistability and hidden chaotic attractors in a new simple 4-D chaotic system with chaotic 2-torus behaviour, *Int. J. Dyn. Control*, 2017. doi: 10.1007/s40435-017-0332-8.
108. Zhang, G., Wu, F., Wang, C., and Ma, J., Synchronization behaviors of coupled systems composed of hidden attractors, *Int. J. Mod. Phys. B*, vol. 31, art. num. 1750180.
109. Messias, M. and Reinol, A., On the formation of hidden chaotic attractors and nested invariant tori in the Sprott A system, *Nonlinear Dyn.*, 2017, vol. 88, no. 2, pp. 807–821.
110. Brzeski, P., Wojewoda, J., Kapitaniak, T., Kurths, J., and Perlikowski, P., Sample-based approach can outperform the classical dynamical analysis—experimental confirmation of the basin stability method, *Sci. Rep.*, 2017, no. 7, art. no. 6121.
111. Wei, Z., Moroz, I., Sprott, J., Akgul, A., and Zhang, W., Hidden hyperchaos and electronic circuit application in a 5D self-exciting homopolar disc dynamo, *Chaos*, vol. 27, no. 3, art. no. 033101.
112. Chaudhuri, U. and Prasad, A., Complicated basins and the phenomenon of amplitude death in coupled hidden attractors, *Phys. Lett. A*, 2014, vol. 378, no. 9, pp. 713–718.
113. Jiang, H., Liu, Y., Wei, Z., and Zhang, L., Hidden chaotic attractors in a class of two-dimensional maps, *Nonlinear Dyn.*, 2016, vol. 85, no. 4, pp. 2719–2727.
114. Volos, C., Pham, V.-T., Zambrano-Serrano, E., Munoz-Pacheco, J.M., Vaidyanathan, S., and Tlelo-Cuautle, E., Analysis of a 4-D hyperchaotic fractional-order memristive system with hidden attractors, *Advances in Memristors, Memristive Devices and Systems*, Berlin: Springer-Verlag, 2017, pp. 207–235.
115. Rocha, R. and Medrano-T, R.-O., Stablity analysis and mapping of multiple dynamics of Chua's circuit in full-four parameter space, *Int. J. Bifurcation Chaos Appl. Sci. Eng.*, 2015, vol. 25, art. no. 1530037.
116. Bao, B., Jiang, P., Wu, H., and Hu, F., Complex transient dynamics in periodically forced memristive Chua's circuit, *Nonlinear Dyn.*, 2015, vol. 79, pp. 2333–2343.
117. Andrievsky, B.R., Kuznetsov, N.V., Leonov, G.A., and Seledzhi, S.M., Hidden oscillations in stabilization system of flexible launcher with saturating actuators, *IFAC Proceedings Volumes*, 2013, vol. 46, no. 19, pp. 37–41.
118. Andrievsky, B.R., Kuznetsov, N.V., Leonov, G.A., and Pogromsky, A., Hidden oscillations in aircraft flight control system with input saturation, *IFAC Proceedings Volumes*, 2013, vol. 46, no. 12, pp. 75–79.
119. Leonov, G.A., Kuznetsov, N.V., Kiseleva, M.A., Solovyeva, E.P., and Zaretskiy, A.M., Hidden oscillations in mathematical model of drilling system actuated by induction motor with a wound rotor, *Nonlinear Dyn.*, 2014, vol. 77, nos. 1–2, pp. 277–288.
120. Danca, M.-F., Kuznetsov, N., and Chen, G., Unusual dynamics and hidden attractors of the Rabinovich–Fabrikant system, *Nonlinear Dyn.*, 2017, vol. 88, pp. 791–805.
121. Kuznetsov, N., Leonov, G., Yuldashev, M., and Yuldashev, R., Hidden attractors in dynamical models of phase-locked loop circuits: limitations of simulation in MATLAB and SPICE, *Commun. Nonlinear Sci. Numer. Simul.*, 2017, vol. 51, pp. 39–49.
122. Chen, G., Kuznetsov, N., Leonov, G., and Mokaev, T., Hidden attractors on one path: Glukhovsky–Dolzhansky, Lorenz, and Rabinovich systems, *Int. J. Bifurcation Chaos Appl. Sci. Eng.*, vol. 27, no. 8, art. no. 1750115.
123. Danca, M.-F. and Kuznetsov, N., Hidden chaotic sets in a Hopfield neural system, *Chaos Solitons Fractals*, 2017, vol. 103, pp. 144–150.
124. Piiroinen, P.T. and Kuznetsov, Y.A., An event-driven method to simulate Filippov systems with accurate computing of sliding motions, *ACM Trans. Math. Software (TOMS)*, 2008, vol. 34, no. 3, p. 13.

125. Kiseleva, M.A. and Kuznetsov, N.V., Coincidence of Gelig-Leonov-Yakubovich, Filippov, and Aizerman–Pyatnitskii definitions, *Vestn. St. Petersb. Univ. Math.*, 2015, vol. 48, no. 2, pp. 66–71.
126. Barabanov, N.E., On the Kalman problem, *Sib. Math. J.*, 1988, vol. 29, no. 3, pp. 333–341.
127. Fitts, R.E., Two counterexamples to Aizerman's conjecture, *IEEE Trans. Automat. Control*, 1966, vol. 11, no. 3, pp. 553–556.
128. Bernat, J. and Llibre, J., Counterexample to Kalman and Markus–Yamabe conjectures in dimension larger than 3, *Dyn. Contin. Discrete Impuls. Syst.*, 1996, vol. 2, no. 3, pp. 337–379.
129. Meisters, G., A biography of the Markus–Yamabe conjecture, http://www.math.unl.edu/gmeisters1/papers/HK1996.pdf.
130. Glutsyuk, A.A., Meetings of the Moscow Mathematical Society (1997), *Russian Math. Surveys*, 1998, vol. 53, no. 2, pp. 413–417.
131. Andronov, A.A., Vitt, E.A., and Khaikin, S.E., *Theory of Oscillators*, Oxford: Pergamon, 1966.
132. Leonov, G.A., Bragin, V.O., and Kuznetsov, N.V., Algorithm for constructing counterexamples to the Kalman problem, *Dokl. Math.*, 2010, vol. 82, no. 1, pp. 540–542.
133. Bragin, V.O., Vagaitsev, V.I., Kuznetsov, N.V., and Leonov, G.A., Algorithms for finding hidden oscillations in nonlinear systems. The Aizerman and Kalman conjectures and Chua's circuits, *J. Comput. System Sci. Int.*, 2011, vol. 50, no. 4, pp. 511–543.
134. Leonov, G.A., *Mathematical Problems of Control Theory: An Introduction*, Singapore: World Sci., 2001.

PII

ANALYSIS OF OSCILLATIONS IN DISCONTINUOUS LURIE SYSTEMS VIA LPRS METHOD

by

E.D. Akimova, I.M. Boiko, N.V. Kuznetsov, R.N. Mokaev 2019

Vibroengineering PROCEDIA, Vol. 25, PP. 177–181,
https://doi.org/10.21595/vp.2019.20817

Analysis of oscillations in discontinuous Lurie systems via LPRS method

E. D. Akimova[1], I. M. Boiko[2], N. V. Kuznetsov[3], R. N. Mokaev[4]
[1, 3, 4]Saint-Petersburg State University, 7/9 Universitetskaya emb., Saint-Petersburg, Russia
[2]Khalifa University of Science and Technology, Abu Dhabi, UAE
[3, 4]University of Jyväskylä, P.O. Box 35 (Agora), Jyväskylä, Finland
[3]Institute for Problems in Mechanical Engineering RAS, St. Petersburg, Russia
[3]Corresponding author
E-mail: [1]*akimova.el.dm@gmail.com*, [2]*igor.boiko@ku.ac.ae*, [3]*nkuznetsov239@gmail.com*, [4]*mokaev.ruslan@gmail.com*

Received 10 May 2019; accepted 17 May 2019
DOI https://doi.org/10.21595/vp.2019.20817

Check for updates

Copyright © 2019 E. D. Akimova, et al. This is an open access article distributed under the Creative Commons Attribution License, which permits unrestricted use, distribution, and reproduction in any medium, provided the original work is properly cited.

Abstract. We discuss advantages and limitations of the harmonic balance method and the locus of a perturbed relay system (LPRS) method in the problem of finding periodic oscillations. In this paper we present the results of using harmonic balance method and LPRS method while investigating a 3rd order dynamic system in Lurie form. In this system a symmetric periodic oscillation is found, while other two asymmetric periodic motions are not found using both methods.

Keywords: global stability, harmonic balance method, periodic oscillations.

1. Introduction

The necessity of studying stability and limiting dynamical regimes (attractors) arises in classical theoretical and applied problems. In [1] the classification of oscillations as being hidden or self-excited was proposed: self-excited oscillations can be visualized numerically by a trajectory starting from a point in a neighborhood of unstable equilibrium. In contrast, the basin of attraction for a hidden oscillation is not connected with equilibria and, it is necessary to develop special analytical and numerical methods to find initial points for their visualization. For nonlinear systems with a unique equilibrium and bounded solutions, the question that arises is how to find a class of systems for which the condition of the impossibility of generation of self-excited oscillations implies the absence of hidden oscillations.

Among engineers, one of the most widely used methods for searching and analyzing oscillations in nonlinear control systems is the harmonic balance method. It was developed in the 1920-1930s in the works of van der Pol [2] and Krylov and Bogolyubov [3] and later developed in the works of their followers (see [4-6]). It is known [1] that the harmonic balance method is an approximate method for determining the frequency and amplitude of periodic solutions. Moreover, the harmonic balance method may not predict hidden periodic oscillations [1].

The latter is true for the locus of a perturbed relay systems approach (LPRS method), that was developed in [7, 8] for Lurie systems with relay nonlinearities, despite the fact that the LPRS method makes it possible in many cases to predict oscillations not discoverable by the harmonic balance method.

In this article, using the example of known dynamical system with coexisting self-excited periodic oscillations, we will show that these methods may not reveal self-excited oscillations.

2. Oscillations in relay systems

Consider the following system with one scalar relay nonlinearity in the Lurie form:

$$\dot{\mathbf{x}} = \mathbf{A}\mathbf{x} + \mathbf{B}\,\mathrm{sign}(\sigma), \quad \sigma = -\mathbf{C}\mathbf{x}, \tag{1}$$

where $\mathbf{x} \in \mathbb{R}^n$ is a state vector, $\sigma \in \mathbb{R}^1$, $\mathbf{A} \in \mathbb{R}^{n\times n}$, $\mathbf{B} \in \mathbb{R}^{n\times 1}$, $\mathbf{C} \in \mathbb{R}^{1\times n}$ are matrices, all quantities are real. We consider the solution of system Eq. (1) in the Filippov sense [9].

2.1. Harmonic balance method

The classical harmonic balance method (e.g., see [10]) for system Eq. (1) computes a periodic oscillation $a\cos\omega_0 t$ in the following way: introduce a linearization coefficient k so that matrix $\mathbf{A} + k\mathbf{BC}$ has purely imaginary eigenvalues $\pm j\omega_0$ $(\omega_0 > 0)$, with the rest of its eigenvalues having negative real parts. Values of ω_0 and k can be found from equations:

$$Im\, W(j\omega_0) = 0, \quad k = -\left(Re\, W(j\omega_0)\right)^{-1}, \tag{2}$$

where W is the transfer function of system Eq. (1).

Finally, the amplitude a can be found from the following harmonic balance equation:

$$\int_0^{\frac{2\pi}{\omega_0}} (\mathrm{sign}(a\cos\omega_0 t) - k\, a\cos\omega_0 t) a\cos\omega_0 t\, dt = 0. \tag{3}$$

Solving equation Eq. (3), we get:

$$a = \frac{4}{\pi k}. \tag{4}$$

2.2. LPRS method

Consider another method of analysis of periodic motions in relay feedback systems. The locus of a perturbed relay system (LPRS) method [7, 8] can be considered as a further development of Tsypkin's ideas [11] on exact analysis of discontinuous systems. The basic concept of the method is as follows.

For system Eq. (1), following [8], we define a function $J(\omega)$ which contains information on the frequency and amplitude of periodic oscillations. In this paper we apply a matrix state-space description approach to construct LPRS function for system Eq. (1):

$$J(\omega) = -0.5\mathbf{C}\left[\mathbf{A}^{-1} + \frac{2\pi}{\omega}\left(\mathbf{I} - e^{\frac{2\pi}{\omega}\mathbf{A}}\right)^{-1} e^{\frac{\pi}{\omega}\mathbf{A}}\right]\mathbf{B} + j\frac{\pi}{4}\mathbf{C}\left(\mathbf{I} + e^{\frac{\pi}{\omega}\mathbf{A}}\right)^{-1}\left(\mathbf{I} - e^{\frac{\pi}{\omega}\mathbf{A}}\right)\mathbf{A}^{-1}\mathbf{B}. \tag{5}$$

Suppose we have computed the LPRS of a given system. Then there is a finite number of points of intersection of the LPRS and the horizontal axis. The following equation defines a frequency of a possible symmetric periodic solution of system Eq. (1):

$$Im\, J(\omega_0) = 0. \tag{6}$$

Therefore, an actual periodic motion can be found only among these candidate points. Note that formula Eq. (6) is a necessary condition for the existence of the frequency of symmetric periodic motion in the system (the actual existence of a periodic motion depends on a number of other factors [8]).

3. Example: Atherton's system

Consider a relay control system in Lurie form, introduced by D. Atherton in [12], with the following matrices:

$$\mathbf{A} = \begin{pmatrix} 0 & 1 & 0 \\ 0 & 0 & 1 \\ 10d & 2d-10 & d-2 \end{pmatrix}, \quad \mathbf{B} = \begin{pmatrix} 0 \\ 0 \\ 1 \end{pmatrix}, \quad \mathbf{C} = \begin{pmatrix} 1 \\ 0 \\ 0 \end{pmatrix}^T, \tag{7}$$

where d is a parameter.

The linear part of system Eq. (7) is defined by the transfer function:

$$W_{Ath}(s) = \frac{1}{(s-d)(s^2+2s+10)}, \tag{8}$$

and the stationary set is as follows:

$$\Lambda_{Ath} = \left\{ (x_1, x_2, x_3) \in \mathbb{R}^3 \,|\, x_2 = x_3 = 0, \;\; x_1 \in \left\{ -\frac{1}{10d}, \frac{1}{10d} \right\} \right\}. \tag{9}$$

From Eq. (2) we get value of ω_0:

$$\begin{aligned} &Im\, W_{Ath}(j\omega_0) = 0 \Leftrightarrow Im\, \frac{-1}{j{\omega_0}^3 + (2-d){\omega_0}^2 - (10-2d)j\omega_0 + 10d} = 0 \Leftrightarrow \\ &\Leftrightarrow \frac{{\omega_0}^3 - (10-2d)\omega_0}{({\omega_0}^3 - (10-2d)\omega_0)^2 + \left((2-d){\omega_0}^2 + 10d\right)^2} = 0 \underset{\omega_0 \neq 0}{\Longleftrightarrow} \\ &\underset{\omega_0 \neq 0}{\Longleftrightarrow} {\omega_0}^2 = 10 - 2d \underset{\omega_0 > 0}{\Longleftrightarrow} \omega_0 = \sqrt{10-2d}, \end{aligned} \tag{10}$$

and from:

$$Re\, W_{Ath}(j\omega_0) = -\frac{(2-d){\omega_0}^2 + 10d}{({\omega_0}^3 - (10-2d)\omega_0)^2 + \left((2-d){\omega_0}^2 + 10d\right)^2}, \tag{11}$$

we get $k = 2d^2 - 4d + 20$.

Next, from Eq. (4) we get value of amplitude a:

$$a = \frac{4}{\pi k} \Leftrightarrow a = \frac{2}{\pi(d^2 - 2d + 10)}. \tag{12}$$

For the value $d = 1.2$ we find frequency ω_{hb} of a periodic solution as 2.75681. Now using formula Eq. (5) we build LPRS for system Eq. (7) (see Fig. 1).

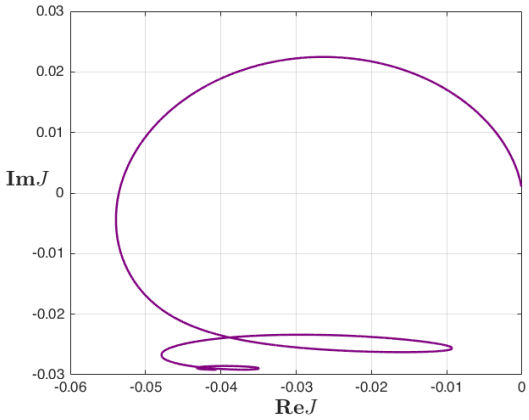

Fig. 1. The LPRS for system Eq. (7) for $d = 1.2$ and $\omega \in [0.5, 10]$

Solving equation Eq. (6) using MATLAB function "vpasolve()" with a given tolerance 10^{-8}, we find frequency of periodic solution as $\omega_{LPRS} = 2.739991399$. Initial data this periodic solution is given in Table 1.

We can examine orbital stability of the oscillations using the following approach proposed in [13] and generalized for the linear parts containing delays and integrators in [8]. It is formulated as the following theorem:

Theorem 1. Periodic motions in system Eq. (1) are locally orbitally asymptotically stable if and only if all eigenvalues of the matrix:

$$\Phi_0 = \left[\mathbf{I} - \frac{\mathbf{v}\left(\frac{T}{2} - 0\right)\mathbf{C}}{\mathbf{C}\mathbf{v}\left(\frac{T}{2} - 0\right)}\right] e^{\mathbf{A}\frac{T}{2}}, \tag{13}$$

where $T = 2\pi/\omega$ is the period of the oscillations, $\mathbf{v}$ is the value of the velocity matrix at the time of the relay switch, in the periodic motion, $\mathbf{v}\left(\frac{T}{2} - 0\right) = 2\left(\mathbf{I} + e^{\mathbf{A}\frac{T}{2}}\right)^{-1} e^{\mathbf{A}\frac{T}{2}}\mathbf{B}$, have magnitudes less than one.

For system Eq. (7) the corresponding eigenvalues are $\lambda_1 = 1.457$, $\lambda_2 = 0.279$, $\lambda_3 = 0$. Since one of eigenvalues has magnitude greater than 1, the motion is not orbitally stable. Therefore, a symmetric periodic solution exists but it is orbitally unstable and cannot reveal itself as an oscillation.

3.1. Numerical modeling

Using special computational package [14] and initial data from Table 2 we can visualize two self-excited (with respect to rest segment) asymmetric periodic solutions (see Fig. 2), that cannot be found using harmonic balance method and LPRS method.

Table 1. Parameters of two asymmetric solutions of system Eq. (7)

ω	2.608029064355592
T	2.409169971705080
λ	0.296489410929823

Table 2. Initial data of two asymmetric solutions of system Eq. (7)

x_1	$\pm$0.000000000312706
x_2	$\mp$0.110095383325227
x_3	$\pm$0.037742341170832

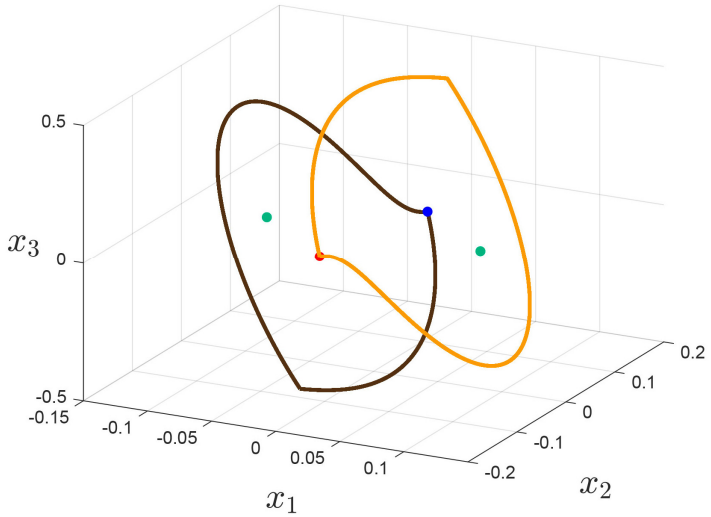

Fig. 2. Trajectories with initial data from Table 3

4. Conclusions

In this paper it is shown that the harmonic balance method and the LPRS method may not predict the existence of all self-excited oscillations. A symmetric periodic solution exists but it is orbitally unstable and cannot reveal itself as an oscillation. Although the LPRS does not detect hidden and self-excited asymmetric oscillations, it would be possible to develop a certain extension to the LPRS method to solve these problems.

Acknowledgements

This work was supported by the Russian Science Foundation 19-41-02002.

References

[1] **Leonov G. A., Kuznetsov N. V.** Hidden attractors in dynamical systems. From hidden oscillations in Hilbert- Kolmogorov, Aizerman, and Kalman problems to hidden chaotic attractors in Chua circuits. International Journal of Bifurcation and Chaos in Applied Sciences and Engineering, Vol. 23, 2013, p. 1330002.

[2] **Van Der Pol B.** On relaxation-oscillations. Philosophical Magazine and Journal of Science, Vol. 7, Issue 2, 1926, p. 978-992.

[3] **Krylov N. M., Bogolyubov N. N.** Introduction to Nonlinear Mechanics. Princeton University Press, 1947, (in Russian).

[4] **Bulgakov B. V.** Self-excited oscillations of control systems. Prikladnaya Matematika and Mekhanika, Vol. 7, Issue 2, 1943, p. 97-108, (in Russian).

[5] **Goldfarb L. S.** Certain nonlinearities in control systems. Automatica and Telemekhanika, Vol. 8, Issue 5, 1947, p. 349-383, (in Russian).

[6] **Massera J. L.** Contributions to stability theory. Annals of Mathematics, Vol. 64, 1956, p. 182-206.

[7] **Boiko I. M.** Oscillations and transfer properties of relay servo systems – the locus of a perturbed relay system approach. Automatica, Vol. 41, 2005, p. 677-683.

[8] **Boiko I.** Discontinuous Control Systems: Frequency-Domain Analysis and Design. Springer London, 2008.

[9] **Filippov A. F.** Differential Equations with Discontinuous Right-Hand Sides. Kluwer, Dordrecht, 1988.

[10] **Khalil H. K.** Nonlinear Systems. Prentice Hall, 2002.

[11] **Tsypkin Ya.Z.** Relay Control Systems. University Press, Cambridge, 1984.

[12] **Atherton D. P.** Correspondence: analytical determination of limit cycles for a class of third-order non-linear system. International Journal of Control, Vol. 21, Issue 6, 1975, p. 1021-1023.

[13] **Astrom K. J., et al.** Adaptive Control, Filtering and Signal Processing. The IMA Volumes in Mathematics and its Applications, Vol. 74, 1995.

[14] **Piiroinen P. T., Kuznetsov Yu A.** An event-driven method to simulate Filippov systems with accurate computing of sliding motions. ACM Transactions on Mathematical Software (TOMS), Vol. 34, Issue 3, 2008, p. 13.

PIII

COUNTEREXAMPLES TO THE KALMAN CONJECTURES

by

N.V. Kuznetsov, O.A. Kuznetsova, D.V. Koznov, R.N. Mokaev, B.R. Andrievsky
2018

IFAC-PapersOnLine, Vol. 51, I. 33, PP. 138–143,
https://doi.org/10.1016/j.ifacol.2018.12.107

Available online at www.sciencedirect.com

ScienceDirect

IFAC PapersOnLine 51-33 (2018) 138–143

Counterexamples to the Kalman Conjectures ⋆

N.V. Kuznetsov [*,**,***], **O.A. Kuznetsova** [*,***], **D. Koznov** [*], **R.N. Mokaev** [*,***], **B. Andrievsky** [*,**],

[*] *Faculty of Mathematics and Mechanics, Federal State Budgetary Educational Institution of Higher Education "Saint Petersburg State University", Russia*
[**] *Institute for Problems of Mechanical Engineering of RAS, Russia*
[***] *Dept. of Mathematical Information Technology, University of Jyväskylä, Jyväskylä, Finland*

Abstract: In the paper counterexamples to the Kalman conjecture with smooth nonlinearity basing on the Fitts system, that are periodic solution or hidden chaotic attractor are presented. It is shown, that despite the fact that Kalman's conjecture (as well as Aizerman's) turned out to be incorrect in the case of $n > 3$, it had a huge impact on the theory of absolute stability, namely, the selection of the class of nonlinear systems whose stability can be studied with linear methods.

© 2018, IFAC (International Federation of Automatic Control) Hosting by Elsevier Ltd. All rights reserved.

Keywords: Kalman conjecture, Fitts system, Barabanov system, point-mapping method, hidden attractor

1. INTRODUCTION

In the middle of the past century the theory of absolute stability was rapidly developed [Lurie and Postnikov, 1944, Bulgakov, 1943, Aizerman, 1949, Letov, 1965, Pliss, 1958, LaSalle and Lefschetz, 1961, Yakubovich, 1958, Aizerman and Gantmakher, 1963, Andronov et al., 1966, Gelig et al., 1978].history

For continuous and discontinuous nonlinearities one of the challenging problems is the selection of classes of systems for which it is possible to obtain a necessary and sufficient condition for absolute stability. The history of attempts to solve this problem is connected with the Aizermans' [Aizerman, 1949] and Kalmans' [Kalman, 1957] conjectures about absolute stability of control systems with nonlinearity satysfying Routh-Hurwitz criterion. In the present paper the differences in the behavior of systems with continuous and discontinuous nonlinearities that are counterexamples to the Kalman conjecture are considered.

Aizerman's conjecture was complitely investigated in two-dimensional case [Malkin, 1952, Erugin, 1952, Krasovsky, 1952]. It turned out to be true except for the special case when trajectories tend to infinity.

In 1957 R.E. Kalman, being unaware of Aizerman's research, proposed a statement concerning restrictions on the derivative of nonlinearity to be in the Hurwitz angle.

Kalman conjecture is more rigorous than Aizermans' one, so it turned out to be valid for two- and three-dimensional cases [Leonov et al., 1996]. These cases are natural for applied mechanical problems, so it is necessary to emphasize Kalmans' scientific intuition.

Unlike the continuous-time case, Kalman conjecture is false in general for two-dimensional discrete-time systems [Alli-Oke et al., 2012].

⋆ This work was supported by the grant NSh-2858.2018.1 for the Leading Scientific Schools of Russia (2018-2019).

By now Kalman conjecture remains unsolved in the general case.

2. KALMAN CONJECTURE

Consider the following system with one scalar non-linearity in the Lur'e form

$$\dot{x} = Ax + b\varphi(\sigma), \qquad \sigma = c^* x, \tag{1}$$

where A is a constant $n \times n$ matrix, b and c - constant n-dimensional vectors, all quantities are real, $*$ is the sign of transposition, φ is a smooth scalar function with $\varphi(0) = 0$ and the following condition is satisfied at differentiability points:

$$k_1 \le \varphi'(\sigma) \le k_2, \qquad \sigma \in (-\infty, +\infty), \tag{2}$$

where k_1 is a number or $-\infty$, k_2 is a number or $+\infty$.

In 1957, R.E. Kalman formulated the following conjecture: if a linear system $\dot{x} = Ax + kbc^* x$, $k \in [k_1, k_2]$, is globally asymptotically stable, then the system (1) is also globally asymptotically stable. Let us recall that a system is globally asymptotically stable if its zero solution is Lyapunov stable and $\lim_{t\to+\infty} |x(t, x_0)| = 0$ for any $x_0 \in \mathbb{R}^n$.

3. HISTORY

The first counterexample to the Kalman conjecture were obtained due to experiments by Fitts [1966], who studied oscillations in nonlinear feedback systems.

Further attempts to construct counterexamples were mainly related to the consideration of systems with discontinuous piecewise-linear nonlinearities and integration of such systems in sections of linearity [Andronov et al., 1966].

In the beginning of the past century the concept of discontinuous system appeared in study of various applied mechanical problems, e.g. vibrations in a mechanical model with dry friction [den Hartog, 1930], damping flutter in aircraft control systems with dry friction [Keldysh, 1944], autopilot construction problem [Andronov and Bautin, 1955].

2405-8963 © 2018, IFAC (International Federation of Automatic Control) Hosting by Elsevier Ltd. All rights reserved.
Peer review under responsibility of International Federation of Automatic Control.
10.1016/j.ifacol.2018.12.107

Andronov et al. [1966] introduced the idea of trajectory "sewing" and developed all the necessary "ingredients" of discontinuous systems theory. Later, the elements of the discontinuous systems theory were rigorously formulated in [Wazewski, 1961, Filippov, 1988].

At first the development of the theory of absolute stability was related to the names of its founders Lurie and Postnikov [1944]. They tried to solve the problem of absolute stability of automatic control systems using Lyapunov function method. Popov [1961, 1973] developed original and effective criterion in the form of frequency sufficient condition for absolute stability. The conjecture that sufficient conditions of absolute stability, obtained by using of frequency methods, are also necessary conditions was refuted by Yakubovich [1967], who constructed an absolutely stable system, for which the Popov's frequency condition is not satisfied, and later by Pyatnitsky [1973]. Important results by Yakubovich [1962] and Kalman [1963] resulted in a well-known Kalman-Yakubovich-Popov lemma (see [Barabanov et al., 1996]).

Also it was natural to generalize various concepts of Lyapunov's stability theory and frequency approach to the discontinuous systems theory. The first corresponding results and new different approaches were obtained by representatives of the scientific school of V.A. Yakubovich ([Yakubovich, 1967, 1975, Gelig et al., 1978, Barabanov et al., 1996]).

Mention that similar results independently obtained in [Shevitz and Paden, 1994].

Later results given in [Gelig et al., 1978] were developed and new methods of stability analysis of discontinuous control systems were presented. Note that only sufficient conditions for absolute stability of discontinuous systems were stated [Gelig et al., 1978].

Now let us consider two counterexamples to Kalman conjecture and verify the fulfillment of analytical sufficient conditions for global asymptotic stability of corresponding systems.

4. FITTS COUNTEREXAMPLE

As already mentioned, the first counterexample to the Kalman conjecture was proposed by Fitts [Fitts, 1966], who performed the computer simulation of system (1) with the transfer function

$$W(p) = \frac{p^2}{((p+\beta)^2+0.9^2)\,((p+\beta)^2+1.1^2)} \tag{3}$$

and the cubic nonlinearity $\varphi(\sigma) = K\sigma^3$. As a result of the simulation, Fitts discovered periodic solutions of the system (1) for the values of parameters $m_1 = 0.9$, $m_2 = 1.1$, $K = 10$ and $\beta \in (0.01, 0.75)$. However, later N.E. Barabanov showed in [Barabanov, 1988] that the results of the experiments were incorrect for a part of the parameters that Fitts considered, specifically, for $\beta \in (0.572, 0.75)$. The Kalman conjecture was further discussed and doubts in the counterexamples of Fitts and Barabanov were raised in [Bernat and Llibre, 1996, Glutsyuk, 1998, Meisters, 1996].

4.1 Fitts' counterexample variation

Let us present the following novel variation of Fitts' counterexample. Consider system (1) with $n = 4$ defined by transfer function (3) from Fitts' counterexample with the nonlinearity

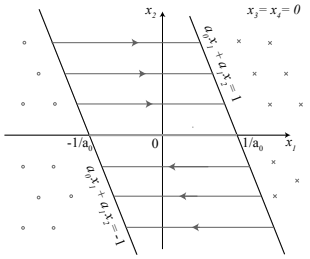

Fig. 1. Sliding mode manifold $\{(x_1,x_2,x_3,x_4) \in \mathbb{R}^4 \mid x_3 = x_4 = 0, -1 \le a_0x_1 + a_1x_2 \le 1\}$ for the Fitts system (4). Arrowed lines define the motion on the surface, thick green line defines the rest segment.

$\varphi(\sigma) = \operatorname{sign}(\sigma)$. Deriving the system from transfer function (3), one obtains [Leonov, 2001]:

$$\begin{aligned} \dot{x}_1 &= x_2, \\ \dot{x}_2 &= x_3, \\ \dot{x}_3 &= x_4, \\ \dot{x}_4 &= -a_0x_1 - a_1x_2 - a_2x_3 - a_3x_4 + \operatorname{sign}(-x_3), \end{aligned} \tag{4}$$

where $a_0 = (m_1^2+\beta^2)(m_2^2+\beta^2)$, $a_1 = 2\beta(m_1^2+m_2^2+2\beta^2)$, $a_2 = m_1^2+m_2^2+6\beta^2$, $a_3 = 4\beta$.

Here

$$A = \begin{pmatrix} 0 & 1 & 0 & 0 \\ 0 & 0 & 1 & 0 \\ 0 & 0 & 0 & 1 \\ -a_0 & -a_1 & -a_2 & -a_3 \end{pmatrix}, b = \begin{pmatrix} 0 \\ 0 \\ 0 \\ 1 \end{pmatrix}, c = \begin{pmatrix} 0 \\ 0 \\ -1 \\ 0 \end{pmatrix}. \tag{5}$$

Sliding mode manifold for the system (4) is given by:

$$D_{\text{fitts}} = \{(x_1,x_2,x_3,x_4) \in \mathbb{R}^4 \mid x_3 = x_4 = 0, \\ -1 \le a_0x_1 + a_1x_2 \le 1\},$$

Moreover, a sliding mode is described by the equations

$$\dot{x}_1 = x_2, \dot{x}_2 = 0, \dot{x}_3 = 0, \dot{x}_4 = 0, \tag{6}$$

so for the point $(x_{01}, x_{02}, 0, 0) \in D_{\text{fitts}}$ one gets $x_1(t) = x_{02}t + x_{01}, x_2(t) \equiv x_{02}$. The rest segment is

$$\Lambda_{\text{fitts}} = \{(x_1,x_2,x_3,x_4) \in \mathbb{R}^4 \mid x_2 = x_3 = x_4 = 0, \tag{7}$$

$$-\tfrac{1}{a_0} \le x_1 \le \tfrac{1}{a_0}\}. \tag{8}$$

4.2 Stability of Rest Segment

If there are trajectories that tend to some periodic solution of the system or infinity, then one can say that the system is not globally asymptotically stable.

Hidden and self-excited classification. Since is not proven that system (4) is globally asymptotically stable, one can expect the existence of a nontrivial attractor in the phase space. First let us recall the definition of attractor.

Consider system

$$\dot{\mathrm{x}} = f(\mathrm{x}, t), \tag{9}$$

where $\mathrm{x} \in \mathbb{R}^n$, $f : \mathbb{R}^n \to \mathbb{R}^n$ Define by $\mathrm{x}(t, \mathrm{x}_0)$ a solution of (9) such that $\mathrm{x}(0, \mathrm{x}_0) = \mathrm{x}_0$.

Definition 1. For system (9), a bounded closed invariant set K is

(i) a *(local) attractor* if it is a locally attractive set (i.e. $\lim_{t\to+\infty} \operatorname{dist}(K, \mathrm{x}(t, \mathrm{x}_0)) = 0 \ \forall \mathrm{x}_0 \in K(\varepsilon)$, where $K(\varepsilon)$ is a certain ε-neighborhood of set K),

(ii) a *global attractor* if it is a globally attractive set (i.e. $\lim_{t\to+\infty} \mathrm{dist}(K, \mathrm{x}(t,\mathrm{x}_0)) = 0 \ \forall \mathrm{x}_0 \in \mathbb{R}^n$),

where $\mathrm{dist}(K,\mathrm{x}) = \inf_{v\in K} ||v-\mathrm{x}||$ is the distance from the point $\mathrm{x} \in \mathbb{R}^n$ to the set $K \subset \mathbb{R}^n$ (see, e.g. [Leonov et al., 2015]).

Since the whole phase space is a global attractor and any finite union of attractors is again an attractor, it is reasonable to consider only minimal global and local attractors, i.e. the smallest bounded closed invariant set possessing the property (ii) or (i).

Localization and analysis of attractors is one of the main tasks of the investigation of dynamical systems. While trivial attractors (stable equilibrium points) can be easily found analytically, the search of periodic and chaotic attractors can turn out to be a challenging problem. For numerical localization of an attractor one needs to choose an initial point in the basin of attraction and observe how the trajectory, starting from this initial point, after a transient process visualizes the attractor. Leonov and Kuznetsov introduced in [Leonov et al., 2011, Leonov and Kuznetsov, 2011, Kuznetsov and Leonov, 2014] a classification of attractors based on the simplicity of finding the basins of attraction in the phase space.

Definition 2. An attractor is called a *self-excited attractor* if its basin of attraction intersects with any open neighborhood of an equilibrium, otherwise, it is called a *hidden attractor*.

Self-excited attractors can be easily visualized because its basin of attraction is connected with an unstable equilibrium and, therefore, can be localized numerically. For a hidden attractor, its basin of attraction is not connected with equilibria and, thus, the search and visualization of hidden attractors in the phase space may be a difficult task.

Further using a special computational package [Piiroinen and Kuznetsov, 2008] and Andronov's point-mapping method [Andronov and Maier, 1947], it will be shown that in system (4), for certain values of the β parameter it is possible to localize hidden attractors. Also it will be shown that this hidden attractors coexist with periodic solutions.

4.3 Trajectories computation

We performed numerical simulation in the vicinity $\varepsilon = 0.1$ of the rest segment (7) in the subspace (x_1, x_4) while $x_2 = x_3 = 0$. In our experiment for integration of solutions we used computational package from [Piiroinen and Kuznetsov, 2008]. Trajectories with initial point in the vicinity tended to a periodic solution (see Fig. 2).

4.4 Trajectories sewing

Let's write down the solutions of linear systems $\dot{\mathrm{x}} = A\mathrm{x} + b$ and $\dot{\mathrm{x}} = A\mathrm{x} - b$ given by (5) in the corresponding regions $\Sigma^+ = \{\mathrm{x} = (x_1,x_2,x_3,x_4) \in \mathbb{R}^4 \mid x_3 < 0\}$, $\Sigma^- = \{\mathrm{x} = (x_1,x_2,x_3,x_4) \in \mathbb{R}^4 \mid x_3 > 0\}$. Trajectories of (4) in three regions of phase space as the solutions of the linear systems may be obtained analytically without using numerical methods for solving ordinary differential equations and sewing them when switching modes. This gives the trajectory released from the point $(x_{01},x_{02},x_{03},x_{04}) = (10,10,10,10)$ for parameters values $m_1 = 0.9, m_2 = 1.1, \beta = 0.03$ on the time interval $t \in [0,500]$ and precision of 32 digits. Calculation shows that this trajectory attracts to the periodic orbit (see Fig. 3).

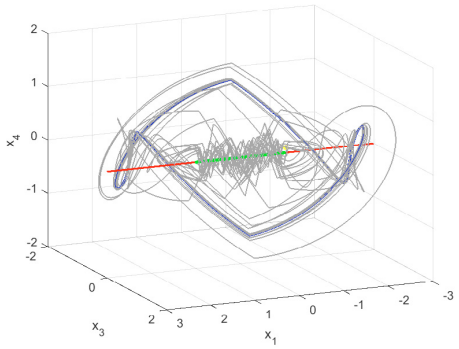

Fig. 2. Trajectory (gray) released from the point (-1.105017,0,0,0.05) (yellow) from vicinity of rest segment Λ_{fitts} tends to periodic solution (blue). $\beta = 0.03$

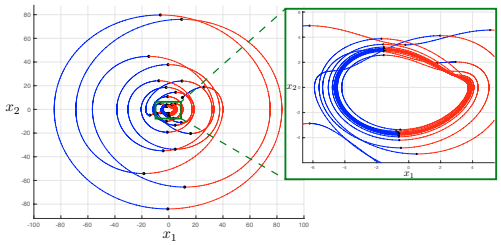

Fig. 3. Modeling of the system (4) for $\beta = 0.03$. Trajectories of the system $\dot{x} = Ax + b$ (red) are being sewed with the trajectories of the system $\dot{x} = Ax - b$ (blue) at the switching mode points (black).

4.5 Point-mapping method

This result can be clarified using Andronov's point-mapping method [Andronov and Maier, 1947]. Note that periodic solution of the system (4) consists of two parts: $\mathrm{x}^+(t,\mathrm{x}_0^+) \in \Sigma^+$, $t \in [0, T_+^{\mathrm{sw}}]$ (mode I) and $\mathrm{x}^-(t,\mathrm{x}_0^-) \in \Sigma^-$, $t \in [0, T_-^{\mathrm{sw}}]$ (mode II). Wherein $\mathrm{x}^\pm(0,\mathrm{x}_0^\pm) = \mathrm{x}_0^\pm = (x_{01}^\pm, x_{02}^\pm, 0, x_{04}^\pm)$, where $x_{04}^+ < 0$, $x_{04}^- > 0$ and $\mathrm{x}^\pm(T_\pm^{\mathrm{sw}}, \mathrm{x}_0^\pm) = \mathrm{x}_0^\mp$. Therefore the following equality holds:

$$\mathrm{x}^-(T_-^{\mathrm{sw}}, \mathrm{x}_0^-) = \mathrm{x}_0^+ = \mathrm{x}^+(-T_+^{\mathrm{sw}}, \mathrm{x}_0^-). \qquad (10)$$

By the analogy with Sec. 4.4 for solutions $\mathrm{x}^\pm(t,\mathrm{x}_0^\pm)$, the solution can be found analytically. For parameters $m_1 = 0.9$, $m_2 = 1.1$, $\beta = 0.03$ the values, found with the help of MATLAB software, are given in Tab. 1. Using the coordinates of the initial point $(x_{01}^-, x_{02}^-, 0, x_{04}^-)$ we can localize orbitally asymptotically stable periodic solution (see Fig. 8). Note that this periodic solution coexists with periodic solution obtained in 4.3.

4.6 Strange attractor

Now we are going to use continuation method for numerical localization of nonperiodic strange attractor in the system (4). It is often used for hidden attractors localization [Leonov et al., 2010, Bragin et al., 2011, Leonov and Kuznetsov, 2011, 2013]. In this method, a sequence of systems is considered and each corresponds to a specially chosen parameter with values in a certain interval. It is assumed that for the first (initial) system the initial data for numerical localization of periodic (or chaotic) solutions can be obtained analytically. Thus, we can

Table 1. Coordinates of the point on the periodic solution of the system (4) for $\beta = 0.03$ and the duration of the modes I and II.

x_{01}^-	$-0.625205162606931095343423624907 23$
x_{02}^-	$-3.732409707265061046582527856259 4$
x_{04}^-	3.475416972869712079398927411163 6
T_+^{sw}	6.086116329959190440192942793354 3
T_-^{sw}	3.255814324139461747057143591736 8

consider a system with an initial self-excited attractor as an initial system. Then we can numerically trace the transformation of the initial solution in the transition from one system to another. At the same time, the initial data for the solution of the next system is the endpoint of the solution of the previous system. The latter system corresponds to a system for which a hidden attractor is sought. As a result, if there is no loss of stability bifurcation, then it is possible to find hidden attractor.

Consider an interval $\beta \in [0.03, 0.1]$ and choose the partition with the step 0.0175. For fixed $m_1 = 0.9$, $m_2 = 1.1$ and for each $\beta = \beta^j = 0.03 + 0.0175j$, $j = 0, \ldots, 4$ we will integrate the solution $\mathrm{x}^j(t)$ of the system (4) on the time interval $[0, T]$, $T = 2000$.

We use as initial data for the system with $\beta = \beta^{j+1}$ the endpoint of the solution with $\beta = \beta^j$, i.e. $\mathrm{x}^{j+1}(0) := \mathrm{x}^j(T)$. Here we can integrate the solutions both using the procedure described in Sec. 4.3 and special computational package described in [Piiroinen and Kuznetsov, 2008] for modeling solutions in Filippov sense. Using the second option and performing the continuation method we localized strange nonperiodic attractor (see Fig. 6,Fig. 7). Also note that this attractor coexist with periodic solution (see Fig. 9, Fig. 10).

This strange attractor (as well as periodic solution for $\beta = 0.03$) remains under the reverse scenario of discontinuous Aizerman – Pyatnitsky approximation [Aizerman and Pyatnitskiy, 1974], i.e. transition from nonlinearity $\varphi(\sigma) = \psi_0(\sigma) = \operatorname{sign}\sigma$ to $\varphi(\sigma) = \psi_N(\sigma)$ nonlinearity where

$$\varphi(\sigma) = \psi_N(\sigma) \equiv \begin{cases} -1, & \sigma \le -N, \\ \frac{1}{N}\sigma, & -N \le \sigma \le N, \\ 1, & \sigma \ge N \end{cases} \qquad (11)$$

for sufficiently small values of N (e.g. for $N = 0.05$) in the system (4).

Then using continuation method we consider nonlinearity $\varphi(\sigma) = \chi_\varepsilon(\sigma) \equiv \psi_N(\sigma) + \varepsilon\,(\tanh(\sigma/N) - \psi_N(\sigma))$ for ε increasing from 0 to 1 with the step 0.1 to implement transition from piecewise-differentiable nonlinearity (11) (corresponding to $\varphi(\sigma) = \chi_0(\sigma) = \psi_N(\sigma)$) to smooth nonlinearity $\varphi(\sigma) = \chi_1(\sigma) = \tanh(\sigma/N)$. During this transition the local strange attractor obtained in the previous steps is preserved (see Fig. 4–5).

Thus in the system (1) with $\varphi(\sigma) = \tanh(\sigma/N)$ for sufficient small values of N there is strange attractor and for $k_1 < 0$ and $k_2 = +\infty$ Kalman conjecture is wrong.

5. BARABANOV SYSTEM

In 1988 N.E. Barabanov constructed the following counterexample to the Kalman conjecture:

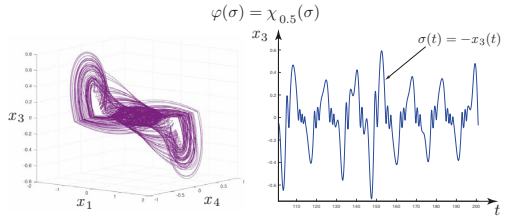

Fig. 4. Strange attractor in the system (4) for $\beta = 0.1$ and $\varphi(\sigma) = \chi_\varepsilon(\sigma) \equiv \psi_N(\sigma) + \varepsilon\,(\tanh(\sigma/N) - \psi_N(\sigma))$, $N = 0.01$, $\varepsilon = 0.5$.

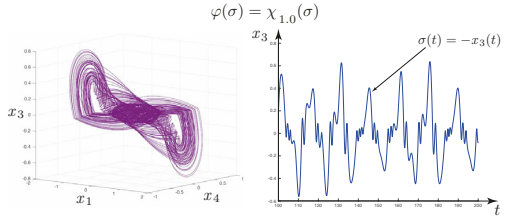

Fig. 5. Strange attractor in the system (4) for $\beta = 0.1$ and $\varphi(\sigma) = \chi_\varepsilon(\sigma) \equiv \psi_N(\sigma) + \varepsilon\,(\tanh(\sigma/N) - \psi_N(\sigma))$, $N = 0.01$, $\varepsilon = 1$.

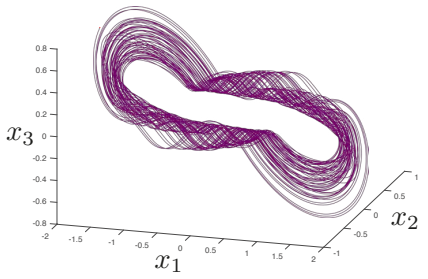

Fig. 6. Projection of the strange attractor in the system (4) for $\beta = 0.1$ in the subspace (x_1, x_2, x_3).

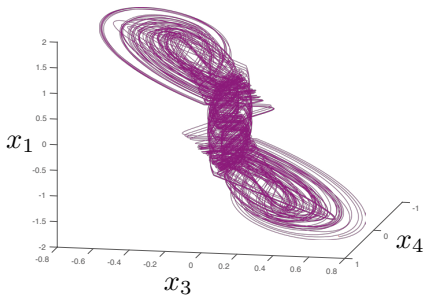

Fig. 7. Projection of the strange attractor in the system (4) for $\beta = 0.1$ in the subspace (x_1, x_3, x_4).

$$\begin{aligned} \dot{x}_1 &= x_2, \\ \dot{x}_2 &= -x_4, \\ \dot{x}_3 &= x_1 - 2x_4 - \varphi(x_4), \\ \dot{x}_4 &= x_1 + x_3 - x_4 - \varphi(x_4), \end{aligned} \qquad (12)$$

where $\varphi = \operatorname{sign}(\sigma)$. In this case

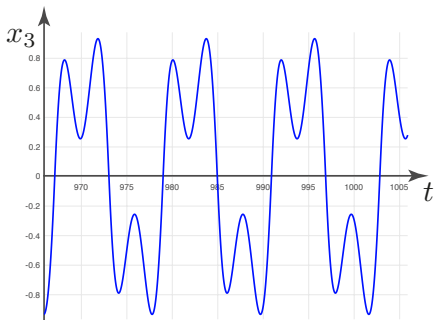

Fig. 8. Periodic solution of the system (4) for $\beta = 0.03$.

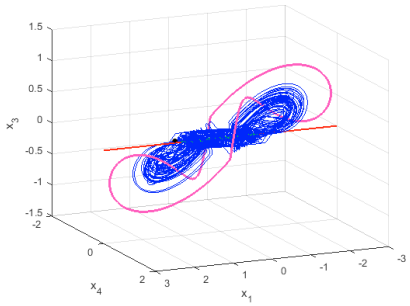

Fig. 9. Coexisting periodic solution and chaotic attractor in (4) for $\beta = 0.1$ in the subspace (x_1, x_3, x_4)

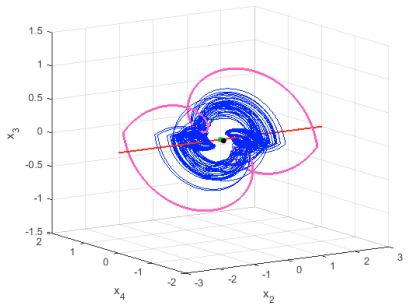

Fig. 10. Coexisting periodic solution and chaotic attractor in (4) for $\beta = 0.1$ in the subspace (x_2, x_3, x_4)

$$A = \begin{pmatrix} 0 & 1 & 0 & 0 \\ 0 & 0 & 0 & -1 \\ 1 & 0 & 0 & -2 \\ 1 & 0 & 1 & -1 \end{pmatrix}, \qquad b = \begin{pmatrix} 0 \\ 0 \\ -1 \\ -1 \end{pmatrix}, \qquad c = \begin{pmatrix} 0 \\ 0 \\ 0 \\ 1 \end{pmatrix}.$$

Sliding mode manifold for system (12) is

$$D_{\text{bar}} = \{(x_1, x_2, x_3, x_4) \in \mathbb{R}^4 \mid x_4 = 0, x_2 = C_1, \\ x_1 = C_1 t + C_2, x_3 = C_3 e^{-t}, -1 \le x_1 + x_3 \le 1\}$$

Rest segment for the system (12) is

$$\Lambda_{\text{bar}} = \{(x_1, x_2, x_3, x_4) \in \mathbb{R}^4 \mid x_2 = x_3 = x_4 = 0, \\ -1 \le x_1 \le 1\}.$$

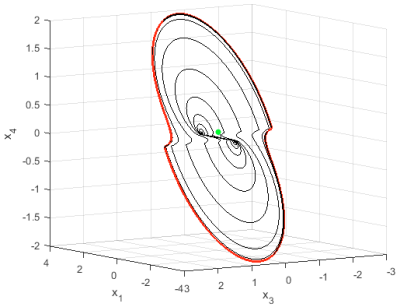

Fig. 11. Trajectory (black) released from the point $(0,0,0,\varepsilon)$ (green) and tends to the periodic solution (red) in the subspace (x_1, x_3, x_4). $T = 5000$.

5.1 Trajectories computation

For the Barabanov system the trajectories released from the vicinity of the rest segment have been numerically found by a simulation. In our experiment vicinity radius is $\varepsilon = 0.1$ in the space (x_1, x_4) (in this case we take $x_2 = x_3 = 0$). Resulting trajectories tended to the periodic solutions of the system (12), see Fig. 11.

6. CONCLUSION

In this paper we presented counterexamples to the Kalman conjecture with smooth nonlinearity basing on the Fitts system, that are periodic solution or hidden chaotic attractor. However, despite the fact that Kalman's conjecture (as well as Aizerman's) turned out to be incorrect in the case of $n > 3$, it had a huge impact on the theory of absolute stability, namely, the selection of the class of nonlinear systems whose stability can be studied with linear methods.

REFERENCES

Aizerman, M.A. (1949). On a problem concerning the stability in the large of dynamical systems. *Uspekhi Mat. Nauk (in Russian)*, 4, 187–188.

Aizerman, M.A. and Gantmakher, F.B. (1963). *Absolute Stability of Control Systems*. Izd Akad Nauk SSSR, Moscow.

Aizerman, M. and Pyatnitskiy, E. (1974). Foundations of a theory of discontinuous systems: I. *Autom.Remote Control*, 35, 1066–1079.

Alli-Oke, R., Carrasco, J., Heath, W., and Lanzon, A. (2012). A robust Kalman conjecture for first-order plants. *IFAC Proceedings Volumes (IFAC-PapersOnline)*, 7, 27–32. doi: 10.3182/20120620-3-DK-2025.00161.

Andronov, A.A., Vitt, E.A., and Khaikin, S.E. (1966). *Theory of Oscillators*. Pergamon Press, Oxford.

Andronov, A. and Bautin, N. (1955). The theory of stabilization of the course of a neutral aeroplane by means of an automatic pilot having the constant speed of a servomechanism i. *Izvestiya Akad. Nauk SSSR, Ser. Tekhn. Nauk*, 6, 3–32. (in Russian).

Andronov, A. and Maier, A. (1947). On the Vyshnegradkii problem in the theory of direct control. *Avtomatika i Telemekhanika (in Russian)*, 8(5).

Barabanov, N.E. (1988). On the Kalman problem. *Sib. Math. J.*, 29(3), 333–341.

Barabanov, N., Gelig, A., Leonov, G., Likhtarnikov, A., Matveev, A., Smirnova, V., and Fradkov, A. (1996). The frequency theorem (the yakubovich-kalman lemma) in control theory. *Automatic Remote Control*, 10(9), 3–40.

Bernat, J. and Llibre, J. (1996). Counterexample to Kalman and Markus-Yamabe conjectures in dimension larger than 3. *Dynamics of Continuous, Discrete and Impulsive Systems*, 2(3), 337–379.

Bragin, V., Vagaitsev, V., Kuznetsov, N., and Leonov, G. (2011). Algorithms for finding hidden oscillations in nonlinear systems. The Aizerman and Kalman conjectures and Chua's circuits. *Journal of Computer and Systems Sciences International*, 50(4), 511–543. doi:10.1134/S106423071104006X.

Bulgakov, B.V. (1943). Self-excited oscillations of control systems. *Prikl. Mat. Mekh. (in Russian)*, 7(2), 97–108.

den Hartog, J. (1930). Forced vibrations with combined viscous and coulomb damping. *The London, Edinburgh, and Dublin Philosophical Magazine and Journal of Science*, 9(59), 801–817.

Erugin, N.P. (1952). A problem in the theory of stability of automatic control systems. *Prikl. Mat. Mekh. (in Russian)*, (5), 620–628.

Filippov, A.F. (1988). *Differential equations with discontinuous right-hand sides*. Kluwer, Dordrecht.

Fitts, R.E. (1966). Two counterexamples to Aizerman's conjecture. *Trans. IEEE*, AC-11(3), 553–556.

Gelig, A., Leonov, G., and Yakubovich, V. (1978). *Stability of Nonlinear Systems with Nonunique Equilibrium (in Russian)*. Nauka. (English transl: Stability of Stationary Sets in Control Systems with Discontinuous Nonlinearities, 2004, World Scientific).

Glutsyuk, A.A. (1998). Meetings of the Moscow mathematical society (1997). *Russian mathematical surveys*, 53(2), 413–417.

Kalman, R.E. (1957). Physical and mathematical mechanisms of instability in nonlinear automatic control systems. *Transactions of ASME*, 79(3), 553–566.

Kalman, R. (1963). Lyapunov functions for the problem of lurie in automatic control. *Proc. Nat. Acad. Sci. USA*, 49, 201–205. (in Russian).

Keldysh, M. (1944). On dampers with a nonlinear characteristic. *Tr. TsAGI (in Russian)*, 557, 26–37.

Krasovsky, N.N. (1952). Theorems on the stability of motions determined by a system of two equations. *Prikl. Mat. Mekh. (in Russian)*, 16(5), 547–554.

Kuznetsov, N. and Leonov, G. (2014). Hidden attractors in dynamical systems: systems with no equilibria, multistability and coexisting attractors. *IFAC Proceedings Volumes*, 47, 5445–5454. doi:10.3182/20140824-6-ZA-1003.02501.

LaSalle, J. and Lefschetz, S. (1961). *Stability by Liapunov's direct method: with applications*. Academic Press, New-York-London.

Leonov, G. (2001). *Mathematical problems of control theory. An introduction*. World Scientific, Singapore.

Leonov, G., Bragin, V., and Kuznetsov, N. (2010). Algorithm for constructing counterexamples to the Kalman problem. *Doklady Mathematics*, 82(1), 540–542. doi: 10.1134/S1064562410040101.

Leonov, G. and Kuznetsov, N. (2011). Algorithms for searching for hidden oscillations in the Aizerman and Kalman problems. *Doklady Mathematics*, 84(1), 475–481. doi: 10.1134/S1064562411040120.

Leonov, G. and Kuznetsov, N. (2013). Hidden attractors in dynamical systems. From hidden oscillations in Hilbert-Kolmogorov, Aizerman, and Kalman problems to hidden chaotic attractors in Chua circuits. *International Journal of Bifurcation and Chaos*, 23(1). doi: 10.1142/S0218127413300024. art. no. 1330002.

Leonov, G., Kuznetsov, N., and Mokaev, T. (2015). Homoclinic orbits, and self-excited and hidden attractors in a Lorenz-like system describing convective fluid motion. *Eur. Phys. J. Special Topics*, 224(8), 1421–1458. doi:10.1140/epjst/e2015-02470-3.

Leonov, G., Kuznetsov, N., and Vagaitsev, V. (2011). Localization of hidden Chua's attractors. *Physics Letters A*, 375(23), 2230–2233. doi:10.1016/j.physleta.2011.04.037.

Leonov, G., Ponomarenko, D., and Smirnova, V. (1996). *Frequency-Domain Methods for Nonlinear Analysis. Theory and Applications*. World Scientific, Singapore.

Letov, A.M. (1965). *Stability of Nonlinear Controlled Systems*. Gostekhizdat (In Russian), Moscow. (in Russian).

Lurie, A.I. and Postnikov, V.N. (1944). To the stability theory of controlled systems. *Applied Mathematics and Mechanics (in Russian)*, 8(3), 246–248.

Malkin, I.G. (1952). On the stability of automatic control systems. *Prikl. Mat. Mekh. (in Russian)*, (16(4)), 495–499.

Meisters, G. (1996). A biography of the Markus-Yamabe conjecture. *http://www.math.unl.edu/ gmeisters1/papers/HK1996.pdf*.

Piiroinen, P.T. and Kuznetsov, Y.A. (2008). An event-driven method to simulate Filippov systems with accurate computing of sliding motions. *ACM Transactions on Mathematical Software (TOMS)*, 34(3), 13.

Pliss, V.A. (1958). *Some Problems in the Theory of the Stability of Motion (in Russian)*. Izd LGU, Leningrad.

Popov, V.M. (1961). On the absolute stability of nonlinear controlled systems. *Avtomatika i Telemekhanika*, 8, 961–970. (in Russian).

Popov, V.M. (1973). *Hyperstability of Control Systems*. Springer-Verlag, New York.

Pyatnitsky, E. (1973). On the existence of absolute stability systems, for which the criterion of V.-M. Popov is not satisfied. *Avtomatika i Telemekhanika*, 1, 30–37. (in Russian).

Shevitz, D. and Paden, B. (1994). Lyapunov stability theory of nonsmooth systems. *IEEE Transactions on Automatic Control*, 39, 1910–1914.

Wazewski, T. (1961). Sur une condition équivalente l'équation au contingent. *Bull. Acad. Polon. Sci.*, 9, 865–867.

Yakubovich, V.A. (1958). On boundedness and stability in large of solutions of some nonlinear differential equations. *Doklady Akademii Nauk SSSR (in Russian)*, 121(6), 984–986.

Yakubovich, V. (1962). Solving some matrix inequalities, which are meeting in control theory. *Doklady Acad. Nauk SSSR*, 143, 1304–1307. (in Russian).

Yakubovich, V. (1967). Frequency conditions of absolute stability of the control systems with some non-linear and linear non-stationary blocks. *Avtomatika i Telemekhanika*, 5–30. (in Russian).

Yakubovich, V. (1975). *Methods of the theory of absolute stability*. Nauka, Moscow. (in Russian).

PIV

COEXISTENCE OF HIDDEN ATTRACTORS AND MULTISTABILITY IN COUNTEREXAMPLES TO THE KALMAN CONJECTURE

by

N.V. Kuznetsov, O.A. Kuznetsova, T.N. Mokaev, R.N. Mokaev, M.V. Yuldashev, R.V. Yuldashev 2019 (accepted to IFAC-PapersOnLine)

Proceedings of the 11th IFAC Symposium on Nonlinear Control Systems

Coexistence of hidden attractors and multistability in counterexamples to the Kalman conjecture

N.V. Kuznetsov [*,**,***], **O.A. Kuznetsova** [*], **T.N. Mokaev** [*], **R.N. Mokaev** [*,**], **M.V. Yuldashev** [*], **R.V. Yuldashev** [*]

[*] *Faculty of Mathematics and Mechanics, St. Petersburg State University, Russia*
[**] *Dept. of Mathematical Information Technology, University of Jyväskylä, Jyväskylä, Finland*
[***] *Institute for Problems in Mechanical Engineering RAS, Russia*

Abstract: The Aizerman and Kalman conjectures played an important role in the theory of global stability for control systems and set two directions for its further development – the search and formulation of sufficient stability conditions, as well as the construction of counterexamples for these conjectures. From the computational perspective the latter problem is nontrivial, since the oscillations in counterexamples are hidden, i.e. their basin of attraction does not intersect with a small neighborhood of an equilibrium. Numerical calculation of initial data of such oscillations for their visualization is a challenging problem. Up to now all known counterexamples to the Kalman conjecture were constructed in such a way that one locally stable limit cycle (hidden oscillation) co-exists with a locally stable equilibrium. In this paper we demonstrate a multistable configuration of three co-existing hidden oscillations (limit cycles) and a locally stable equilibrium in the phase space of the fourth-order system, which provides a new class of counterexamples to the Kalman conjecture.

Keywords: global stability, hidden attractors, multistability, Kalman conjecture, periodic oscillations

1. INTRODUCTION

The necessity to study stability and limit dynamical regimes (attractors) arises in classical theoretical and applied problems. One of the first such problems is related to the design of automatic control systems, which ensure the transition of the controlled object to the operating regime and its stability with respect to external disturbances. The first dynamical models of control systems were constructed in a way that the operating regime corresponded to the unique globally stable equilibrium state. After that models with oscillating operating regimes (periodic attractors) and chaotic regimes (chaotic attractors) were obtained. Later on, multistable models with different co-existing regimes (attractors) were discovered. Control of system states and their transfer into the basin of attraction of a desired attractor is the subject for study of the oscillation control theory (see e.g. [Fradkov and Pogromsky, 1998, Fradkov and Evans, 2005]). One of the first theoretical problems on multistability is the second part of the famous Hilbert's 16th problem on the number and mutual disposition of coexisting periodic attractors in two-dimensional polynomial systems. For chaotic multidimensional dynamical systems a similar problem on the number and mutual disposition of chaotic attractors and, in particular, their dependence on the degree of polynomials in the model is discussed in [Leonov and Kuznetsov, 2015, Kuznetsov et al., 2018].

For nonlinear systems with a unique equilibrium and bounded solutions, the question arose: how to find a class of systems for which the condition for the absence of the possibility for birth of self-excited oscillations implies the absence of hidden oscillations [1] and the global stability of the equilibrium. This problem has its origins in the Watt governor stability studies. In 1877, I.A. Vyshnegradsky [Vyshnegradsky, 1877] for the closed dynamic model "machine + governor" studied an approximate linear mathematical model without dry friction and proposed the stability conditions of the desired operating regime corresponding to the equilibrium state (trivial attractor). However, the question about a rigorous proof of the Vyshnegradsky problem on the validity of the linearization procedure for a system by discarding dry friction remained open. In 1885, M.H. Léauté showed [Léauté, 1885] the

[1] In 2009, G.A. Leonov and N.V. Kuznetsov proposed the classification of oscillations as being hidden or self-excited and laid the foundations of the *theory of hidden oscillations*, which reflects the modern stage of development of the A.A. Andronov's theory of oscillations. Self-excited oscillations can be visualized numerically by a trajectory starting from a point in a neighborhood of an unstable equilibrium. In contrast, the basin of attraction for a hidden oscillation is not connected with equilibria and, thus is necessary to develop a special analytical-numerical methods to find initial points for their visualization. The current progress in the development of theory of hidden oscillations was recently presented at a plenary lecture at the 5th IFAC Conference on Analysis and Control of Chaotic Systems (see `https://chaos2018.dc.wtb.tue.nl`).

possibility of the appearance of limit periodic oscillations in dynamical models of control systems with dry friction. After that, publications appeared (see e.g. [Zhukovsky, 1909, p. 6]), which criticized Vyshnegradsky approach and questioned his conclusions. In response to this criticism, A.A. Andronov and A.G. Maier [Andronov and Maier, 1944] provided a rigorous global analysis of the nonlinear model of the Watt governor with dry friction and proved the sufficiency of the Vyshnegradsky conditions for the absence of limit oscillations and global stability of the operating regime [2] (i.e. the existence of a rest segment that attracts trajectories from any initial data). Further development and generalization of the results by Vyshnegradsky, Andronov and Maier were done by G.A. Leonov in [Leonov, 1971] (see also survey [Leonov et al., 2017]).

In 1949, inspirited by the discussion of the work [Andronov and Maier, 1944] at the Andronov's scientific seminar in the Institute of Automation and Remote Control (USSR Academy of Sciences, Moscow) [Bissell, 1998], M.A. Aizerman formulated a new problem. His question was whether the sufficient conditions of global stability of a class of nonlinear Lurie systems with a unique equilibrium coincide with the necessary stability conditions when the smooth nonlinearity belongs to the sector of linear stability [Aizerman, 1949]. Independently, a similar conjecture was later advanced by R.E. Kalman in 1957, with the additional requirement that the derivative of nonlinearity belong to the linear stability sector [Kalman, 1957]: *"If $\varphi(\sigma)$ in Fig. 1 is replaced by constants k corresponding to all possible values of $\varphi'(\sigma)$, and it is found that the closed-loop system is stable for all such k, then it is intuitively clear that the system must be monostable; i.e. all transient solutions will converge to a unique, stable critical point."*

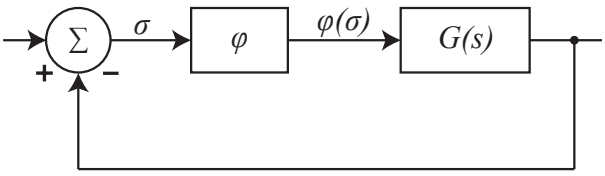

Fig. 1. Nonlinear control system. $G(s)$ is a linear transfer function, $\varphi(\sigma)$ is a single-valued smooth function [Kalman, 1957].

Kalman's statement can be reformulated in the following:

Conjecture 1. (The Kalman Conjecture). Consider the following control system in the Lurie form

$$\dot{\mathrm{x}} = A\mathrm{x} + b\varphi(\sigma), \quad \sigma = c^*\mathrm{x}, \tag{1}$$

where A is a constant $n \times n$ matrix, b and c are constant n-dimensional columns, with all values being, sign $*$ denotes the transpose, and φ is a smooth scalar function with $\varphi(0) = 0$, satisfying the condition

$$k_1 < \varphi'(\sigma) < k_2, \quad \sigma \in (-\infty, +\infty), \tag{2}$$

where k_1 is a number or $-\infty$, and k_2 is a number or $+\infty$. If the linear system $\dot{\mathrm{x}} = A\mathrm{x} + kbc^*\mathrm{x}$, with $k \in (k_1, k_2)$ is asymptotically stable, then system (1) is stable in large (i.e. a zero solution of system (1) is asymptotically stable and any solution tends to zero as $t \to +\infty$).

[2] This result was specially remarked when in 1946 A.A. Andronov was elected to the Academy of Sciences of the USSR where he became the first academician in control theory.

The Aizerman and Kalman conjectures played an important role in the theory of global stability for control systems and set two directions for its further development – the search and formulation of sufficient stability conditions (see pioneering works [Popov, 1961, Kalman, 1963, Gelig et al., 1978]), as well as the construction of counterexamples for these conjectures. From the computational perspective, the latter problem is nontrivial, since the oscillations in counterexamples are hidden, i.e. their basin of attraction does not intersect with small neighborhood of an equilibrium. Numerical calculation of initial data of such oscillations for their visualization is a challenging problem. Up to now all known counterexamples to the Kalman conjecture were constructed in such a way that one locally stable limit cycle (hidden oscillation) co-exists with a locally stable equilibrium. In this paper we demonstrate a multistable configuration of three co-existing hidden oscillations (limit cycles) and a locally stable equilibrium in the phase space of the fourth-order system, which provides a new class of counterexamples to the Kalman conjecture.

2. PREVIOUS COUNTEREXAMPLES TO KALMAN CONJECTURE

First known attempt to construct counterexamples to the Kalman conjecture was made by R.E. Fitts [Fitts, 1966], who experimentally studied a fourth-order system with a cubic nonlinearity. As a result, Fitts experimentally observed a periodic solution of considered system. Later on, N.E. Barabanov [Barabanov, 1988] claimed that some Fitts' results are not true and suggested to use discontinuous nonlinearity $\mathtt{sign}(\cdot)$ to derive counterexamples analytically. His work also raised critical discussions in [Bernat and Llibre, 1996, Meisters, 1996, Glutsyuk, 1998]. In particular, Bernat and Llibre [1996] pointed out the necessity to rigorously analyze non-local bifurcations while smoothing discontinuous nonlinearities. They suggested to start the procedure for constructing counterexamples with a piecewise linear nonlinearity $\mathtt{sat}(\cdot)$. In [Bragin et al., 2010, 2011, Leonov and Kuznetsov, 2011], it was introduced an effective approach for construction of counterexamples to the Kalman conjecture relying on an analytical-numerical search for periodic solutions by applying harmonic balance and numerical continuation methods and using smooth nonlinearity $\mathtt{tanh}(\cdot)$. For discrete-time systems Heath et al. [2015] demonstrated that Kalman conjecture is false even for second-order systems using counterexamples with stable periodic solutions [3]. Also construction of counterexamples to the Kalman conjecture is discussed in [Burkin and Khien, 2014].

3. COEXISTING LIMIT CYCLES

To construct numerically a new counterexample to the Kalman conjecture providing three co-existing limit cycles we combined Fitts' linear system, Barabanov's idea

[3] Remark that the difference between the dimensions of the phase spaces of a discrete-time system and a continuous-time system defined by autonomous ODE, for which the Kalman conjecture is not true, is equal to 2. This value coincides with the difference between the dimensions of the spaces in which chaos can occur (for discrete-time systems the dimension is equal to 1, for continuous-time systems – 3).

of considering $\mathtt{sign}(\cdot)$, and the idea from [Leonov and Kuznetsov, 2011] to use numerical continuation procedure while passing from $\mathtt{sign}(\cdot)$ to $\mathtt{tanh}(\cdot)$.

Consider the control system in the Lurie form (1) with

$$A=\begin{pmatrix} 0 & 1 & 0 & 0 \\ 0 & 0 & 1 & 0 \\ 0 & 0 & 0 & 1 \\ -a_0 & -a_1 & -a_2 & -a_3 \end{pmatrix},\ b=\begin{pmatrix} 0 \\ 0 \\ 0 \\ 1 \end{pmatrix},\ c=\begin{pmatrix} 0 \\ 0 \\ -1 \\ 0 \end{pmatrix}, \quad (3)$$

and $a_0=(m_1^2+\beta^2)(m_2^2+\beta^2)$, $a_1=2\beta(m_1^2+m_2^2+2\beta^2)$, $a_2=m_1^2+m_2^2+6\beta^2$, $a_3=4\beta$, $m_1=0.9, m_2=1.1, \beta=0.03$, $\varphi(\sigma)=\mathtt{tanh}(\sigma/\varepsilon)$, $\varepsilon=0.01$. The linear part of system (1) is defined by the transfer function

$$W(p)=\frac{p^2}{((p+\beta)^2+m_1^2)\,((p+\beta)^2+m_2^2)}. \quad (4)$$

Initial data for visualization of periodic oscillations were obtained using Andronov point mapping method [Andronov et al., 1966] [4] for system (1), (3) with non-linearity $\varphi(\sigma)=\mathtt{sign}(\sigma)$ and numerical continuation method [5] for smoothing the discontinuous nonlinearity (see e.g. [Leonov and Kuznetsov, 2013, Leonov et al., 2017]). Corresponding initial points for each stable limit cycle are presented below in Table 1. In system (1), (3) with the smooth nonlinearity $\varphi(\sigma)=\mathtt{tanh}(\sigma/\varepsilon)$, $\varepsilon=0.01$ for obtained initial points the trajectories were numerically integrated, which after the transient process allows us to visualize three hidden periodic attractors (see Fig. 2 and Table 2 with initial data). For each periodic attractor, an additional analysis of the local basin of attraction was carried out by choosing a grid of points in the vicinity of the periodic attractor and checking the attraction of all the trajectories with initial data from these points to the periodic attractor.

Table 1. Initial data for modeling of the three periodic attractors for system (1), (3) with nonlinearity $\varphi(\sigma)=\mathtt{sign}(\sigma)$.

	1st and 2nd	3rd
x_1	±0.62520516260693109	−2.113517446278802
x_2	±3.73240970726506105	0.664336179538623
x_3	0	0.891912878629890
x_4	∓3.47541697286971208	0.278600965570120

Table 2. Initial data for modeling of the three periodic attractors for system (1), (3) with nonlinearity $\varphi(\sigma)=\mathtt{tanh}(\sigma/\varepsilon)$, $\varepsilon=0.01$.

	1st and 2nd	3rd
x_1	±0.625216695745867	−2.11395731851229
x_2	±3.73239217905780	0.663680374961913
x_3	0	0.891701229667371
x_4	∓3.47341560599714	0.279201499188914

[4] Other methods for searching periodic oscillations of dynamical models with $\mathtt{sign}(\cdot)$ nonlinearity can be found e.g. in [Tsypkin, 1984, Boiko, 2008].

[5] The idea is to consider system (1), (3) with the nonlinearity $\varphi(\sigma)=\mathtt{sign}(\sigma)+\mu(\mathtt{tanh}(\sigma/\varepsilon)-\mathtt{sign}(\sigma))$, $\mu\in[0,1]$ and to switch from the system with nonlinearity $\mathtt{sign}(\cdot)$ to the system with a smooth nonlinearity $\mathtt{tanh}(\cdot)$ by varying the parameter μ from 0 to 1 with some small step. During the switching on each next step, the initial point for a trajectory to be integrated is chosen as the last point of the trajectory integrated on the previous step.

3.1 Sector of linear stability

It can be seen that the eigenvalues of the Jacobi matrix at the zero equilibrium are

$$-\beta\pm m_1 i, \qquad -\beta\pm m_2 i,$$

and, thus this equilibrium is locally stable.

Consider the matrix

$$A+kbc^*=\begin{pmatrix} 0 & 1 & 0 & 0 \\ 0 & 0 & 1 & 0 \\ 0 & 0 & 0 & 1 \\ -a_0 & -a_1 & -a_2-k & -a_3 \end{pmatrix}. \quad (5)$$

Characteristic polynomial of the matrix (5) is

$$\lambda^4+a_3\lambda^3+(a_2+k)\lambda^2+a_1\lambda+a_0. \quad (6)$$

Using Routh-Hurwitz criterion it is possible to show that for each $\beta>0$ the linear system $\dot{\mathrm{x}}=A\mathrm{x}+k\,b\,c^*\mathrm{x}$, given by matrices (3), is globally asymptotically stable for

$$k\in\big(-4\beta^2-\tfrac{(m_1^2-m_2^2)^2}{2(2\beta^2+m_1^2+m_2^2)},+\infty\big).$$

All the roots of the characteristic polynomial (6) have negative real parts, iff all the leading principal minors

$$\Delta_1=a_3=4\beta, \qquad \Delta_2=a_3(a_2+k)-a_1,$$
$$\Delta_3=a_1a_3k-a_1^2+a_1a_2a_3-a_0a_3^2, \qquad \Delta_4=a_0\Delta_3$$

of the Hurwitz matrix

$$\begin{pmatrix} a_3 & a_1 & 0 & 0 \\ 1 & a_2+k & a_0 & 0 \\ 0 & a_3 & a_1 & 1 \\ 0 & 1 & a_2+k & a_0 \end{pmatrix}$$

are positive. This implies the inequality $k>\frac{a_0a_3^2+a_1^2-a_1a_2a_3}{a_1a_3}$, which defines a sector of linear stability.

3.2 Describing function method and Popov criterion

Let us show that the application of the classical describing function method [6] and Popov method to system (1), (3) demonstrates the necessity of their further development to be able to obtain the necessary and sufficient conditions for the birth of oscillations and stability.

Suppose system (1), (3) has periodic solution with amplitude a and frequency ω_0. Hence, according to the harmonic balance method, frequency of this solution can be found from the following equality $\operatorname{Im}W(i\omega_0)=0$ and, therefore, $\omega_0=\sqrt{\beta^2+\frac{m_1^2+m_2^2}{2}}>0$. Also, from the equality $\operatorname{Re}W(i\omega_0)=0$ we can get a coefficient of harmonic linearization

$$k_{\mathrm{hl}}=-\frac{1}{\operatorname{Re}W(i\omega_0)}=-\left(4\beta^2+\frac{(m_1^2-m_2^2)^2}{2(2\beta^2+m_1^2+m_2^2)}\right)<0.$$

The describing function is defined as follows:

[6] Describing function method belongs to the approximate methods of analysis of control systems and there exist various examples of systems for which it leads to incorrect results in both prediction of stability (see e.g. [Bragin et al., 2011, Leonov and Kuznetsov, 2013]) and prediction of the existence of oscillations (see e.g. [Leonov and Kuznetsov, 2018a,b]).

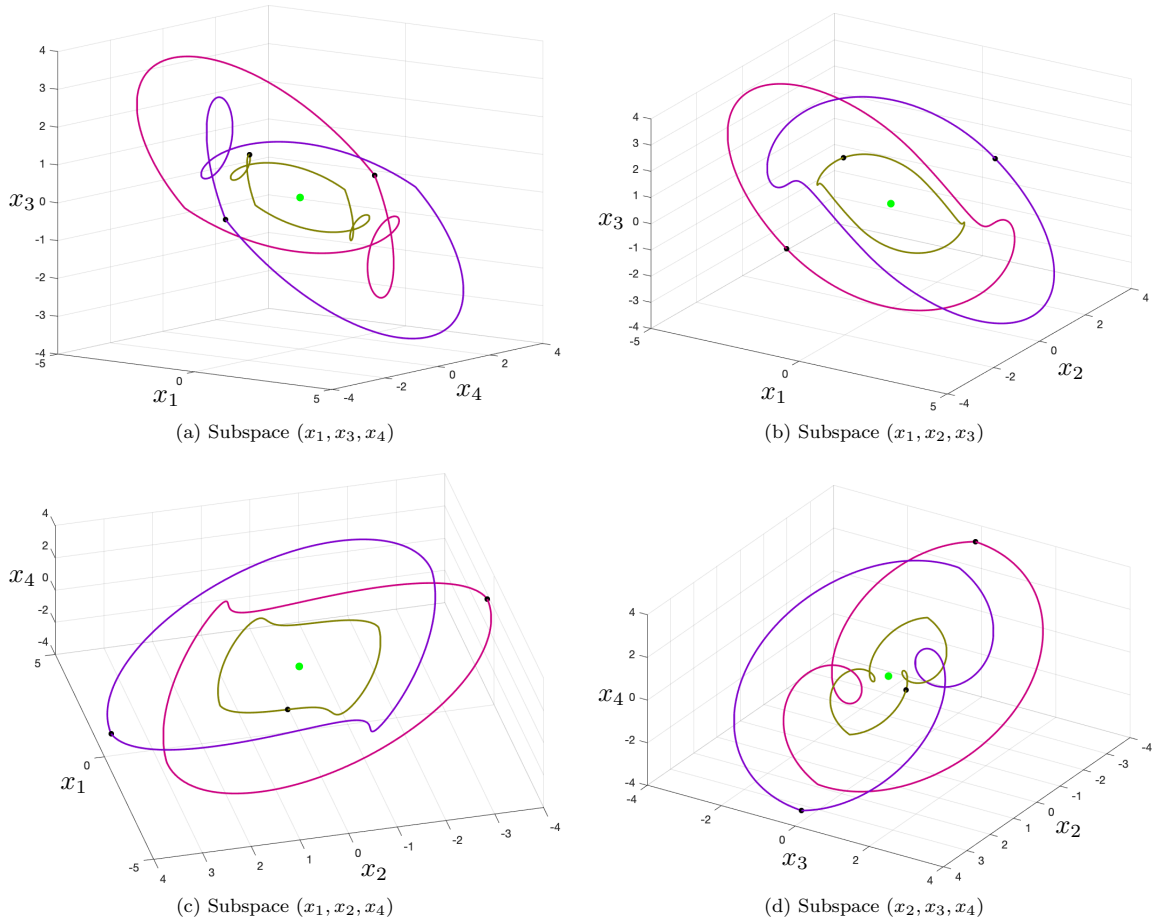

(a) Subspace (x_1, x_3, x_4)

(b) Subspace (x_1, x_2, x_3)

(c) Subspace (x_1, x_2, x_4)

(d) Subspace (x_2, x_3, x_4)

Fig. 2. Co-existence of a stable equilibrium (light green) and three hidden limit cycles, two large symmetric ones (red and purple), and a small one (dark green), in the phase space of system (1), (3) with $\varphi(\sigma) = \texttt{tanh}(\sigma/\varepsilon)$, $\varepsilon = 0.01$.

$$\Phi(a) = \int_0^{\frac{2\pi}{\omega_0}} \tanh(\cos(\omega_0 t)a)\cos(\omega_0 t)dt - \\ -ak_{\text{hl}} \int_0^{\frac{2\pi}{\omega_0}} (\cos(\omega_0 t))^2 dt \geq -\frac{\pi a k_{\text{hl}}}{\omega_0}. \tag{7}$$

If $a \neq 0$, then $\Phi(a) > 0$ and there is no such a that $\Phi(a) = 0$. Therefore, there are no periodic solutions in the system (1) according to the describing function method.

Consider the Popov criterion on the absolute stability (see e.g. [Popov, 1961, p. 961],[Yakubovich et al., 2004, p. 79]) for system (1), (3) and non-linearity $\varphi(\sigma) = \texttt{tanh}(\sigma)$. First two conditions of the Popov criterion, i.e. asymptotic stability of the linear part and $0 \leq \frac{\tanh(\sigma)}{\sigma} \leq \infty, \sigma \neq 0, \tanh(0) = 0$, are satisfied. The third condition of the Popov criterion has the following form:

$$\text{Re}[(1 + i\omega\vartheta)W(i\omega)] = \text{Re}\, W(i\omega) - \omega\vartheta\, \text{Im}\, W(i\omega) \geq 0 \Leftrightarrow \\ -\omega^2(\omega^4 - \omega^2 a_2 + a_0) \geq 2\vartheta\omega^4\beta\left(-2\omega^2 + \frac{a_1}{2\beta}\right).$$

If $\omega = 0$, then this inequality holds. Else, if $\omega \neq 0$, then this condition takes the form:

$$(4\vartheta\beta - 1)\omega^4 - (\vartheta a_1 - a_2)\omega^2 - a_0 \geq 0. \tag{8}$$

Note that since $a_0 > 0$, then for each $\vartheta \geq 0$ there exists small enough $\omega > 0$ such that (8) is not true. Therefore, the conditions of the criterion are not satisfied.

4. CONCLUSION

Thus, the results obtained here show the limits of applicability of existing analytical methods and demonstrate the difficulty of identifying classes of systems for which it is possible to match the necessary and sufficient conditions for global stability.

In the general case, when considering various nonlinearities, it is possible to synthesize systems with a large number of coexisting attractors (equilibria, limit cycles, chaotic attractors), see e.g. [Wang and Chen, 2013, Zhang and Chen, 2017, Stankevich et al., 2017, Kuznetsov et al., 2017, Chen et al., 2017]. However, in these examples the nonlinearities were non-scalar, or the derivatives of the nonlinearities changed their signs. Therefore, these nonlinearities did not satisfy the conditions of Kalman conjecture. In this article, we demonstrate new counterex-

ample to the Kalman conjecture with three co-existing stable limit cycles. The mutual disposition of co-existing attractors in counterexamples to the Kalman conjecture (depending on the dimension of the system) and possibility of managing the number of attractors (e.g. finding the maximum possible number of attractors) are open problems for the further study.

ACKNOWLEDGEMENTS

We acknowledge support form the Russian Scientific Foundation (project 19-41-02002, sections 2-4) and the Leading Scientific Schools of Russia (project NSh-2858.2018.1, section 1).

REFERENCES

M.A. Aizerman. On a problem concerning the stability in the large of dynamical systems. *Uspekhi Mat. Nauk (in Russian)*, 4:187–188, 1949.

A.A. Andronov and A.G. Maier. The Mizes problem in the theory of direct control and the theory of point transformations of surfaces. *Dokl. Akad. Nauk SSSR*, 43(2), 1944. (in Russian).

A.A. Andronov, E.A. Vitt, and S.E. Khaikin. *Theory of Oscillators*. Pergamon Press, Oxford, 1966.

N.E. Barabanov. On the Kalman problem. *Sib. Math. J.*, 29(3):333–341, 1988.

J. Bernat and J. Llibre. Counterexample to Kalman and Markus-Yamabe conjectures in dimension larger than 3. *Dynamics of Continuous, Discrete and Impulsive Systems*, 2(3):337–379, 1996.

C. Bissell. A.A. Andronov and the development of Soviet control engineering. *IEEE Control Systems Magazine*, 18:56–62, 1998.

I. Boiko. *Discontinuous Control Systems: Frequency-Domain Analysis and Design*. Springer London, Limited, 2008.

V.O. Bragin, N.V. Kuznetsov, and G.A. Leonov. Algorithm for construction of counterexamples to Aizerman's and Kalman's conjecture. *IFAC Proceedings Volumes (IFAC-PapersOnline)*, 4(1):24–28, 2010. doi: 10.3182/20100826-3-TR-4016.00008.

V.O. Bragin, V.I. Vagaitsev, N.V. Kuznetsov, and G.A. Leonov. Algorithms for finding hidden oscillations in nonlinear systems. The Aizerman and Kalman conjectures and Chua's circuits. *Journal of Computer and Systems Sciences International*, 50(4):511–543, 2011. doi: 10.1134/S106423071104006X.

I.M. Burkin and N.N. Khien. Analytical-numerical methods of finding hidden oscillations in multidimensional dynamical systems. *Differential Equations*, 50(13):1695–1717, 2014.

G. Chen, N.V. Kuznetsov, G.A. Leonov, and T.N. Mokaev. Hidden attractors on one path: Glukhovsky-Dolzhansky, Lorenz, and Rabinovich systems. *International Journal of Bifurcation and Chaos in Applied Sciences and Engineering*, 27(8), 2017. art. num. 1750115.

R.E. Fitts. Two counterexamples to Aizerman's conjecture. *Trans. IEEE*, AC-11(3):553–556, 1966.

A.L. Fradkov and R.J. Evans. Control of chaos: Methods and applications in engineering. *Annual Reviews in Control*, 29(1):33–56, 2005.

A.L. Fradkov and A.Yu. Pogromsky. *Introduction to control of oscillations and chaos*. World Scientific Series of Nonlinear Science, 1998.

A.Kh. Gelig, G.A. Leonov, and V.A. Yakubovich. *Stability of Nonlinear Systems with Nonunique Equilibrium (in Russian)*. Nauka, 1978. [English transl: Stability of Stationary Sets in Control Systems with Discontinuous Nonlinearities, 2004, World Scientific].

A.A. Glutsyuk. Meetings of the Moscow mathematical society (1997). *Russian mathematical surveys*, 53(2):413–417, 1998.

W.P. Heath, J. Carrasco, and M. de la Sen. Second-order counterexamples to the discrete-time Kalman conjecture. *Automatica*, 60:140–144, 2015.

R.E. Kalman. Physical and mathematical mechanisms of instability in nonlinear automatic control systems. *Transactions of ASME*, 79(3):553–566, 1957.

R.E. Kalman. Lyapunov functions for the problem of Lur'e in automatic control. *Proc. Nat. Acad. Sci. USA*, 49(2):201–205, 1963.

N.V. Kuznetsov, O.A. Kuznetsova, G.A. Leonov, T.N. Mokaev, and N.V. Stankevich. Hidden attractors localization in Chua circuit via the describing function method. *IFAC-PapersOnLine*, 50(1):2651–2656, 2017.

N.V. Kuznetsov, G.A. Leonov, T.N. Mokaev, A. Prasad, and M.D. Shrimali. Finite-time Lyapunov dimension and hidden attractor of the Rabinovich system. *Nonlinear Dynamics*, 92(2):267–285, 2018. doi: 10.1007/s11071-018-4054-z.

M.H. Léauté. Mémoire sur les oscillations à longue période dans les machines actionnées par des moteurs hydrauliques et sur les moyens de prévenir ces oscillations. *Journal de l'école Polytechnique (in French)*, 55:1–126, 1885.

G.A. Leonov. Concerning stability of nonlinear controlled systems with non-single equilibrium state. *Automation and Remote Control*, 32(10):1547–1552, 1971.

G.A. Leonov and N.V. Kuznetsov. Algorithms for searching for hidden oscillations in the Aizerman and Kalman problems. *Doklady Mathematics*, 84(1):475–481, 2011. doi: 10.1134/S1064562411040120.

G.A. Leonov and N.V. Kuznetsov. Hidden attractors in dynamical systems. From hidden oscillations in Hilbert-Kolmogorov, Aizerman, and Kalman problems to hidden chaotic attractors in Chua circuits. *International Journal of Bifurcation and Chaos in Applied Sciences and Engineering*, 23(1), 2013. doi: 10.1142/S0218127413300024. art. no. 1330002.

G.A. Leonov and N.V. Kuznetsov. On differences and similarities in the analysis of Lorenz, Chen, and Lu systems. *Applied Mathematics and Computation*, 256:334–343, 2015. doi: 10.1016/j.amc.2014.12.132.

G.A. Leonov and N.V. Kuznetsov. On the Keldysh problem of flutter suppression. *AIP Conference Proceedings*, 1959(1), 2018a. doi: 10.1063/1.5034578. art. num. 020002.

G.A. Leonov and N.V. Kuznetsov. On flutter suppression in the Keldysh model. *Doklady Physics*, 63(9):366–370, 2018b.

G.A. Leonov, N.V. Kuznetsov, M.A. Kiseleva, and R.N. Mokaev. Global problems for differential inclusions. Kalman and Vyshnegradskii problems and Chua circuits. *Differential Equations*, 53(13):1671–1702, 2017.

G. Meisters. A biography of the Markus-Yamabe conjecture. *http://www.math.unl.edu/~gmeisters1/papers/HK1996.pdf*, 1996.

V.M. Popov. On absolute stability of non-linear automatic control systems. *Automatika i Telemekhanika (in Russian)*, 22(8):961–979, 1961.

N.V. Stankevich, N.V. Kuznetsov, G.A. Leonov, and L. Chua. Scenario of the birth of hidden attractors in the Chua circuit. *International Journal of Bifurcation and Chaos in Applied Sciences and Engineering*, 27(12), 2017. art. num. 1730038.

Ya.Z. Tsypkin. *Relay Control Systems*. Univ Press, Cambridge, 1984.

I.A. Vyshnegradsky. On regulators of direct action. *Izvestiya St. Petersburg Technological Inst.*, 1, 1877. (in Russian).

X. Wang and G. Chen. Constructing a chaotic system with any number of equilibria. *Nonlinear Dynamics*, 71(3): 429–436, 2013.

V.A. Yakubovich, G.A. Leonov, and A.Kh. Gelig. *Stability of Stationary Sets in Control Systems with Discontinuous Nonlinearities*. World Scientific, Singapure, 2004.

X. Zhang and G. Chen. Constructing an autonomous system with infinitely many chaotic attractors. *Chaos: An Interdisciplinary Journal of Nonlinear Science*, 27 (7):071101, 2017.

N.Ye. Zhukovsky. *Theory of regulation of the course of machines*. Tipo-litgr. T-va I. N. Kushnerev and Co., 1909. (in Russian).

PV

HARMONIC BALANCE METHOD AND STABILITY OF DISCONTINUOUS SYSTEMS

by

E.V. Kudryashova E.V., Kuznetsov N.V., Kuznetsova O.A., Leonov G.A., Mokaev R.N 2019

In: Matveenko V., Krommer M., Belyaev A., Irschik H. (eds) Dynamics and Control of Advanced Structures and Machines. Springer, Cham, PP. 99–107, https://doi.org/10.1007/978-3-319-90884-7_11

Harmonic Balance Method and Stability of Discontinuous Systems

Kudryashova E. V., Kuznetsov N. V., Kuznetsova O. A.,
Leonov G. A., and Mokaev R. N.

Abstract The development of the theory of discontinuous dynamical systems and differential inclusions was not only due to research in the field of abstract mathematics but also a result of studies of particular problems in mechanics. One of first methods, used for the analysis of dynamics in discontinuous mechanical systems, was the harmonic balance method developed in the thirties of the 20th century. In our work the results of analysis obtained by the method of harmonic balance, which is an approximate method, are compared with the results obtained by rigorous mathematical methods and numerical simulation.

1 Introduction

The development of the theory of discontinuous dynamical systems and differential inclusions was not only due to research in the field of abstract mathematics in the thirties of the last 20th century but also a result of studies of particular problems in mechanics. In the thirties and forties of the 20th century J. Hartog, A. Andronov, N. Bautin, M. Keldysh were among the first who rigorously treated the mathematical peculiarities of discontinuous dynamical models [1, 2, 3] on the examples of mechanical models. One of first methods, used for the analysis of stability and oscillations in discontinuous dynamical models, was the harmonic balance method (or the describing function method) developed in the thirties of the 20th century

Kudryashova E. V., Kuznetsov N. V. Kuznetsova O. A. Leonov G. A., Mokaev R. N.
Saint-Petersburg State University, 7/9 Universitetskaya emb., Saint-Petersburg, 199034, Russia
e-mail: nkuznetsov239@gmail.com

Leonov, G. A.
Institute of Problems of Mechanical Engineering RAS, 61 Bolshoj pr. V.O., Saint-Petersburg, 199178, Russia

Kuznetsov N. V., Mokaev R. N.
University of Jyväkylä, P.O. Box 35 (Agora), Jyväkylä, FI-40014, Finland

[4]. This method is not strictly mathematically justified and is one of approximate methods of analysis of oscillation in nonlinear systems. Nowadays we can apply various rigorous analytical and reliable numerical methods, which have been developed from that time till now: mathematical theory of differential inclusions (see, e.g. [5, 6, 7, 8, 9] and others), direct Lyapunov method and frequency methods (see, e.g. [6, 10]), special numerical approaches for solving differential inclusions (see, e.g. [11, 12, 13]).

In our work for the Hartog, Keldysh and modified Fitss models we compare the results of analysis obtained by the method of harmonic balance with the results obtained by rigorous mathematical methods and numerical simulation.

2 Hartog model

In 1930, J. Hartog studied vibrations in a mechanical model with dry friction[1] described by the following equation [1].

$$m\ddot{x}+kx=-\varphi(\dot{x}),\quad \varphi(\dot{x})=F_0\mathrm{sign}(\dot{x}) \tag{1}$$

where $m>0$ is a mass, $k>0$ is spring stiffness, $F_0>0$ is the dry friction coefficient. Following the mechanical sense, Hartog defined $\mathrm{sign}(0)$ as a value from $[-F_0,F_0]$ and, thus, the discontinuous differential equation (1) has a segment of equilibria (rest segment).

Follow the theory of differential inclusion, for the model (1) we consider the discontinuity manifold: $S=\{\dot{x}:\ \dot{x}=0\}$ on the phase space $(x,\dot{x})$, define $\varphi(\dot{x})$ on S as the set $[-F_0,+F_0]$, and get differential inclusion

$$m\ddot{x}+kx\in-\hat{\varphi}(\dot{x}),\quad \hat{\varphi}(\dot{x})=\begin{cases}\varphi(\dot{x}), & \text{if } \dot{x}\neq 0,\\ [-F_0,+F_0], & \text{if } \dot{x}=0.\end{cases} \tag{2}$$

The solutions of (2) are considered in the sense of Filippov [5]. Remark that here solutions cannot slide on the discontinuity manifold S, but can tend to the rest segment:

$$\Lambda=\{\ -F_0/k\le x\le F_0/k,\dot{x}=0\}\subset S,$$

or pierce the manifold $S\backslash\Lambda$. The phase portrait of (2) is shown in Fig. 1.

For equation (2), the harmonic balance methods states that there is no periodic oscillations for any values of the parameters. This result can be rigorously justified by the analog direct Lyapunov method for differential inclusions [6, Lemma 1.5, p.58]. Consider Lyapunov function

$$V(x,\dot{x})=\frac{1}{2}(m\dot{x}^2+kx^2). \tag{3}$$

[1] The history of the dry friction law can be found, e.g, in [14].

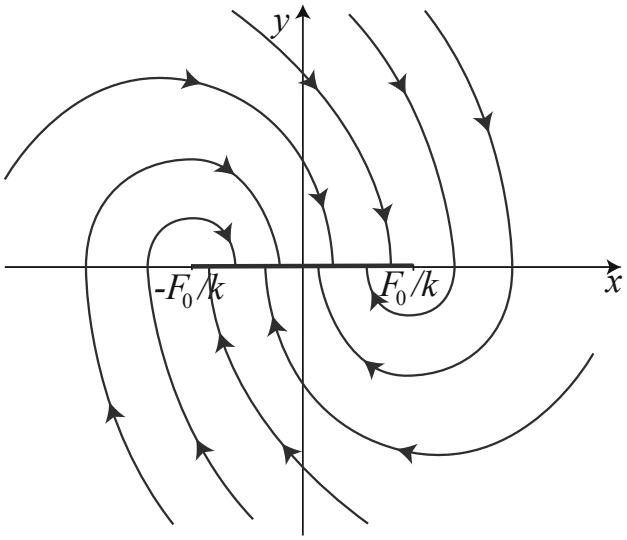

Fig. 1 Phase portrait of system (1): trajectories tend toward the rest segment $\{|x| \le F_0/k,\ y = 0\}$.

Then we have

$$\dot{V}(x,\dot{x}) = -F_0\dot{x}\mathrm{sign}(\dot{x}) < 0, \quad \forall \dot{x} \notin S$$

and the equality $V(x(t),\dot{x}(t)) \equiv \mathrm{const}$ can hold only for $x \in \Lambda$. Thus, any solution of (2) converges to the rest segment Λ.

3 Two-dimensional Keldysh model

M. Keldysh, in 1944, studied a two-dimensional model of damping flutter in aircraft control systems with dry friction [3]

$$J\ddot{x} + kx = -\mu\dot{x} - \varphi(\dot{x}), \quad \mu = \lambda - h,\ \varphi(\dot{x}) = (F_0 + \kappa\dot{x}^2)\mathrm{sign}(\dot{x}), \tag{4}$$

where $J > 0$ is the moment of inertia, $k > 0$ is sprig stiffness, $h\dot{x}$ is an excitation force proportional to the angular velocity $\dot{x}$, $f(\dot{x}) = \lambda\dot{x} + \varphi(\dot{x})$ is the nonlinear characteristic of hydraulic damper with dry friction, $F_0 > 0$ is the dry friction coefficient, $\lambda > 0$ and $\kappa > 0$ are parameters of the hydraulic damper.

Using the harmonic balance method, Keldysh formulated the following result: *If*

$$-2.08\sqrt{F_0\kappa} = \delta_K < \mu$$

then all trajectories of (4) converge to the rest segment; If $\mu < -2.08\sqrt{F_0\kappa}$ *then there are two periodic trajectories (limit cycles)* $\approx a_{\pm}\cos(\omega t)$ *with amplitudes*

$$a_{\pm}(\mu) = \frac{3}{8\kappa}\sqrt{\frac{J}{k}}\left(\pi\mu \pm \sqrt{\pi^2\mu^2 - \frac{32}{3}\kappa F_0}\right); \tag{5}$$

Other trajectories behave as follows. The trajectories, emerging from infinity, tend to the external limit cycle. The domain between two limit cycles is filled with trajectories unwinding from the internal (unstable) limit cycle and winding onto external (stable) limit cycle. The stability domain bounded by the internal limit cycle is filled with trajectories tending to one of the possible equilibrium on the rest segment.

By analogy with the above consideration of the Hartog model, we transform the Keldysh model to the differential inclusion

$$J\ddot{x} + kx + \mu\dot{x} \in -\hat{\varphi}(\dot{x}), \quad \hat{\varphi}(\dot{x}) = \begin{cases} \varphi(\dot{x}) & \dot{x} \neq 0, \\ [-F_0, +F_0] & \dot{x} = 0, \end{cases} \tag{6}$$

consider Lyapunov function (3) with $m = J$, and get

$$\dot{V}(x,\dot{x}) = -\mu\dot{x}^2 - \dot{x}\varphi(\dot{x}) < 0, \quad \forall \dot{x} \notin S.$$

Thus, if $\dot{x}\varphi(\dot{x}) > 0$ for $\dot{x} \neq 0$, i.e.

$$-2\sqrt{F_0\kappa} < \mu,$$

then any solution of (6) converges to the rest segment Λ [15]. Here the estimate obtained by direct Lyapunov method is close to the Keldysh estimate obtained by the harmonic balance method.

To check the second part of Keldysh's result we use numerical simulation [13]. The qualitative behavior of trajectories in the case of two coexisting limit cycles is shown in Fig. 2.

Fig. 2 Numerical experiment with $F_0 = 0.2, J = 1, k = 1, \kappa = 1$. Outer trajectory winds onto stable limit cycle, inner trajectory unwinds from unstable limit cycle and winds onto the stable limit cycle (hidden attractor). Left subfigure: $\mu = -1.3967\delta_K$: $a_+(\mu) >> a_-(\mu) > F_0$. Right subfigure: $\mu = -1.7847\delta_K$: $a_+(\mu) >> F_0 > a_-(\mu)$.

Here the largest limit cycle is a hidden attractor [16, 17, 18, 19, 20, 21, 22, 23] and corresponds to the flutter. Fig. 3 shows the bifurcation of collision of the limit cycles and the rest segment. In the right subfigure of Fig. 3, both limit cycles have disappeared and trajectories tend to the rest segment while the second part of the Keldysh estimate is valid.

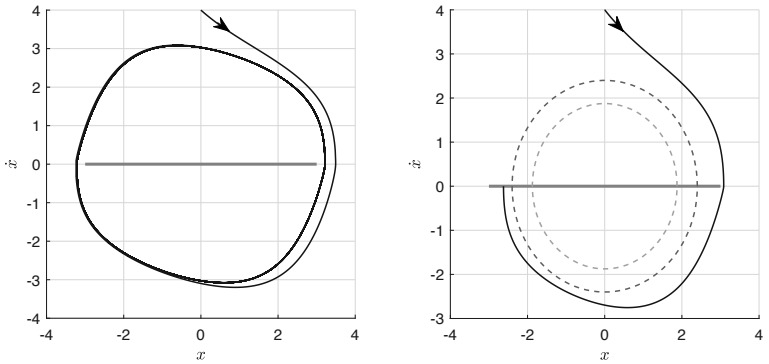

Fig. 3 Numerical experiment with $F_0 = 3, J = 1, k = 1, \kappa = 1$. Left subfigure: $\mu = -1.0713\delta_K$, $a_+(\mu) \gtrapprox F_0 > a_-(\mu)$; outer trajectory winds onto stable limit cycle, internal unstable limit cycle is not revealed numerically (due to stiffness). Right subfigure: $\mu = -1.0076\delta_K$, $F_0 \gtrapprox a_+(\mu) > a_-(\mu)$ (dash circles); outer trajectory approaches the stationary segment, both limit cycles have disappeared.

4 Discontinuous modification of the Fitts counterexample

It is known that the harmonic balance method may lead to wrong conclusion on the global stability. For example, it states that the Aizerman and Kalman conjectures on the global stability of nonlinear control systems are valid, while various counterexamples with hidden attractors have been found (see, e.g. [24, 25, 26, 27, 28, 29, 30, 16, 31, 32]). Consider a modification of one of first counterexamples to the Kalman conjecture [33]

$$\begin{aligned} &\dot{x}_1 = x_2, \qquad \dot{x}_2 = x_3, \qquad \dot{x}_3 = x_4, \\ &\dot{x}_4 \in -a_0 x_1 - a_1 x_2 - a_2 x_3 - a_3 x_4 + \hat{\varphi}(-x_3), \quad \hat{\varphi}(\dot{x}) = \begin{cases} \operatorname{sign}(-x_3) & x_3 \neq 0, \\ [-1,1] & x_3 = 0, \end{cases} \end{aligned} \tag{7}$$

where $a_i > 0$.

The sliding mode surface for the system (7) is given by

$$D = \{(x_1, x_2, x_3, x_4) \in \mathbb{R}^4 \;\big|\; x_3 = x_4 = 0, -1 \le a_0 x_1 + a_1 x_2 \le 1\}$$

and the rest segment is

$$\Lambda = \{(x_1,x_2,x_3,x_4) \in \mathbb{R}^4 \;\big|\; x_2 = x_3 = x_4 = 0, -\tfrac{1}{a_0} \le x_1 \le \tfrac{1}{a_0}\}.$$

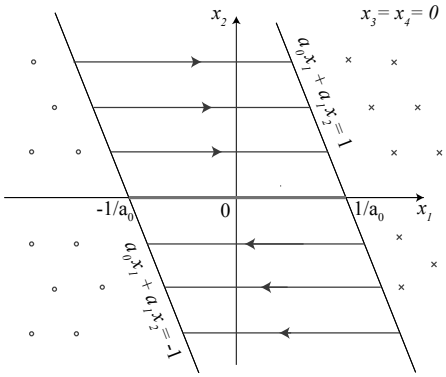

Fig. 4 Sliding mode surface $\{(x_1,x_2,x_3,x_4) \in \mathbb{R}^4 \;\big|\; x_3 = x_4 = 0, -1 \le a_0x_1 + a_1x_2 \le 1\}$ for system (7). Arrowed lines define the motion on the surface, thick line defines the rest segment.

This system has infinite sector of the linear stability and, thus, the harmonic balance method can not reveal any periodic solutions [16]. However, for parameters $a_0 = 0.981919$, $a_1 = 0.121308$, $a_2 = 2.0254$, $a_3 = 0.12$ it can be found numerically periodic solution (see Fig. 5) with initial data [34, 33]

$$\begin{aligned}(x_1^0,x_2^0,x_3^0,x_4^0) = (&-0.625205162606931095343423624907 23,\\ &-3.732409707265061046582527856259 4,\ 0,\\ &3.475416972869712079398927411163 6)\end{aligned}$$

Using the continuation procedure and passing from parameters $a_0 = 0.981919$, $a_1 = 0.121308$, $a_2 = 2.0254$, $a_3 = 0.12$ to parameters $a_0 = 1.0004$, $a_1 = 4.08$, $a_2 = 2.08$, $a_3 = 0.4$ it is possible to localize non-periodic oscillating solution (see Fig. 6).

Conclusions

While harmonic balance method is widely used for study of stability and oscillations of nonlinear dynamical systems, it may lead to wrong results. Some limitations of the use of harmonic balance method for the study of systems with dry friction and rest segment are demonstrated.

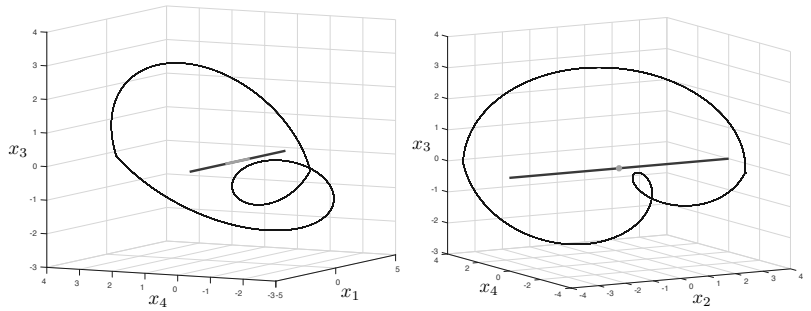

Fig. 5 Periodic solution of system (7) for parameters $a_0 = 0.981919$, $a_1 = 0.121308$, $a_2 = 2.0254$, $a_3 = 0.12$. Thick dark gray line defines the projection of the sliding mode surface on the corresponding three-dimensional hyperspace (x_1, x_3, x_4) (or (x_2, x_3, x_4)), light gray line (or dot) defines the projection of the rest segment.

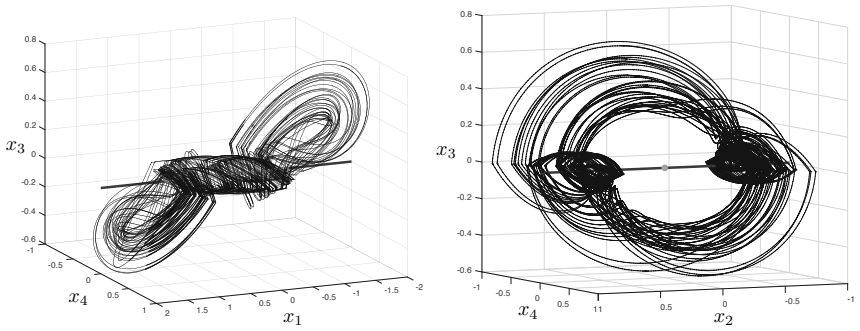

Fig. 6 Non-periodic oscillating solution of system (7) for parameters $a_0 = 1.0004$, $a_1 = 4.08$, $a_2 = 2.08$, $a_3 = 0.4$ Thick dark gray line defines the projection of the sliding mode surface on the corresponding three-dimensional hyperspace (x_1, x_3, x_4) (or (x_2, x_3, x_4)), light gray line (or dot) defines the projection of the rest segment.

This work was supported by the grant NSh-2858.2018.1 of the President of Russian Federation for the Leading Scientific Schools of Russia (2018-2019).

References

1. J.D. Hartog, The London, Edinburgh, and Dublin Philosophical Magazine and Journal of Science **9**(59), 801 (1930)
2. N. Andronov, A.A. Bautin, Dokl. Akad. Nauk SSSR (in Russian) **43**(5), 197 (1944)
3. M. Keldysh, Tr. TsAGI (in Russian) **557**, 26 (1944)
4. N. Krylov, N. Bogolyubov, *Introduction to non-linear mechanics (in Russian)* (AN USSR, Kiev, 1937). (English transl: Princeton Univ. Press, 1947)
5. A.F. Filippov, *Differential equations with discontinuous right-hand sides* (Kluwer, Dordrecht, 1988)

6. A. Gelig, G. Leonov, V. Yakubovich, *Stability of Nonlinear Systems with Nonunique Equilibrium (in Russian)* (Nauka, 1978). (English transl: Stability of Stationary Sets in Control Systems with Discontinuous Nonlinearities, 2004, World Scientific)
7. Y. Orlov, *Discontinuous Systems: Lyapunov Analysis and Robust Synthesis under Uncertainty Conditions*. Communications and Control Engineering (Springer, 2008)
8. I. Boiko, *Discontinuous Control Systems: Frequency-Domain Analysis and Design* (Springer London, Limited, 2008)
9. S. Adly, *A Variational Approach to Nonsmooth Dynamics: Applications in Unilateral Mechanics and Electronics*. SpringerBriefs in Mathematics (Springer International Publishing, 2018)
10. G. Leonov, D. Ponomarenko, V. Smirnova, *Frequency-Domain Methods for Nonlinear Analysis. Theory and Applications* (World Scientific, Singapore, 1996)
11. M. Aizerman, E. Pyatnitskiy, Automation and Remote Control (in Russian) (7, 8), 33 (1974)
12. A. Dontchev, F. Lempio, SIAM Review **34**(2), 263 (1992)
13. P.T. Piiroinen, Y.A. Kuznetsov, ACM Transactions on Mathematical Software (TOMS) **34**(3), 13 (2008)
14. V. Zhuravlev, Herald of the Bauman Moscow State Technical University. Series Natural Sciences. (2(53)), 21 (2014)
15. G. Leonov, N. Kuznetsov, Doklady Physics (2018). Submitted
16. G. Leonov, N. Kuznetsov, International Journal of Bifurcation and Chaos **23**(1) (2013). DOI 10.1142/S0218127413300024. art. no. 1330002
17. G. Leonov, N. Kuznetsov, T. Mokaev, Eur. Phys. J. Special Topics **224**(8), 1421 (2015). DOI 10.1140/epjst/e2015-02470-3
18. N. Kuznetsov, Lecture Notes in Electrical Engineering **371**, 13 (2016). DOI 10.1007/978-3-319-27247-4_2. (Plenary lecture at International Conference on Advanced Engineering Theory and Applications 2015)
19. M. Kiseleva, E. Kudryashova, N. Kuznetsov, O. Kuznetsova, G. Leonov, M. Yuldashev, R. Yuldashev, International Journal of Parallel, Emergent and Distributed Systems (2018). https://doi.org/10.1080/17445760.2017.1334776
20. N. Stankevich, N. Kuznetsov, G. Leonov, L. Chua, International Journal of Bifurcation and Chaos **27**(12) (2017). art. num. 1730038
21. G. Chen, N. Kuznetsov, G. Leonov, T. Mokaev, International Journal of Bifurcation and Chaos **27**(8) (2017). art. num. 1750115
22. N. Kuznetsov, G. Leonov, T. Mokaev, A. Prasad, M. Shrimali, Nonlinear dynamics (2018). https://doi.org/10.1007/s11071-018-4054-z
23. M.F. Danca, M. Fečkan, N. Kuznetsov, G. Chen, Nonlinear Dynamics **91**(4), 2523 (2018)
24. V.A. Pliss, *Some Problems in the Theory of the Stability of Motion (in Russian)* (Izd LGU, Leningrad, 1958)
25. R.E. Fitts, Trans. IEEE **AC-11**(3), 553 (1966)
26. N.E. Barabanov, Sib. Math. J. **29**(3), 333 (1988)
27. J. Bernat, J. Llibre, Dynamics of Continuous, Discrete and Impulsive Systems **2**(3), 337 (1996)
28. G. Leonov, V. Bragin, N. Kuznetsov, Doklady Mathematics **82**(1), 540 (2010). DOI 10.1134/S1064562410040101
29. V. Bragin, V. Vagaitsev, N. Kuznetsov, G. Leonov, Journal of Computer and Systems Sciences International **50**(4), 511 (2011). DOI 10.1134/S106423071104006X
30. G. Leonov, N. Kuznetsov, Doklady Mathematics **84**(1), 475 (2011). DOI 10.1134/S1064562411040120
31. R. Alli-Oke, J. Carrasco, W. Heath, A. Lanzon, IFAC Proceedings Volumes (IFAC-PapersOnline) **7**, 27 (2012). DOI 10.3182/20120620-3-DK-2025.00161
32. W.P. Heath, J. Carrasco, M. de la Sen, Automatica **60**, 140 (2015)
33. G. Leonov, N. Kuznetsov, M. Kiseleva, R. Mokaev, Differential Equations **53**(13), 1671 (2017)
34. G. Leonov, R. Mokaev, Doklady Mathematics **96**(1), 1 (2017). DOI 10.1134/S1064562417040111

PVI

STABILITY AND CHAOTIC ATTRACTORS OF MEMRISTOR-BASED CIRCUIT WITH A LINE OF EQUILIBRIA

by

N.V. Kuznetsov, T.N. Mokaev, E.V. Kudryashova, O.A. Kuznetsova, R.N. Mokaev, M.V. Yuldashev, R.V. Yuldashev 2020

Lecture Notes in Electrical Engineering, PP. 639–644,
https://doi.org/10.1007/978-3-030-14907-9_62

Stability and chaotic attractors of memristor-based circuit with a line of equilibria

N.V. Kuznetsov[1,2,3], T.N. Mokaev[1], E.V. Kudryashova[1], O.A. Kuznetsova[1], R.N. Mokaev[1,2], M.V. Yuldashev[1], and R.V. Yuldashev[1]

[1] St. Petersburg State University, Peterhof, St. Petersburg, Russia, nkuznetsov239@gmail.com,
[2] University of Jyväskylä, Jyväskylä, Finland,
[3] Institute of Problems of Mechanical Engineering RAS, Russia

Abstract. This report investigates the stability problem of memristive systems with a line of equilibria on the example of SBT memristor-based Wien-bridge circuit. For the considered system, conditions of local and global partial stability are obtained, and chaotic dynamics is studied.

Keywords: partial stability, memristor, chaos, hidden attractors

1 Introduction

In 1971, Leon Chua suggested the concept of a memristor [1] as an electrical component that regulates the flow of electrical current in a circuit and remembers the amount of charge that has previously flowed through it. Nowadays, various types of memristors are developing for the realization of memory, computations and many other applications (see e.g. [2–4]).

Consider the dynamical model of SBT memristor-based Wien-bridge circuit [5]:

$$\begin{cases} \dot{x} = \frac{1}{C_1}\big(\frac{1}{R_5}(y-x) - (A+B+g(\varphi)+G)x\big), \\ \dot{y} = \frac{1}{C_2}\big(\frac{1}{R_2}\big(\frac{R_4}{R_3}\,y - z\big) - \frac{1}{R_1}y - \frac{1}{R_5}(y-x)\big), \\ \dot{z} = \frac{1}{C_3}\big(\frac{1}{R_2}\big(\frac{R_4}{R_3}\,y - z\big)\big), \\ \dot{\varphi} = x, \end{cases} \tag{1}$$

where $g(\varphi) = |\varphi|$, the parameters $C_{1,2,3}$, $R_{1,2,3,4,5}$, A, B are positive, and G is negative. Using the notation $\alpha_i = \frac{1}{C_i}$, $(i = 1, 2, 3)$, $\beta_1 = \frac{1}{R_1}$, $\beta_2 = \frac{1}{R_2}$, $\beta_3 = \frac{R_4}{R_3}$, $\beta_4 = \frac{1}{R_5}$ we rewrite system (1) as follows:

$$\begin{cases} \dot{x} = f_1(x,y,z,\varphi) = \alpha_1\big(\beta_4(y-x) - (A+B+g(\varphi)+G)x\big), \\ \dot{y} = f_2(x,y,z,\varphi) = \alpha_2\big(\beta_2\big(\beta_3 y - z\big) - \beta_1 y - \beta_4(y-x)\big), \\ \dot{z} = f_3(x,y,z,\varphi) = \alpha_3\big(\beta_2\big(\beta_3 y - z\big)\big), \\ \dot{\varphi} = f_4(x,y,z,\varphi) = x. \end{cases} \tag{2}$$

Equating the right-hand of system (2) to zero we obtain a line of equilibria:

$$E = \{(x,y,z,\varphi) \,\big|\, x = y = z = 0,\ \varphi \in \mathbb{R})\}. \tag{3}$$

2 Local stability analysis

Let us analyze the local stability of the equilibrium points on the line of equilibria E. Here for simplicity, we approximate continuous function $g(\varphi) = |\varphi|$ by a smooth function $g(\varphi) = \varphi \tanh(\rho\,\varphi) \geq 0$, where $\rho \gg 1$. Since for an arbitrary equilibrium $(0,0,0,\varphi_0) \in E$ we have

$$\begin{aligned}\left.\frac{\partial f_1(x,y,z,\varphi)}{\partial\varphi}\right|_{(0,0,0,\varphi_0)} &= \lim_{h\to 0}\frac{f_1(x,y,z,\varphi+h)|_{(0,0,0,\varphi_0)} - f_1(x,y,z,\varphi)|_{(0,0,0,\varphi_0)}}{h} = \\ &= \lim_{h\to 0}\frac{(\alpha_1 x(g(\varphi+h)-g(\varphi)))|_{(0,0,0,\varphi_0)}}{h} = 0,\end{aligned}$$

the Jacobi matrix at $(0,0,0,\varphi_0)$ can be expressed as:

$$J = \begin{pmatrix} -\alpha_1(A + Bg(\varphi_0) + G + \beta_4) & \alpha_1\beta_4 & 0 & 0 \\ \alpha_2\beta_4 & \alpha_2(\beta_2\beta_3 - \beta_1 - \beta_4) & -\alpha_2\beta_2 & 0 \\ 0 & \alpha_3\beta_2\beta_3 & -\alpha_3\beta_2 & 0 \\ 1 & 0 & 0 & 0 \end{pmatrix}. \tag{4}$$

The characteristic polynomial for the Jacobi matrix J is as follows:

$$\det(\lambda I - J) = \lambda\big(\lambda^3 + P_2\lambda^2 + P_1\lambda + P_0\big), \tag{5}$$

where

$$\begin{aligned} P_2 &= \alpha_1\,(A + Bg(\varphi_0) + G + \beta_4) + \alpha_2\,(\beta_1 - \beta_2\,\beta_3 + \beta_4) + \alpha_3\beta_2, \\ P_1 &= \alpha_1\alpha_2\left((A + Bg(\varphi_0) + G + \beta_4)\,(\beta_1 - \beta_2\,\beta_3 + \beta_4) - \beta_4^2\right) + \\ &\quad + \alpha_1\alpha_3\,((A + Bg(\varphi_0) + G + \beta_4)\,\beta_2) + \alpha_2\,\alpha_3\,\beta_2\,(\beta_1 + \beta_4)\,, \\ P_0 &= \alpha_1\alpha_2\alpha_3\,\beta_2\left((A + Bg(\varphi_0) + G + \beta_4)\,(\beta_1 + \beta_4) - \beta_4^2\right). \end{aligned} \tag{6}$$

Expression (5) indicates that the characteristic equation of Jacobi matrix J has a zero eigenvalue with corresponding eigenvector $(0,0,0,1)^*$, and three non-zero eigenvalues. Since the central manifold of each equilibrium $p \in E$ is placed on the line of equilibria E, local dynamics of the nonlinear system near p is described by the local dynamics of linearized system (see, e.g. *Shoshitaishvili reduction principle* [6] and related results). Thus, if p has three eigenvalues with negative real parts, then it is locally stable.

According to the Routh-Hurwitz criterion of stability, all the non-zero eigenvalues of (5) have negative real parts, iff $P_2 > 0$, $P_0 > 0$ and $P_2P_1 - P_0 > 0$. Left-hand side of the latter inequality has the form of quadratic equation:

$$P_2\,P_1 - P_0 = Q_2\,\nu^2 + Q_1\,\nu + Q_0 \tag{7}$$

with respect to $\nu = \alpha_1 Bg(\varphi_0)$, where

$$\begin{aligned} Q_2 &= \alpha_2\,(\beta_1 - \beta_2\,\beta_3 + \beta_4) + \alpha_3\beta_2, \\ Q_1 &= Q_2^2 + \alpha_1\left(2\,(A + G + \beta_4)\,Q_2 - \alpha_2\beta_4^2\right), \\ Q_0 &= \alpha_1\left((A + G + \beta_4)\,Q_2 - \alpha_2\beta_4^2\right)((A + G + \beta_4)\,\alpha_1 + Q_2) \\ &\quad + \alpha_2\alpha_3\beta_2\left(\alpha_1\beta_4^2 + (\beta_1 + \beta_4)\,Q_2\right). \end{aligned} \tag{8}$$

The discriminant of (7) has the following form:

$$\mathcal{D} = \left(Q_2^2 + \alpha_1\alpha_2\,\beta_4^2\right)^2 - 4\alpha_2\,\alpha_3\,\beta_2\,Q_2\left((\beta_1+\beta_4)\,Q_2 + \alpha_1\beta_4^4\right). \tag{9}$$

For stability of all points on the line of equilibria (3), the branches of parabola Eq. (7) has to be directed upwards, i.e. the inequality $Q_2 > 0$ is needed. Since $\nu = \alpha_1 Bg(\varphi_0) \geq 0$ for all $\varphi_0 \in \mathbb{R}$, to satisfy the inequality $P_2P_1 - P_0 > 0$ it is necessary and sufficient to have either no real roots (i.e $\mathcal{D} < 0$), or all negative roots of the Eq. (7). The latter condition is satisfied, iff $\mathcal{D} \geq 0$, $Q_1 > 0$, $Q_0 > 0$. Inequalities $P_2 > 0$, $P_0 > 0$ are satisfied for all $\varphi_0 \in \mathbb{R}$, iff

$$\begin{aligned} (P_2 \geq) \quad & \underbrace{\alpha_1\,(A+G+\beta_4) + \alpha_2\,(\beta_1 - \beta_2\,\beta_3 + \beta_4) + \alpha_3\beta_2}_{=\kappa_1} > 0, \\ (P_0 \geq) \quad & \underbrace{\alpha_1\alpha_2\alpha_3\,\beta_2\left((A+G+\beta_4)\,(\beta_1+\beta_4) - \beta_4^2\right)}_{=\kappa_2} > 0. \end{aligned} \tag{10}$$

Thus, it is possible to formulate the following statement

Lemma 1. *If the values of parameters $\alpha_{1,2,3}$, $\beta_{1,2,3,4}$, A, B, G are such that the conditions $\kappa_1 > 0$, $\kappa_2 > 0$, $Q_2 > 0$, and*

$$\mathcal{D} \geq 0, \quad Q_1 > 0, \quad Q_0 > 0, \qquad \textit{or} \qquad \mathcal{D} < 0 \tag{11}$$

hold, then each point at the line of equilibria E is locally Lyapunov stable[4].

3 Global stability analysis

In order to study the global stability of the line (3) let us consider the following Lyapunov function:

$$V = \tfrac{1}{2}\left(\tfrac{x^2}{\alpha_1} + \tfrac{y^2}{\alpha_2} + \tfrac{z^2}{\alpha_3}\right), \tag{12}$$

which has the following derivative along the solutions of system (2):

$$\begin{aligned} \dot{V} &= -(\beta_4+A+Bg(\varphi)+G)x^2 + 2\beta_4 xy - (\beta_1 - \beta_2\beta_3 + \beta_4)y^2 + (\beta_2(\beta_3-1))yz - \beta_2 z^2 \\ &= -\gamma_1\left(x - \tfrac{\beta_4 y}{\gamma_1}\right)^2 - \gamma_2\left(y - \tfrac{1}{2}\tfrac{\beta_2(\beta_3-1)z}{\gamma_2}\right)^2 - \gamma_3 z^2, \end{aligned} \tag{13}$$

where

$$\gamma_1 = \beta_4+A+Bg(\varphi)+G, \qquad \gamma_2 = \beta_1 - \beta_2\beta_3 + \beta_4\left(1 - \tfrac{\beta_4}{\gamma_1}\right), \qquad \gamma_3 = \beta_2\left(1 - \tfrac{\beta_2(\beta_3-1)^2}{4\gamma_2}\right). \tag{14}$$

[4] For any $\varepsilon > 0$ there exists $\delta > 0$, such that, if $|u(0) - u_{eq}| < \delta$, then $|u(t) - u_{eq}| < \varepsilon$ is valid for all $t > 0$. Recall that *local asymptotic stability* of u_{eq} means that u_{eq} is locally Lyapunov stable and also there exists $\delta > 0$, such that if $|u(0) - u_{eq}| < \delta$, then $\lim_{t\to\infty} |u(t) - u_{eq}| = 0$. Thus, due to the noise, the state of the physical model could drift along the line of equilibria.

Since $B > 0$, we have

$$\gamma_1 \geq \underbrace{\beta_4 + A + G}_{=\mu_1}, \qquad \gamma_2 \geq \underbrace{\beta_1 - \beta_2\beta_3 + \beta_4\left(1 - \frac{\beta_4}{\mu_1}\right)}_{=\mu_2}, \qquad \gamma_3 \geq \underbrace{\beta_2\left(1 - \frac{\beta_2(\beta_3-1)^2}{4\mu_2}\right)}_{=\mu_3}. \tag{15}$$

Thus, it is possible to formulate the following statement

Lemma 2. *If the values of parameters $\alpha_{1,2,3}$, $\beta_{1,2,3,4}$, A, B, G are such that the conditions $\mu_1 > 0$, $\mu_2 > 0$, $\mu_3 > 0$ hold, then the line of equilibria E is partially globally stable, i.e. for any ellipsoidal cylinder $\varepsilon = V(x, y, z)$ defined by (12) with a sufficiently small radius ε and for any trajectory from outside it there exists a moment of time T after which the trajectory enters the cylinder and remain there (see, e.g. [7]).*

4 Chaotic attractors

For parameters $\alpha_1 = 10^8$, $\alpha_2 = \alpha_3 = 5 \cdot 10^7$, $\beta_1 = \beta_2 = 4 \cdot 10^{-5}$, $\beta_3 = 2.5$, $\beta_4 = 2.22 \cdot 10^{-5}$, $A = 0.0676$, $B = 0.3682$, $G = -0.0677$ chaotic attractors [5] can be found in system (2) (see Fig. 1). These attractors are self-excited ones with respect to some unstable points on the line of equilibria E according to the definition from [8–13]. However since there is a continuum of unstable equilibria on E, the unstable manifold of which may from attractors, the revealing of all co-existing attractors is a challenging task, and, thus, attractors is such systems sometimes are also called "hidden". For their search one can use, e.g., various evolutionary algorithms [14, 15]. The search of all co-existing attractors and determination of their mutual disposition in dynamical systems can be regarded as a generalization [16] of the second part of Hilbert's 16th problem on the number and mutual disposition of limit cycles in two-dimensional polynomial systems. Remark, that since there is an unbounded line of equilibria E in system (1), one has to consider cylindrical absorbing sets and unbounded attractors.

One can see that the region of parameters given by the conditions of Lemma 1 does not coincide with the region of parameters corresponding to the conditions of Lemma 2. When all equilibria are locally stable, the following cases are of interest:

(a) system (1) can be partially globally stable when all trajectories tend to the line of equilibria E;
(b) system (1) may have hidden attractors with respect to E;
(c) system (1) can be dichotomic (some trajectories can tend to infinity in the (x, y, z) subspace).

When some of the equilibria on E are unstable, the following cases are of interest:

(a) system (1) can be gradient-like (i.e. when all trajectories except unstable equilibria tend to the stable equilibria on E);
(b) system (1) can be partially dissipative (all trajectories do not leave an absorbing cylinder; in this case system (1) can have self-excited attractors);
(c) system (1) can be dichotomic.

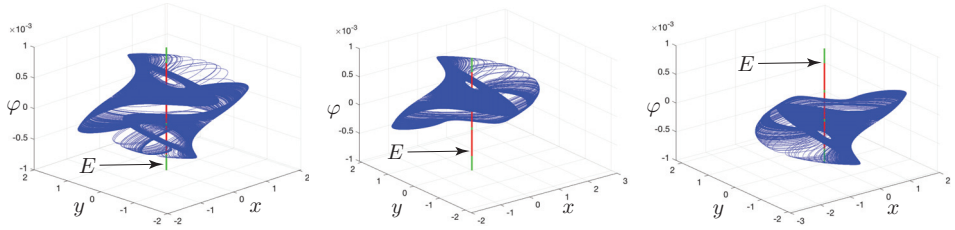

(a) Initial point $u_0 = (10^{-2}, 0, 0, 0)$. (b) Initial point $u_0 = (10^{-2}, 0, 0, 5 \cdot 10^{-4})$. (c) Initial point $u_0 = (10^{-2}, 0, 0, -5 \cdot 10^{-4})$.

Fig. 1: Self-excited chaotic attractors (blue) in system (2) for parameters $\alpha_1 = 10^8$, $\alpha_2 = \alpha_3 = 5 \cdot 10^7$, $\beta_1 = \beta_2 = 4 \cdot 10^{-5}$, $\beta_3 = 2.5$, $\beta_4 = 2.22 \cdot 10^{-5}$, $A = 0.0676$, $B = 0.3682$, $G = -0.0677$, which are visualized by trajectories with initial data in vicinity of the line of equilibria E (stable equilibria are green, unstable – red).

Conclusion

In this report we discussed some basic ideas of the stability theory for memristive systems with a line of equilibria. For the SBT memristor-based Wien-bridge chaotic circuit the conditions of local and global partial stability are obtained. Using [17, 18], various other memristive circuits can be studied similarly. More detailed studies and results will be included in the forthcoming survey *"Theory of stability for memristive systems with a line of equilibria"* [19].

Acknowledgements

The authors wish to thank Prof. Leon Chua (University of California, Berkeley, USA) for the fruitful discussions and valuable comments on memristive systems. This work was supported by the Leading Scientific Schools of Russia grant NSh-2858.2018.1.

References

1. Chua, L.: Memristor-the missing circuit element. IEEE Transactions on circuit theory 18(5), 507–519 (1971)
2. Tetzlaff, R.: Memristors and memristive systems. Springer (2013)
3. Adamatzky, A., Chen, G.: Chaos, CNN, memristors and beyond: A festschrift for Leon Chua. World Scientific (2013)
4. Vaidyanathan, S., Volos, C.: Advances in memristors, memristive devices and systems, vol. 701. Springer (2017)
5. Guo, M., Gao, Z., Xue, Y., Dou, G., Li, Y.: Dynamics of a physical SBT memristor-based Wien-bridge circuit. Nonlinear Dynamics 93(3), 1681–1693 (2018)
6. Shoshitaishvili, A.N.: Bifurcations of topological type of a vector field near a singular point. Trudy Semin. Im. IG Petrovskogo 1, 279–309 (1975)

7. Rumyantsev, V.V., Oziraner, A.S.: Stability and Partial Motion Stabilization. Nauka, Moscow (1987), (in Russian)
8. Leonov, G., Kuznetsov, N.: Hidden attractors in dynamical systems. From hidden oscillations in Hilbert-Kolmogorov, Aizerman, and Kalman problems to hidden chaotic attractors in Chua circuits. International Journal of Bifurcation and Chaos 23(1) (2013), art. no. 1330002
9. Leonov, G., Kuznetsov, N., Mokaev, T.: Homoclinic orbits, and self-excited and hidden attractors in a Lorenz-like system describing convective fluid motion. The European Physical Journal Special Topics 224(8), 1421–1458 (2015)
10. Dudkowski, D., Jafari, S., Kapitaniak, T., Kuznetsov, N., Leonov, G., Prasad, A.: Hidden attractors in dynamical systems. Physics Reports 637, 1–50 (2016)
11. Stankevich, N., Kuznetsov, N., Leonov, G., Chua, L.: Scenario of the birth of hidden attractors in the Chua circuit. International Journal of Bifurcation and Chaos 27(12) (2017), art. num. 1730038
12. Chen, G., Kuznetsov, N., Leonov, G., Mokaev, T.: Hidden attractors on one path: Glukhovsky-Dolzhansky, Lorenz, and Rabinovich systems. International Journal of Bifurcation and Chaos 27(8) (2017), art. num. 1750115
13. Kuznetsov, N., Leonov, G., Mokaev, T., Prasad, A., Shrimali, M.: Finite-time Lyapunov dimension and hidden attractor of the Rabinovich system. Nonlinear Dynamics 92(2), 267–285 (2018)
14. Zelinka, I.: A survey on evolutionary algorithms dynamics and its complexity – Mutual relations, past, present and future. Swarm and Evolutionary Computation 25, 2–14 (2015)
15. Zelinka, I.: Evolutionary identification of hidden chaotic attractors. Engineering Applications of Artificial Intelligence 50, 159–167 (2016)
16. Leonov, G., Kuznetsov, N.: On differences and similarities in the analysis of Lorenz, Chen, and Lu systems. Applied Mathematics and Computation 256, 334–343 (2015)
17. Corinto, F., Ascoli, A., Gilli, M.: Nonlinear dynamics of memristor oscillators. IEEE Transactions on Circuits and Systems I: Regular Papers 58(6), 1323–1336 (2011)
18. Corinto, F., Forti, M.: Memristor circuits: Flux-charge analysis method. IEEE Trans. on Circuits and Systems 63(11), 1997–2009 (2016)
19. Kuznetsov, N.V., Kuznetsova, O.A., Kudryashova, E.V., Mokaev, T.N., Mokaev, R.N., Yuldashev, M.V., Yuldashev, R.V., Chua, L.: Theory of stability for memristive systems with a line of equilibria (2018)

PVII

HOMOCLINIC BIFURCATIONS AND CHAOS IN THE FISHING PRINCIPLE FOR THE LORENZ-LIKE SYSTEMS

by

G.A. Leonov, R.N. Mokaev, N.V. Kuznetsov, T.N. Mokaev 2020

International Journal of Bifurcation and Chaos, Vol. 30 (accepted, preprint https://arxiv.org/pdf/1802.07694.pdf)

International Journal of Bifurcation and Chaos
© World Scientific Publishing Company

Homoclinic Bifurcations and Chaos in the Fishing Principle for the Lorenz-like Systems

G. A. Leonov
Faculty of Mathematics and Mechanics, St. Petersburg State University, Peterhof, St. Petersburg, Russia

R. N. Mokaev
Faculty of Mathematics and Mechanics, St. Petersburg State University, Peterhof, St. Petersburg, Russia
Faculty of Information Technology, University of Jyväskylä, Jyväskylä, Finland

N. V. Kuznetsov
Faculty of Mathematics and Mechanics, St. Petersburg State University, Peterhof, St. Petersburg, Russia
Faculty of Information Technology, University of Jyväskylä, Jyväskylä, Finland
Institute for Problems in Mechanical Engineering RAS, Russia
nkuznetsov239@gmail.com

T. N. Mokaev
Faculty of Mathematics and Mechanics, St. Petersburg State University, Peterhof, St. Petersburg, Russia

Received (to be inserted by publisher)

In this article using analytical method called Fishing principle we obtain the region of parameters, where the existence of a homoclinic orbit to a zero saddle equilibrium in the Lorenz-like system is proved. For a qualitative description of the different types of homoclinic bifurcations, a numerical analysis of the obtained region of parameter is organized, which leads to the discovery of new bifurcation scenarios.

Keywords: Lorenz system, Lorenz-like system, Lorenz attractor, homoclinic orbit, homoclinic bifurcation, strange attractor

1. Introduction

In 1963, famous meteorologist E. Lorenz discovered [Lorenz, 1963] a strange attractor in the following Rayleigh-Bénard convection model:

$$\begin{cases} \dot{x} = -\sigma(x-y), \\ \dot{y} = rx - dy - xz, \\ \dot{z} = -bz + xy, \end{cases} \tag{1}$$

where $d = 1$, $\sigma > 0$ is a Prandtl number, $r > 0$ is a Rayleigh number, $b > 0$ is a parameter that determines the ratio of the vertical and horizontal dimensions of a convection cell. Equations (1) are also encountered in other mechanical and physical problems, for example, in the problem of fluid convection in a closed annular tube [Rubenfeld & Siegmann, 1977], for describing the mechanical model of a chaotic water wheel [Tel & Gruiz, 2006], the model of a dissipative oscillator with an inertial nonlinearity [Neimark & Landa, 1992], and the dynamics of a single-mode laser [Oraevsky, 1981].

Later on, for $d \neq 1$ it was suggested various Lorenz-like systems, such as Chen system [Chen & Ueta, 1999] ($d = -c$, $c > \frac{\sigma}{2}$, $r = c - \sigma$), Lu system [Lu & Chen, 2002] ($d = -c$, $c > 0$, $r = 0$), and Tigan-Yang systems [Tigan & Opris, 2008; Yang & Chen, 2008] ($d = 0$), which have dynamics differing in certain aspect form the Lorenz system dynamics (see corresponding discussions e.g. in [Leonov & Kuznetsov, 2015; Barboza, 2018]).

Using the following smooth change of variables (see, e.g. [Leonov, 2016]):

$$\eta := \sigma(y - x), \quad \xi := z - \tfrac{x^2}{b} \tag{2}$$

one can reduce system (1) to the form

$$\begin{cases} \dot{x} = \eta, \\ \dot{\eta} = -(\sigma + d)\eta + \sigma\xi x + \sigma(r - d)x - \frac{\sigma}{b}x^3, \\ \dot{\xi} = -b\xi - \frac{(2\sigma - b)}{b\sigma}x\eta. \end{cases} \tag{3}$$

Then, by changing

$$t := \sqrt{\sigma(r - d)}t, \quad x := \frac{x}{\sqrt{b(r - d)}}, \quad \vartheta := \frac{\eta}{\sqrt{b\sigma}(r - d)}, \quad u := \frac{\xi}{r - d}$$

system (3) can be reduced to the form

$$\begin{cases} \dot{x} = \vartheta, \\ \dot{\vartheta} = -\lambda\vartheta - xu + x - x^3, \\ \dot{u} = -\alpha u - \beta x\vartheta, \end{cases} \tag{4}$$

$$\lambda = \frac{(\sigma + d)}{\sqrt{\sigma(r - d)}}, \quad \alpha = \frac{b}{\sqrt{\sigma(r - d)}}, \quad \beta = \frac{2\sigma - b}{\sigma}.$$

Using the following change of variables (see, e.g. [Leonov, 2013]):

$$\nu := y, \quad u := z - x^2$$

the well-known Shimizu-Morioka system [Shimizu & Morioka, 1980; Leonov *et al.*, 2015a]

$$\begin{cases} \dot{x} = y, \\ \dot{y} = (1 - z)x - \lambda y, \\ \dot{z} = -\alpha(z - x^2) \end{cases} \tag{5}$$

with $\beta = 2$ can be also transformed to form (4).

The following Lorenz-like system from [Ovsyannikov & Turaev, 2017]:

$$\begin{cases} \dot{X} = Y, \\ \dot{Y} = X - \lambda Y - XZ - X^3, \\ \dot{Z} = -\alpha Z + BX^2 \end{cases} \tag{6}$$

can be also reduced to the system of form (4) by using the following change the variables:

$$X := \sqrt{\tfrac{\alpha}{B+\alpha}}\, x, \quad Y := \sqrt{\tfrac{\alpha}{B+\alpha}}\, y, \quad Z := z + \tfrac{B}{B+\alpha}x^2, \tag{7}$$

and if $\beta = \frac{2B}{B+\alpha} < 2$.

Thus, in this article it is convenient for us to consider and study system (4). Its equilibria have the following form:

$$S_0 = (0, 0, 0), \quad S_\pm = (\pm 1, 0, 0). \tag{8}$$

It is easy to show that for positive α, β, λ the equilibrium state S_0 is always a saddle, and $S_\pm$ are stable equilibria if $\beta < \frac{\lambda(\lambda\alpha + \alpha^2 + 2)}{(\lambda + \alpha)}$.

The seminal work [Lorenz, 1963] initiated the development of chaotic dynamics and, in particular, the description of scenarios of transition to chaos. An important role in such scenarios plays a homoclinic bifurcation, when in the phase of dynamical system a homoclinic orbit appear. This bifurcation is related to global changes of system's dynamics, such as changes in basins of attraction of attractors and the emergence of chaotic behavior [Wiggins, 1988; Shilnikov *et al.*, 1998, 2001; Homburg & Sandstede, 2010; Afraimovich *et al.*, 2014], and is applied in various fields of science, for instance, in mechanics, chemistry and theory of population (see, e.g, [Kuznetsov *et al.*, 1992; Champneys, 1998; Argoul *et al.*, 1987]). Difficulties in studying of dynamics in the vicinity of a homoclinic orbit was noted by Poincaré [Poincare, 1892, 1893, 1899]. In this paper for the Lorenz-like system (4) we analytically prove the existence of a homoclinic orbit and make an attempt to study the various scenarios of homoclinic bifurcation numerically.

2. Existence problem of homoclinic orbit. Analytical method.

Definition 2.1. The homoclinic orbit $\mathrm{x}(t)$ of an autonomous system of differential equations

$$\dot{\mathrm{x}} = f(\mathrm{x}, q), \quad t \in \mathbb{R}, \quad \mathrm{x} \in \mathbb{R}^n \tag{9}$$

for a given value of parameter $q \in \mathbb{R}^m$ is a phase trajectory that is doubly asymptotic to a saddle equilibrium $\mathrm{x}_0 \in \mathbb{R}^n$, i.e.

$$\lim_{t\to+\infty} \mathrm{x}(t) = \lim_{t\to-\infty} \mathrm{x}(t) = \mathrm{x}_0.$$

Here $f(\mathrm{x}, q)$ is a smooth vector-function, $\mathbb{R}^n = \{\mathrm{x}\}$ is a phase space of system (9). Let $\gamma(s), s \in [0, 1]$ be a smooth path in the space of the parameter $\{q\} = \mathbb{R}^m$. Consider the following Tricomi problem [Tricomi, 1933; Leonov, 2012] for system (9) and the path $\gamma(s)$: *is there a point* $q_0 \in \gamma(s)$ *for which system* (9) *with* q_0 *has a homoclinic orbit?*

Consider system (9) with $q = \gamma(s)$ and introduce the following notions. Let $\mathrm{x}(t, s)^+$ be an outgoing separatrix of the saddle point x_0 (i.e. $\lim\limits_{t\to-\infty} \mathrm{x}(t, s)^+ = \mathrm{x}_0$) with a one-dimensional unstable manifold. Define by $\mathrm{x}_\Omega(s)^+$ the point of the first crossing of separatrix $\mathrm{x}(t, s)^+$ with the closed set Ω:

$$\mathrm{x}(t, s)^+ \notin \Omega, \quad t \in (-\infty, T),$$

$$\mathrm{x}(T, s)^+ = \mathrm{x}_\Omega(s)^+ \in \Omega.$$

If there is no such crossing, we assume that $\mathrm{x}_\Omega(s)^+ = \emptyset$ (the empty set).

Now let us formulate a general method for proving the existence of homoclinic trajectories for systems (9) called the *Fishing principle* [Leonov *et al.*, 2015c; Leonov, 2012, 2013, 2014].

Theorem 1. *Suppose that for the path* $\gamma(s)$ *there is an* $(n-1)$*-dimensional bounded manifold* Ω *with a piecewise-smooth edge* $\partial\Omega$ *that possesses the following properties:*

(i) *for any* $\mathrm{x} \in \Omega \setminus \partial\Omega$ *and* $s \in [0, 1]$*, the vector* $f(\mathrm{x}, \gamma(s))$ *is transversal to the manifold* $\Omega \setminus \partial\Omega$*;*

(ii) *for any* $s \in [0, 1]$*,* $f(\mathrm{x}_0, \gamma(s)) = 0$*, the point* $\mathrm{x}_0 \in \partial\Omega$ *is a saddle;*

(iii) *for* $s = 0$ *the inclusion* $\mathrm{x}_\Omega(0)^+ \in \Omega \setminus \partial\Omega$ *is valid;*

(iv) *for* $s = 1$ *the relation* $\mathrm{x}_\Omega(1)^+ = \emptyset$ *is valid (i.e.* $\mathrm{x}_\Omega(1)^+$ *is an empty set);*

(v) *for any* $s \in [0, 1]$ *and* $\mathrm{y} \in \partial\Omega \setminus \mathrm{x}_0$ *there exists a neighborhood* $U(\mathrm{y}, \delta) = \{\mathrm{x} \in \mathbb{R}^n \mid |\mathrm{x} - \mathrm{y}| < \delta\}$ *such that* $\mathrm{x}_\Omega(s)^+ \notin U(\mathrm{y}, \delta)$*.*

If conditions (i)–(v) are satisfied, then there exists $s_0 \in [0, 1]$ *such that* $\mathrm{x}(t, s_0)^+$ *is a homoclinic orbit of the saddle point* x_0*.*

For the further investigation of system (4) we prove several auxiliary statements using the Lyapunov function

$$V(x, \vartheta, u) = \vartheta^2 - \frac{u^2}{\beta} - x^2 + \frac{x^4}{2}, \tag{10}$$

which has the following derivative along the solutions of system (4):

$$\frac{dV}{dt} = (\mathrm{grad}V, f) = 2\left(-\lambda\vartheta(t)^2 + \frac{\alpha}{\beta}u(t)^2\right). \tag{11}$$

Lemma 1. *Let $\lambda = 0$ and $\beta > 0$. Then the separatrix*

$$\lim_{t\to-\infty} x(t) = \lim_{t\to-\infty} \vartheta(t) = \lim_{t\to-\infty} u(t) = 0$$

starting from the saddle $x = \vartheta = u = 0$ tends to infinity as $t \to +\infty$.

Proof. Assume the contrary. Then in this case the separatrix has an ω-limit point x_0, ϑ_0, u_0. From (11) we can obtain that the arc of trajectory $\tilde{x}(t)$, $\tilde{\vartheta}(t)$, $\tilde{u}(t)$, $t \in [0, T]$ with initial data $\tilde{x}(0) = x_0$, $\tilde{\vartheta}(0) = \vartheta_0$, $\tilde{u}(0) = u_0$ also consists of ω-limit points and satisfies the relation $\tilde{u}(t) = 0$, $\forall\, t \in [0, T]$. Then from the third equation of (4) we can obtain that $\tilde{\vartheta}(t)\tilde{x}(t) = 0$, $\forall t \in [0, T]$. This implies the following:

$$(\tilde{x}(t)^2)^\bullet = 2\,\tilde{x}(t)\,\tilde{\vartheta}(t) = 0, \quad \forall t \in [0, T].$$

Thus, $\tilde{x}(t) = \text{const}$, $\tilde{\vartheta}(t) = 0$, $\tilde{u}(t) = 0$, $\forall\, t \in [0, T]$. Then it is easy to see that $\tilde{x}(t)$, $\tilde{\vartheta}(t)$, $\tilde{u}(t)$ are an equilibrium point. From (11) and the relation $V(0, 0, 0) = 0 > -1/2 = V(\pm 1, 0, 0)$ it follow that $\tilde{x}(t) = \tilde{\vartheta}(t) = \tilde{u}(t) \equiv 0$. But in this case the trajectory $x(t), \vartheta(t), u(t)$ is a homoclinic one and $V(x(t), \vartheta(t), u(t)) \equiv 0$.

Then from (11) it follows that $u(t) \equiv 0$. Repeating the arguments that we held earlier for $\tilde{x}(t), \tilde{\vartheta}(t), \tilde{u}(t)$, we get that $x(t) = \vartheta(t) = u(t) \equiv 0$. The latter contradicts the assumption that $x(t), \vartheta(t), u(t)$ is a separatrix of the saddle $x = \vartheta = u = 0$.

Thus, the separatrix $x(t), \vartheta(t), u(t)$ has no ω-limit points and tends to infinity as $t \to +\infty$. ■

Consider system (4) with $\lambda \geq 0$, $\beta > 0$, and assume that

$$\alpha(\sqrt{\lambda^2 + 4} + \lambda) > 2(\beta - 2). \tag{12}$$

Inequality (12) implies that there exists a number $L > 0$, such that

$$L > \frac{\sqrt{\lambda^2 + 4} - \lambda}{2}, \qquad \frac{\beta L}{\alpha + 2L} < 1. \tag{13}$$

Introduce the notions $K = \frac{\beta L}{\alpha + 2L} < 1$ and $M = 1 - K$.

Consider the separatrix $x^+(t)$, $\vartheta^+(t)$, $u^+(t)$ of the zero saddle point of system (4), where $x(t)^+ > 0$, $\forall t \in (-\infty, \tau)$, τ is a number, and $\lim\limits_{t\to-\infty} x(t)^+ = 0$ (i.e. positive outgoing separatrix is considered).

Lemma 2. *Let the following inequality holds:*

$$x^+(t) \geq 0, \qquad \forall\, t \in (-\infty, \tau] \tag{14}$$

and $M > 0$. Then there exists a number $R > 0$ (independent of parameter τ) such that $x^+(t) \leq R$, $|\vartheta^+(t)| \leq R$, $|u^+(t)| \leq R$ for all $t \in (-\infty, \tau]$.

Proof. Define the manifold Φ as follows:

$$\Phi = \left\{ x \in [0,\, x_0],\, \vartheta \leq \min\left\{ Lx,\, \sqrt{\vartheta_0^2 + x^2 - \tfrac{M}{2}x^4} \right\},\, u \geq -Kx^2 \right\}.$$

Here ϑ_0 is an arbitrary positive number (e.g., $\vartheta_0 = 1$), and x_0 is a positive root of the equation

$$\vartheta_0^2 + x^2 - \frac{M}{2}x^4 = 0. \tag{15}$$

Inequalities (13), $K > 0$ and $\vartheta \leq Lx$ in a small vicinity of $x = \vartheta = 0$ implies that at a certain time interval $(-\infty, \tau_1)$, $\tau_1 < \tau$ the separatrix $x^+(t)$, $\vartheta^+(t)$, $u^+(t)$ belongs to Φ. In order to prove that the separatrix belongs to Φ for all $t \in (-\infty, \tau]$ consider the parts of the boundary of $\Phi \cap \{x > 0\}$ and show that they transversal. These boundaries are the following surfaces or the parts of surfaces:

$$\begin{aligned}
\delta_1\Phi &= \left\{ (x, \vartheta, u) \in \mathbb{R}^3 \;\middle|\; x \in (0,\, x_0),\, \vartheta = Lx,\, u \geq -Kx^2 \right\},\\
\delta_2\Phi &= \left\{ (x, \vartheta, u) \in \mathbb{R}^3 \;\middle|\; x \in (0,\, x_0),\, \vartheta^2 = \vartheta_0^2 + x^2 - \tfrac{M}{2}x^4,\, u \geq -Kx^2 \right\},\\
\delta_3\Phi &= \left\{ (x, \vartheta, u) \in \mathbb{R}^3 \;\middle|\; x \in (0,\, x_0),\, \vartheta < Lx,\, u = -Kx^2 \right\},\\
\delta_4\Phi &= \left\{ (x, \vartheta, u) \in \mathbb{R}^3 \;\middle|\; x = x_0,\; \vartheta < 0 \right\}.
\end{aligned}$$

Consider a solution $x(t)$, $\vartheta(t)$, $u(t)$ of system (4), which at the point t is on the surface $\delta_1\Phi$. From (13) it follows that

$$\frac{d\vartheta}{dx} = -\lambda + \frac{1-x^2-u}{L} < -\lambda + \frac{1-Mx^2}{L} < -\lambda + \frac{1}{L}, \qquad \forall\, x \in (0,\, x_0].$$

Thus, we have

$$\frac{d\vartheta}{dx} < L, \qquad \forall\, x \in (0,\, x_0], \quad v = Lx, \quad u \geq -Kx^2.$$

So the surface $\delta_1\Phi$ is transversal and if $x(t)$, $\vartheta(t)$, $u(t)$ is on the surface $\delta_1\Phi$, then for this solution there exists a number $\varepsilon(t)$ such that $\vartheta(\tau) - Lx(\tau) < 0$, $\forall \tau \in (t, t+\varepsilon(t))$.

Now consider a solution $x(t)$, $\vartheta(t)$, $u(t)$ of system (4), which at the point t is on the surface $\delta_2\Phi$ and consider the function $V(x,\vartheta) = \vartheta^2 - x^2 + \frac{M}{2}x^4$. On the set $\delta_2\Phi$ the following relations hold

$$V = 0, \qquad \dot{V}(x,\vartheta) = -2\lambda\vartheta^2(t) - 2\vartheta(t)x(t)\big(u(t) + Kx^2(t)\big) < 0.$$

This implies transversality of $\delta_2\Phi$ and if $x(t)$, $\vartheta(t)$, $u(t)$ is on the surface $\delta_2\Omega$, then for this solution there exists a number $\varepsilon(t)$ such that $V(x(\tau),\vartheta(\tau)) < 0$, $\forall \tau \in (t, t+\varepsilon(t))$.

Consider a solution $x(t)$, $\vartheta(t)$, $u(t)$ of system (4), which at the point t is on the surface $\delta_3\Phi$. Then

$$(u + Kx^2)^{\bullet} = -\alpha u - \beta x\vartheta + 2Kx\vartheta = x((-\beta + 2K)v + \alpha Kx) \;=\; \frac{\alpha\beta x}{\alpha + 2L}(Lx - v) > 0.$$

This implies transversality of $\delta_3\Phi$ and if $x(t)$, $\vartheta(t)$, $u(t)$ is on the surface $\delta_2\Phi$, then for this solution there exists a number $\varepsilon(t)$ such that $u(\tau) + Kx^2(\tau) > 0$, $\forall \tau \in (t, t+\varepsilon(t))$. Transversality of $\delta_4\Phi$ is obvious.

From the relations proved above and the obvious inequality $\dot{x}(t) < 0$ for $x(t) = x_0$, $\vartheta(t) < 0$ it follows that the separatrix $(x^+(t),\, \vartheta^+(t),\, u^+(t))$ belongs to Φ for all $t \in (-\infty,\, \tau]$.

Notice that the third equation of system (4) yields the relations

$$(u + \frac{\beta}{2}x^2)^{\bullet} + \alpha(u + \frac{\beta}{2}x^2) \;=\; \frac{\alpha\beta}{2}x^2.$$

Taking into account the boundedness of $x^+(t)$, i.e. $x^+(t) \in (0,\, x_0)$ for all $t \in (-\infty,\, \tau]$, it follows the boundedness of $u^+(t)$ on $(-\infty,\, \tau]$:

$$u^+(t) + \frac{\beta}{2}(x^+(t))^2 \leq \frac{\beta}{2}x_0^2, \quad \forall t \in (-\infty,\, \tau].$$

Hence, we have the estimate

$$u^+(t) \leq \frac{\beta}{2}x_0^2, \quad \forall t \in (-\infty,\, \tau]. \tag{16}$$

The second equation of system (4) and boundedness of $x^+(t)$ and $u^+(t)$ on $(-\infty,\, \tau]$ yields the boundedness of $\vartheta^+(t)$ for $\lambda > 0$ and boundedness of $\dot{\vartheta}^+(t)$ for $\lambda = 0$. From the first equation of the system (4) and from the boundedness of $x^+(t)$ and $\dot{\vartheta}^+(t)$ it follows the boundedness of $\vartheta^+(t)$ on $(-\infty,\, \tau]$. This implies the assertion of the lemma. ■

Lemma 3. *Suppose inequality* (12) *and the following inequality:*

$$\lambda^2 > 4\left[\left(1 + \tfrac{\beta}{2}\right)\, x_0^2 - 1\right] \tag{17}$$

hold, where x_0 *– is the positive root of equation* (15)*. Then* $x^+(t) > 0$, $\forall\, t \in (-\infty, +\infty)$.

Proof. Here the conditions of Lemma 2 are satisfied. Therefore, if $x^+(t) > 0, \forall\, t \in (-\infty, \tau)$, then $x^+(t) \in \Omega$, $\forall\, t \in (-\infty, \tau)$ and relation (16) holds. If $x^+(\tau) = 0$, then there exists a time moment $T < \tau$ such that for any $P > 0$ we have

$$\vartheta^+(T) = -Px^+(T), \quad \vartheta^+(t) > -Px^+(t), \quad \forall\, t \in (-\infty,\, T). \tag{18}$$

For the relation $\vartheta(T) = -Px(T)$ we have the following:

$$\frac{d\vartheta}{dx} > -\lambda + \tfrac{D}{P}, \qquad D = \left(1 + \frac{\beta}{2}\right) x_0^2 - 1.$$

It is clear that if $P = \frac{\lambda}{2} + \sqrt{\frac{\lambda^2}{4} - D}$, then

$$\frac{d}{dx}(\vartheta + Px) > P - \lambda + \tfrac{D}{P} = 0 \tag{19}$$

on Ω. Here we use condition (17).

From (19) it follows that

$$(\vartheta(T)^+)^\bullet + P(x(T)^+)^\bullet > 0.$$

It follows that there is no $T < \tau$, such that $v^+(T) = -P\,x^+(T)$, which contradicts relations (18). This implies Lemma 3. ■

The obtained lemmas and the Fishing principle (see Theorem 1) allows us to formulate for system (4) the following result.

Theorem 2. *Consider a smooth path $\lambda(s)$, $\alpha(s)$, $\beta(s)$, $s \in [0,\ 1)$ in the parameter space of system (4). Let*

$$\begin{gathered} \lambda(0) = 0, \quad \lim_{s\to 1} \lambda(s) = +\infty, \\ \limsup_{s\to 1} \alpha(s) < +\infty, \quad \limsup_{s\to 1} \beta(s) < +\infty \end{gathered} \tag{20}$$

and the following condition holds:

$$\alpha(s)(\sqrt{\lambda(s)^2 + 4} + \lambda(s)) > 2(\beta(s) - 2), \ \ \forall s \in [0, 1). \tag{21}$$

Then there exists $s_0 \in (0, 1)$ such that system (4) with $\alpha(s_0)$, $\beta(s_0)$, $\lambda(s_0)$ has a homoclinic orbit.

Proof. Here we present the sketch of the proof using the Fishing principle (Theorem 1), and Lemmas 1, 2, 3. We choose the set Ω as follows:

$$\Omega = \left\{(x, \vartheta, u) \in \mathbb{R}^3 \ \middle|\ x = 0, \vartheta \le 0, \vartheta^2 + u^2 \le R^2\right\},$$

where R is a sufficiently large positive number. Conditions (i) and (ii) in Theorem 1 are satisfied for any $s \in [0, 1)$.

Lemmas 1 and 2 imply that, for $s = 0$ condition (iii) in Theorem 1 holds, while Lemmas 1 and 3 imply that, for $s = s_1$ sufficiently close to 1 condition (iv) in Theorem 1 is satisfied.

Condition (v) holds, since system (4) has the solution

$$x(t) \equiv \vartheta(t) \equiv 0, \quad u(t) = u(0)\exp(-\alpha t),$$

which satisfies

$$\lim_{t\to-\infty} u(t) = \infty.$$

Consequently, for large $|t|$, $t < 0$, the solutions with initial data from a small neighborhood of the point $x = \vartheta = 0$, $u = u_0$ leave the cylinder $\left\{(x, \vartheta, u) \in \mathbb{R}^3 \ \middle|\ \vartheta^2 + u^2 \le R^2\right\}$, where R is a sufficiently large positive number. Therefore, by Lemma 1, condition (v) in Theorem 1 holds.

Hence, a path with $s \in [0, s_1]$ satisfies the conditions of Theorem 1, and therefore there exists s_0, for which the assertion of the Theorem 2 holds. ■

Corollary 2.1. *If $\beta(s) \in (0, 2)$ and conditions (20) hold for any $s \in [0, 1)$, then there exists $s_0 \in (0, 1)$ such that system (4) with $\alpha(s_0)$, $\beta(s_0)$, $\lambda(s_0)$ has a homoclinic orbit.*

The statement of Corollary 2.1 was proved previously in [Leonov, 2016].

Corollary 2.2. *Of particular interest to this study is the following path:*

$$\lambda(s) = \frac{s}{\sqrt{1-s}}, \qquad \alpha(s) = \delta\sqrt{1-s}, \qquad \beta(s) \equiv \beta \in (0,\ 2+\delta), \qquad s \in [0,\ 1), \qquad \delta > 0. \tag{22}$$

This path satisfies all conditions of Theorem 2, and therefore there exists a number $s_0 \in (0,\ 1)$ *such that system* (4) *with parameters* (22) *and* $s = s_0$ *has a homoclinic orbit.*

In this case, conditions (22) describe the region of the parameters $\mathcal{B}_{\delta,\beta} = \{\ (\delta,\beta)\ \big|\ \delta > 0,\ \beta \in (0, 2+\delta)\}$ in the parameter plane (δ,β) (see Fig. 1). The eigenvalues and eigenvectors of the matrix of the linear part

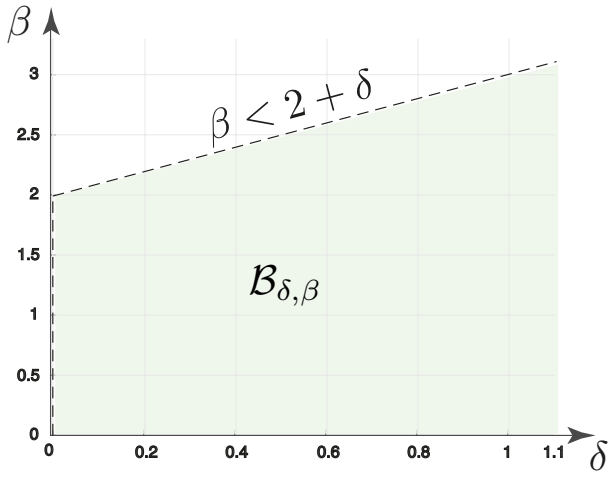

Figure 1. Region of parameters $\mathcal{B}_{\delta,\beta}$ (light green) in the plane (δ,β), for which there exists a homoclinic orbit in system (4).

of (4) at the saddle S_0 have the following form:

$$\begin{aligned}
&\lambda^{\mathrm{s}} = -\alpha = -\delta\sqrt{1-s}, && \mathrm{v}^{\mathrm{s}} = (0,\ 0,\ 1),\\
&\lambda^{\mathrm{ss}} = \tfrac{1}{2}\big(-\sqrt{\lambda^2+4} - \lambda\big) = -\tfrac{1}{\sqrt{1-s}}, && \mathrm{v}^{\mathrm{ss}} = \big(-\sqrt{1-s},\ 1,\ 0\big),\\
&\lambda^{\mathrm{u}} = \tfrac{1}{2}\big(\sqrt{\lambda^2+4} - \lambda\big) = \sqrt{1-s}, && \mathrm{v}^{\mathrm{u}} = \big(\tfrac{1}{\sqrt{1-s}},\ 1,\ 0\big),
\end{aligned} \tag{23}$$

where v^{s}, v^{ss}, v^{u} are mutually perpendicular and the saddle value $\sigma_0 = \lambda^{\mathrm{u}} + \lambda^{\mathrm{s}} = (1-\delta)\sqrt{1-s}$ is negative if $\delta > 1$, zero if $\delta = 1$, and positive if $\delta \in (0,1)$. The equilibrium S_0 has stable and unstable local invariant manifolds $\dim W^{\mathrm{s}}_{\mathrm{loc}} = 2$ and $\dim W^{\mathrm{u}}_{\mathrm{loc}} = 1$, respectively, intersecting at S_0.

Remark 2.1. The result of Corollary 2.2 for path (22) with $\beta \in (0,2)$ and $\delta = 1$ was proved in [Leonov, 2015, 2016] and later repeated in [Ovsyannikov & Turaev, 2017] (taking into account transformation (7)).

All the homoclinic bifurcations observed previously in [Leonov, 2012, 2013, 2016] during the variation of bifurcation parameter s within the interval $(0,1)$ are described by the following two scenarios: either the change of attracting equilibria for separatrices of the saddle zero equilibrium (this case is related to the classical Lorenz system with parameters $\sigma = 10$, $b = 8/3$ and $r \approx 13.926$), or the collision of two stable limit cycles with a saddle equilibrium and merging into one stable limit cycle (see description of these scenarios e.g. in [Sparrow, 1982; Wiggins, 1988; Shilnikov *et al.*, 2001]). Here, using numerical simulations, we describe for $\delta < 1$ several new homoclinic bifurcation scenarios.

3. Numerical analysis of a homoclinic bifurcation in the Lorentz-like system

Homoclinic bifurcation phenomena is related to the mathematical description of the transition to chaos called in literature as *Shilnikov chaos*. Numerical analysis and visualization of Shilnikov chaos is a difficult task, since it requires the study of unstable structures that are sensitive to errors in numerical methods.

3.1. *Numerical experiments*

In this article, to study numerically scenarios of homoclinic bifurcations with different signs of the saddle value σ_0 we consider the region of parameters $\mathcal{B}_{\delta,\beta} = \{\ (\delta,\beta)\ \big|\ \delta \in (0,\ 1.1],\ \beta \in (0, 2+\delta)\}$ in the $\delta\beta$-plane, which satisfies conditions (22), and for points filling the region $\mathcal{B}_{\delta,\beta}$ calculate an approximate interval $[\underline{s}\,, \overline{s}] \subset (0,1)$, such that within it there exist a homoclinic orbit. We select a grid of points $\mathcal{B}_{\rm grid} \subset \mathcal{B}_{\delta,\beta}$ with the predefined partitioning steps $\delta_{\rm grid} = \beta_{\rm grid} = 0.01$ and for each point $(\delta_{\rm curr}, \beta_{\rm curr}) \in \mathcal{B}_{\rm grid}$ we choose the partition $0 < s^0_{\rm step} < 2s^0_{\rm step} < \ldots, (N-1)s^0_{\rm step} < 1$ of the interval $(0,1)$ with step $s^0_{\rm step} = \frac{1}{N} = 0.001$. For the system (4) with parameters $\delta_{\rm curr}, \beta_{\rm curr}, \lambda(s_{\rm curr}), \alpha(s_{\rm curr})$ we integrate numerically the separatrix $(x_{\rm sepa}(t), \vartheta_{\rm sepa}(t), u_{\rm sepa}(t))$ of the saddle equilibrium S_0 of system (4) on the chosen time interval $t \in [0, T_{\rm trans}]$ using the `ode45` solver in MATLAB with best available values of relative and absolute tolerances.

To determine possible existence of limit sets (stable limit cycles, or chaotic attractors) and exclude transient process we also numerically integrate trajectories $x_{\rm lim}(t), \vartheta_{\rm lim}(t), u_{\rm lim}(t)$ with initial data $(x_{\rm lim}(0), \vartheta_{\rm lim}(0), u_{\rm lim}(0)) = (x_{\rm sepa}(T_{\rm trans}), \vartheta_{\rm sepa}(T_{\rm trans}), u_{\rm sepa}(T_{\rm trans}))$ on the chosen interval $t \in [0, T_{\rm lim}]$. Resulting trajectories $(x_{\rm sepa}(t), \vartheta_{\rm sepa}(t), u_{\rm sepa}(t))$ and $(x_{\rm lim}(t), \vartheta_{\rm lim}(t), u_{\rm lim}(t))$ are colored according to the gradient between blue to red colors, corresponding to the integration time interval (this helps us to detect possible untwisting of trajectories). Note that due to symmetry of the system (4) it is sufficient to integrate only one separatrix $\Gamma^+(t) = (x_{\rm sepa}(t), \vartheta_{\rm sepa}(t), u_{\rm sepa}(t))$ and the second one can be expressed as $\Gamma^-(t) := (-x_{\rm sepa}(t), -\vartheta_{\rm sepa}(t), u_{\rm sepa}(t))$. When equilibria $S_\pm$ are saddle-foci, we also integrate the separatrix of the S_+ in the described above manner.

In numerical integration of trajectories via `ode45` we use the event handler ODE Event Location to detect the following events:

- *separatrix $\Gamma^+(t)$ tends to infinity.* For the values of parameter s close to 0 system (4) is not dissipative in the sense of Levinson, and the separatrix of the saddle equilibrium S_0 slowly untwists to "infinity". If the separatrix leaves the ball with the big enough radius $R_{\rm inf}$, the integration is terminated.
- *separatrix $\Gamma^+(t)$ tends to equilibrium S_+ (or $\Gamma^-(t)$ to S_-), towards which it is released.* If for some $s = s_{\rm cr}$ the separatrix tends to nearest equilibrium state, then for $s > s_{\rm cr}$ there will be no other bifurcations. At this point it is possible to terminate the variation of parameter s and skip the next pair $(\delta,\beta) \in \mathcal{B}_{\rm grid}$. To verify the attraction to the equilibrium state we detect the event of falling into its small vicinity of the radius $\varepsilon_{\rm eq}$.

If for a fixed pair $(\delta,\beta) \in \mathcal{B}_{\rm grid}$ during the scanning of the interval $(0,1)$ with the step $s^0_{\rm step}$ there are two consecutive values $\underline{s}, \overline{s} \in (0,1)$ such that the behavior of the separatrices $\Gamma^\pm(t)$ changes as we go from the parameters $\lambda(\underline{s})$, $\alpha(\underline{s})$ to the parameters $\lambda(\overline{s})$, $\alpha(\overline{s})$, then the segment $[\underline{s}\,, \overline{s}]$ is also scanned with the $s^{i+1}_{\rm step} = 0.1 s^i_{\rm step}$, $i = 0, 1, \ldots$. This consecutive reduction of the partitioning step allows us to find the boundary values $\underline{s}$, $\overline{s}$ which specify a bifurcation with a certain accuracy $\overline{s} - \underline{s} > \varepsilon_{\rm threshold}$. All the values parameters of the described numerical procedure are outlined in Table 3.1.

Table 1. Values of the parameters of the numerical procedure for scanning the region $\mathcal{B}_{\delta,\beta}$.

$\delta_{\rm grid}$	$\beta_{\rm grid}$	$s^0_{\rm step}$	$\varepsilon_{\rm threshold}$	$T_{\rm trans}$	$T_{\rm lim}$	$R_{\rm inf}$	$\varepsilon_{\rm eq}$
10^{-2}	10^{-2}	10^{-3}	10^{-12}	$4 \cdot 10^3$	10^3	100	10^{-1}

After the described scanning of the region $\mathcal{B}_{\delta,\beta}$ for each grid point $(\delta,\beta) \in \mathcal{B}_{\rm grid}$ the values $\underline{s}, \overline{s} \in (0,1)$ are found numerically, such that the change of the parameter s on the interval $[\underline{s}\,, \overline{s}] \subset (0,1)$ specifies a homoclinic bifurcation. Further, the type of homoclinic bifurcation is refined by numerical analysis of the behavior of the Poincaré map on the corresponding sections $\Sigma^{\rm in}$, $\Sigma^{\rm out}$, chosen in the neighborhood of the saddle S_0 (Fig. 2). The section $\Sigma^{\rm in}$ is chosen perpendicular to the vector $\mathrm{v}^{\rm s}$ at a distance of $\varepsilon^{\rm in}$ from S_0, the section $\Sigma^{\rm out}$ – is perpendicular to the vector $\mathrm{v}^{\rm u}$ and is located at a distance of $\varepsilon^{\rm out}$ from S_0. On the section $\Sigma^{\rm in}$ a rectangular grid of points $\Sigma^{\rm in}_{\rm grid}$ with sides collinear to the vectors $\mathrm{v}^{\rm u}$ and $\mathrm{v}^{\rm ss}$ is chosen. We match the color according to the color scale (from blue to red) to each row of grid points, starting with the row that lies at the intersection of $\Sigma^{\rm in}$ and the plane $\{\mathrm{v}^{\rm s}, \mathrm{v}^{\rm ss}\}$, and paint the grid in this way (Fig. 3).

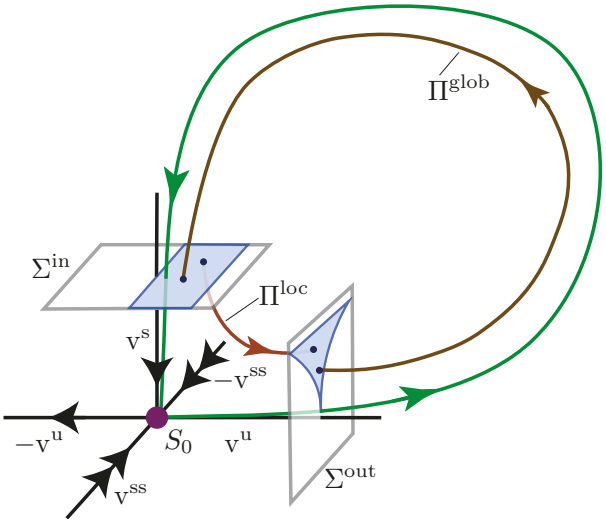

Figure 2. Poincaré sections Σ^{in} and Σ^{out} in the neighborhood of the saddle $S_0 = (0, 0, 0)$ of the system (4).

Next, the evolution of the Poincare map $\Pi = \Pi^{glob} \circ \Pi^{loc} : \Sigma^{in} \to \Sigma^{in}$ of the given grid of points Σ^{in}_{grid} is numerically studied. In our experiment, the maps $\Pi^{loc} : \Sigma^{in} \to \Sigma^{out}$ and $\Pi^{glob} : \Sigma^{out} \to \Sigma^{in}$ are simulated in MATLAB using numerical procedure `ode45` and built-in event handler ODE Event Location to determine the moment of hitting on the corresponding section. To accelerate the described calculations we also use the MATLAB Parallel Computing Toolbox.

During the numerical simulations we found that for a sufficiently small rectangle after the first Poincaré map its image falls inside its domain. Therefore, from the rectangular grid of points it is possible to "cut out" the middle part and to consider the half frame in the experiment. The size of the cutted-out part is chosen in such a way that the intersection point of the separatrix $\Gamma^+(t)$ released from the saddle S_0 with the section Σ^{in} belongs to it along with its small neighborhood. This approach allows us to avoid the simulation of trajectories which are close to the homoclinic loop and which require calculations over large time intervals.

Numerical studies show that in the region covered by the given grid points, there are 4 regions with different homoclinic bifurcations (Fig. 4). In the yellow region marked with by (Ⅰ) before bifurcation separatrices $\Gamma^{\pm}(t)$ were attracted to the opposite equilibria $S_{\mp}$ and after bifurcation – to the nearest ones, i.e. to $S_{\pm}$. In this case, during the inverse bifurcation (i.e. while moving in the direction from $s = 1$ to $s = 0$), two unstable limit cycles are born from the homoclinic butterfly. This scenario corresponds to the case of the homoclinic bifurcation in classical Lorenz system [Lorenz, 1963] with parameters $\sigma = 10$, $b = 8/3$, $r \approx 13.926$ (see e.g. [Sparrow, 1982; Wiggins, 1988; Shilnikov *et al.*, 2001]).

In the blue region marked by (Ⅲ) during the bifurcation, one large stable "eight"-type limit cycle collides with the saddle equilibrium S_0 and splits into two stable limit cycles around $S_{\pm}$. Numerical analysis of the separatrices behavior for all $\delta \in [1, 1.1]$, $\beta \in (0, 2 + \delta)$ within the chosen partition and the dynamics analysis of the grid points Σ^{in}_{grid} on the Poincaré section Σ^{in} under the successive action of Poincaré map $\Pi : \Sigma^{in} \to \Sigma^{in}$ give us a reason to think that there is no chaotic attractors in the vicinity of the homoclinic bifurcation in the case of zero and negative saddle values σ_0.

Also, two new scenarios of homoclinic bifurcation, which was not described in [Leonov, 2012, 2013, 2016], are found. In the red area marked with (Ⅳ), depending on values of parameters δ, β, two symmetric limit cycles $\Theta^{\pm}$ around $S_{\pm}$ coexist with either one stable "eight"-type limit cycle, or a strange attractor which attract the separatrices $\Gamma^{\pm}(t)$. Then this attractor (periodic or strange) loses stability and separatrices $\Gamma^{\pm}(t)$ are attracted to the opposite limit cycles $\Theta^{\mp}$. After the bifurcation the separatrices $\Gamma^{\pm}(t)$ are attracted to the nearest limit cycles $\Theta^{\pm}$. As in the case of classical Lorenz system, in this case during

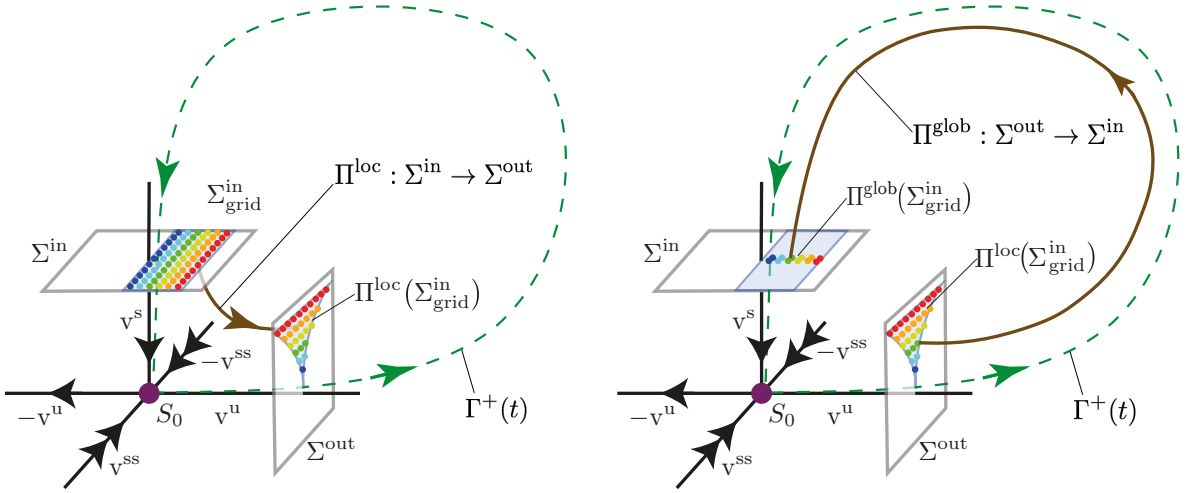

(a) $\Pi^{\mathrm{loc}}:\Sigma^{\mathrm{in}}\to\Sigma^{\mathrm{out}}$ maps rectangular grid of points $\Sigma^{\mathrm{in}}_{\mathrm{grid}}$ to a "half bowtie" shape grid $\Pi^{\mathrm{loc}}(\Sigma^{\mathrm{in}}_{\mathrm{grid}})$.

(b) $\Pi^{\mathrm{glob}}:\Sigma^{\mathrm{out}}\to\Sigma^{\mathrm{in}}$ shrinks $\Pi^{\mathrm{loc}}(\Sigma^{\mathrm{in}}_{\mathrm{grid}})$ into a "stick" shape grid $\Pi^{\mathrm{glob}}(\Sigma^{\mathrm{in}}_{\mathrm{grid}})$.

Figure 3. Rectangular grid of points $\Sigma^{\mathrm{in}}_{\mathrm{grid}}$ and its image $\Pi^{\mathrm{glob}}(\Sigma^{\mathrm{in}}_{\mathrm{grid}})$ on the Poincare section Σ^{in}.

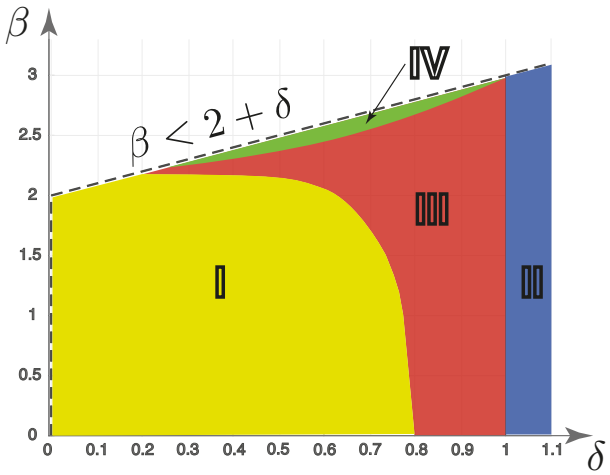

Figure 4. Different types of homoclinic bifurcations in the system (4).

the inverse bifurcation scenario, two unstable limit cycles are born from the homoclinic butterfly, but here they separetes two stable cycles $\Theta^{\pm}$. For example, for parameter values $\delta = 0.9$, $\beta = 0.2$, the dynamics of separatrices in the phase space is shown in Fig. 5 and the dynamics of the grid of points $\Sigma^{\mathrm{in}}_{\mathrm{grid}}$ before and after bifurcation is presented in Fig. 9 and Fig. 10), respectively. For parameter values $\delta = 0.5$, $\beta = 2.2$ the case of coexistence of two symmetric limit cycles $\Theta^{\pm}$ around $S_{\pm}$ with a strange attractor defined by the separatrix $\Gamma^{+}(t)$ is presented in Fig. 6. Note that here one could consider two types of vicinities of the bifurcation point in the parameter space: $[\underline{s}, \overline{s}]$ and $[\underline{s}', \overline{s}]$, where $[\underline{s}, \overline{s}] \subset [\underline{s}', \overline{s}]$. In the vicinity $[\underline{s}, \overline{s}]$ a simple bifurcation is observed in which, as described just above, there is a change in attracting limit cycles $\Theta^{\pm}$ for the separatrices $\Gamma^{\pm}(t)$ of the saddle S_0. At the same time, on the interval $[\underline{s}', \underline{s})$ the chaotic behavior of the separatrices $\Gamma^{\pm}(t)$ can be observed, which can make one to think that the homoclinic bifurcation is embedded in the strange attractor.

In the green region marked with ($\mathbb{IV}$), when an unstable homoclinic orbit occurs, one strange attractor

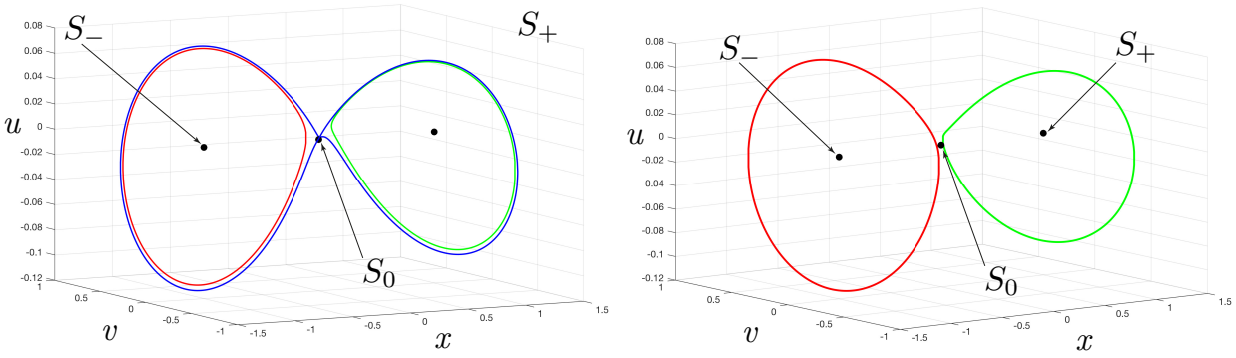

(a) $\underline{s} = 0.060131460578$ **(b)** $\overline{s} = 0.060131460581$

Figure 5. Homoclinic bifurcation for $\delta = 0.9$, $\beta = 0.2$.

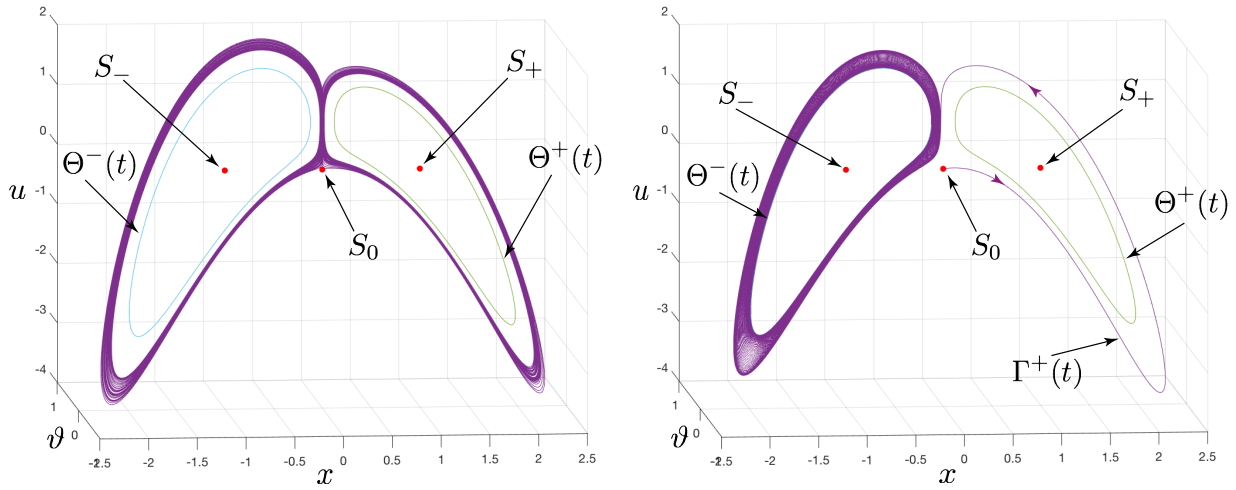

(a) $\underline{s}' = 0.7979407438278198$ **(b)** $\underline{s} \in [0.7979407447814941, 0.8059291805341841]$

Figure 6. Behavior of separatrix $\Gamma^+(t)$ of saddle S_0 and separatrices of saddle-foci $S_\pm$ before homoclinic bifurcation for $\delta = 0.5$, $\beta = 2.2$. Homoclinic bifurcation occurs on the interval $s \in [\underline{s}, \overline{s}]$, where $\overline{s} = 0.8059291805416346$.

split into two (or, if we track the change in the parameter s from 1 to 0, then we can say that two strange attractors merge into one strange attractor). For example, for parameter values $\delta = 0.9$, $\beta = 2.899$, the dynamics of separatrices in the phase space is shown in Fig. 7 and the dynamics of the grid of points $\Sigma^{\text{in}}_{\text{grid}}$ before and after bifurcation is presented in Fig. 11 and Fig. 12), respectively.

For numerical verification of the behavior of the Poincaré map $\Pi : \Sigma^{\text{in}} \to \Sigma^{\text{in}}$ for the case of splitting attractors we perform the following test. Consider the grid of points $\Sigma^{\text{attr}}_{\text{grid}}$ corresponding to the intersection between one of the attractors and the Poincaré section Σ^{in} and color it according to the scale (from blue to red). We save the coordinates of grid points assuming that approximately this grid represents the line segment. Next, we calculate the image of $\Sigma^{\text{attr}}_{\text{grid}}$ under the action of the Poincaré and after that for each point $\mathrm{x}_0 \in \Sigma^{\text{attr}}_{\text{grid}}$ we compare its coordinate with the coordinate of $\Pi(\mathrm{x}_0)$. As a result of this experiment, we have obtained that, under the indicated assumptions, the Poincaré map behaves approximately the same way as the know one-dimensional tent map with parameter ≈ 2 (Fig. 8). Using special methods for finite-time Lyapunov exponents and finite-time Lyapunov dimension estimations (see e.g. [Leonov *et al.*, 2015c,b; Kuznetsov *et al.*, 2018a]), we calculate the corresponding values of the largest finite-time Lyapunov exponent, $\mathrm{LE}_1(t_{\text{end}}, \mathrm{x}_0) = 0.0316 > 0$, and local finite-time

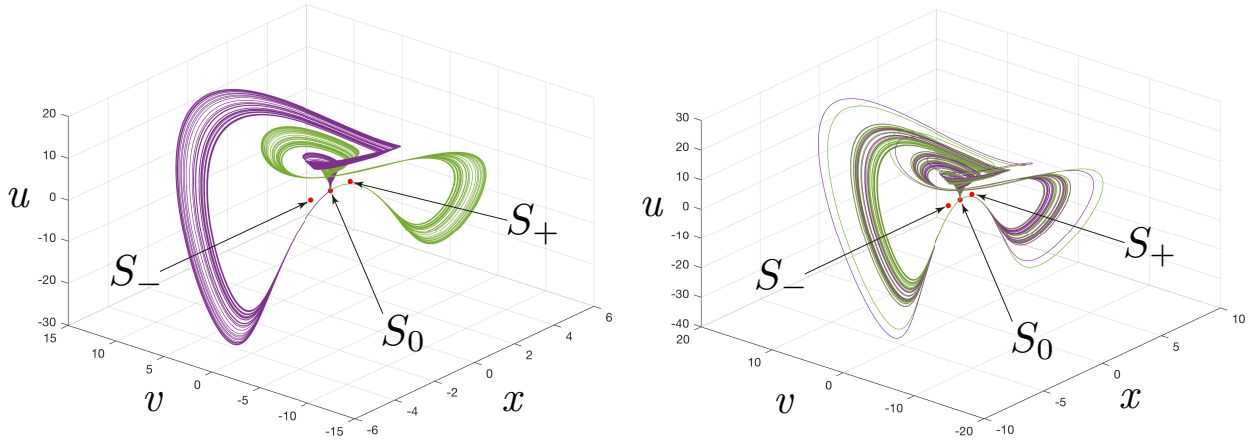

(a) $\overline{s} = 0.7957...$ **(b)** $\underline{s} = 0.7955...$

Figure 7. Homoclinic bifurcation of the two merging attractors at $\delta = 0.9$, $\beta = 2.899$.

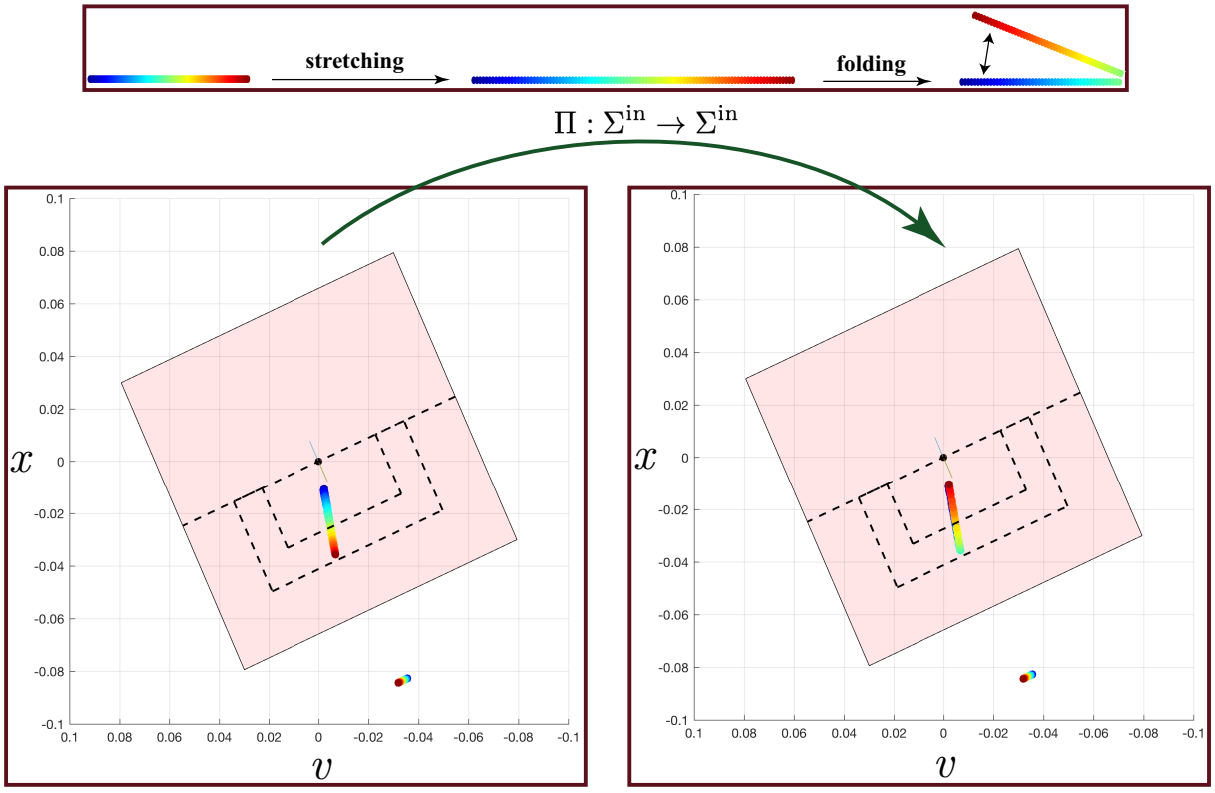

Figure 8. Behavior of the Poincaré map $\Pi : \Sigma^{\text{in}} \to \Sigma^{\text{in}}$ before the homoclinic bifurcation of merging attractors for system (4) with $\delta = 0.9$, $\beta = 2.899$.

Lyapunov dimension, $\text{LD}(t_{\text{end}}, \text{x}_0) = 2.0131$ for one of the attractors along the trajectory[1] with initial

[1]Remark that in numerical studying of long-term behavior of trajectories of nonlinear systems one usually could face the following problems. On the one hand, the result of numerical integration of trajectories via approximate methods is strongly influenced by round-off errors in the general case accumulate over a large time interval and do not allow tracking the "true" trajectory without the use of special methods and approaches [Galias & Zgliczyński, 1998; Tucker, 1999; Liao & Wang, 2014; Lozi & Pchelintsev, 2015; Kehlet & Logg, 2017]. On the other hand, the problem arises of distinguishing between the established behavior defined by the *sustain* limit sets (periodic orbits, strange attractors) from the so-called *transient behavior* corresponding to a *transient set* in phase space, which nevertheless can exist for a long time [Grebogi *et al.*, 1983; Lai & Tel, 2011; Chen *et al.*, 2017; Kuznetsov *et al.*, 2018a].

data $x_0 = (-0.0479075467563750, 8.41428910156156, 13.7220943173008)$ and time interval $[0, t_{\text{end}} = 1000]$. These numerical experiments give us a reason to think that the considered attractor (and the symmetric one) is strange.

Numerical simulations of separatrices outside the region $\mathcal{B}_{\delta,\beta}$ (i.e. for the case $\beta > 2 + \delta$) show that system (4) in this region is not dissipative in the sense of Levinson and separatrices tend to infinity. Thus, numerically we obtain that outside the region $\mathcal{B}_{\delta,\beta}$ there are no homoclinic bifurcations.

Remark that according to the description of the numerical experiments on the study of homoclinic bifurcation scenarios all the attractors (periodic and chaotic) obtained here for system (4) are *self-excited*, i.e. they could be revealed numerically by the integration of trajectories, started in small neighborhoods of unstable equilibria. However, there may also exist *hidden attractors*[2], which basins of attraction are not connected with equilibria and which are "hidden" somewhere in the phase space. The search for hidden attractors may be a challenging task, especially in the case when dynamical system is not dissipative in the sense of Levinson and so it is necessary to consider an unbounded set of initial data for their visualization.

The classical Lorenz attractor in system (1) with $\sigma = 10$, $r = 28$, and $b = 8/3$ is a self-excited one with respect to all equilibria, and it is still an open question[3] [Kuznetsov, 2016a, p. 14] whether for some parameters there exists a hidden Lorenz attractor (see corresponding discussion, e.g. in [Leonov & Kuznetsov, 2015; Leonov *et al.*, 2015c; Chen *et al.*, 2017; Sprott & Munmuangsaen, 2018; Kuznetsov & Mokaev, 2019]). However, there are a number of physical dynamical models representing generalizations of the Lorenz system, which possess hidden chaotic attractors (see e.g. [Leonov *et al.*, 2015b,c; Kuznetsov *et al.*, 2018a; Chen *et al.*, 2017]).

4. Conclusion

In the papers [Leonov *et al.*, 2015c; Leonov, 2012, 2013], it is suggested the effective analytical approach, called Fishing principle, which allows one not only to prove the existence of a homoclinic orbit to a saddle equilibrium in the phase space of dynamical system, but also to organize a convenient analytical-numerical study of homoclinic bifurcation scenarios, which are observed while changing the particular bifurcation parameter s within the Fishing principle (see Eq. (22)).

However, subsequent studies [Leonov & Mokaev, 2018; Leonov, 2018] have shown the practical difficulties of the numerical implementation of this approach related to the calculations with finite accuracy and round-off errors. In this paper we overcome these difficulties as much as possible while remaining within the framework of standard calculations in MATLAB.

We prove analytically the existence of homoclinic orbit to a saddle zero equilibrium in the Lorenz-like system (4) and perform a numerical scanning of the corresponding parameter region $\mathcal{B}_{\delta,\beta}$, where during the variation of parameter $s \in (0, 1)$ homoclinic bifurcations occur. As a result, classical Lorenz scenarios of homoclinic bifurcations were observed as well as two new scenarios of homoclinic bifurcations in system (4) were found numerically, e.g., the homoclinic bifurcation of two merging strange attractors.

It is the beginning of study of these types of homoclinic bifurcations. Further studies and refinements of the obtained numerical results may require consideration of general numerical approaches for the analysis of homoclinic bifurcations (see e.g. [Champneys *et al.*, 1996; Homburg & Sandstede, 2010; Doedel & Oldeman, 2012]).

5. Acknowledgment

This work was supported by the Russian Science Foundation (project 19-41-02002). We dedicate this work to the memory of our scientific father — Gennady A. Leonov, with whom we had started it in 2018 and

[2]The classification of attractors as being hidden or self-excited was proposed by G.A. Leonov and N.V. Kuznetsov in 2009 [Leonov & Kuznetsov, 2013; Leonov *et al.*, 2015c; Kuznetsov *et al.*, 2018a]. This classification became a basis for the *theory of hidden oscillations* [Kuznetsov, 2016b, 2018a,b, 2019, 2020], which represents the genesis of the modern era of Andronov's theory of oscillations.

[3]This question is related to the "chaotic" generalization [Leonov & Kuznetsov, 2015] of the second part of Hilbert's 16th problem *on the number and mutual disposition of attractors and repellers in the chaotic multidimensional dynamical systems and, in particular, their dependence on the degree of polynomials in the model.*

finished after his sudden passing away [Kuznetsov *et al.*, 2018b].

References

Afraimovich, V. S., Gonchenko, S. V., Lerman, L. M., Shilnikov, A. L. & Turaev, D. V. [2014] "Scientific heritage of L.P. Shilnikov," *Regular and Chaotic Dynamics* **19**, 435–460.

Argoul, F., Arneodo, A. & Richetti, P. [1987] "Experimental evidence for homoclinic chaos in the Belousov-Zhabotinskii reaction," *Physics Letters A* **120**, 269–275.

Barboza, R. [2018] "On Lorenz and Chen systems," *International Journal of Bifurcation and Chaos* **28**, 1850018.

Champneys, A. [1998] "Homoclinic orbits in reversible systems and their applications in mechanics, fluids and optics," *Physica D: Nonlinear Phenomena* **112**, 158–186.

Champneys, A., Kuznetsov, Y. & Sandstede, B. [1996] "A numerical toolbox for homoclinic bifurcation analysis," *International Journal of Bifurcation and Chaos* **6**, 867–888.

Chen, G., Kuznetsov, N., Leonov, G. & Mokaev, T. [2017] "Hidden attractors on one path: Glukhovsky-Dolzhansky, Lorenz, and Rabinovich systems," *International Journal of Bifurcation and Chaos in Applied Sciences and Engineering* **27**, art. num. 1750115.

Chen, G. & Ueta, T. [1999] "Yet another chaotic attractor," *International Journal of Bifurcation and Chaos* **9**, 1465–1466.

Doedel, E. & Oldeman, B. [2012] "AUTO-07P: Continuation and bifurcation software for ordinary differential equations," URL http://www.hds.bme.hu/~fhegedus/BubbleDynamics/AUTO/auto.pdf.

Galias, Z. & Zgliczyński, P. [1998] "Computer assisted proof of chaos in the Lorenz equations," *Physica D* **115**, 165–188.

Grebogi, C., Ott, E. & Yorke, J. [1983] "Fractal basin boundaries, long-lived chaotic transients, and unstable-unstable pair bifurcation," *Physical Review Letters* **50**, 935–938.

Homburg, A. J. & Sandstede, B. [2010] "Homoclinic and heteroclinic bifurcations in vector fields," *Handbook of dynamical systems* **3**, 379–524.

Kehlet, B. & Logg, A. [2017] "A posteriori error analysis of round-off errors in the numerical solution of ordinary differential equations," *Numerical Algorithms* **76**, 191–210.

Kuznetsov, N. [2016a] "Hidden attractors in fundamental problems and engineering models. A short survey," *Lecture Notes in Electrical Engineering* **371**, 13–25, doi:10.1007/978-3-319-27247-4_2, (Plenary lecture at International Conference on Advanced Engineering Theory and Applications 2015).

Kuznetsov, N. [2018a] "Plenary lecture "Theory of hidden oscillations"," *5th IFAC Conference on Analysis and Control of Chaotic Systems*.

Kuznetsov, N. [2018b] "Plenary lecture "Theory of hidden oscillations"," *11th Russian Multiconference on Control Problems*.

Kuznetsov, N. [2019] "Invited lecture "Theory of hidden oscillations and stability of control systems"," *XII All-Russian Congress on Fundamental Problems of Theoretical and Applied Mechanics (Ufa, Russia)*, (https://www.youtube.com/watch?v=843m-rI5nTM).

Kuznetsov, N. [2020] "Theory of hidden oscillations and stability of control systems," *Journal of Computer and Systems Sciences International* **1**.

Kuznetsov, N., Leonov, G., Mokaev, T., Prasad, A. & Shrimali, M. [2018a] "Finite-time Lyapunov dimension and hidden attractor of the Rabinovich system," *Nonlinear Dynamics* **92**, 267–285, doi: 10.1007/s11071-018-4054-z.

Kuznetsov, N. & Mokaev, T. [2019] "Numerical analysis of dynamical systems: unstable periodic orbits, hidden transient chaotic sets, hidden attractors, and finite-time Lyapunov dimension," *Journal of Physics: Conference Series* **1205**, doi:10.1088/1742-6596/1205/1/012034, art. num. 012034.

Kuznetsov, N. V. [2016b] *Analytical-numerical methods for the study of hidden oscillations (Habilitation thesis, in Russian)* (Saint-Petersburg State University).

Kuznetsov, N. V., Abramovich, S., Fradkov, A. L. & Chen, G. [2018b] "In Memoriam: Gennady Alekseevich Leonov." *International Journal of Bifurcation and Chaos* **28**, 1–5.

Kuznetsov, Y., Muratori, S. & Rinaldi, S. [1992] "Bifurcations and chaos in a periodic predator-prey

model," *International Journal of Bifurcation and Chaos* **2**, 117–128.
Lai, Y. & Tel, T. [2011] *Transient Chaos: Complex Dynamics on Finite Time Scales* (Springer, New York).
Leonov, G. [2012] "General existence conditions of homoclinic trajectories in dissipative systems. Lorenz, Shimizu-Morioka, Lu and Chen systems," *Physics Letters A* **376**, 3045–3050.
Leonov, G. [2013] "Shilnikov chaos in Lorenz-like systems," *International Journal of Bifurcation and Chaos* **23**, doi:10.1142/S0218127413500582, art. num. 1350058.
Leonov, G. [2014] "Fishing principle for homoclinic and heteroclinic trajectories," *Nonlinear Dynamics* **78**, 2751–2758.
Leonov, G. [2015] "Cascade of bifurcations in Lorenz-like systems: Birth of a strange attractor, blue sky catastrophe bifurcation, and nine homoclinic bifurcations," *Doklady Mathematics* **92**, 563–567.
Leonov, G. [2016] "Necessary and sufficient conditions of the existence of homoclinic trajectories and cascade of bifurcations in Lorenz-like systems: birth of strange attractor and 9 homoclinic bifurcations," *Nonlinear Dynamics* **84**, 1055–1062.
Leonov, G. [2018] "Lyapunov functions in the global analysis of chaotic systems," *Ukrainian Mathematical Journal* **70**, 42–66, doi:10.1007/s11253-018-1487-y.
Leonov, G., Alexeeva, T. & Kuznetsov, N. [2015a] "Analytic exact upper bound for the Lyapunov dimension of the Shimizu-Morioka system," *Entropy* **17**, 5101–5116, doi:10.3390/e17075101.
Leonov, G. & Kuznetsov, N. [2013] "Hidden attractors in dynamical systems. From hidden oscillations in Hilbert-Kolmogorov, Aizerman, and Kalman problems to hidden chaotic attractors in Chua circuits," *International Journal of Bifurcation and Chaos in Applied Sciences and Engineering* **23**, doi:10.1142/S0218127413300024, art. no. 1330002.
Leonov, G. & Kuznetsov, N. [2015] "On differences and similarities in the analysis of Lorenz, Chen, and Lu systems," *Applied Mathematics and Computation* **256**, 334–343, doi:10.1016/j.amc.2014.12.132.
Leonov, G., Kuznetsov, N. & Mokaev, T. [2015b] "Hidden attractor and homoclinic orbit in Lorenz-like system describing convective fluid motion in rotating cavity," *Communications in Nonlinear Science and Numerical Simulation* **28**, 166–174, doi:10.1016/j.cnsns.2015.04.007.
Leonov, G., Kuznetsov, N. & Mokaev, T. [2015c] "Homoclinic orbits, and self-excited and hidden attractors in a Lorenz-like system describing convective fluid motion," *The European Physical Journal Special Topics* **224**, 1421–1458, doi:10.1140/epjst/e2015-02470-3.
Leonov, G. & Mokaev, R. [2018] "Numerical simulations of the Lorenz-like system: Asymptotic behavior of solutions, chaos and homoclinic bifurcations," *Abstracts of the International Scientific Conference on Mechanics "The Eight Polyakhov's Reading"*, p. 264.
Liao, S. & Wang, P. [2014] "On the mathematically reliable long-term simulation of chaotic solutions of Lorenz equation in the interval [0,10000]," *Science China Physics, Mechanics and Astronomy* **57**, 330–335.
Lorenz, E. [1963] "Deterministic nonperiodic flow," *J. Atmos. Sci.* **20**, 130–141.
Lozi, R. & Pchelintsev, A. [2015] "A new reliable numerical method for computing chaotic solutions of dynamical systems: the Chen attractor case," *International Journal of Bifurcation and Chaos* **25**, 1550187.
Lu, J. & Chen, G. [2002] "A new chaotic attractor coined," *Int. J. Bifurcation and Chaos* **12**, 1789–1812.
Neimark, Y. I. & Landa, P. S. [1992] *Stochastic and Chaotic Oscillations* (Kluwer Academic Publishers, Dordrecht, The Netherlands).
Oraevsky, A. N. [1981] "Masers, lasers, and strange attractors," *Quantum Electronics* **11**, 71–78.
Ovsyannikov, I. & Turaev, D. [2017] "Analytic proof of the existence of the Lorenz attractor in the extended Lorenz model," *Nonlinearity* **30**, 115.
Poincare, H. [1892, 1893, 1899] *Les methodes nouvelles de la mecanique celeste. Vol. 1-3* (Gauthiers-Villars, Paris), [English transl. edited by D. Goroff: American Institute of Physics, NY, 1993].
Rubenfeld, L. A. & Siegmann, W. L. [1977] "Nonlinear dynamic theory for a double-diffusive convection model," *SIAM Journal on Applied Mathematics* **32**, 871–894.
Shilnikov, L. P., Shilnikov, A. L., Turaev, D. V. & Chua, L. [1998] *Methods of Qualitative Theory in Nonlinear Dynamics: Part 1* (World Scientific).
Shilnikov, L. P., Shilnikov, A. L., Turaev, D. V. & Chua, L. [2001] *Methods of Qualitative Theory in*

Nonlinear Dynamics: Part 2 (World Scientific).

Shimizu, T. & Morioka, N. [1980] "On the bifurcation of a symmetric limit cycle to an asymmetric one in a simple model," *Physics Letters A* **76**, 201 – 204.

Sparrow, C. [1982] *The Lorenz Equations: Bifurcations, Chaos, and Strange Attractors*, Applied Mathematical Sciences (Springer New York).

Sprott, J. & Munmuangsaen, B. [2018] "Comment on "A hidden chaotic attractor in the classical Lorenz system"," *Chaos, Solitons & Fractals* **113**, 261–262.

Tel, T. & Gruiz, M. [2006] *Chaotic dynamics: An introduction based on classical mechanics* (Cambridge University Press).

Tigan, G. & Opris, D. [2008] "Analysis of a 3D chaotic system," *Chaos, Solitons & Fractals* **36**, 1315–1319.

Tricomi, F. [1933] "Integrazione di unequazione differenziale presentatasi in elettrotechnica," *Annali della R. Shcuola Normale Superiore di Pisa* **2**, 1–20.

Tucker, W. [1999] "The Lorenz attractor exists," *Comptes Rendus de l'Academie des Sciences - Series I - Mathematics* **328**, 1197 – 1202.

Wiggins, S. [1988] *Global bifurcations and chaos: analytical methods*, Vol. 73 (Springer-Verlag).

Yang, Q. & Chen, G. [2008] "A chaotic system with one saddle and two stable node-foci," *International Journal of Bifurcation and Chaos* **18**, 1393–1414, doi:10.1142/S0218127408021063.

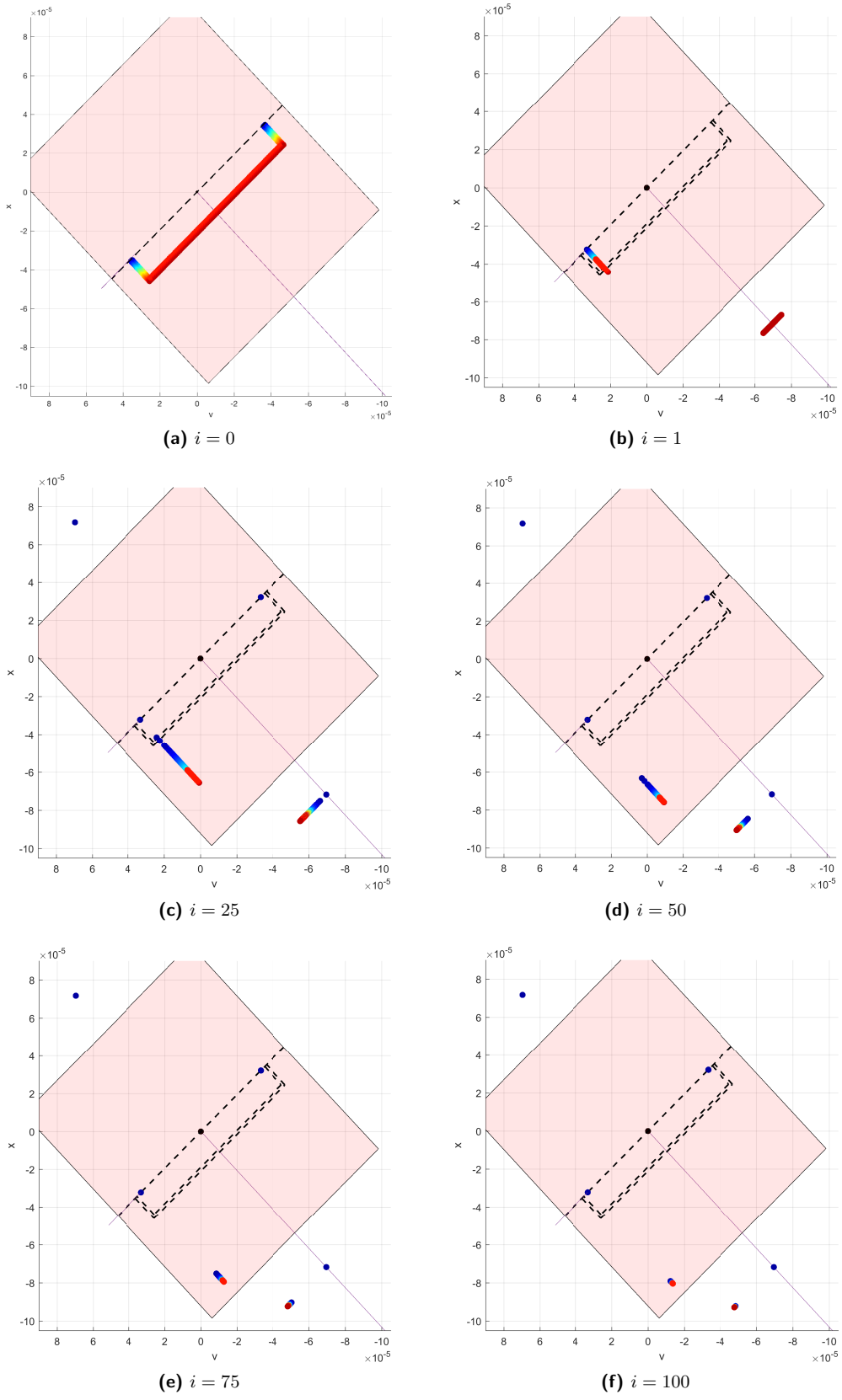

(a) $i = 0$ **(b)** $i = 1$

(c) $i = 25$ **(d)** $i = 50$

(e) $i = 75$ **(f)** $i = 100$

Figure 9. Dynamics of the half-frame of points $\Sigma^{\text{in}}_{\text{grid}}$ on the section Σ^{in} under repeated applications of the Poincaré map $\Pi^i : \Sigma^{\text{in}} \to \Sigma^{\text{in}}$, $i = 1, 2, \ldots$, for $\delta = 0.9$, $\beta = 0.2$, $\underline{s} = 0.060131460578$ (before bifurcation).

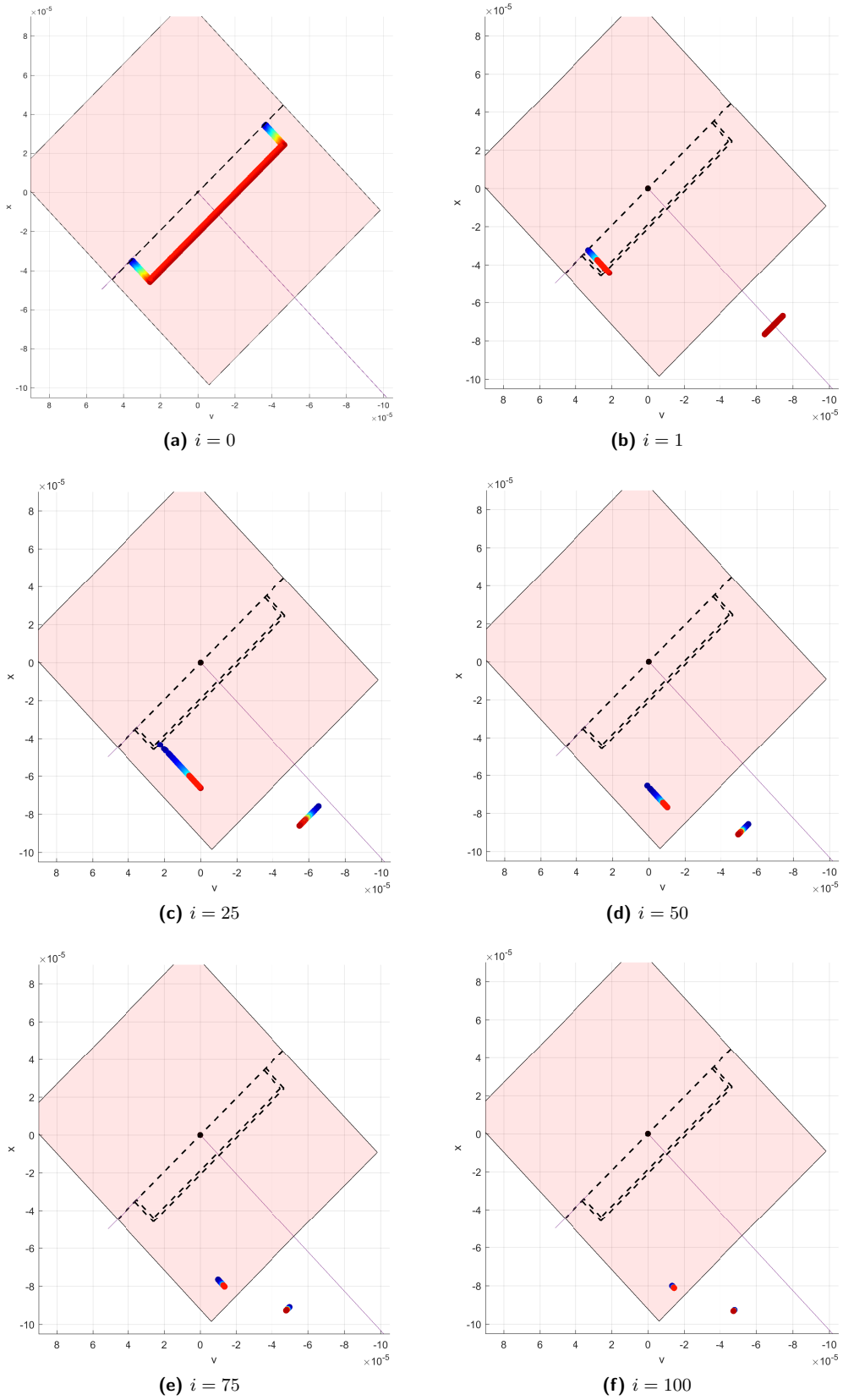

(a) $i = 0$ **(b)** $i = 1$

(c) $i = 25$ **(d)** $i = 50$

(e) $i = 75$ **(f)** $i = 100$

Figure 10. Dynamics of the half-frame of points $\Sigma^{\text{in}}_{\text{grid}}$ on the section Σ^{in} under repeated applications of the Poincaré map $\Pi^i : \Sigma^{\text{in}} \to \Sigma^{\text{in}}$, $i = 1, 2, \ldots$, for $\delta = 0.9$, $\beta = 0.2$, $\overline{s} = 0.060131460581$ (after bifurcation).

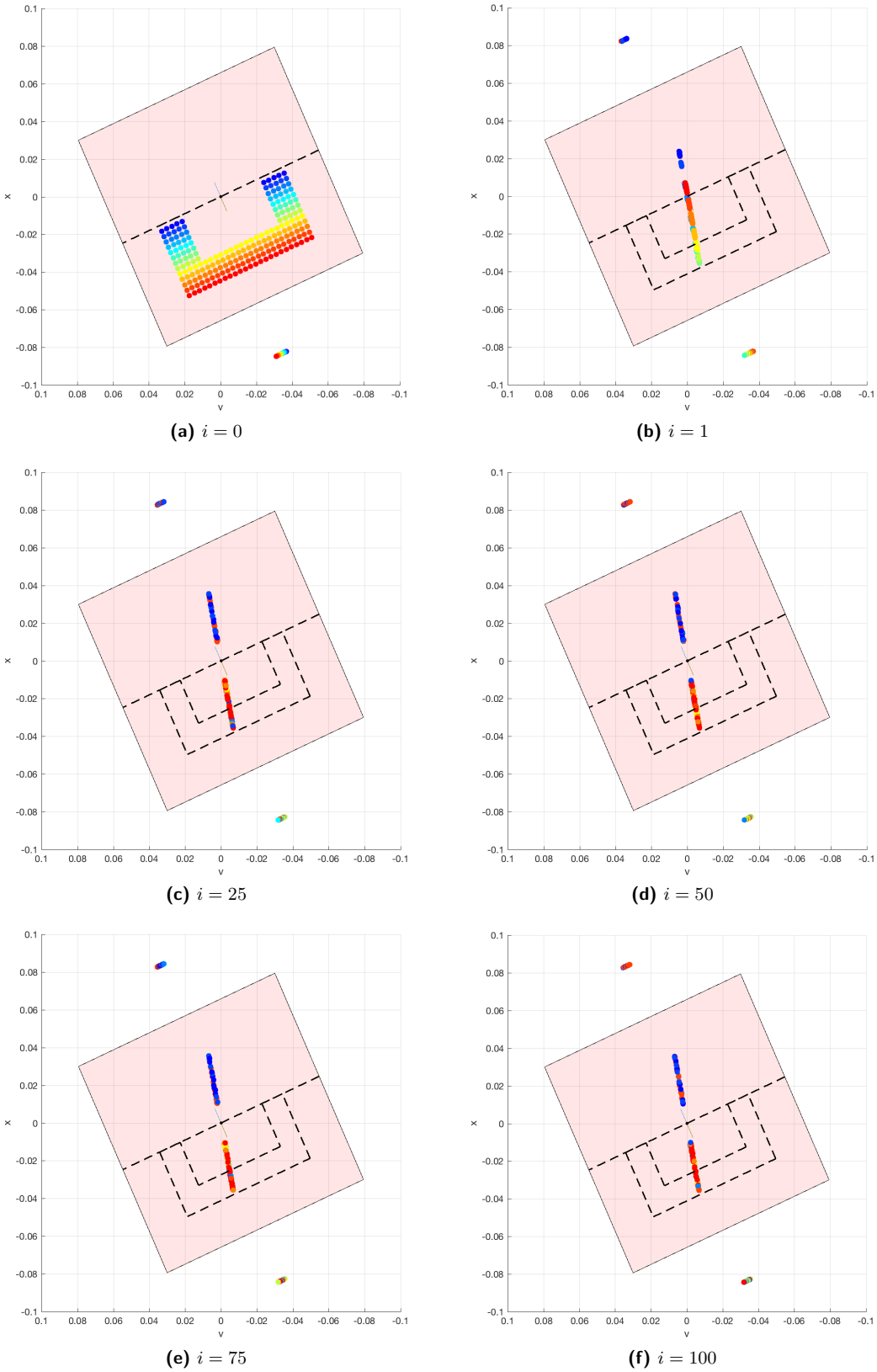

(a) $i = 0$ **(b)** $i = 1$

(c) $i = 25$ **(d)** $i = 50$

(e) $i = 75$ **(f)** $i = 100$

Figure 11. Dynamics of the half-frame of points $\Sigma^{\text{in}}_{\text{grid}}$ on the section Σ^{in} under repeated applications of the Poincaré map $\Pi^i : \Sigma^{\text{in}} \to \Sigma^{\text{in}}$, $i = 1, 2, \ldots$, for $\delta = 0.9$, $\beta = 2.899$, $\underline{s} = 0.7955$ (before bifurcation).

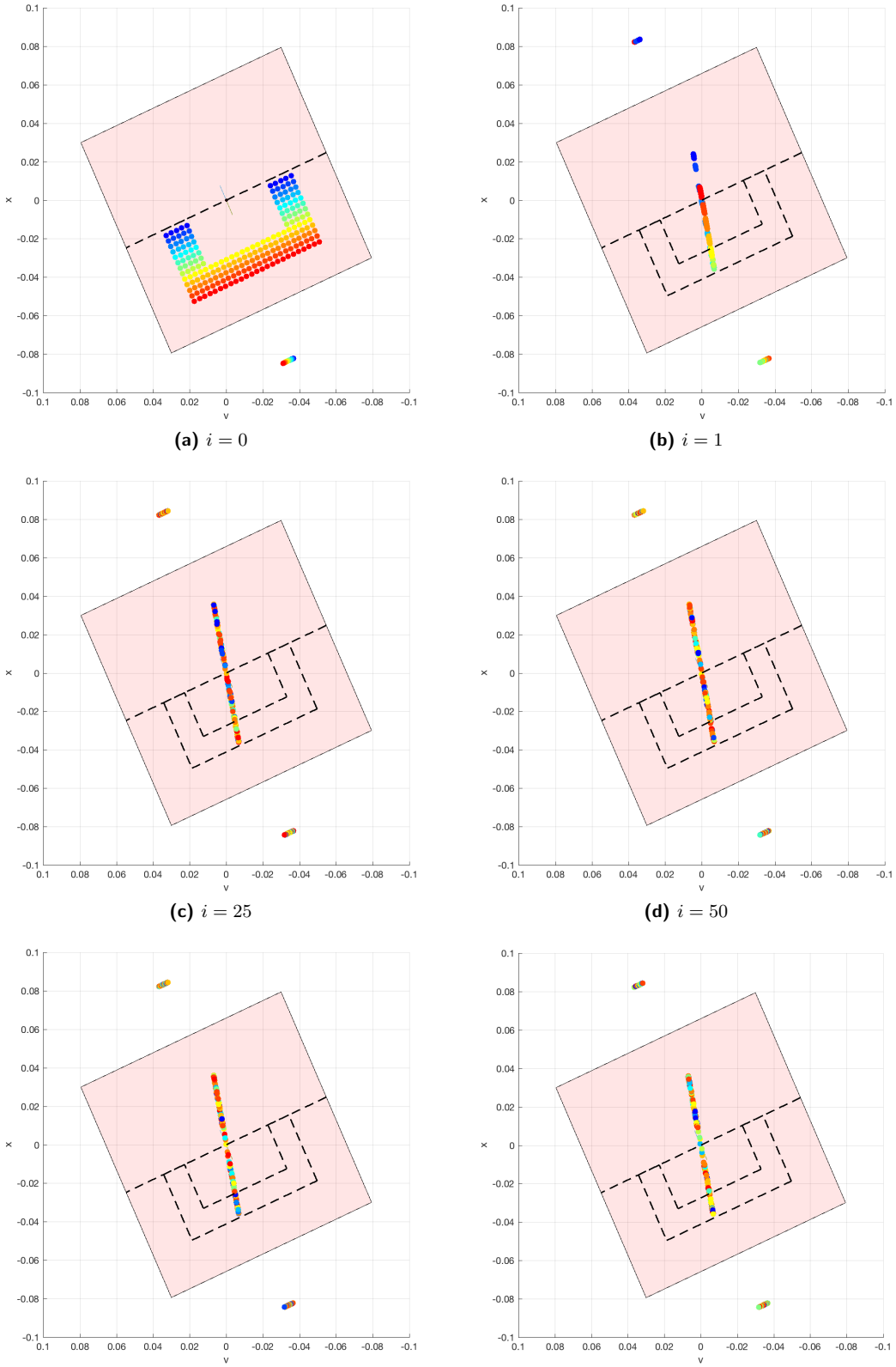

(a) $i = 0$ **(b)** $i = 1$

(c) $i = 25$ **(d)** $i = 50$

(e) $i = 75$ **(f)** $i = 100$

Figure 12. Dynamics of the half-frame of points $\Sigma^{\text{in}}_{\text{grid}}$ on the section Σ^{in} under repeated applications of the Poincaré map $\Pi^i : \Sigma^{\text{in}} \to \Sigma^{\text{in}}$, $i = 1, 2, \ldots$, for $\delta = 0.9$, $\beta = 2.899$, $\overline{s} = 0.7958$ (after bifurcation).

PVIII

A LOWER-BOUND ESTIMATE OF THE LYAPUNOV DIMENSION FOR THE GLOBAL ATTRACTOR OF THE LORENZ SYSTEM

by

N.V. Kuznetsov, T.N. Mokaev, R.N. Mokaev, O.A. Kuznetsova,
E.V. Kudryashova 2019

preprint, arXiv:1910.08740, https://arxiv.org/pdf/1910.08740.pdf

A lower-bound estimate of the Lyapunov dimension for the global attractor of the Lorenz system

N. V. Kuznetsov,[1,2,3,*] T. N. Mokaev,[1] R. N. Mokaev,[1,2] O. A. Kuznetsova,[1] and E. V. Kudryashova[1]

[1] *Faculty of Mathematics and Mechanics, St. Petersburg State University, Peterhof, St. Petersburg, Russia*
[2] *Faculty of Information Technology, University of Jyväskylä, Jyväskylä, Finland*
[3] *Institute for Problems in Mechanical Engineering RAS, Russia*

(Dated: October 29, 2019)

In this short report, for the classical Lorenz attractor we demonstrate the applications of the Pyragas time-delayed feedback control technique and Leonov analytical method for the Lyapunov dimension estimation and verification of the Eden's conjecture. The problem of reliable numerical computation of the finite-time Lyapunov dimension along the trajectories over large time intervals is discussed.

arXiv:1910.08740v2 [nlin.CD] 27 Oct 2019

I. LORENZ ATTRACTOR AND PYRAGAS STABILIZATION OF EMBEDDED UNSTABLE PERIODIC ORBITS

Consider the classical Lorenz system [1]

$$\begin{cases} \dot{x} = -\sigma(x-y), \\ \dot{y} = rx - y - xz, \\ \dot{z} = -bz + xy, \end{cases} \tag{1}$$

with physically sound parameters $\sigma, r > 0$, and $b \in [0, 4]$. For $r < 1$ it has only one globally stable equilibrium $S_0 = (0,\, 0,\, 0)$, and for $r > 1$ the equilibrium S_0 turns into a saddle, while two new symmetric equilibria appear:

$$S_\pm = \big(\pm\sqrt{b(r-1)}, \pm\sqrt{b(r-1)}, r-1\big), \tag{2}$$

which stability depends on the values of parameters.

System (1) is dissipative in the sense of Levinson (see e.g. [2]), i.e. there exist a global bounded absorbing set containing global attractor $\mathcal{A}_{\text{glob}}$, and in some cases this attractor exhibits chaotic behavior. For some values of parameters, it is possible to observe a case of multistability, when the global attractor consists of several local attractors. To get a visualization of such attractors one needs to choose an initial point in the basin of attraction of a particular attractor and observe how the trajectory, starting from this initial point, after a transient process visualizes the attractor: an attractor is called a *self-excited attractor* if its basin of attraction intersects with any open neighborhood of an equilibrium, otherwise, it is called a *hidden attractor* [2–5]. It was discovered numerically by E. Lorenz that in the phase space of system (1) with parameters $r = 28$, $\sigma = 10$, $b = 8/3$ there exist a *chaotic attractor* $\mathcal{A}$, which is self-excited with respect to all equilibria S_0, $S_\pm$.

The "skeleton" of a chaotic attractor comprises embedded unstable periodic orbits (UPOs) (see e.g. [6–8]), and one of the effective methods among others for the computation of UPOs is the *delay feedback control* (DFC) approach, suggested by K. Pyragas [9] (see also discussions in [10–12]). This approach allows Pyragas and his progeny to stabilize and study UPOs in various chaotic dynamical systems. Nevertheless, some general analytical results have been obtained [13], showing that DFC has a certain limitation, called the odd number limitation (ONL), which is connected with an odd number of real Floquet multipliers larger than unity. In order to overcome ONL, later Pyragas suggested a modification of the classical DFC technique, which was called the unstable delayed feedback control (UDFC) [14].

Rewrite system (1) in a general form

$$\dot{u} = f(u). \tag{3}$$

Let $u^{\text{upo}}(t, u_0^{\text{upo}_1})$ be its UPO with period $\tau > 0$, $u^{\text{upo}}(t-\tau, u_0^{\text{upo}_1}) = u^{\text{upo}}(t, u_0^{\text{upo}_1})$, and initial condition $u_0^{\text{upo}_1} = u^{\text{upo}}(0, u_0^{\text{upo}_1})$. To compute the UPO and overcome ONL, we add the UDFC in the following form:

$$\begin{aligned} \dot{u}(t) &= f(u(t)) + KB\,\big[F_N(t) + w(t)\big], \\ \dot{w}(t) &= \lambda_c^0 w(t) + (\lambda_c^0 - \lambda_c^\infty) F_N(t), \\ F_N(t) &= C^* u(t) - (1-R)\sum_{k=1}^{N} R^{k-1} C^* u(t-kT), \end{aligned} \tag{4}$$

where $0 \le R < 1$ is an extended DFC parameter, $N = 1, 2, \ldots, \infty$ defines the number of previous states involved in delayed feedback function $F_N(t)$, $\lambda_c^0 > 0$, and $\lambda_c^\infty < 0$ are additional unstable degree of freedom parameters, B, C are vectors and $K > 0$ is a feedback gain. For initial condition $u_0^{\text{upo}_1}$ and $T = \tau$ we have

$$F_N(t) \equiv 0,\ w(t) \equiv 0,$$

and, thus, the solution of system (4) coincides with the periodic solution of initial system (3).

For the Lorenz system (1) with parameters $r = 28$, $\sigma = 10$, $b = 8/3$ using (4) with $B^* = (0, 1, 0)$, $C^* = (0, 1, 0)$, $R = 0.7$, $N = 100$, $K = 3.5$, $\lambda_c^0 = 0.1$, $\lambda_c^\infty = -2$, one can stabilize a period-1 UPO $u^{\text{upo}_1}(t, u_0)$ with period $\tau_1 = 1.5586$ from the initial point $u_0 = (1, 1, 1)$, $w_0 = 0$ (see Fig. 1). Results of this experiment could be repeated using various other numerical approaches (see

* Corresponding author: nkuznetsov239@gmail.com

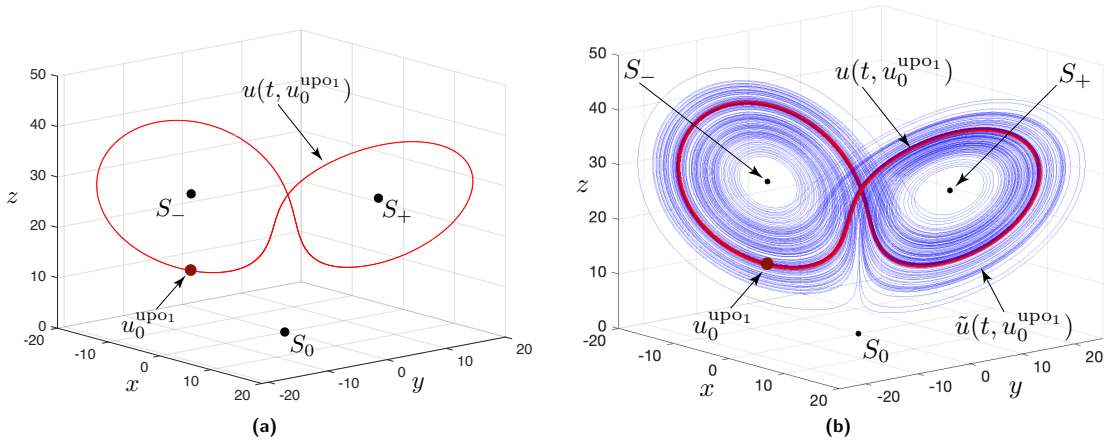

Figure 1: Period-1 UPO $u^{\text{upo}_1}(t)$ (red, period $\tau_1 = 1.5586$) stabilized using UDFC method, and pseudo-trajectory $\tilde{u}(t, u_0^{\text{upo}_1})$ (blue, $t \in [0, 100]$) in system (1) with parameters $r = 28$, $\sigma = 10$, $b = 8/3$.

e.g. [15–17]), and are in agreement with similar results on the existence of UPOs embedded in the Lorenz attractor [18, 19]. However, the Pyragas procedure, in general, is more convenient for UPOs numerical visualization.

For the initial point $u_0^{\text{upo}_1} \approx (-6.2262, -11.0027, 13.0515)$ on the UPO $u^{\text{upo}_1}(t) = u(t, u_0^{\text{upo}_1})$ we numerically compute the trajectory of system (4) without the stabilization (i.e. with $K = 0$) on the time interval $[0, T = 100]$ (see Fig. 1b). We denote it by $\tilde{u}(t, u_0^{\text{upo}_1})$ to distinguish this pseudo-trajectory from the periodic orbit $u(t, u_0^{\text{upo}_1})$. One can see that on the initial small time interval $[0, T_1 \approx 11]$, even without the control, the obtained trajectory $\tilde{u}(t, u_0^{\text{upo}_1})$ traces approximately the "true" periodic orbit $u(t, u_0^{\text{upo}_1})$. But for $t > T_1$, without a control, the trajectory $\tilde{u}(t, u_0^{\text{upo}_1})$ diverge from $u^{\text{upo}_1}(t, u_0^{\text{upo}_1})$ and visualize a local chaotic attractor $\mathcal{A}$.

Remark that in numerical computation of trajectory over a finite-time interval it is also difficult to distinguish a *sustained chaos* from a *transient chaos* (a transient chaotic set in the phase space, which can persist for a long time) [20]. This challenging task is related to an open problem about the existence of a hidden chaotic attractor in the Lorenz system (1) (see e.g. discussions in [2, 21–23]).

II. LYAPUNOV DIMENSION ESTIMATION AND EDEN CONJECTURE

Following [24, 25], let us outline the concept of the *finite-time Lyapunov dimension*, which is convenient for carrying out numerical experiments with finite time.

For a fixed $t \geq 0$ let us consider the map $u(t, \cdot) : \mathbb{R}^3 \to \mathbb{R}^3$ defined by the shift operator along the solutions of system (1): $u(t, u_0)$, $u_0 \in \mathbb{R}^3$. Since system (1) possesses an absorbing set, the existence and uniqueness of solutions of system (1) for $t \in [0, +\infty)$ take place and, therefore, the system generates a *dynamical system* $\big(\{u(t, \cdot)\}_{t \geq 0}, (\mathbb{R}^3, |\cdot|)\big)$.

Consider linearization of system (1) along the solution $u(t, u_0)$ and its 3×3 fundamental matrix of solutions $\Phi(t, u_0)$: $\dot{\Phi}(t, u_0) = Df((u(t, u_0))\Phi(t, u_0)$, where $\Phi(0, u_0) = I$ is a unit 3×3 matrix. Denote by $\sigma_i(t, u_0) = \sigma_i(\Phi(t, u_0))$, $i = 1, 2, 3$, the singular values of $\Phi(t, u_0)$ (i.e. the square roots of the eigenvalues of the symmetric matrix $\Phi(t, u_0)^* \Phi(t, u_0)$ with respect to their algebraic multiplicity)[1], ordered so that $\sigma_1(t, u_0) \geq \sigma_2(t, u_0) \geq \sigma_3(t, u_0) > 0$ for any $u_0 \in \mathbb{R}^3$ and $t > 0$.

Consider a set of *finite-time Lyapunov exponents* at the point u_0:

$$\text{LE}_i(t, u_0) = \frac{1}{t} \ln \sigma_i(t, u_0), \ t > 0, \quad i = 1, 2, 3. \tag{5}$$

Here, the set $\{\text{LE}_i(t, u_0)\}_{i=1}^3$ is ordered by decreasing (i.e. $\text{LE}_1(t, u_0) \geq \text{LE}_2(t, u_0) \geq \text{LE}_3(t, u_0)$ for all $t > 0$). The *finite-time local Lyapunov dimension* [24, 25] can be defined via an analog of the *Kaplan-Yorke formula* with respect to the set of ordered finite-time Lyapunov exponents $\{\text{LE}_i(t, u_0)\}_{i=1}^3$:

$$\dim_{\text{L}}(t, u_0) = j(t, u_0) + \frac{\text{LE}_1(t, u_0) + \cdots + \text{LE}_{j(,u_0)}(t, u_0)}{|\text{LE}_{j(t,u_0)+1}(t, u_0)|}, \tag{6}$$

where $j(t, u_0) = \max\{m : \sum_{i=1}^m \text{LE}_i(t, u_0) \geq 0\}$. Then the *finite-time Lyapunov dimension* of dynamical system with respect to a set $\mathcal{A}$ is defined as:

$$\dim_{\text{L}}(t, \mathcal{A}) = \sup_{u_0 \in \mathcal{A}} \dim_{\text{L}}(t, u_0). \tag{7}$$

[1] Symbol * denotes the transposition of matrix.

The *Douady–Oesterlé theorem* [26] implies that for any fixed $t > 0$ the finite-time Lyapunov dimension on a compact invariant set $\mathcal{A}$, defined by (7), is an upper estimate of the Hausdorff dimension: $\dim_{\mathrm{H}} \mathcal{A} \le \dim_{\mathrm{L}}(t, \mathcal{A})$. The best estimation is called the *Lyapunov dimension* [24]

$$\dim_{\mathrm{L}} \mathcal{A} = \inf_{t>0} \sup_{u_0 \in \mathcal{A}} \dim_{\mathrm{L}}(t, u_0) = \\ = \liminf_{t \to +\infty} \sup_{u_0 \in \mathcal{A}} \dim_{\mathrm{L}}(t, u_0).$$

We use the *adaptive algorithm for the computation of the finite-time Lyapunov dimension and exponents* for trajectories on the local attractor $\mathcal{A}$ [25]. In order to distinguish the corresponding values for the stabilized UPO $u(t, u_0^{\mathrm{upo}_1})$ with a period $\tau_1 = 1.5586$ and for the pseudo-trajectory $\tilde{u}(t, u_0^{\mathrm{upo}_1})$ computed without Pyragas stabilization in our experiment we use the following notations for finite-time Lyapunov dimensions: $\dim_{\mathrm{L}}(u(t,\cdot), u_0^{\mathrm{upo}_1})$ and $\dim_{\mathrm{L}}(\tilde{u}(t,\cdot), u_0^{\mathrm{upo}_1})$, respectively.

The comparison of the obtained values of finite-time Lyapunov dimensions computed along the stabilized UPO and the trajectory without stabilization gives us the following results. On the initial small part of the time interval, one can indicate the coincidence of these values with a sufficiently high accuracy. For the UPO and for the unstabilized trajectory the finite-time local Lyapunov dimensions $\dim_{\mathrm{L}}(u(t,\cdot), u_0^{\mathrm{upo}_1})$ and $\dim_{\mathrm{L}}(\tilde{u}(t,\cdot), u_0^{\mathrm{upo}_1})$ coincide up to the 4th decimal place inclusive on the interval $[0, t_m^1 \approx 7\tau_1]$. After $t > t_m^1$ the difference in values becomes significant and the corresponding graphics diverge in such a way that the part of the graph corresponding to the unstabilized trajectory is lower than the part of the graph corresponding to the UPO (see Fig. 2b, Fig. 3).

The Jacobi matrix at the saddle-foci equilibria $S_\pm$ has simple eigenvalues, which give the following: $\dim_{\mathrm{L}} S_\pm = 2.0136$. The UPO u^{upo_1} with period $\tau_1 = 1.5586$ has the following Floquet multipliers: $\rho_1 = 4.7127$, $\rho_2 = 1$, $\rho_3 = -1.19 \cdot 10^{-10}$ and corresponding Lyapunov exponents: $\{\frac{1}{\tau_1} \log \rho_i\}_{i=1}^3$. Thus, for the local Lyapunov dimension of this UPO we obtain: $\dim_{\mathrm{L}} u^{\mathrm{upo}_1} = 2.0678 \lessapprox 2.0679 = \dim_{\mathrm{L}}(u(100,\cdot), u_0^{\mathrm{upo}_1})$.

Using an effective analytical technique, proposed by Leonov [24, 27], which is based on a combination of the Douady-Oesterlé approach and the direct Lyapunov method, it is possible to obtain [28, 29] the exact formula of the Lyapunov dimension for the global attractor $\mathcal{A}_{\mathrm{glob}}$ of the Lorenz system (1):

$$\dim_{\mathrm{L}} \mathcal{A}_{\mathrm{glob}} = 3 - \frac{2(\sigma+b+1)}{\sigma+1+\sqrt{(\sigma-1)^2+4\sigma r}} \qquad (8)$$

for the case, when $r\sigma > (\sigma + b)(b + 1)$.

III. CONCLUSION

In this note, for the Lorenz system (1) with classical values of parameters $r = 28$, $\sigma = 10$, $b = 8/3$ we have studied the Eden conjecture [30, p.98] and obtained the following relations:

$$\dim_{\mathrm{L}} \mathcal{A}_{\mathrm{glob}} = \dim_{\mathrm{L}} S_0 = 3 - \frac{2(\sigma+b+1)}{\sigma+1+\sqrt{(\sigma-1)^2+4\sigma r}} = 2.4013 > \\ > \dim_{\mathrm{L}} \mathcal{A} \ge \dim_{\mathrm{L}} u^{\mathrm{upo}_1} = 2.0678 > \dim_{\mathrm{L}}(\tilde{u}(100,\cdot), u_0^{\mathrm{upo}_1}) \\ = 2.0621 > \dim_{\mathrm{L}} S_\pm = 2.0136.$$

Here, since the global Lorenz attractor contains a period-1 UPO: $\mathcal{A}_{\mathrm{glob}} \supset u^{\mathrm{upo}_1}$, we have the following lower-bound estimate for the Lyapunov dimension: $\dim_{\mathrm{L}} \mathcal{A}_{\mathrm{glob}} \ge 2.0678 = \dim_{\mathrm{L}} u^{\mathrm{upo}_1}$. Similar experiment and results for the Rössler system [31] are presented in [32, 33].

Concerning the time of integration, remark that while the time series obtained from a *physical experiment* are assumed to be reliable on the whole considered time interval, the time series produced by the integration of *mathematical dynamical model* can be reliable on a limited time interval only due to computational errors (caused by finite precision arithmetic and numerical integration of ODE). Thus, in general, the closeness of the real trajectory $u(t, u_0)$ and the corresponding pseudo-trajectory $\tilde{u}(t, u_0)$ calculated numerically can be guaranteed on a limited short time interval only.

In our experiment, if we continue computation over a long time interval $[0, 10000]$ of FTLD along the stabilized UPO and the pseudo-trajectory obtained without Pyragas stabilization, as a result, completely different values will be obtained (see Fig. 3). Evolution of $\dim_{\mathrm{L}}(u(t,\cdot), u_0^{\mathrm{upo}_1})$ along the stabilized UPO will tend to the analytical value $\dim_{\mathrm{L}} u^{\mathrm{upo}_1} = 2.0678$, computed via Floquet multipliers, while evolution of $\dim_{\mathrm{L}}(\tilde{u}(t,\cdot), u_0^{\mathrm{upo}_1})$ along the pseudo-trajectory will converge to the value 2.0622[2]. These results are in good agreement with the rigorous analysis of the time interval choices for reliable numerical computation of trajectories for the Lorenz system: the time interval for reliable computation with 16 significant digits and error 10^{-4} is estimated as $[0, 36]$, with error 10^{-8} is estimated as $[0, 26]$ (see [47, 48]), and reliable computation for a longer time interval, e.g. $[0, 10000]$ in [49], is a challenging task that requires significant increase of the precision of the floating-point representation and the use of supercomputers. Analytical aspects of this problem are related to the shadowing theory (see e.g. [50]).

[2] The following results on the dimension of the Lorenz attractor with parameters $r = 28$,$\sigma = 10$,$b = 8/3$ can be found in the literature. In [34, p. 193] and [35, p. 3529] the fractal (box-counting, capacity) dimension is estimated as $\mathbf{2.06 \pm 0.01}$. For the correlation dimension the following results are known: $\mathbf{2.05 \pm 0.01}$ in [34, p. 193] and [36, p. 456]; $\mathbf{2.06 \pm 0.03}$ in [37, p. 47]; $\mathbf{2.049 \pm 0.096}$ in [38, p. 1874]; $\mathbf{2.05}$ in [39, p. 80]. For the Lyapunov dimension the following values have been computed: $\mathbf{2.063}$ in [40, p. 92] and [41, p. 1957]; $\mathbf{2.05}$ in [42, p. 267]; $\mathbf{2.062}$ in [38, p. 1874], [43, p. 115] and [44, p. 53]; $\mathbf{2.06215}$ [45, p. 033124-3] and [39, p. 83]. Also, let us mention estimates for the global attractor: $2.401 \le \dim_{\mathrm{L}} \mathcal{A}_{\mathrm{glob}} \le 2.409$ [46, p. 170] and $\dim_{\mathrm{L}} \mathcal{A}_{\mathrm{glob}} \approx 2.401...$ in [42, p. 267].

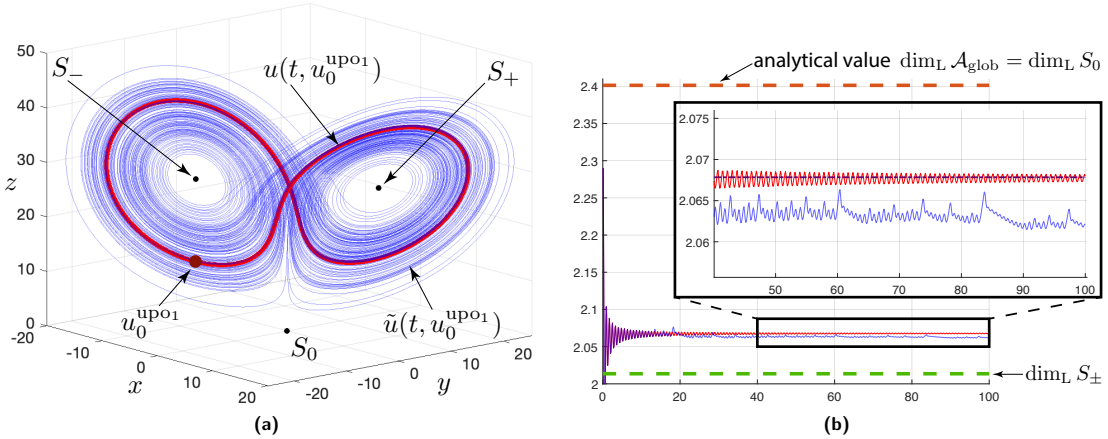

Figure 2: Evolution of FTLDs $\dim_{\mathrm{L}}(u(t,\cdot), u_0^{\mathrm{upo}_1})$ (red) and $\dim_{\mathrm{L}}(\tilde{u}(t,\cdot), u_0^{\mathrm{upo}_1})$ (blue) computed on the time interval $t \in [0, 100]$ along the UPO $u^{\mathrm{upo}_1}(t) = u(t, u_0^{\mathrm{upo}_1})$ (red) and the trajectory $\tilde{u}(t, u_0^{\mathrm{upo}_1})$ (blue) integrated without stabilization, respectively. Both trajectories start from the point $u_0^{\mathrm{upo}_1} = (-6.2262, -11.0027, 13.0515)$.

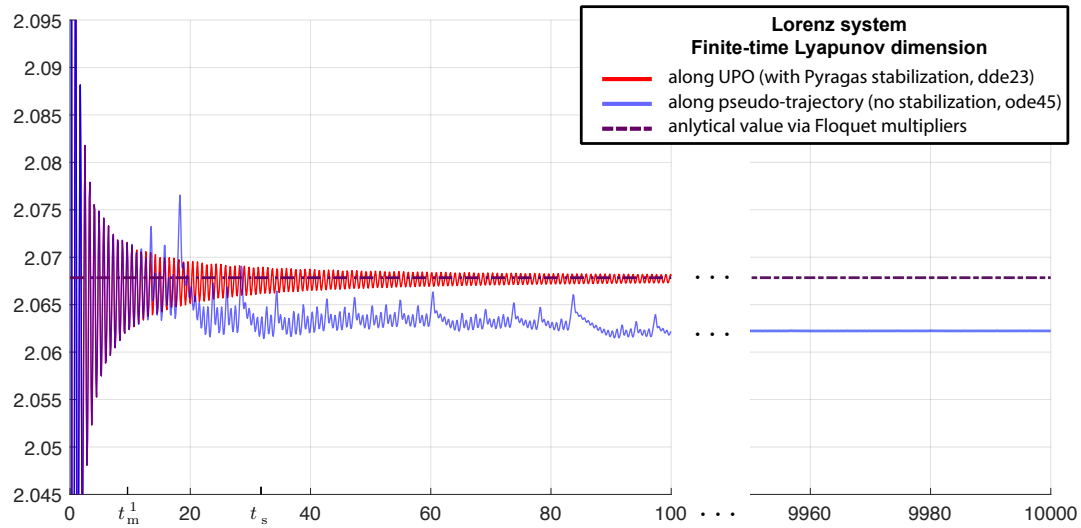

Figure 3: Evolution of FTLDs $\dim_{\mathrm{L}}(u(t,\cdot), u_0^{\mathrm{upo}_1})$ (red) and $\dim_{\mathrm{L}}(\tilde{u}(t,\cdot), u_0^{\mathrm{upo}_1})$ (blue) computed on the long time interval $t \in [0, 10000]$ along the UPO $u^{\mathrm{upo}_1}(t) = u(t, u_0^{\mathrm{upo}_1})$ (red) and the trajectory $\tilde{u}(t, u_0^{\mathrm{upo}_1})$ (blue) integrated without stabilization, respectively. Both trajectories start from the point $u_0^{\mathrm{upo}_1} = (-6.2262, -11.0027, 13.0515)$.

ACKNOWLEDGEMENT

This work was supported by the Russian Science Foundation 19-41-02002.

[1] E. Lorenz, Deterministic nonperiodic flow, J. Atmos. Sci. 20 (2) (1963) 130–141.

[2] G. Leonov, N. Kuznetsov, T. Mokaev, Homoclinic orbits, and self-excited and hidden attractors in a Lorenz-like system describing convective fluid motion, The Eu-

ropean Physical Journal Special Topics 224 (8) (2015) 1421–1458. doi:10.1140/epjst/e2015-02470-3.

[3] G. Leonov, N. Kuznetsov, V. Vagaitsev, Localization of hidden Chua's attractors, Physics Letters A 375 (23) (2011) 2230–2233. doi:10.1016/j.physleta.2011.04.037.

[4] G. Leonov, N. Kuznetsov, Hidden attractors in dynamical systems. From hidden oscillations in Hilbert-Kolmogorov, Aizerman, and Kalman problems to hidden chaotic attractors in Chua circuits, International Journal of Bifurcation and Chaos in Applied Sciences and Engineering 23 (1), art. no. 1330002. doi:10.1142/S0218127413300024.

[5] N. Kuznetsov, Hidden attractors in fundamental problems and engineering models. A short survey, Lecture Notes in Electrical Engineering 371 (2016) 13–25, (Plenary lecture at International Conference on Advanced Engineering Theory and Applications 2015). doi:10.1007/978-3-319-27247-4_2.

[6] V. Afraımovic, V. Bykov, L. Silnikov, On the origin and structure of the Lorenz attractor 234 (2) (1977) 336–339.

[7] D. Auerbach, P. Cvitanović, J.-P. Eckmann, G. Gunaratne, I. Procaccia, Exploring chaotic motion through periodic orbits, Physical Review Letters 58 (23) (1987) 2387.

[8] P. Cvitanović, Periodic orbits as the skeleton of classical and quantum chaos, Physica D: Nonlinear Phenomena 51 (1-3) (1991) 138–151.

[9] K. Pyragas, Continuous control of chaos by selfcontrolling feedback, Phys. Lett. A. 170 (1992) 421–428.

[10] N. Kuznetsov, G. Leonov, M. Shumafov, A short survey on Pyragas time-delay feedback stabilization and odd number limitation, IFAC-PapersOnLine 48 (11) (2015) 706–709. doi:10.1016/j.ifacol.2015.09.271.

[11] G. Chen, X. Yu, On time-delayed feedback control of chaotic systems, IEEE Transactions on Circuits and Systems I: Fundamental Theory and Applications 46 (6) (1999) 767–772.

[12] J. Lehnert, P. Hövel, V. Flunkert, P. Guzenko, A. Fradkov, E. Schöll, Adaptive tuning of feedback gain in time-delayed feedback control, Chaos: An Interdisciplinary Journal of Nonlinear Science 21 (4) (2011) 043111.

[13] E. Hooton, A. Amann, Analytical limitation for time-delayed feedback control in autonomous systems, Phys. Rev. Lett. 109 (2012) 154101.

[14] K. Pyragas, Control of chaos via an unstable delayed feedback controller, Phys. Rev. Lett. 86 (2001) 2265–2268.

[15] D. Viswanath, The Lindstedt–Poincaré technique as an algorithm for computing periodic orbits, SIAM review 43 (3) (2001) 478–495.

[16] V. Budanov, Undefined frequencies method, Fundam. Prikl. Mat. 22 (2018) 59–71, (in Russian).

[17] A. Pchelintsev, A. Polunovskiy, I. Yukhanova, The harmonic balance method for finding approximate periodic solutions of the Lorenz system, Tambov University Reports. Series: Natural and Technical Sciences 24 (2019) 187–203, (in Russian).

[18] Z. Galias, W. Tucker, Short periodic orbits for the Lorenz system, in: 2008 International Conference on Signals and Electronic Systems, IEEE, 2008, pp. 285–288.

[19] R. Barrio, A. Dena, W. Tucker, A database of rigorous and high-precision periodic orbits of the Lorenz model, Computer Physics Communications 194 (2015) 76–83.

[20] C. Grebogi, E. Ott, J. Yorke, Fractal basin boundaries, long-lived chaotic transients, and unstable-unstable pair bifurcation, Physical Review Letters 50 (13) (1983) 935–938.

[21] G. Leonov, N. Kuznetsov, On differences and similarities in the analysis of Lorenz, Chen, and Lu systems, Applied Mathematics and Computation 256 (2015) 334–343. doi:10.1016/j.amc.2014.12.132.

[22] G. Chen, N. Kuznetsov, G. Leonov, T. Mokaev, Hidden attractors on one path: Glukhovsky-Dolzhansky, Lorenz, and Rabinovich systems, International Journal of Bifurcation and Chaos in Applied Sciences and Engineering 27 (8), art. num. 1750115.

[23] J. Sprott, B. Munmuangsaen, Comment on "A hidden chaotic attractor in the classical Lorenz system", Chaos, Solitons & Fractals 113 (2018) 261–262.

[24] N. Kuznetsov, The Lyapunov dimension and its estimation via the Leonov method, Physics Letters A 380 (25-26) (2016) 2142–2149. doi:10.1016/j.physleta.2016.04.036.

[25] N. Kuznetsov, G. Leonov, T. Mokaev, A. Prasad, M. Shrimali, Finite-time Lyapunov dimension and hidden attractor of the Rabinovich system, Nonlinear Dynamics 92 (2) (2018) 267–285. doi:10.1007/s11071-018-4054-z.

[26] A. Douady, J. Oesterle, Dimension de Hausdorff des attracteurs, C.R. Acad. Sci. Paris, Ser. A. (in French) 290 (24) (1980) 1135–1138.

[27] G. Leonov, On estimations of Hausdorff dimension of attractors, Vestnik St. Petersburg University: Mathematics 24 (3) (1991) 38–41, [Transl. from Russian: Vestnik Leningradskogo Universiteta. Mathematika, 24(3), 1991, pp. 41-44].

[28] G. Leonov, N. Kuznetsov, N. Korzhemanova, D. Kusakin, Lyapunov dimension formula for the global attractor of the Lorenz system, Communications in Nonlinear Science and Numerical Simulation 41 (2016) 84–103. doi:10.1016/j.cnsns.2016.04.032.

[29] G. Leonov, Lyapunov functions in the global analysis of chaotic systems, Ukrainian Mathematical Journal 70 (1) (2018) 42–66.

[30] A. Eden, An abstract theory of L-exponents with applications to dimension analysis (PhD thesis), Indiana University, 1989.

[31] O. Rössler, An equation for continuous chaos, Physics Letters A 57 (5) (1976) 397–398.

[32] N. Kuznetsov, T. Mokaev, Numerical analysis of dynamical systems: unstable periodic orbits, hidden transient chaotic sets, hidden attractors, and finite-time Lyapunov dimension, Journal of Physics: Conference Series 1205 (1), art. num. 012034. doi:10.1088/1742-6596/1205/1/012034.

[33] N. Kuznetsov, T. Mokaev, E. Kudryashova, O. Kuznetsova, M.-F. Danca, On lower-bound estimates of the Lyapunov dimension and topological entropy for the Rossler systems, 15th IFAC Workshop on Time Delay SystemsAccepted.

[34] P. Grassberger, I. Procaccia, Measuring the strangeness of strange attractors, Physica D: Nonlinear Phenomena 9 (1-2) (1983) 189–208.

[35] R. Benzi, G. Paladin, G. Parisi, A. Vulpiani, On the multifractal nature of fully developed turbulence and chaotic systems, Journal of Physics A: Mathematical and General 17 (18) (1984) 3521.

[36] H. Strogatz, Nonlinear Dynamics and Chaos. With Applications to Physics, Biology, Chemistry, and Engineering, Westview Press, 1994.
[37] G. Malinetskii, A. Potapov, On calculating the dimension of strange attractors, USSR Computational Mathematics and Mathematical Physics 28 (4) (1988) 39–49.
[38] J. Sprott, G. Rowlands, Improved correlation dimension calculation, International Journal of Bifurcation and Chaos 11 (07) (2001) 1865–1880.
[39] A. Fuchs, Nonlinear dynamics in complex systems, Springer, 2013.
[40] E. Lorenz, The local structure of a chaotic attractor in four dimensions, Physica D: Nonlinear Phenomena 13 (1-2) (1984) 90–104.
[41] J. Nese, J. Dutton, R. Wells, Calculated attractor dimensions for low-order spectral models, Journal of the atmospheric sciences 44 (15) (1987) 1950–1972.
[42] C. R. Doering, J. Gibbon, On the shape and dimension of the Lorenz attractor, Dynamics and Stability of Systems 10 (3) (1995) 255–268.
[43] J. Sprott, Chaos and time-series analysis, Oxford University Press, Oxford, 2003.
[44] M. Lappa, Thermal convection: patterns, evolution and stability, John Wiley & Sons, 2009.
[45] J. Sprott, Maximally complex simple attractors, Chaos: An Interdisciplinary Journal of Nonlinear Science 17 (3) (2007) 033124.
[46] A. Eden, C. Foias, R. Temam, Local and global Lyapunov exponents, Journal of Dynamics and Differential Equations 3 (1) (1991) 133–177, [Preprint No. 8804, The Institute for Applied Mathematics and Scientific Computing, Indiana University, 1988]. doi:10.1007/BF01049491.
[47] B. Kehlet, A. Logg, Quantifying the computability of the Lorenz system using a posteriori analysis, in: Proceedings of the VI Int. conf. on Adaptive Modeling and Simulation (ADMOS 2013), 2013.
[48] B. Kehlet, A. Logg, A posteriori error analysis of round-off errors in the numerical solution of ordinary differential equations, Numerical Algorithms 76 (1) (2017) 191–210.
[49] S. Liao, P. Wang, On the mathematically reliable long-term simulation of chaotic solutions of Lorenz equation in the interval [0,10000], Science China Physics, Mechanics and Astronomy 57 (2) (2014) 330–335.
[50] S. Pilyugin, Theory of shadowing of pseudotrajectories in dynamical systems, Differencialnie Uravnenia i Protsesy Upravlenia (Differential Equations and Control Processes) 4 (2011) 96–112.